SIDE-CHAIN FUNCTIONALIZED LUMINESCENT POLYMERS FOR ORGANIC LIGHT-EMITTING DIODE APPLICATIONS

A Dissertation
Presented to
The Academic Faculty

by

Alpay Kimyonok

In Partial Fulfillment
of the Requirements for the Degree
Doctor of Philosophy in the
School of Chemistry and Biochemistry

Georgia Institute of Technology
August 2008

SIDE-CHAIN FUNCTIONALIZED LUMINESCENT POLYMERS

FOR ORGANIC LIGHT-EMITTING DIODE APPLICATIONS

Approved by:

Dr. Marcus Weck, Advisor
School of Chemistry and Biochemistry
Georgia Institute of Technology

Dr. Joseph Perry
School Chemistry and Biochemistry
Georgia Institute of Technology

Dr. Jean-Luc Brédas
School of Chemistry and Biochemistry
Georgia Institute of Technology

Dr. Laren M. Tolbert
School of Chemistry and Biochemistry
Georgia Institute of Technology

Dr. Christopher Jones
School of Chemical and Biomolecular Engineering
Georgia Institute of Technology

Date Approved: June 24, 2008

ACKNOWLEDGEMENTS

First, I would like to thank to my advisor, Marcus Weck, not only for his invaluable scientific guidance, but also for his contribution to my writing and presentation skills. He showed me by example that presenting (or selling) a scientific work is as important as the science itself. I would also like to thank to the past and present members of the Weck Group for their help and support. I was lucky to have two mentors, Dr. Xian-Yong Wang, and Dr. Amy Meyers, who helped me to grasp the fundamentals of my research projects. I also want to thank Dr. Kunsang Yoon for being a great lab partner and for his patience for my loud Turkish music. I should also mention Si Kyung Yang with whom I had many discussions about the priorities in life. I spent a good amount of time with my dear friend Dr. William Sommer both in restaurants and in CRC, and I will certainly not forget the fun we had together. Finally, I must mention Dr. Nandita Madhavan, Kim Arrowood, Kamlesh Nair, and Dr. Ke Feng, the members of "Weck United", who made my final year less unbearable. I will especially miss the extensive gossiping with Nandita and Kim about the department and our boss.

I would also like to thank my committee members, Professors Jean-Luc Brédas, Christopher Jones, Laren Tolbert, and Joseph Perry for their valuable inputs. I also thank to the Bunz Group, the El-Sayed Group, the Jones Group, and the Perry Group for allowing me to use their equipments. I was fortunate enough to be a part of a project that involved intense collaboration with the Brédas Group, the Marder Group, and the Kippelen Group. I thank to the every member of the project for their contributions. I especially thank to Andreas Haldi for his friendship and for the devices he fabricated.

TABLE OF CONTENTS

LIST OF TABLES

LIST OF FIGURES

LIST OF SCHEMES

LIST OF ABBREVIATIONS

AIBN	2,2′-azo-bis(isobutyronitrile)
Alq_3	Aluminum tris(8-hydroxyquinoline)
BCP	2,9-dimethyl-4,7-diphenyl-1,10-phenanthroline
BINAP	2,2′-bis(diphenylphosphino)-1,1′-binaphthyl
btpy	2-benzo[b]thiophen-2-yl-pyridine
CBP	4,4′-(dicarbazol-9-yl)biphenyl
DCC	Dicyclohexylcarbodiimide
DFT	Density functional theory
DMAP	N,N-Dimethylaminopyridine
DMSO	Dimethylsulfoxide
DSC	Differential scanning calorimeter
EL	Electroluminescence
EQE	External quantum yield
ETL	Electron-transport layer

fac	Facial
GPC	Gel permeation chromotography
HOMO	Highest occupied molecular orbital
HTL	Hole-transport layer
IR	Infrared
$Ir(btpy)_3$	Tris(2- benzo[b]thiophen-2-yl-pyridine) iridium (III)
$Ir(btpy)_2acac$	Bis(2-benzo[b]thiophen-2-yl-pyridine)(acetlyacetonato) iridium (III)
$Ir(ns)_2acac$	Bis(2-phenylbenzothiazole)(acetlyacetonato) iridium (III)
$Ir(ppf)_3$	Tris(2-(2,4-difluoro-phenyl)pyridinato) iridium (III)
$Ir(ppy)_3$	Tris(2-phenylpyridine) iridium (III)
$Ir(pq)_3$	Tris(2-phenylquinoline) iridium (III)
$Ir(pq)_2acac$	Bis(2-phenylquinoline)(acetlyacetonato) iridium (III)
ITO	Indium tin oxide
KHMDS	Potassium hexamethyldisilazane
LC	Ligand-centered
LCD	Liquid crystal display
LEC	Light-emitting electrochemical cell

LED	Light-emitting diode
LUMO	Lowest unoccupied molecular orbital
mer	meridianal
MLCT	Metal to ligand charge transfer
M_n	Number average molecular weight
M_w	Weight average molecular weight
NMR	Nuclear magnetic resonance
OLED	Organic light-emitting diode
PBD	2-(4-biphenylyl-5-(4-tertbutylphenyl)-1,2,3-oxadiazole
Pd_2dba_3	Tris(dibenzylideneacetone)dipalladium(0)
PDI	Polydispersity index
PL	Photoluminescence
PMMA	Poly(methyl methacrylate)
ppf	2-(2,4-difluoro-phenyl)pyridine
ppy	2-phenylpyridine
pq	2-phenylquinoline
Pt(acac)(ppf)	(2-(2,4-difluoro-phenyl)pyridinato) platinum (II)

ROMP	Ring-opening metathesis polymerization
TEMPO	2,2,6,6-tetramethyl-piperidine-1-oxyl
TFA	Trifluoro acetic acid
T_g	Glass transition temperature
TGA	Thermogravimetric analysis
THF	Tetrahydrofuran
TPD	N,N′-bis(m-tolyl)-N,N′-diphenyl-1,1′-biphenyl-4,4′-diamine
UV	Ultraviolet
Ybq_3	Ytterbium tris(8-hydroxyquinoline)

SUMMARY

The major drawback for the fabrication of the small molecule based OLEDs is that these molecules are difficult to process. They have to be either vacuum-deposited or doped into a host material, often resulting in phase separation and poor device performance. A more appealing strategy is the employment of polymers that can be solution-processed, which is less costly compared to vacuum deposition technique. In addition to the reduced cost, solution processability allows for large surface area fabrication. Furthermore, polymers are suitable for flexible displays, and the emission properties of the polymers can be tailored by various synthetic strategies. Finally, polymers can be multi-functional; more than one electroactive group such as electron- and hole-transport compounds along with the emissive material can be incorporated into polymers, thus, creating materials that can combine properties of different layers in just one layer.

This thesis aims to provide a detailed understanding of side-chain functionalized polymers as emissive materials for OLEDs. The proceeding chapters will discuss the syntheses and photophysical properties of these solution-processable materials as well as the effects of metal types, polymer backbones, chain lengths, spacer types and lengths, host types, and concentrations of the metal complexes on the emission properties and device performance.

The polymers were functionalized with host materials along with the metal complexes to enhance the charge transport and to obtain energy transfer from the host to the complex. The physical and photophysical properties of the polymers were tuned by changing the backbone and the metal complex. Poly(norbornene)s, poly(cyclooctene)s, and poly(styrene)s were studied. The differences in the glass transition temperatures and

PDIs of the polymers indicated that device performances might be affected by the polymer type due to the differences in the processability of the polymers. In addition to the backbone, it was found that device performance is dependent on various parameters such as molecular weight, metal loading, spacer type, and spacer length. In each case, it was found that the polymer backbone does not interfere with the basic photopysical properties of the metal complexes.

The two main classes of metal complexes studied in this thesis are metalloquinolates and iridium complexes. It was shown that the emission properties of poly(cyclooctene)s containing 8-hydroxyquinolines in their side-chains could be altered by simply changing the metal. Green- and near IR-emitting polymers were synthesized by employing aluminum and ytterbium, respectively. On the other hand, for the iridium complexes, changes in color were achieved by varying the ligands. Iridium containing polymers with emission spectra that span the entire visible spectrum were synthesized by employing the appropriate ligands. It was demonstrated that OLEDs with high efficiencies can be fabricated by using these polymers as the emissive layer.

CHAPTER 1

INTRODUCTION TO ORGANIC LIGHT EMITTING DIODES

1.1 Abstract

This chapter presents a basic introduction to organic light-emitting diodes. Fundamentals of device operation are discussed, and examples for the materials employed in OLEDs are presented. Furthermore, mechanism of light emission is discussed in detail. Finally, OLEDs based on electroluminescent polymers are described.

1.2 Background Information

Organic light-emitting diode technology has been advancing rapidly as the next-generation technology that can compete with liquid crystal displays (LCDs), today's dominant flat panel display technology. Compared to LCDs, OLEDs feature wider viewing angle, lower power consumption and operating voltages, lighter weight, faster data display, and brighter, more saturated colors.[1,2] Furthermore, OLEDs do not require backlight to function, another significant advantage of OLEDs over LCDs.[3] Even though OLED technology is still an emerging technology, devices containing OLEDs are already on the market. It has been proposed that the OLED market will exceed $3 billion by 2008.[4]

1.3 Device Operation

Electroluminescence, in which light emission is obtained by the recombination of opposite charges injected from two electrodes, has received increasing attention over the past two decades.[1,5] Although organic electroluminescent materials have been known

since the 1950s,[6] intense research on organic compounds as key components in light-emitting diodes (LED) did not begin until 1987 when Tang and VanSlyke discovered *tris*-8-hydroxyquinoline aluminum (Alq_3) as an efficient emissive layer in LED devices.[7] Since then, small molecule organic compounds, organometallic complexes, conjugated polymers, and polymers containing photoactive groups have been the focus of extensive research in academia and industry due to their promise as low cost materials and the ease of modification of the emission wavelength of these materials using simple synthetic procedures.

In the simplest LED structure, emissive material is placed between two electrodes (Figure 1.1). The high work function electrode (anode) is in most devices indium tin oxide (ITO), which is transparent and allows the light generated to exit the device.[1] There are several choices for the low work function electrode (cathode) that include Ag, Al, Mg, and Ca.[1] Under an applied voltage, electrons are injected from the cathode and the holes are injected from the anode. In order to facilitate the charge transport, additional layers such as electron-transport or hole-transport layers are usually deposited between the electrodes and the emissive layer.[1,5,6] Light emission is dependent on the efficient charge trapping in the emissive layer. When electrons and holes are trapped, electron-hole binding results due to the Coulombic attraction of the opposite charges. This electron-hole pair is referred to as an exciton. Light emission is obtained by the radiative recombination of the excitons.[8] HOMO and LUMO levels of each layer are decisive in terms of device performance.[5] Electron-transport materials have low LUMOs, which facilitate the electron injection from the cathode.[9] If they have low-lying HOMOs, they can also serve as hole-blocking material by blocking the holes at the interface of the emissive layer and the electron-transport layer. The most widely used electron-transport compounds are oxadiazoles, metalloquinolates, triazoles, triazines, phenanthrolines, and siloles (Figure 1.2).[9] On the other hand, triarylamines (Figure 1.3) are used almost exclusively as hole-transport compounds due to their high HOMOs and

LUMOs,[10] which facilitate hole injection from the anode and electron blocking at the interface of the emissive layer and the hole-transport layer, respectively.

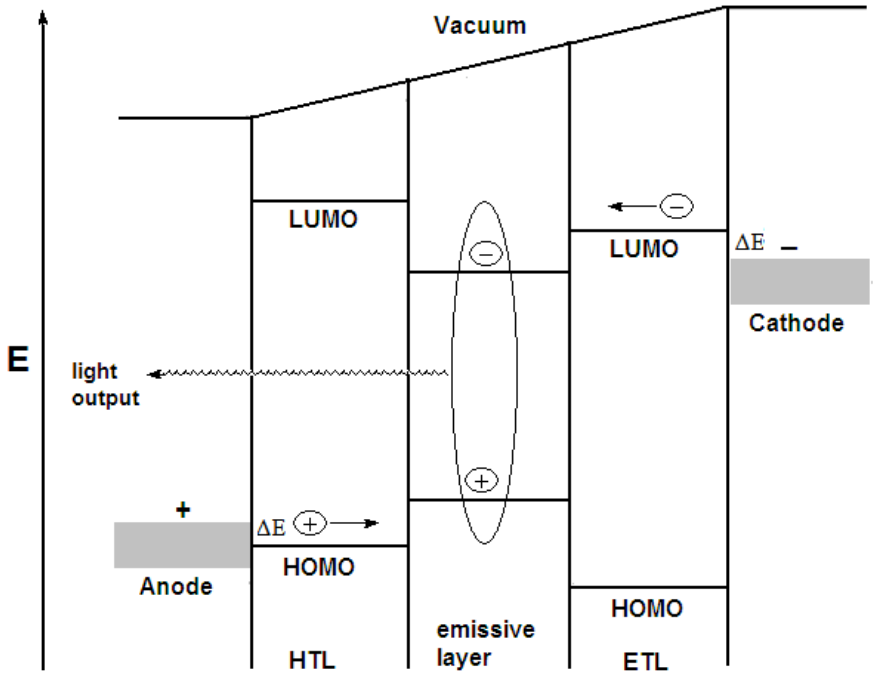

Figure 1.1 Schematic energy-level diagram for a device containing an anode, hole-transport layer (HTL), emissive layer, electron-transport layer (ETL), and a cathode (ΔE = energy barrier for charge injection from the electrodes).

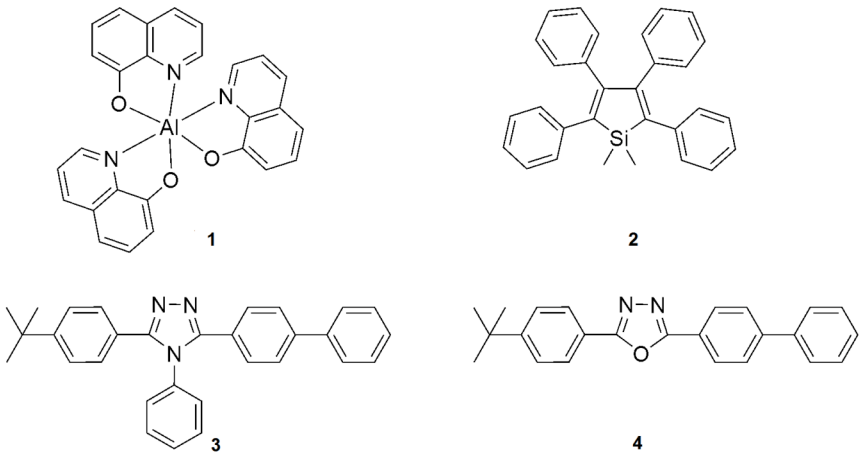

Figure 1.2 Examples of electron-transport compounds based on metalloquinolates (**1**), siloles (**2**), triazoles (**3**), and oxadiazoles (**4**).

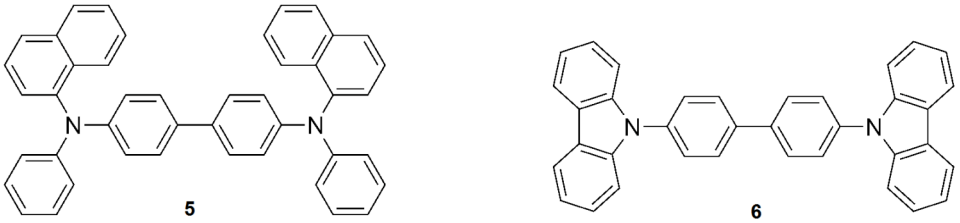

Figure 1.3 Examples of hole-transport compounds: NPD (**5**), and CBP (**6**).

Three main terms are used to describe device performances: External quantum efficiency, luminous efficiency and power efficiency. The external quantum efficiency is the ratio of luminescence output from the device to luminescence from the emissive layer. The latter term can be viewed as the internal quantum efficiency, which is defined as the ratio of the number of photons produced within the device to the number of electrons flowing in the external circuit.[1] Since not all light produced within the emissive layer can pass through the device, the external quantum efficiency is lower than the internal quantum efficiency. Another factor that determines the quality of the device is the luminous efficiency (cd/A), which is defined as the ratio of luminance (cd/m^2) to the current density (A/m^2).[11] Finally, the power efficiency (lm/W) is the ratio of the light output in lumens divided by the electrical input in watts. Thanks to the extensive research on small molecule-based OLEDs, the efficiencies of devices now reach high values. For example, a maximum external quantum efficiency of 19% and a power efficiency of 60 lm/W with a luminous efficiency of 86 cd/A were obtained for devices with organometallic complexes as the emissive compounds.[12] Even at a luminance of 1000 cd/m^2 (luminance of a laptop screen is around 100 cd/m^2), an external quantum efficiency of 14% was observed.[12]

1.4 Emission Pathways

The most common emissive materials for OLEDs are either fluorescent or phosphorescent. Figure 1.4 shows a partial energy diagram for a photoluminescence system. Upon light absorption, an electron is transferred from the ground state to a singlet excited state. The electronic state and vibrational level of the excited electron depends on the energy of the absorbed photon. Transitions from the ground state to the triplet states are spin-forbidden and thus highly improbable.[13] The excited electron relaxes to the lowest vibrational level of the lowest singlet excited state by vibrational relaxation in 10^{-13} to 10^{-11} seconds.[14] This process is referred as internal conversion. Once the electron is at the lowest vibrational level of the lowest excited singlet state, there are several possibilities for further relaxation. Fluorescence occurs when light is generated by the relaxation from the singlet excited state to the ground state. This process usually takes about 10^{-9} seconds.[14] The efficiency of fluorescence is dependent on competing factors such as radiation-less relaxation to the ground state or intersystem crossing to a triplet state.[15] Phosphorescence occurs when light is produced from the transition from an excited triplet state to the ground state.[14] Phosphorescence lifetime is much longer than that of fluorescence and can range from microseconds to minutes. The main advantage of the phosphorescent compounds over the fluorescent compounds is that 100% photoluminescence quantum efficiency is possible for phosphorescent compounds, provided that there is an efficient intersystem crossing from the singlet excited state to the triplet excited state.[8] This can be achieved by employing heavy metal complexes, which have strong spin-orbit coupling that leads to singlet-triplet mixing, which in turn results in efficient phosphorescence.[12,16,17]

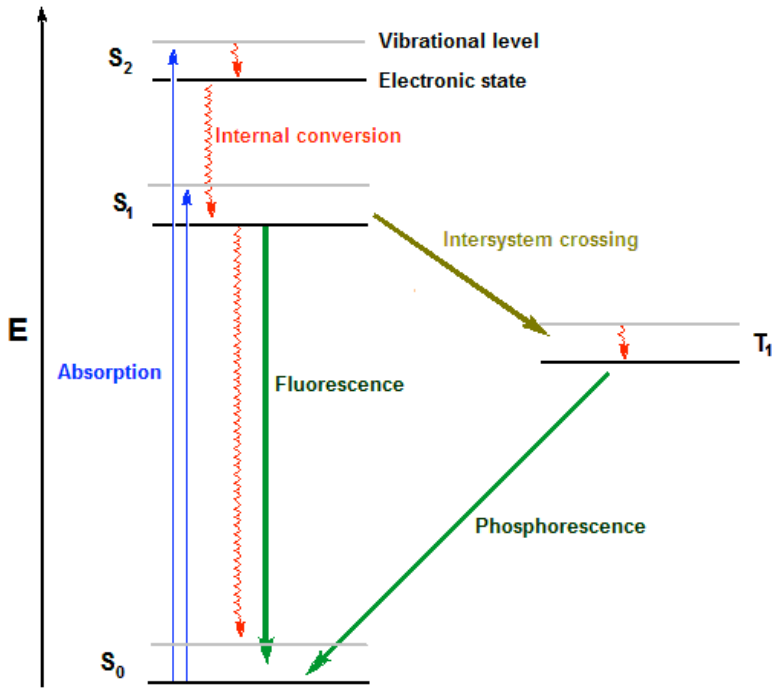

Figure 1.4 Partial energy diagram for photoluminescence.

Another type of emission can be obtained by the employment of lanthanide complexes as the emitting layer. In these complexes, emission stems from the lanthanide metal ion, the ligands are only responsible for the energy transfer into the metal.[18] Emission bands of the lanthanide complexes are much narrower than those of fluorescent or phosphorescent compounds due to their 4f electrons, which are responsible for their photoluminescence properties. The efficient shielding of 4f electrons from the external forces by the overlying $5s^2$ and $5p^6$ orbitals results in a small splitting of the excited states arising from the f^n configuration.[19] The small splitting of the excited states together with the weak vibronic couplings due to ion centered electronic states give rise to sharp absorption and emission bands. In lanthanide complexes, the lanthanide ions are excited via intramolecular energy transfer from the triplet excited states of the ligands.[20] In order to have an efficient energy transfer to the lanthanide ions, the triplet states of the ligands should be slightly above the metal ion's emitting levels.[19] The excitation of the ligands

and the transfer to the triplet states are described in Figure 1.4. Fig 1.5 shows the energy transfer to the lanthanide ion. Lanthanide complexes can produce both visible and near infrared emission. For example, Tb^{+3} and Eu^{+3} chelates are used to obtain green and red emission, respectively, whereas near IR emissions are observed for Yb^{+3}, Nd^{+3}, and Er^{+3} complexes.[19]

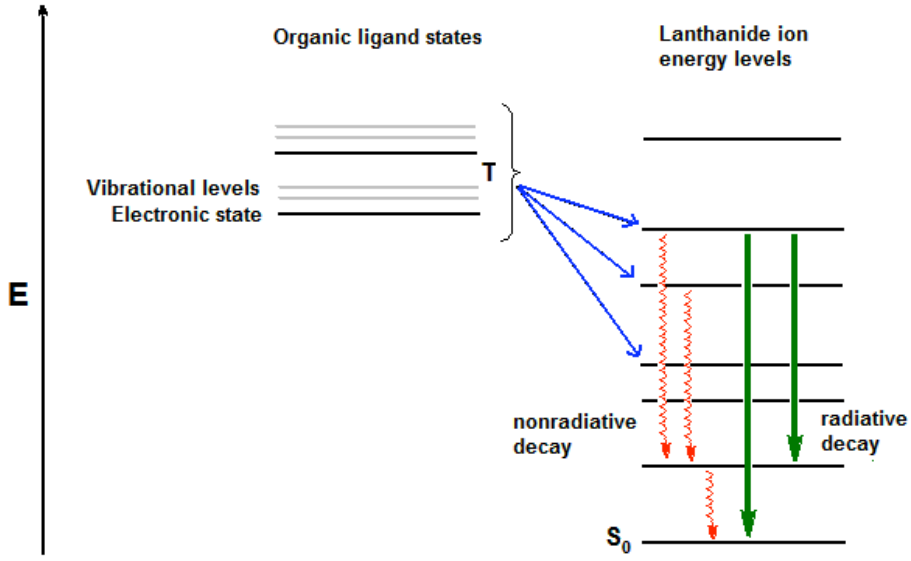

Figure 1.5 Energy transfer from the triplet states of the ligand to the lanthanide.

1.5 OLEDs with Polymers

The major drawback for the fabrication of the small molecule based OLEDs is that these molecules (organic dyes or organometallic complexes) are difficult to process. They have to be either vacuum-deposited or doped into a host material, often resulting in phase separation and poor device performance.[21] A more appealing strategy is the employment of polymers that can be solution-processed, which is less costly compared to vacuum deposition techniques.[22] In addition to the reduced cost, solution processability allows for large surface area fabrication.[23] Furthermore, polymers are suitable for flexible displays, and the emission properties of the polymers can be tailored by various synthetic strategies.[24,25] Finally, polymers can be multi-functional; more than one

electroactive group such as electron- and hole-transport compounds along with the emissive material can be incorporated into polymers, thus, creating materials that can combine properties of different layers in just one layer.[23-26]

There are basically two different types of emissive polymers: Conjugated polymers, for which the polymer backbone is responsible for the emission, and nonconjugated polymers with side-chain photoactive groups that can generate light.[22-25] Figure 1.6 shows examples of emissive polymers. Apart from the emissive layer, polymers can also be used as electron- or hole-transport layers. Poly(p-phenylenevinylene)s, poly(thiophene)s, and oxadiazole containing polymers are widely used as electron-transport polymers.[9] On the other hand, poly(N-vinyl carbazole)s and polymers with triarylamines are the most common hole-transport polymers.[10]

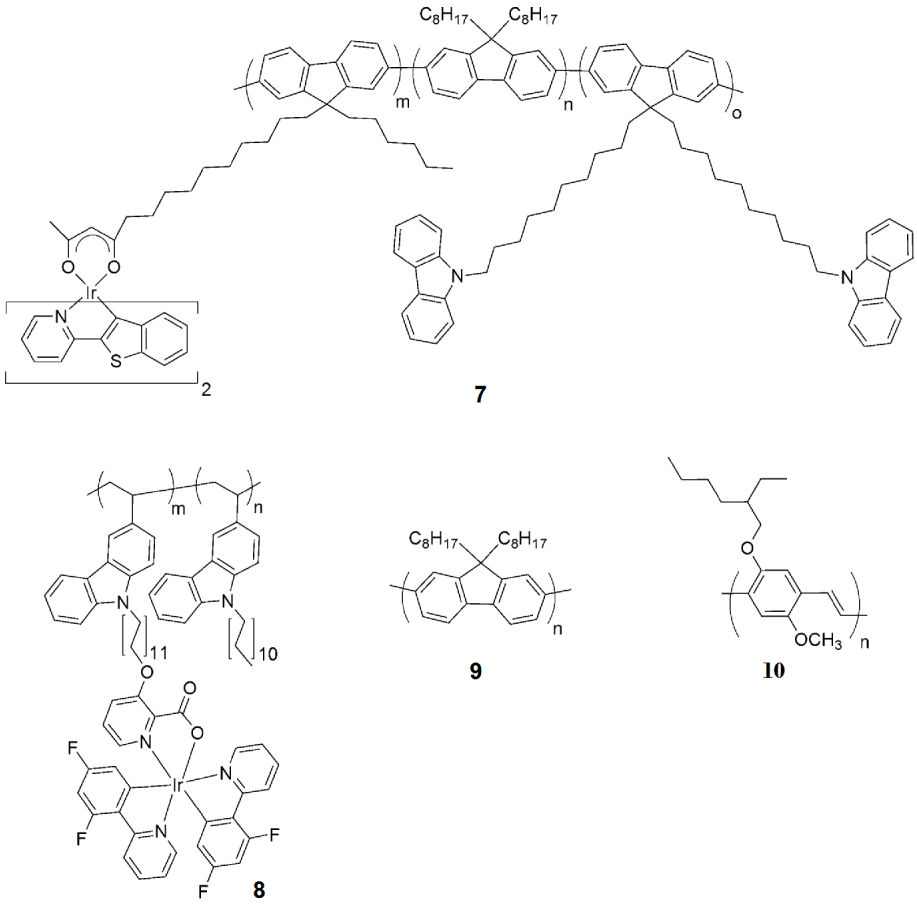

Figure 1.6 Examples of emissive polymers based on side-chain iridium complexes (**7** and **8**), poly(fluorene) (**9**), and poly(para-phenylene vinylene) (**10**).

Efficiencies of the devices with a polymeric emissive layer have been increasing steadily over the last ten years, although there is still need for significant improvements. The external quantum efficiencies of these devices are lower than 10% and the luminous efficiencies are around 5 cd/A (a more detailed discussion of device performances will be given in the next chapter). Although these efficiencies are lower than those of equivalent devices based on vacuum-deposited material, they demonstrate the promise that this new strategy holds for OLEDs. In the next chapter, employment of emissive metal complexes and their polymeric analogs in OLEDs is described, and strategies to enhance the performances of polymer-based OLEDs are discussed.

1.6 References

(1) Friend, R. H.; Gymer, R. W.; Holmes, A. B.; Burroughes, J. H.; Marks, R. N.; Taliani, C.; Bradley, D. D. C.; Dos Santos, D. A.; Brédas, J. L.; Logdlund, M.; Salaneck, W. R. Electroluminescence in Conjugated Polymers *Nature* **1999**, *397*, 121.

(2) Allen, K. J. Reel to Real: Prospects for Flexible Displays *Proc. IEEE* **2005**, *93*, 1394.

(3) Burrows, P. E.; Gu, G.; Bulovic, V.; Shen, Z.; Forrest, S. R.; Thompson, M. E. Achieving Full-Color Organic Light-Emitting Devices for Lightweight, Flat-Panel Displays *IEEE Trans. Electron Devices* **1997**, *44*, 1188.

(4) www.universaldisplay.com.

(5) Sheats, J. R.; Antoniadis, H.; Hueschen, M.; Leonard, W.; Miller, J.; Moon, R.; Roitman, D.; Stocking, A. Organic Electroluminescent Devices *Science* **1996**, *273*, 884.

(6) Bernius, M. T.; Inbasekaran, M.; O'Brien, J.; Wu, W. S. Progress with Light-Emitting Polymers *Adv. Mater.* **2000**, *12*, 1737.

(7) Tang, C. W.; Vanslyke, S. A. Organic Electroluminescent Diodes *Appl. Phys. Lett.* **1987**, *51*, 913.

(8) Yersin, H. Triplet Emitters for OLED Applications. Mechanisms of Exciton Trapping and Control of Emission Properties *Top. Curr. Chem.* **2004**, *241*, 1.

(9) Thelakkat, M.; Schmidt, H. W. Low Molecular Weight and Polymeric Heterocyclics as Electron Transport Hole-Blocking Materials in Organic Light-Emitting Diodes *Polym. Adv. Technol.* **1998**, *9*, 429.

(10) Thelakkat, M. Star-Shaped, Dendrimeric and Polymeric Triarylamines as Photoconductors and Hole Transport Materials for Electro-Optical Applications *Macromol. Mater. Eng.* **2002**, *287*, 442.

(11) Hung, L. S.; Chen, C. H. Recent Progress of Molecular Organic Electroluminescent Materials and Devices *Mater. Sci. Eng., R* **2002**, *39*, 143.

(12) Adachi, C.; Baldo, M. A.; Thompson, M. E.; Forrest, S. R. Nearly 100% Internal Phosphorescence Efficiency in an Organic Light-Emitting Device *J. Appl. Phys.* **2001**, *90*, 5048.

(13) Lower, S. K.; El-Sayed, M. A. The Triplet State and Molecular Electronic Processes in Organic Molecules *Chem. Rev.* **1966**, *66*, 199.

(14) Hercules, D. M. *Fluorescence and Phosphorescence Analysis: Principles and Applications*; Interscience Publishers: New York, 1966.

(15) Kasha, M. Characterization of Electronic Transitions in Complex Molecules *Discuss. Faraday Soc.* **1950**, *9*, 14.

(16) Adachi, C.; Baldo, M. A.; Forrest, S. R.; Lamansky, S.; Thompson, M. E.; Kwong, R. C. High-Efficiency Red Electrophosphorescence Devices *Appl. Phys. Lett.* **2001**, *78*, 1622.

(17) Ikai, M.; Tokito, S.; Sakamoto, Y.; Suzuki, T.; Taga, Y. Highly Efficient Phosphorescence from Organic Light-Emitting Devices with an Exciton-Block Layer *Appl. Phys. Lett.* **2001**, *79*, 156.

(18) Crosby, G. A.; Kasha, M. Intramolecular Energy Transfer in Ytterbium Organic Chelates *Spectrochim. Acta* **1958**, *10*, 377.

(19) Kido, J.; Okamoto, Y. Organo Lanthanide Metal Complexes for Electroluminescent Materials *Chem. Rev.* **2002**, *102*, 2357.

(20) Curry, R. J.; Gillin, W. P. Electroluminescence of Organolanthanide Based Organic Light Emitting Diodes *Curr. Opin. Solid State Mater. Sci.* **2001**, *5*, 481.

(21) Gong, J.-R.; Wan, L.-J.; Lei, S.-B.; Bai, C.-L.; Zhang, X.-H.; Lee, S.-T. Direct Evidence of Molecular Aggregation and Degradation Mechanism of Organic Light-Emitting Diodes under Joule Heating: an STM and Photoluminescence Study *J. Phys. Chem. B* **2005**, *109*, 1675.

(22) Bradley, D. D. C.; Grell, M.; Grice, A.; Tajbakhsh, A. R.; O'Brien, D. F.; Bleyer, A. Polymer Light Emission: Control of Properties through Chemical Structure and Morphology *Opt. Mater.* **1998**, *9*, 1.

(23) Bradley, D. D. C. Conjugated Polymer Electroluminescence *Synth. Met.* **1993**, *54*, 401.

(24) Greiner, A. Design and Synthesis of Polymers for Light-Emitting Diodes *Polym. Adv. Technol.* **1998**, *9*, 371.

(25) Kimyonok, A.; Wang, X. Y.; Weck, M. Electroluminescent Poly(quinoline)s and Metalloquinolates *Polym. Rev.* **2006**, *46*, 47.

(26) Scherf, U.; List, E. J. W. Semiconducting Polyfluorenes - Towards Reliable Structure-Property Relationships *Adv. Mater.* **2002**, *14*, 477.

CHAPTER 2

INTRODUCTION TO LUMINESCENT METAL COMPLEXES

2.1 Abstract

Employment of luminescent metal complexes as emissive layers in OLEDs is described with a focus on metalloquinolates and iridium complexes. Furthermore, literature reports on polymers with metalloquinolates and iridium complexes are reviewed, and strategies to optimize polymer structures are discussed.

2.2 Introduction

The focus of this thesis is the design and syntheses of polymers with side-chain emissive metal complexes for OLED applications. Additional photoactive groups such as hole-transport compounds are incorporated into the polymers along with the metal complexes in order to enhance the charge mobility, provide energy transfer into the metal complexes and to increase the solubility of the polymers. Three different types of metal complexes are used: Green-emitting fluorescent aluminum tris(8-hydroxyquinoline) (Alq_3), near IR-emitting ytterbium tris(8-hydroxyquinoline) (Ybq_3), and phosphorescent iridium complexes with emission spectra that span the whole visible spectrum. Although aluminum-based systems are significantly cheaper in comparison to the transition metal complexes, higher internal quantum efficiencies have been obtained for OLEDs with iridium complexes due to the intersystem crossing from the singlet to the triplet excited state as discussed in section 1.4. On the other hand, lanthanide complexes are appealing due to the possibility of fabricating near IR-emitting OLEDs. In this chapter the basic

photophysical properties of these complexes will be discussed, and the current literature that describes the polymeric versions of these complexes will be reviewed.

2.3 Metalloquinolates

Over the last two decades, metal-chelates of quinolines have been studied in detail as active compounds in OLED devices.[1,2] In particular, the use of 8-hydroxyquinoline as a ligand in coordination complexes for optical applications has been employed since the discovery of Alq_3 as an electron-transport and emitting layer.[3] Several reasons account for the popularity of metallated 8-hydroxyquinoline-based complexes. First, while the emission stems from the ligands, the type of metal plays an important role in determining the optical properties such as fluorescence quantum yield and excited state lifetimes.[4] Therefore, by simply changing the metal, one can tune the optical properties of the complexes. Second, the incorporation of electron-donating and -withdrawing groups on the ligands changes the electronic properties of the complex, which changes the optical properties, giving the scientist another handle to tune the optical properties. Finally, most metal-hydroxyquinoline complexes are octahedral (Figure 2.1). Since 8-hydroxyquinoline is an unsymmetrical ligand, two different isomers are possible for these metal chelates. In the facial isomer, the oxygen and nitrogen atoms are placed on the faces of the octahedron such that each oxygen atom has a nitrogen atom in the opposite position. In the meridianal isomer, only one oxygen atom is opposite to one of the nitrogens. The meridianal isomer belongs to the symmetry group C1, whereas the symmetry group of the facial isomer is C3. Because the two isomers have different symmetries, they also have two distinct optical properties.

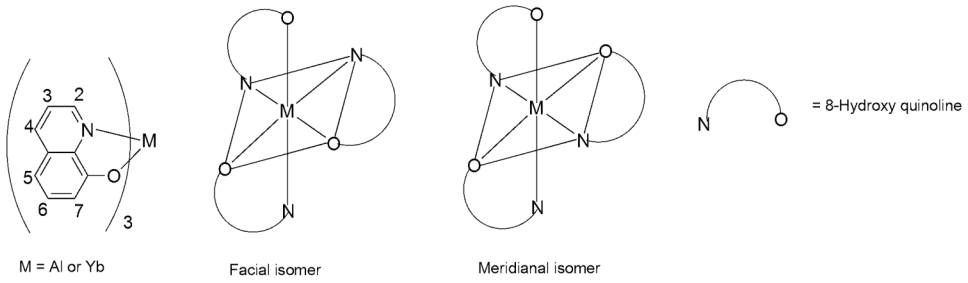

Figure 2.1 Numbering of the quinoline ligand and structures of the facial and the meridianal isomers.

Through simple variations of these parameters, the optical properties and ultimately the photo and electroluminescence of the OLED can be tuned towards more specific applications. Over the next pages, properties of aluminum and ytterbium hydroxyquinolates, and their status in device applications will be discussed.

2.3.1 Aluminum tris(8-hydroxyquinoline)

The vast majority of metal-quinolate complexes employ aluminum as the metal center. Most Alq_3-based systems only use the meridianal form. The first experimental evidence for the presence of *fac*-Alq_3 was reported recently, in 2001.[5] For both isomers, DFT and Ab Initio calculations revealed that the HOMOs are localized on the phenoxides, while the LUMOs are localized on the pyridyl ring.[6,7] It has been suggested that the injection of charges results in only small changes in both the bond lengths and the bond angles, indicating a high structural stability of the molecule.[6] The π-π stacking interactions are mainly due to a pyridyl/pyridyl ring overlap.[8] Since LUMOs are localized on pyridyl rings, overlap of pyridyl rings directly influences the electron mobility behavior of Alq_3.

As described earlier, π-π* transitions in Alq_3 are localized on the ligands, with the HOMOs located on the phenoxides, and the LUMOs on the pyridyl ring. These facts provide the opportunity to tune the emission wavelength by substituting electron-

donating or -withdrawing groups at the proper positions of the ligand.[1] However, it should be noted that substituents affect the intrinsic properties of the complexes, which in turn may affect the device performance. For example, substitution of fluorine at the C5 position resulted in a significant decrease in device performance with luminance only 10 % of analogous Alq_3-based devices.[9]

2.3.2 Polymers with Covalently Attached Alq_3

Covalent conjugation of the quinoline complex to a polymer backbone prevents phase separation, providing a homogeneous layer thereby increasing the charge mobility compared to doped systems. Covalent conjugation first appeared in the literature in 2000, and since then there have only been a limited number of reports in the literature. Three types of polymerization methods have been employed so far: step-growth polymerizations,[10] ring-opening metathesis polymerizations (ROMP),[11-13] and radical polymerizations.[14-19] Examples of the polymers are displayed in Figure 2.2.

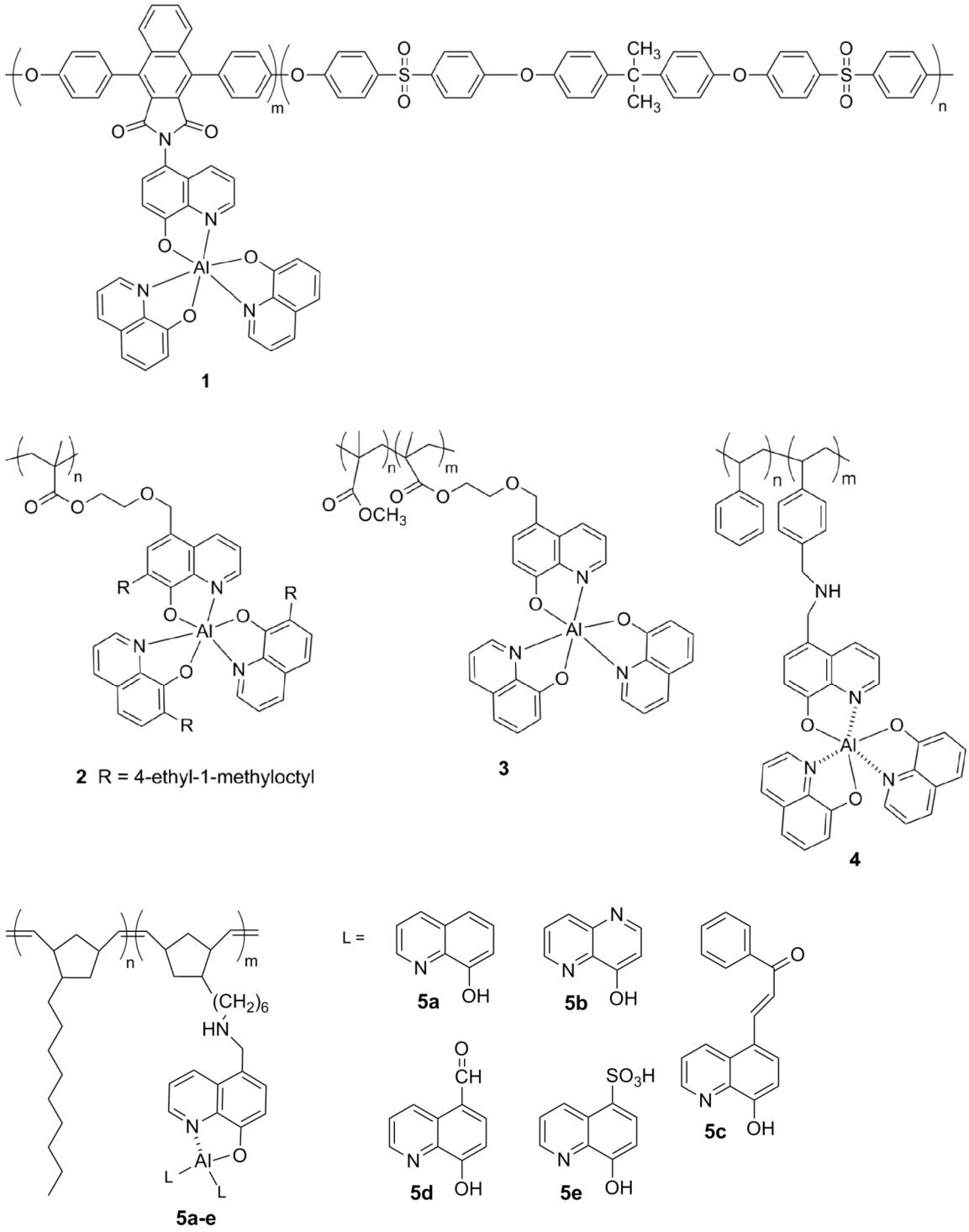

Figure 2.2 Polymers with pendant metal-quinolate complexes.

The first example of a metal quinolate containing polymer is **1**, which is a rigid polymer with a glass-transition temperature of 203 ^{o}C.[10] In this system, Alq_3 was complexed in a post polymerization reaction. The Alq_3 content in the polymer was 11 mol %. Increasing the Alq_3 content further resulted in cross-linking and decreased solubility of the polymer.

The Weck group reported the first synthesis of fully metal-complex functionalized monomers that could be polymerized in a controlled fashion. This strategy minimized the cross-linking, allowed for the controlled formation of copolymers, and ensured full metallation of each hydroxyquinoline moiety.[11] The metal containing monomers were copolymerized with a norbornene monomer containing a pendant alkyl chain to increase solubility (Figure 2.2, polymers **5a**-**e**). Using this approach, the Alq_3 content in the polymer could be increased to 20%.[11] Similar to small molecule chelates, changes in the emission color of the polymers can be obtained by simple ligand substitution (Figure 2.2). As expected, electron-withdrawing groups on the phenoxide ring resulted in a blue shift while increased conjugation of the ligand in **5c** caused a red shift.[13] These effects were observed in solution as well as the solid state (all polymers were solution processable). The same trend was observed when the metal was changed from aluminum to zinc.[12] From these studies we were able to conclude that these polymers retained the photoluminescent properties of the metalloquinolate moiety while gaining the added advantage of being solution processable.

Another class of polymers that can provide good processability are poly(styrene)s. Polymer **4** is a system that contains styrene with functional handles randomly dispersed throughout a poly(styrene) copolymer synthesized via a free radical polymerization followed by the attachment of the hydroxyquinoline (Figure 2.2).[17] Thus, this approach provides a modular backbone for the design of polymer-based metalloquinolates through the complexation of a variety of metals. It was demonstrated that different metals such as aluminum and boron can be introduced to obtain complexes with tunable polymer and

optical properties. The quantum yield of polymer **4** was approximately half of the small molecule Alq_3.[17]

The last polymer that has been functionalized with metal quinolate complexes is PMMA. Contrary to the other systems discussed above, PMMA-based systems have been studied in OLEDs, however, device performances are not promising. Polymer **2** was the first example of a soluble homopolymer having a pendant Alq_3-type complex.[15] The electroluminescence spectrum of **2** showed an emission maximum at 540 nm. This slight red shift was attributed to the presence of the alkyl chain. Polymer **2** was employed as the emission layer in an OLED. The turn-on voltage of the device was 10 V. At around 20 V, the current density was close to 40 mA/cm^2, and luminance was approximately 30 cd/m^2.[15]

The final example of PMMA-based materials is polymer **3** (Figure 2.2).[16] This polymer was prepared by free radical polymerization. The performance of the device made of the crosslinked polymer with aluminum as the metal was very low with an external quantum efficiency of only 0.1%.[20]

The covalent conjugation of Alq_3 to polymer backbones is a very nascent area of research. The first challenge to overcome is the low concentration of complex in the polymers. Nevertheless, increased concentration of the complex and a more thorough examination of this new class of polymers in OLEDs may render this approach superior to the small molecule metal chelates and doped systems

2.3.3 Ytterbium tris(8-hydroxyquinoline)

Current research on OLEDs is focused on the luminescent materials with emission in the visible region. Little attention has been given to the organic materials that emit light in the infrared region. Infrared-emitting materials can be employed in electronic devices, such as organic light-emitting diodes,[21-27] and in photonic

communication networks, especially silica optical fibers.[28-30] Optical fibers based on infrared-emitting materials are potentially useful for high speed data transmission by confining light in a region of high refractive index between regions of low refractive index.[30] Near Infrared region is the optimum wavelength region for light traveling through the optical fibers due to the minimum transmission loss in this region.[30,31]

As discussed in Chapter 1, the design of lanthanide-based infrared emitters includes ligands with energy levels that overlap the energy levels of the lanthanide metal in order for the energy transfer to occur. A wide variety of ligands have been coordinated to different lanthanide metals in order to optimize the energy transfer.[25-28,30,32,33] One ligand that has been used frequently in these studies is 8-hydroxyquinoline.[21,23,28,31,32,34] Lanthanide quinolate complexes have been sublimed into thin films and doped into polymer matrices, producing emission in near infrared region.[32]

There have been only a few studies on ytterbium tris(8-hydroxyquinoline), which has an emission maximum of 980 nm.[35-38] Unfortunately, like the other lanthanide quinolate complexes, OLEDs based on Ybq_3 gave poor device performances.[35] A major problem with these complexes is the concentration quenching that significantly decreases the internal quantum efficiencies of the devices.[25,27] Attaching these complexes to polymer backbones along with comonomers that might function as spacers between the complexes can result in the isolation of the complexes from each other, which in turn might prevent the concentration quenching. There has been no report in the literature on Ybq_3 (or other lanthanide quinolate complex) functionalized polymers.

2.4 Iridium Complexes

Phosphorescent metal complexes are at the center of intense research for organic light emitting diodes.[39-43] Strong spin-orbit coupling in these complexes induces the intersystem crossing from the singlet to the triplet excited state, leading to highly efficient

phosphorescence. Indeed, nearly 100% internal quantum efficiency has been obtained for OLEDs based on transition metal complexes.[44-46] Due to the heavy atom effect on the spin-orbit coupling, complexes containing third-row transition metals have been widely used in OLEDs.[39-43] Of these, iridium complexes exhibit the most promising properties in terms of device performance.[44-52] Octahedral cyclometalated iridium complexes spanning the whole visible spectrum have been synthesized and employed in OLEDs with high external quantum efficiencies.

There are two possible isomers for octahedral iridium complexes: Facial and meridianal (Figure 2.3). Phosphorescence quantum yields of the facial isomers are much higher (usually an order of magnitude higher) than the meriadanal isomers.[52] Therefore, synthesis of isomerically pure complexes is crucial in order to obtain good device performance. Procedures for the selective synthesis of the facial isomer and thermally-induced conversion of the meriadanal isomer to the facial isomer are well established in the literature.[47,48,50,52,53]

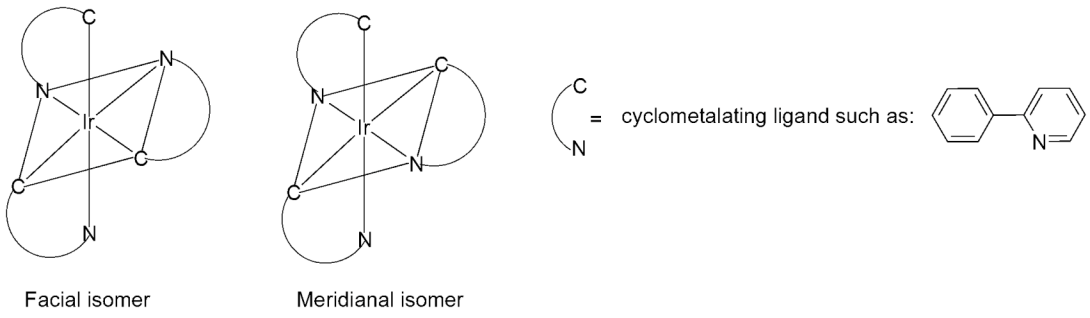

Figure 2.3 Structures of the facial and meridianal isomers of the octahedral iridium complexes

In a typical absorption spectrum of a cyclometalated iridium complex, ligand-centered π-π^* transitions are observed in the high-energy region.[47] In the low-energy region, starting from 350 nm, metal to ligand charge transfer (MLCT) transitions are observed.[47] Strong spin-orbit coupling of the iridium complexes can be observed in the

absorption spectra of the complexes. Both ^{1}MLCT and ^{3}MLCT bands are detected for these complexes.[48] Comparable extinction coefficiencies of ^{3}MLCT bands to spin-allowed ^{1}MLCT bands indicate efficient mixing of singlet and triplet excited states due to the strong spin-orbit coupling. The emission spectra of the complexes with similar absorption spectra can be significantly different due to the relative positions of $^3(\pi\text{-}\pi^*)$ and ^{3}MLCT levels.[48] In general, small Stokes shifts between the absorption and emission bands are observed when the lowest excited state is ^{3}MLCT state. On the other hand, when the lowest excited state is $^3(\pi\text{-}\pi^*)$, large Stokes shifts are observed.[48] Furthermore, in general, emission bands from ^{3}MLCT state are broad and featureless, whereas emission bands from $^3(\pi\text{-}\pi^*)$ states are structured.[54]

It is well-known that the emission spectra of iridium complexes can be tuned by the employment of electron–donating and –withdrawing groups on the ligands of the metal complex or by changing the ligand conjugation length (Figure 2.4). Table 2.1 lists the basic photophysical properties of some of the iridium complexes with different emission colors. Electron-withdrawing fluorine groups on the phenyl ring of $Ir(ppf)_3$ shift the emission towards the blue compared to the parent complex due to the stabilization of HOMO.[52] On the other hand, increased conjugation of $Ir(pq)_3$ leads to a red shift in the emission compared to $Ir(ppy)_3$.[47,48] Another strategy to change the emission maxima of the complexes involves the employment of heteroatoms in the conjugated ring. For example, as in the case of $Ir(btpy)_3$, high polarizibility and basicity of the sulfur can contribute to a red shift in the emission, due to the destabilization of HOMO.[48,50]

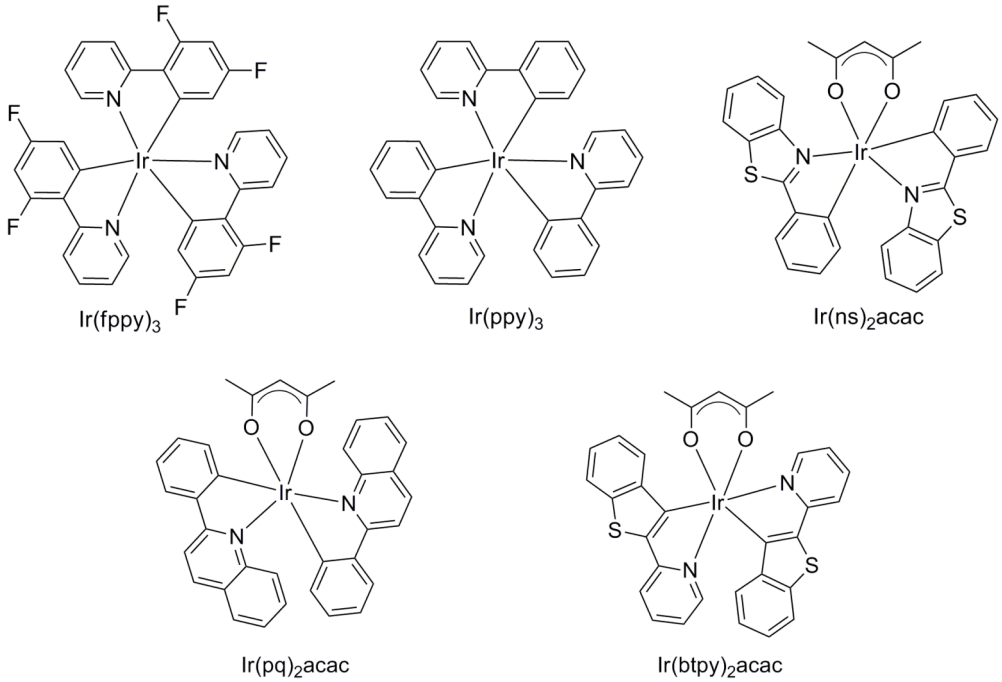

Figure 2.4 Examples of phosphorescent iridium complexes

Table 2.1 Basic photophysical properties of common iridium complexes

Compound	λ_{em} (nm)[a]	Φ[b]	τ (μs)[c]
Ir(fppy)$_3$	468	0.43	1.60
Ir(ppy)$_3$	510	0.40	1.90
Ir(ns)$_2$acac	557	0.26	1.80
Ir(pq)$_2$acac	597	0.10	2.0
Ir(btpy)$_2$acac	612	0.21	5.8

[a]In solution. [b]PL quantum yield in degassed solution. [c]Luminescence lifetime in degassed solution.

2.4.1 Polymers with Covalently Attached Iridium Complexes

There have been two different classes of polymer backbones employed for iridium attachment: Conjugated and nonconjugated backbones. For nonconjugated polymeric systems, iridium complexes are incorporated into the polymers as side-chains with spacers linking the complexes to the polymers. For conjugated systems, two different routes have been employed: side-chain functionalization and placing the complex in the main-chain. Figure 2.5 shows examples of polymers with iridium complexes in the main-chain.[55,56] Polymers **6** and **7** are synthesized via Suzuki coupling reactions. Emission spectrum of **6** is strongly dependent on the chain length. For oligomers (n = 1-3), concentration quenching is observed in neat films due to high contents of the iridium complex. For polymers (n = 15 or 30), even though strong emission of the metal complex is observed in the electroluminescence spectra, a weak fluorene emission is also detected. Furthermore, increased conjugation of the fluorene groups led to a decrease in the triplet energy of poly(fluorene), resulting in an efficiency decline for the metal complex emission due to triplet energy transfer onto fluorene segments.[55] No device performance was reported for polymer **6**. On the other hand, even though not comparable to small molecule-based analogues, OLEDs based on polymer **7** gave good promising performances.[56] All polymers (iridium complex content ranging between 0.4 and 4.2 mol%, molecular weights 20-30 kDa) exhibited EL emission only from the red-emitting metal complex. The best performance was observed for the polymer with 1 mol% iridium complex loading with an external quantum efficiency of 6.5% and luminous efficiency of 2.5 cd/A at the current density of 38 mA/cm^2 and operating voltage of 15.1 V. At 100 mA/cm^2, the efficiency is 5.3%.[56] Careful selection of the metal complex and the polymer length is crucial for the polymers with the complex in the main chain in order to prevent energy transfer from the complex to the triplet level of poly(fluorene) chain. The best results are obtained for red-emitting complexes.

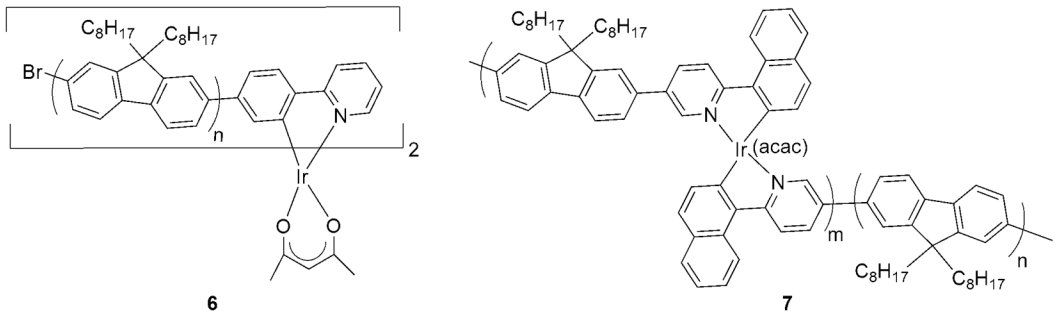

Figure 2.5 Examples of polymers with iridium complexes in the main chain

The most common method for the synthesis of the iridium containing polymers is the attachment of the complex to the polymer through a spacer. Polymers **8** and **9** are examples of side-chain functionalized poly(fluorene)s.[57,58] For polymer **8**, carbazole groups are employed as hole-transport groups along with the emissive iridium complex. Devices with carbazole groups on the polymer gave higher efficiencies and lower turn-on voltages compared to the devices without carbazole groups (k = 0), which demonstrates the ability of multi-functional polymers to combine the properties of different functional units. The best device (polymer properties: m:n:k = 1.3:0:98.7, Mw = 154 kDa, PDI = 2.73, see Figure 2.6) has an EQE of 1.59 and luminous efficiency of 2.8 cd/A at 7V and 65 cd/m^2.[57] A similar polymer, **9**, was used to study the effect of the spacer on the emission properties.[58] Higher PL and EL efficiencies are observed for the polymers with a longer spacer (k = 9) compared to the polymers with a short spacer (k = 1), which is attributed to inhibition of the triplet energy back transfer from the iridium complex to the poly(fluorene) backbone.[58] Increased efficiency upon spatial separation of the complex from the backbone suggests that the covalent linkage of the complex through a spacer is a more promising design strategy than the conjugative linkage of the complex (as in polymer **6**). No detailed device performance was reported for polymer **9**.

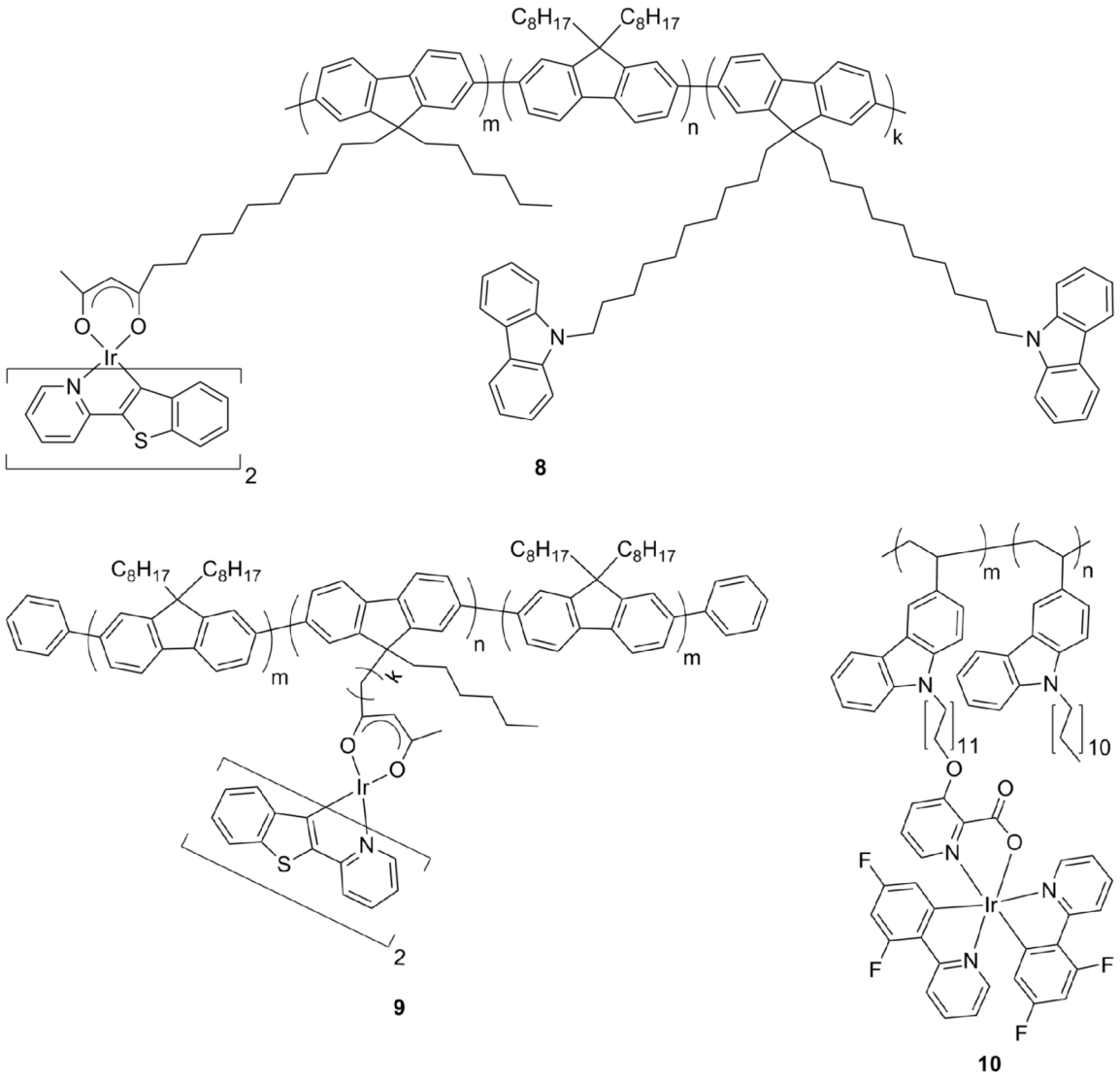

Figure 2.6 Examples of side-chain functionalized polymers

Another strategy for side-chain functionalized polymers is the employment of nonconjugated backbones as supports for the iridium complexes. As discussed above, energy transfer from the backbone to the complex and the triplet energy back transfer from the complex to the backbone are important factors for conjugated polymer based systems. In general, red-emitting complexes are employed in order to have an efficient energy transfer from the blue-emitting poly(fluorene) backbone. Furthermore, triplet levels of red-emitting complexes are lower than the triplet levels of poly(fluorene)s,

making the triplet energy back transfer less probable. It is clear that both the backbone and the complex should be carefully chosen in order to have a good device performance. On the other hand, nonconjugated polymers are not involved in the energy transfer process. Although they affect the charge mobility, their most important function is to provide processability for device fabrication. Polymer **10** is an example of a nonconjugated backbone with a blue-emitting iridium complex as the side-chain.[59] The polymers are synthesized by free radical polymerization. Carbazole groups are used to provide energy transfer into the complex. The best device (polymer properties: m:n = 1:5.7, Mw = 45 kDa, PDI = 2.38) has an EQE less than 1%, and a luminous efficiency of 2.23 cd/A at 10 mA/cm^2.[59]

The Weck group has reported poly(styrene)[60] and poly(norbornene)[61] based iridium complex containing polymers (Figure 2.7). Poly(styrene) is a commodity polymer that is industrially appealing while poly(norbornene)s can be prepared in a controlled fashion, allowing for easy modification of the polymer properties. A more detailed discussion of these polymer backbones will be provided in the proceeding chapters. Polymer **11-13** contain *fac*-Ir(ppy)$_3$, the most widely used iridium complex in OLEDs. On the other hand, polymer **14** contains a cationic iridium complex. These kind of charged complexes are used in light-emitting electrochemical cells (LECs). All four polymers contain comonomers to increase the solubility of the polymers and to decrease the chromophore density on the polymer to prevent concentration quenching. In addition, carbazole groups in polymer **12** can enhance the charge mobility and provide energy transfer into the complex.[60] In all cases, the photophysical properties of the polymers were comparable to the corresponding small molecule analogs.[60,61]

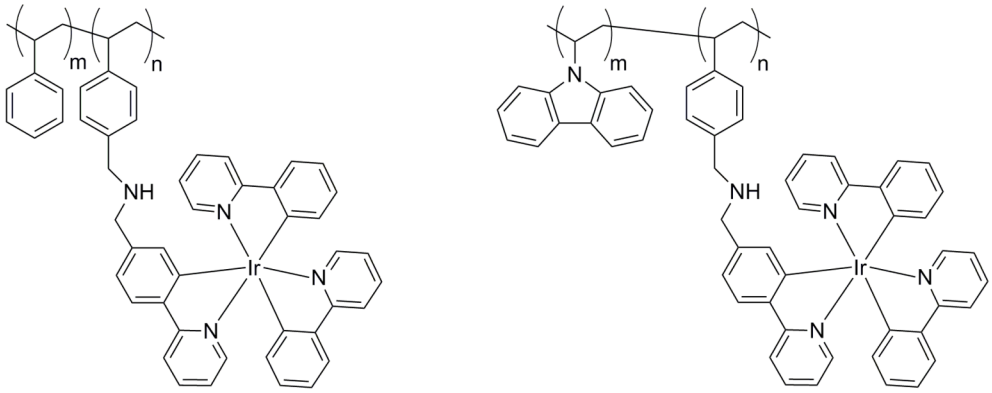

11 12

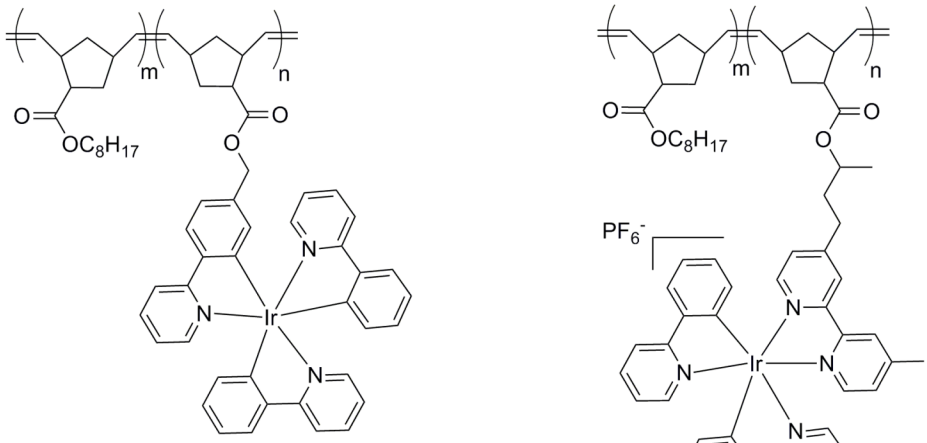

13 14

Figure 2.7 Poly(styrene)s and poly(norbornene)s with iridium complexes

In the examples discussed above, emission stems from the iridium complex and the polymers are used to obtain a single color. On the other hand, white emission is obtained for polymer **15**, which contains a poly(fluorene) backbone for blue emission, a benzothiadiazole type comonomer for green light emission and a side-chain iridium complex for orange light emission.[62] The combination of the emissions from different parts of the polymer resulted in white light with high purity. The best device (m = 0.05 mol%, n = 0.2 mol%, see Figure 2.8) has a maximum luminance efficiency of 6.1 cd/A at 2.2 mA/cm^2.

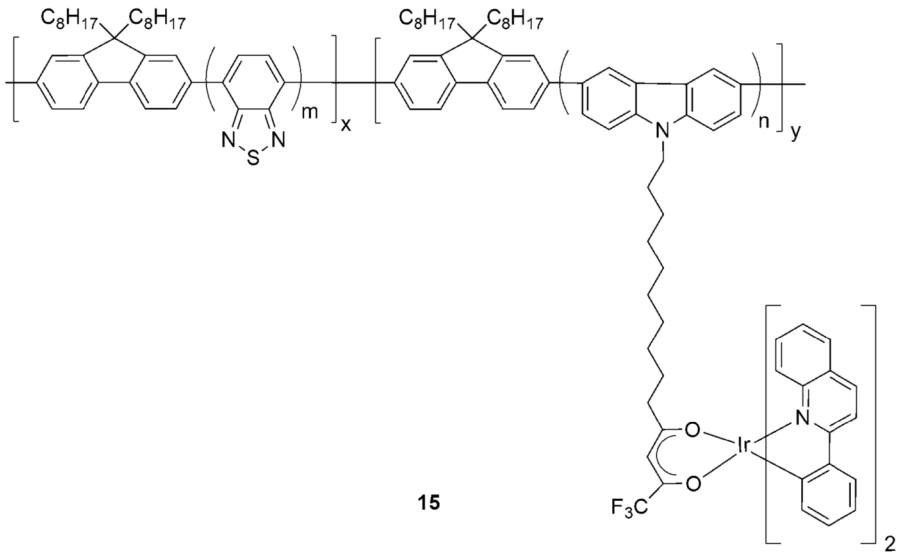

Figure 2.8 Example of a white-emitting polymer

2.5 Design Principles

This thesis aims to provide a detailed understanding of side-chain functionalized polymers as emissive materials for OLEDs. The proceeding chapters will discuss the syntheses and photophysical properties of these solution-processable materials as well as the effects of metal types, polymer backbones, chain lengths, spacer types and lengths, host types, and concentrations of the metal complexes on the emission properties and device performance.

Ring-opening metathesis polymerization (ROMP) is chosen as the polymerization method due to its high tolerance to a wide variety of functional groups. Furthermore, considering that it allows for a high degree of control over molecular weights, ROMP is an ideal polymerization method to study the effect of molecular weight on device performance. The two main classes of the polymer backbones that will be described in the following chapters are poly(cyclooctene)s and poly(norbornene)s. These two backbones have different physical properties, i.e. different glass transition temperatures,

therefore, device performances might be affected by the polymer backbone due to the differences in the processability of the polymers.

Four different metals are studied: Aluminum, ytterbium, iridium and platinum. Chapter 3 describes the syntheses and characterization of 8-hydroxyquinoline functionalized poly(cyclooctene)s. It will be demonstrated that it is possible to tune the emission properties of the polymers by simply changing the metal from aluminum to ytterbium. Furthermore, it will be shown that the host material on the polymers is capable of transferring the absorbed photoexcitation energy into the metal complex.

Chapter 4 describes the ring-opening metathesis polymerization studies of norbornene-based monomers with platinum complexes. In this chapter, the effect of the ligand type on the polymerization behavior of the monomers will be discussed. The rest of the thesis, Chapters 5-8, is focused on the polymers with side-chain iridium complexes. Chapter 5 depicts a system based on poly(cyclooctene)s with side-chain host material and $Ir(ppy)_3$, the most widely employed iridium complex in OLEDs. As in Chapter 3, the interaction between the host and the metal complex in terms of energy transfer will be determined, and it will be shown that the polymer backbone does not interfere with the photophysical properties of the complex.

The majority of the thesis is centered on the fully functionalized monomers that are copolymerized with host materials to obtain a controlled and quantitative metal complex functionalization on the polymer. Another strategy is the modification of polymers with the metal complex in a post polymerization reaction, allowing for attachment of a library of metal complexes onto the polymer backbone. In Chapter 6, it will be shown that polymers with side-chain azide groups can be quantitatively functionalized with metal complexes by taking advantage of the 1,3-dipolar cycloaddition reactions.

The emission properties of the iridium complexes can be tuned by changing the ligands. In Chapter 7, the synthesis of random copolymers containing host moieties and

various iridium complexes in the side-chains that emit in various regions of the visible spectrum, and their photoluminescence and solid-state electroluminescence properties are described. In Chapter 8, one of the polymers discussed in Chapter 7 is used as the model system to study polymer structure-device performance relationships in order to develop general principles that can be used to optimize iridium-containing polymers for OLED applications. It will be shown that the device performance is dependent on various parameters such as molecular weight, iridium loading, spacer type, and spacer length. Finally, in Chapter 9, the final chapter of the thesis, the main findings are summarized and ideas to further optimize the polymer structure are presented.

2.6 References

(1) Chen, C. H.; Shi, J. M. Metal Chelates as Emitting Materials for Organic Electroluminescence *Coord. Chem. Rev.* **1998**, *171*, 161.

(2) Kulkarni, A. P.; Tonzola, C. J.; Babel, A.; Jenekhe, S. A. Electron Transport Materials for Organic Light-Emitting Diodes *Chem. Mater.* **2004**, *16*, 4556.

(3) Tang, C. W.; Vanslyke, S. A. Organic Electroluminescent Diodes *Appl. Phys. Lett.* **1987**, *51*, 913.

(4) Lytle, F. E.; Storey, D. R.; Juricich, M. E. Systematic Atomic Number Effects in Complexes Exhibiting Ligand Luminescence *Spectrochim. Acta, Part A* **1973**, *A 29*, 1357.

(5) Braun, M.; Gmeiner, J.; Tzolov, M.; Coelle, M.; Meyer, F. D.; Milius, W.; Hillebrecht, H.; Wendland, O.; von Schutz, J. U.; Brutting, W. A New Crystalline Phase of the Electroluminescent Material Tris(8-Hydroxyquinoline) Aluminum Exhibiting Blueshifted Fluorescence *J. Chem. Phys.* **2001**, *114*, 9625.

(6) Curioni, A.; Boero, M.; Andreoni, W. Alq_3: Ab Initio Calculations of Its Structural and Electronic Properties in Neutral and Charged States *Chem. Phys. Lett.* **1998**, *294*, 263.

(7) Martin, R. L.; Kress, J. D.; Campbell, I. H.; Smith, D. L. Molecular and Solid-State Properties of Tris-(8-Hydroxyquinolate)-Aluminum *Phys. Rev. B* **2000**, *61*, 15804.

(8) Brinkmann, M.; Gadret, G.; Muccini, M.; Taliani, C.; Masciocchi, N.; Sironi, A. Correlation between Molecular Packing and Optical Properties in Different Crystalline Polymorphs and Amorphous Thin Films of *mer*-Tris(8-Hydroxyquinoline)Aluminum(III) *J. Am. Chem. Soc.* **2000**, *122*, 5147.

(9) Matsumura, M.; Akai, T. Organic Electroluminescent Devices Having Derivatives of Aluminium-Hydroxyquinoline Complex as Light Emitting Materials *Jpn. J. Appl. Phys., Part 1* **1996**, *35*, 5357.

(10) Lu, J. P.; Hlil, A. R.; Meng, Y. Z.; Hay, A. S.; Tao, Y.; D'Iorio, M.; Maindron, T.; Dodelet, J. P. Synthesis and Characterization of a Novel Alq_3-Containing Polymer *J. Polym. Sci., Part A: Polym. Chem.* **2000**, *38*, 2887.

(11) Meyers, A.; Weck, M. Design and Synthesis of Alq_3-Functionalized Polymers *Macromolecules* **2003**, *36*, 1766.

(12) Meyers, A.; South, C.; Weck, M. Design, Synthesis, Characterization and Fluorescent Studies of the First Zinc-Quinolate Polymer *Chem. Commun.* **2004**, 1176.

(13) Meyers, A.; Weck, M. Solution and Solid-State Characterization of Alq_3-Functionalized Polymers *Chem. Mater.* **2004**, *16*, 1183.

(14) Qin, Y.; Pagba, C.; Piotrowiak, P.; Jakle, F. Luminescent Organoboron Quinolate Polymers *J. Am. Chem. Soc.* **2004**, *126*, 7015.

(15) Takayama, T.; Kitamura, M.; Kobayashi, Y.; Arakawa, Y.; Kudo, K. Soluble Polymer Complexes Having Alq_3-Type Pendent Groups *Macromol. Rapid Commun.* **2004**, *25*, 1171.

(16) Du, N. Y.; Tian, R. Y.; Peng, J. B.; Lu, M. G. Synthesis and Photophysical Characterization of the Free-Radical Copolymerization of Metaloquinolate-Pendant Monomers with Methyl Methacrylate *J. Polym. Sci., Part A: Polym. Chem.* **2005**, *43*, 397.

(17) Wang, X. Y.; Weck, M. Poly(styrene)-Supported Alq_3 and Bph_2q *Macromolecules* **2005**, *38*, 7219.

(18) Mei, Q. B.; Du, N. Y.; Lu, M. G. Synthesis, Characterization and Thermal Properties of Metaloquinolate-Containing Polymers *Eur. Polym. J.* **2007**, *43*, 2380.

(19) Du, N. Y.; Tian, R. Y.; Peng, J. B.; Mei, Q. B.; Lu, M. G. Cross-Linked Alq_3-Containing Polymers with Improved Electroluminescence Efficiency Used for OLEDs *Macromol. Rapid Commun.* **2006**, *27*, 412.

(20) Du, N. Y.; Mei, Q. B.; Lu, M. G. Quinolinate Aluminum and Zinc Complexes with Multi-Methyl Methacrylate End Groups: Synthesis, Photoluminescence, and Electroluminescence Characterization *Synth. Met.* **2005**, *149*, 193.

(21) Khreis, O. M.; Curry, R. J.; Somerton, M.; Gillin, W. P. Infrared Organic Light Emitting Diodes Using Neodymium Tris-(8-Hydroxyquinoline) *J. Appl. Phys.* **2000**, *88*, 777.

(22) Gillin, W. P.; Curry, R. J. Erbium (III) Tris(8-Hydroxyquinoline) (Erq): A Potential Material for Silicon Compatible 1.5 μm Emitters *Appl. Phys. Lett.* **1999**, *74*, 798.

(23) Curry, R. J.; Gillin, W. P. 1.54 μm Electroluminescence from Erbium (III) Tris(8-Hydroxyquinoline) (Erq)-Based Organic Light-Emitting Diodes *Appl. Phys. Lett.* **1999**, *75*, 1380.

(24) Hong, Z. R.; Liang, C. J.; Li, R. G.; Zhao, D.; Fan, D.; Li, W. L. Infrared Electroluminescence of Ytterbium Complexes in Organic Light Emitting Diodes *Thin Solid Films* **2001**, *391*, 122.

(25) Sun, R. G.; Wang, Y. Z.; Zheng, Q. B.; Zhang, H. J.; Epstein, A. J. 1.54 μm Infrared Photoluminescence and Electroluminescence from an Erbium Organic Compound *J. Appl. Phys.* **2000**, *87*, 7589.

(26) Kawamura, Y.; Wada, Y.; Yanagida, S. Near-Infrared Photoluminescence and Electroluminescence of Neodymium(III), Erbium(III), and Ytterbium(III) Complexes *Jpn. J. Appl. Phys.* **2001**, *40*, 350.

(27) Slooff, L. H.; Polman, A.; Cacialli, F.; Friend, R. H.; Hebbink, G. A.; van Veggel, F. C. J. M.; Reinhoudt, D. N. Near-Infrared Electroluminescence of Polymer Light-Emitting Diodes Doped with a Lissamine-Sensitized Nd^{3+} Complex *Appl. Phys. Lett.* **2001**, *78*, 2122.

(28) Suzuki, H.; Hattori, Y.; Iizuka, T.; Yuzawa, K.; Matsumoto, N. Organic Infrared Optical Materials and Devices Based on an Organic Rare Earth Complex *Thin Solid Films* **2003**, *438*, 288.

(29) Desurvire, E. The Golden-Age of Optical-Fiber Amplifiers *Phys. Today* **1994**, *47*, 20.

(30) Pitois, C.; Vestberg, R.; Rodlert, M.; Malmstrom, E.; Hult, A.; Lindgren, M. Fluorinated Dendritic Polymers and Dendrimers for Waveguide Applications *Opt. Mater.* **2003**, *21*, 499.

(31) Curry, R. J.; Gillin, W. P. Infra-Red and Visible Electroluminescence from Erq Based OLEDs *Synth. Met.* **2000**, *111*, 35.

(32) Curry, R. J.; Gillin, W. P. Electroluminescence of Organolanthanide Based Organic Light Emitting Diodes *Curr. Opin. Solid State Mater. Sci.* **2001**, *5*, 481.

(33) Harrison, B. S.; Foley, T. J.; Knefely, A. S.; Mwaura, J. K.; Cunningham, G. B.; Kang, T. S.; Bouguettaya, M.; Boncella, J. M.; Reynolds, J. R.; Schanze, K. S. Near-Infrared Photo- and Electroluminescence of Alkoxy-Substituted Poly(p-phenylene) and Nonconjugated Polymer/Lanthanide Tetraphenylporphyrin Blends *Chem. Mater.* **2004**, *16*, 2938.

(34) Iwamuro, M.; Adachi, T.; Wada, Y.; Kitamura, T.; Nakashima, N.; Yanagida, S. Photosensitized Luminescence of Neodymium(III) Coordinated with 8-Quinolinolates in DMSO-D_6 *Bull. Chem. Soc. Jpn.* **2000**, *73*, 1359.

(35) Khreis, O. M., Gillin, W. P.; Somerton, M.; Curry, R. J. *Org. Electron.* **2001**, *2*, 45.

(36) Comby, S.; Imbert, D.; Vandevyver, C.; Bunzli, J. C. G. A Novel Strategy for the Design of 8-Hydroxyquinolinate-Based Lanthanide Bioprobes that Emit in the near Infrared Range *Chem. Eur. J.* **2007**, *13*, 936.

(37) Thompson, J.; Blyth, R. I. R.; Gigli, G.; Cingolani, R. Obtaining Characteristic 4f-4f Luminescence from Rare Earth Organic Chelates *Adv. Funct. Mater.* **2004**, *14*, 979.

(38) Thompson, J.; Blyth, R. I. R.; Arima, V.; Zou, Y.; Fink, R.; Umbach, E.; Gigli, G.; Cingolani, R. 4f Energies in an Organic-Rare Earth Guest-Host System: The Rare Earth Tris-8-Hydroxyquinolines *Mater. Sci. Eng.* **2003**, *B105*, 41.

(39) Friend, R. H.; Gymer, R. W.; Holmes, A. B.; Burroughes, J. H.; Marks, R. N.; Taliani, C.; Bradley, D. D. C.; Dos Santos, D. A.; Brédas, J. L.; Logdlund, M.; Salaneck, W. R. Electroluminescence in Conjugated Polymers *Nature* **1999**, *397*, 121.

(40) Köhler, A.; Wilson, J. S.; Friend, R. H. Fluorescence and Phosphorescence in Organic Materials *Adv. Mater.* **2002**, *14*, 701.

(41) Yersin, H. Triplet Emitters for OLED Applications. Mechanisms of Exciton Trapping and Control of Emission Properties *Top. Curr. Chem.* **2004**, *241*, 1.

(42) Holder, E.; Langeveld, B. M. W.; Schubert, U. S. New Trends in the Use of Transition Metal-Ligand Complexes for Applications in Electroluminescent Devices *Adv. Mater.* **2005**, *17*, 1109.

(43) Lowry, M. S.; Bernhard, S. Synthetically Tailored Excited States: Phosphorescent, Cyclometalated Iridium(III) Complexes and Their Applications *Chem. Eur. J.* **2006**, *12*, 7970.

(44) Adachi, C.; Baldo, M. A.; Forrest, S. R.; Thompson, M. E. High-Efficiency Organic Electrophosphorescent Devices with Tris(2-phenylpyridine)iridium Doped into Electron-Transporting Materials *Appl. Phys. Lett.* **2000**, *77*, 904.

(45) Adachi, C.; Baldo, M. A.; Thompson, M. E.; Forrest, S. R. Nearly 100% Internal Phosphorescence Efficiency in an Organic Light-Emitting Device *J. Appl. Phys.* **2001**, *90*, 5048.

(46) Kawamura, Y.; Brooks, J.; Brown, J. J.; Sasabe, H.; Adachi, C. Intermolecular Interaction and a Concentration-Quenching Mechanism of Phosphorescent Ir(III) Complexes in a Solid Film *Phys. Rev. Lett.* **2006**, *96*.

(47) Lamansky, S.; Djurovich, P.; Murphy, D.; Abdel-Razzaq, F.; Kwong, R.; Tsyba, I.; Bortz, M.; Mui, B.; Bau, R.; Thompson, M. E. Synthesis and Characterization of Phosphorescent Cyclometalated Iridium Complexes *Inorg. Chem.* **2001**, *40*, 1704.

(48) Lamansky, S.; Djurovich, P.; Murphy, D.; Abdel-Razzaq, F.; Lee, H. E.; Adachi, C.; Burrows, P. E.; Forrest, S. R.; Thompson, M. E. Highly Phosphorescent Bis-Cyclometalated Iridium Complexes: Synthesis, Photophysical Characterization, and Use in Organic Light Emitting Diodes *J. Am. Chem. Soc.* **2001**, *123*, 4304.

(49) Adachi, C.; Baldo, M. A.; Forrest, S. R.; Lamansky, S.; Thompson, M. E.; Kwong, R. C. High-Efficiency Red Electrophosphorescence Devices *Appl. Phys. Lett.* **2001**, *78*, 1622.

(50) Tsuboyama, A.; Iwawaki, H.; Furugori, M.; Mukaide, T.; Kamatani, J.; Igawa, S.; Moriyama, T.; Miura, S.; Takiguchi, T.; Okada, S.; Hoshino, M.; Ueno, K. Homoleptic Cyclometalated Iridium Complexes with Highly Efficient Red Phosphorescence and Application to Organic Light-Emitting Diode *J. Am. Chem. Soc.* **2003**, *125*, 12971.

(51) Nazeeruddin, M. K.; Humphry-Baker, R.; Berner, D.; Rivier, S.; Zuppiroli, L.; Graetzel, M. Highly Phosphorescence Iridium Complexes and Their Application in Organic Light-Emitting Devices *J. Am. Chem. Soc.* **2003**, *125*, 8790.

(52) Tamayo, A. B.; Alleyne, B. D.; Djurovich, P. I.; Lamansky, S.; Tsyba, I.; Ho, N. N.; Bau, R.; Thompson, M. E. Synthesis and Characterization of Facial and Meridional Tris-Cyclometalated Iridium(III) Complexes *J. Am. Chem. Soc.* **2003**, *125*, 7377.

(53) Dedeian, K.; Djurovich, P. I.; Garces, F. O.; Carlson, G.; Watts, R. J. A New Synthetic Route to the Preparation of a Series of Strong Photoreducing Agents - *fac* Tris-Ortho-Metalated Complexes of Iridium(III) with Substituted 2-Phenylpyridines *Inorg. Chem.* **1991**, *30*, 1685.

(54) Hercules, D. M. *Fluorescence and Phosphorescence Analysis: Principles and Applications*; Interscience Publishers: New York, 1966.

(55) Sandee, A. J.; Williams, C. K.; Evans, N. R.; Davies, J. E.; Boothby, C. E.; Kohler, A.; Friend, R. H.; Holmes, A. B. Solution-Processible Conjugated Electrophosphorescent Polymers *J. Am. Chem. Soc.* **2004**, *126*, 7041.

(56) Zhen, H. Y.; Luo, C.; Yang, W.; Song, W. Y.; Du, B.; Jiang, J. X.; Jiang, C. Y.; Zhang, Y.; Cao, Y. Electrophosphorescent Chelating Copolymers Based on Linkage Isomers of Naphthylpyridine-Iridium Complexes with Fluorene *Macromolecules* **2006**, *39*, 1693.

(57) Chen, X. W.; Liao, J. L.; Liang, Y. M.; Ahmed, M. O.; Tseng, H. E.; Chen, S. A. High-Efficiency Red-Light Emission from Polyfluorenes Grafted with Cyclometalated Iridium Complexes and Charge Transport Moiety *J. Am. Chem. Soc.* **2003**, *125*, 636.

(58) Evans, N. R.; Devi, L. S.; Mak, C. S. K.; Watkins, S. E.; Pascu, S. I.; Kohler, A.; Friend, R. H.; Williams, C. K.; Holmes, A. B. Triplet Energy Back Transfer in Conjugated Polymers with Pendant Phosphorescent Iridium Complexes *J. Am. Chem. Soc.* **2006**, *128*, 6647.

(59) You, Y.; Kim, S. H.; Jung, H. K.; Park, S. Y. Blue Electrophosphorescence from Iridium Complex Covalently Bonded to the Poly (9-dodecyl-3-vinylcarbazole): Suppressed Phase Segregation and Enhanced Energy Transfer *Macromolecules* **2006**, *39*, 349.

(60) Wang, X. Y.; Prabhu, R. N.; Schmehl, R. H.; Weck, M. Polymer-Based Tris(2-phenylpyridine)iridium Complexes *Macromolecules* **2006**, *39*, 3140.

(61) Carlise, J. R.; Wang, X. Y.; Weck, M. Phosphorescent Side-Chain Functionalized Poly(norbornene)s Containing Iridium Complexes *Macromolecules* **2005**, *38*, 9000.

(62) Jiang, J. X.; Xu, Y. H.; Yang, W.; Guan, R.; Liu, Z. Q.; Zhen, H. Y.; Cao, Y. High-Efficiency White-Light-Emitting Devices from a Single Polymer by Mixing Singlet and Triplet Emission *Adv. Mater.* **2006**, *18*, 1769.

CHAPTER 3

METALLOQUINOLATE FUNCTIONALIZED POLY(CYCLOOCTENE)S

3.1 Abstract

This chapter describes the synthesis and characterization of poly(cyclooctene)s with pendant Alq_3 and Ybq_3. In addition to the metal complexes, the polymers are functionalized with carbazole units in order to increase the solubility of the polymers and to transfer the photoexcitation energy from carbazole units into the metal complexes. All copolymers retained the optical properties associated to their corresponding metal complex analogues. Furthermore, it is established that the polymer backbone does not interfere with the optical properties of the metal complexes.

3.2 Introduction

A basic introduction to metalloquinolates and metalloquinolate functionalized polymers is given in Chapter 2. In this chapter, covalent attachments of Alq_3 and Ybq_3 to poly(cyclooctene) backbones are reported.[1] Poly(cyclooctene)s are known to have a random coil configuration with glass transition temperatures well below 0 ^{o}C.[2] Morphologies of polymers that are employed in OLED devices might change during the device fabrication due to temperature variations that rise above and fall below the T_g of the polymers. As a result, it is difficult to compare the final morphology of the polymer in the device with the initial one and to establish morphology-device performance relationship. Accordingly, it becomes clear that employment of a more flexible backbone with a T_g below room temperature is quite appealing since a low glass transition

temperature assures that there will be no change in the polymer morphology during the device fabrication process, which makes poly(cyclooctene)s desirable materials as metal complex support. The metalloquinolate functionalized polymers described in this chapter also contain carbazole groups to increase the solubility of the polymers and to harvest more light through energy transfer from the carbazole units into the metal complex. Carbazole-based comonomers have been widely used in polymers for OLED applications for their hole-transporting properties and efficient energy transfer.[3-6]

Poly(cyclooctene)s, and poly(norbornene)s are the two main types of backbones that are studied in this thesis. These polymers have distinct physical properties such as different glass transition temperatures (Tg). Furthermore, properties of thin films of solution-processed polymers are dependent on the molecular weight of these polymers,[7,8] i.e. the same type of polymer but with different molecular weights might result in significantly different device performance. Therefore, control over the polymerization is highly desirable. Poly(cyclooctene)s and poly(norbornene)s can be synthesized via ring-opening metathesis polymerization (ROMP), a living polymerization method that allows for a high degree of control over molecular weights.[9-12] Moreover, ruthenium-based ROMP initiators are highly functional-group tolerant, allowing for the polymerization of monomers containing luminescent metal complexes.[3,13-16] Finally, the employment of a living polymerization method such as ROMP allows for the synthesis of controlled copolymers ranging from random copolymers to block copolymers.[17,18]

The basic mechanism of ROMP is described in Figure 3.1. Strained olefins such as norbornenes and cyclooctenes are outstanding monomer candidates, since the polymerization is enthalpically driven by the removal of ring strain. The most common catalysts that are used in ROMP are either molybdenum- or ruthenium-alkylidene complexes.[10] Especially, ruthenium-based initiators developed by Grubbs have become very popular due to their high tolerance to various functional groups and their ability to initiate the polymerization in the presence of air and water.[10] Figure 3.2 shows the

structures of the most widely employed Grubbs' catalysts. All the ring-opening metathesis polymerizations described in this and the proceeding chapters are initiated by Grubbs' third generation initiators, unless stated otherwise.

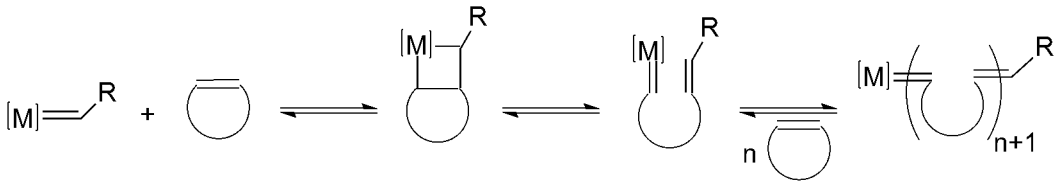

Figure 3.1 Mechanism of ROMP.

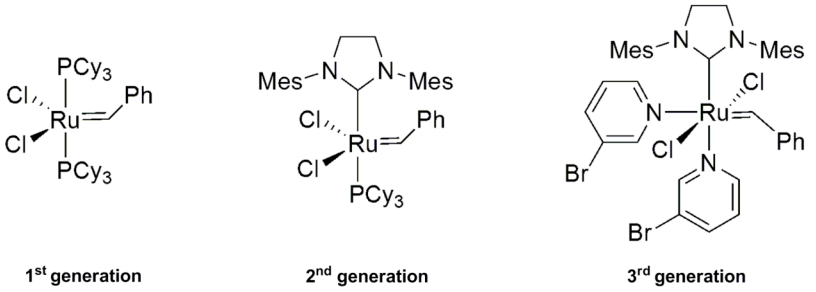

Figure 3.2 Grubbs'olefin metathesis initiators. Cy = Cyclohexyl, Mes = 2,4,6-trimethylphenyl

3.3 Results and Discussion

3.3.1 Ybq_3 Functionalized Poly(cyclooctene)s

Synthesis. The syntheses of the cyclooctene-based quinoline monomer **3** and carbazole monomer **5** are shown in Scheme 3.1. Compound **1** was reacted with **2**[19] in the presence of sodium bicarbonate to yield monomer **3**. Esterification of compound **1** with 6-bromohexanoic acid yielded compound **4**. Carbazole monomer **5** was obtained from the reaction of **4** with commercially available carbazole.

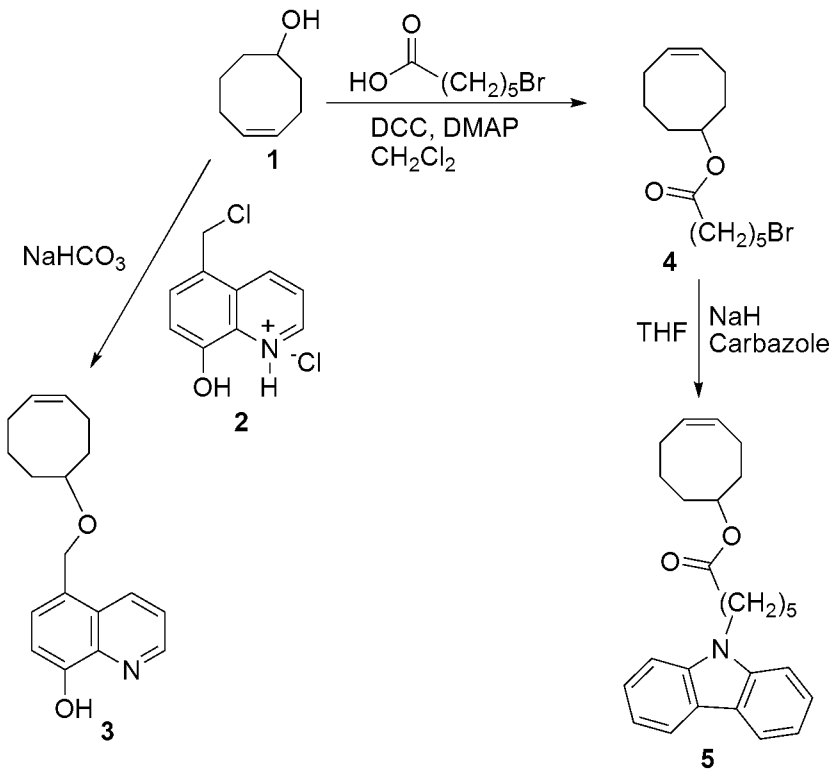

Scheme 3.1 Synthesis of cyclooctene-monomers **3** and **5**.

The copolymerization of **3** and **5** is shown in Scheme 3.2. Ratios of **3** to **5** in copolymers **6a**, **6b**, and **6c** are 1:5, 1:10, 1:20, respectively. Reactions of **6a-c** with Ybq_3 yielded copolymers **7a-c**. The molecular weights of the copolymers are given in Table 3.1. Copolymers **6a-c** showed glass transition temperatures around -15 °C, a clear indication of a flexible polymer backbone. Upon formation of the lanthanide complex, glass transition temperatures of the copolymers increased to around -5 ^{o}C. All the copolymers decomposed around 335 ^{o}C.

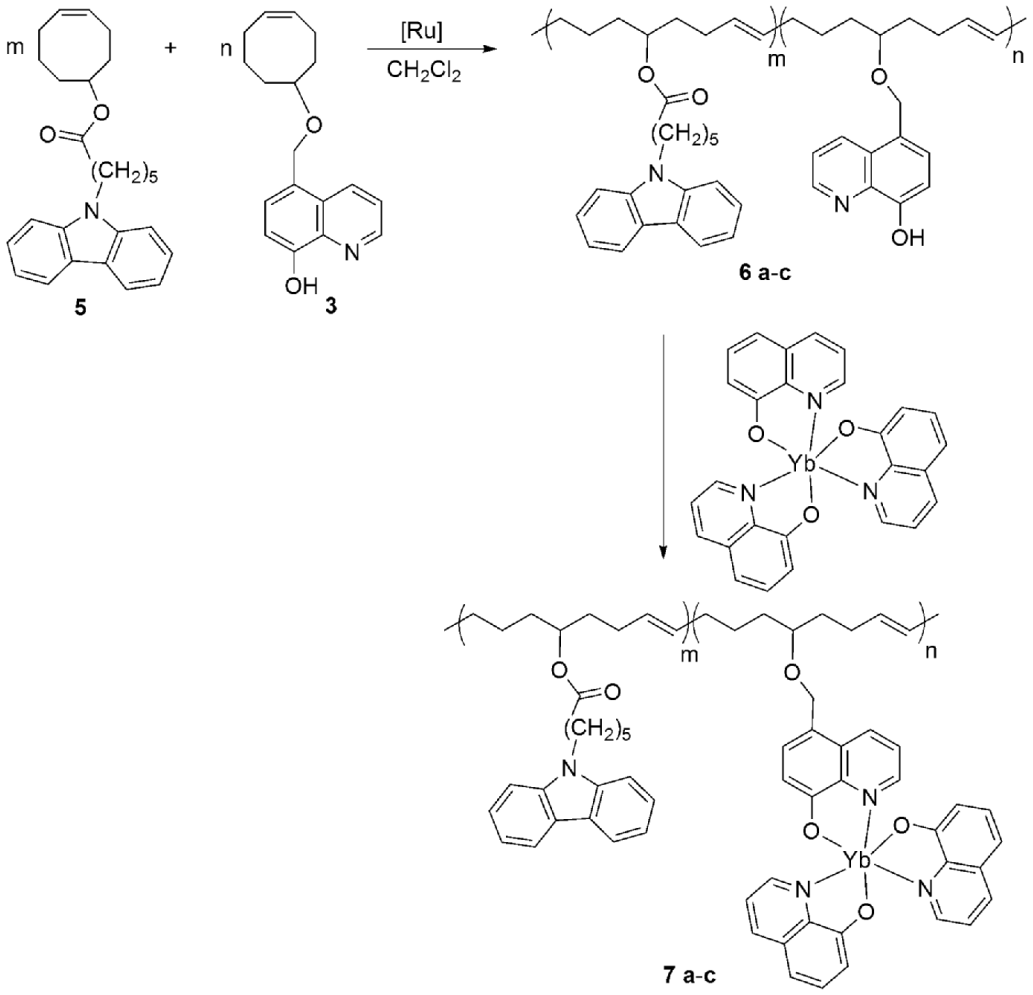

Scheme 3.2 Copolymerization of **3** and **5** and formation of the corresponding Ybq_3-copolymers.

UV/Visible Absorption. Table 3.1 lists the absorption characteristics of **3**, **5**, **6a-c**, and **7a-c**. The absorption spectrum of each copolymer is a combination of both monomers **3** and **5**. Because of the shielding effect discussed in Chapter 1, the metal center itself cannot be excited directly. Instead, the quinoline ligands that are coordinated to the metal center were excited at 380 nm. Complexation of compounds **6a-c** with ytterbium produced absorption bands around 400 nm that indicate the coordination of the metal to the polymers through side-chain quinoline ligands. This absorption characteristic was used to excite the copolymers **7a-c** for the photoluminescence study.

Table 3.1 Characterization data for all monomers and polymers.

Compound	λ_{abs} (nm)	λ_{em} (nm)	M_n (kDa)	M_w (kDa)	PDI
3	319	n/a	n/a	n/a	n/a
5	346, 294	435	n/a	n/a	n/a
6a	346, 331, 294	501	16.5	71	4.3
6b	346, 331, 297	481	12.5	53.5	4.3
6c	346, 331, 294	496	15	61.5	4.0
7a	400, 346, 294	517, 971	11.5	49.5	4.2
7b	402, 346, 297	516, 970	13.5	49.5	3.7
7c	399, 346, 294	518, 975	15	53	3.6

Photoluminescence. The solution photoluminescence of the Ybq_3-copolymers **7a-c** were measured to determine the effect of the concentration of Ybq_3 on the emission properties. While all metallated copolymers were soluble in chloroform, no emission was detected in pure chloroform. However, emission was observed when a mixture of chloroform and DMSO was used. As previously reported, DMSO replaces any water molecules coordinated to the lanthanide metal.[20] The emission of lanthanide-containing compounds in chloroform is dramatically lower than the emission of the same compound in DMSO. In solutions of lanthanide complexes, relatively small energy contents of the long wavelength electronic gap can be readily dissipated by solvent. If the energy of the gap between the lowest emitting level and the nearest non-emitting level is dissipated, radiationless decay occurs. In water, the O-H stretching vibration is very efficient in dissipating energy. If the O-H vibration can be replaced by a less energetic vibration, quenching becomes less efficient. For example, deuterated water is a less efficient quencher due to the lower energy of O-D vibration. The same holds true for the S=O

stretching vibrations of DMSO that are less efficient in quenching the emission than the O-H stretch of water.[20-23]

As shown in Figure 3.3, as the chromophore density in the polymer decreases, the emission intensity also decreases. However, when measuring the photoluminescence of a non-supported Ybq_3 molecule, the emission intensity was significantly lower than the emission of the 1:20 Ybq_3-copolymer. This indicates that the polymer backbone reduces self-quenching of the Ybq_3 chromophore, a reported occurrence for lanthanide-based materials.[24]

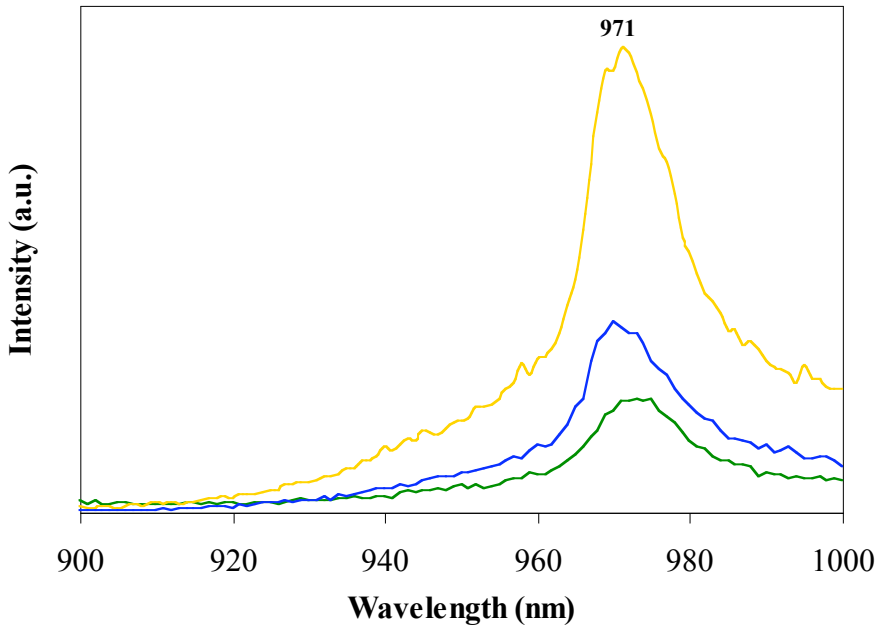

Figure 3.3 Photoluminescence of Ybq_3-copolymers, **7a** 1:5 (—), **7b** 1:10 (—), **7c** 1:20 (—).

3.3.2 Alq_3 Functionalized Poly(cyclooctene)s

Synthesis. The synthetic procedure for polymers **8a-c** has been reported in section 3.3.1. The percentages of the 8-hydroxyquinoline-functionalized monomer in copolymers **8a**, **8b**, and **8c** are 20%, 10%, and 5%, respectively. Scheme 3.3 outlines the synthesis of polymers **9a-c**. Functionalizations of copolymers **8a-c** were accomplished by reacting

them with $AlEt_3$ and 8-hydroxyquinoline, resulting in the target Alq_3-functionalized copolymers **9a-c**.

The molecular weights of polymers **8a-c** are listed in Table 3.2. The polydispersity indices (PDIs) of copolymers **8a-c** are dependent on the monomers and the catalyst ratios. When the results of this section and section 3.3.1 are compared, PDIs are found to be decreasing with decreasing monomer to catalyst ratios. GPC analyses of copolymers **9a-c** were not possible probably due to either the reversible coordination of aluminum to the polymer backbone or the formation of aggregates. Copolymers **8a-c** have glass transition temperatures of approximately –15 ^{o}C. No glass transition temperatures were observed upon the formation of the metal complex functionalized copolymers **9a-c**. Copolymers **9a-c** decomposed around 290 ^{o}C.

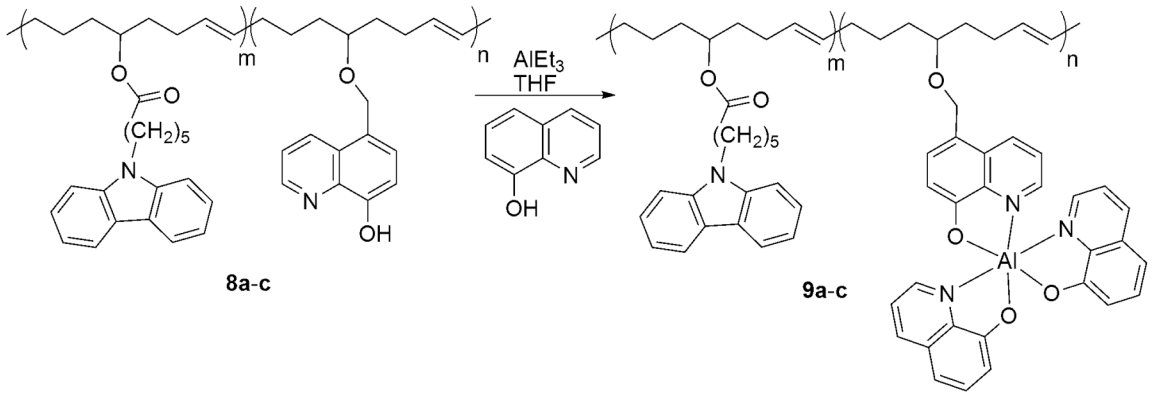

Scheme 3.3 Syntheses of Alq_3 copolymers.

Table 3.2 Polymer characterization data.

Compound	M_n (kDa)	M_w (kDa)	PDI
8a	7.1	15.1	2.12
8b	4.5	10.7	2.39
8c	4.3	9.7	2.27

Photophysical Properties. After establishing the basic polymer properties, photophysical characterizations of the copolymers were carried out. The optical properties of all copolymers are listed in Table 3.3 and shown in Figure 3.4. Complexation of compounds 8a-c with aluminum to produce 9a-c resulted in absorption bands around 390 nm, indicating the coordination of the metal to the polymers through the quinoline ligands in the side-chains.

The photoluminescence spectra of copolymers **9a-c** are shown in Figure 3.4(a) and are almost identical to the reference compound Alq_3. The solution and solid-state emission maxima of all copolymers are almost identical (Table 3.3). These results in combination with the above described absorption spectra suggest that the poly(cyclooctene) backbone does not interfere with the photophysical properties of the pendant metal complexes

Table 3.3 Photophysical properties of the copolymers

Compound	λ_{abs}[a] **(nm)**	λ_{em}[a,b] **(nm)**	λ_{em}[b,c] **(nm)**	Φ[d,e]	τ[f] **(ns)**	τ[g] **(ns)**
9a	331, 345, 388	516	522	0.53	13	15
9b	331, 345, 395	517	520	0.56	12	16
9c	331, 345, 392	514	516	0.45	10	11

[a] in chloroform solutions. [b] all polymers were excited at 380 nm. [c] solid state. [d] in degassed THF solutions. [e] relative to Alq_3. [f] luminescence lifetime in THF solution. [g] luminescence lifetime in degassed THF solution.

To investigate whether energy transfer occurs between the carbazole units and Alq_3, we measured the excitation spectra of polymers **9a-c**. Figure 3.4(b) shows the excitation spectra of **9a-c**, and the absorption spectra of **5** and **9b**. The two local maxima at 330 and 345 nm in the absorption spectra of **9a-c** originate from the carbazole units, while the broad absorption maximum at 380 nm is attributable to the metal complex. The

high intensities of the absorption bands of 330 and 345 nm compared to MLCT bands in the excitation spectra of **9a-c** indicate that there is significant energy transfer from the carbazole units into the metal moieties. These results prove that carbazole groups in copolymers **9a-c** act not only as spacer and solubilizing groups but also as efficient photoactive units that lead to enhanced optical properties. These results in combination with the known hole-transporting ability of carbazole make these copolymers promising candidates as materials for OLED applications.

Finally, the emission quantum yields and lifetimes were measured (Table 3.3). The quantum yields and lifetimes of **9a-c** are almost half of those of Alq_3. The emission lifetimes of **9a-c** are insensitive to oxygen. Since Alq_3 is fluorescent, relaxation time from the excited state to the ground state is significantly shorter than the time necessary for energy transfer to oxygen to occur.[25]

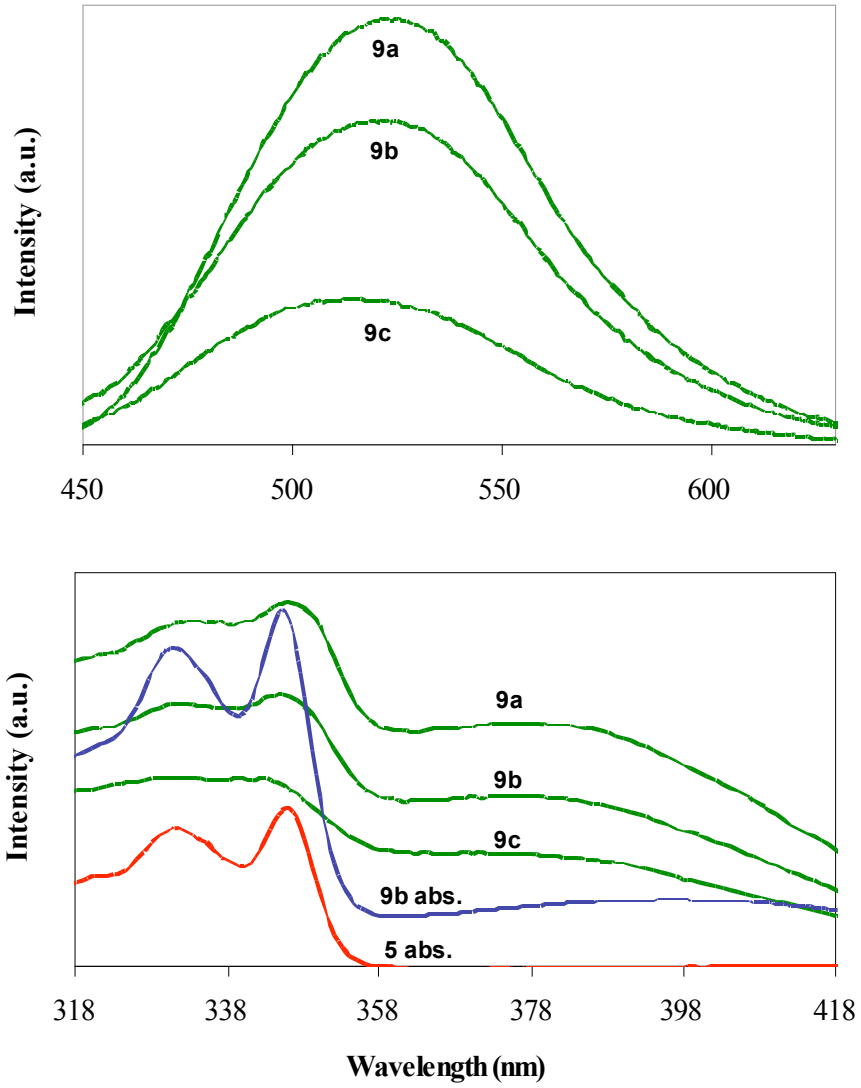

Figure 3.4 Solid state emission spectra of the copolymers (top); solid state excitation spectra of **9a-c** (monitored emission wavelength = 530 nm), and absorption spectra (in chloroform) of **9b**, and **5** (bottom).

3.4 Conclusion

In this chapter, synthesis and characterization of poly(cyclooctene)s containing carbazole and either Alq_3 or Ybq_3 moieties in the side-chains are described. Although the solution emission spectra of Ybq_3 functionalized copolymers exhibited near IR emission around 970 nm, no emission was observed in solid state. On the other hand, the emission

spectra of green-emitting Alq_3 containing copolymers are almost identical to small molecule Alq_3 both in solution and solid state. Excitation spectra of Alq_3 containing copolymers proved significant energy transfer from the carbazole units into the metal complex.

3.5 Experimental

All Reagents were purchased either from Acros Organics or Aldrich and used without further purification. ^{1}H-NMR and ^{13}C-NMR spectra (300 MHz ^{1}H NMR, 75 MHz ^{13}C NMR) were taken using a Varian Mercury Vx 300 spectrometer. All spectra are referenced to residual proton solvent. Abbreviations used include singlet (s), doublet (d), triplet (t), and unresolved multiplet (m). Mass spectral analyses were provided by the Georgia Tech Mass Spectrometry Facility. Gel-permeation chromatography (GPC) analyses were carried out using a Waters 1525 binary pump coupled to a Waters 2414 refractive index detector with methylene chloride as an eluant on American Polymer Standards 10 μm particle size, linear mixed bed packing columns. The flow rate used for all the measurements was 1 mL/min. All GPC measurements were calibrated using poly(styrene) standards and carried out at room temperature. The glass-transition temperature of the polymers (Tg) was measured by differential-scanning calorimetry (DSC). The DSC analyses were performed under an atmosphere of nitrogen using a Mettler Toledo DSC 822e that was calibrated using indium standards. The temperature program provided two heating and cooling cycles between -50 and 100 ^{o}C at 10 ^{o}C/min, with the sample size ranging from 5 to 9 mg. The onset of thermal degradation for the polymers (T_d) was measured by thermal gravimetric analysis (TGA). The TGA analyses were performed under an atmosphere of nitrogen using a Shimadzu TGA-50 and all samples were heated from 25 to 450 ^{o}C at a rate of 10 ^{o}C /min. UV/vis absorption measurements were taken on a Shimadzu UV-2401 PC recording spectrophotometer.

Emission measurements were acquired using a Shimadzu RF-5301 PC spectrofluorophotometer. Lifetime measurements were taken using a PTI model C-72 fluorescence laser spectrophotometer with a PTI GL-3300 nitrogen laser.

Synthesis of 5-(cyclooct-4-enyloxymethyl)-quinolin-8-ol (3). 5-hydroxycyclooctene **1** was prepared according to literature procedure.[26] Monomer **3** was synthesized by stirring chloromethylhydroxyquinoline hydrochloride **2** (1.5 g, 0.0065 mol) and **1** (6.8 g, 0.054 mol) in the presence of excess $NaHCO_3$ at 110 °C for 1.5 hours. Upon cooling, a solid precipitated that was dissolved in CH_2Cl_2, and washed with water. The solvent and the excess alcohol were removed by distillation. The resulting green solid was recrystallized from hexanes to give a white solid (0.87 g, 46 % yield). ^{1}H NMR (300 MHz, $CDCl_3$) δ 8.79 (1H, dd, *J* =1.65, 4.12); 8.49 (1H, dd, *J* =1.65, 8.52); 7.47 (1H, dd, *J* =4.12, 8.52); 7.40 (1H, d, *J* =7.69); 7.10 (1H, d, *J* =7.69); 5.62 (2H, m); 4.80 (2H, dd, *J* =11.26, 22.25); 3.51 (1H, m); 2.35-1.40 (10H, m). ^{13}C NMR (75 MHz, $CDCl_3$) δ 152.4, 147.6, 138.6, 133.9, 130.2, 129.6, 128.7, 127.7, 125.2, 121.9, 109.2, 80.1, 68.7, 34.6, 33.6, 26.1, 25.9, 23.1. MS m/z Calcd. (M^+): 284.2. Found (ESI): 284.2 (M^+).

Synthesis of 6-bromo-hexanoic acid cyclooct-4-enyl ester (4). Dicyclocarbodiimide (7.5 g, 0.036 mol) and N, N-dimethylaminopyridine (0.4 g, 0.0033 mol) were dissolved in 40 mL of anhydrous CH_2Cl_2 and added dropwise to a solution of **1** (3.9 g, 0.031 mol) and 6-bromohexanoic acid (7.6 g, 0.039 mol) in 40 mL of anhydrous CH_2Cl_2 under argon. The solution was stirred overnight at room temperature. The white precipitate that formed during the reaction was filtered off, the filtrate was reduced, and the remaining oil was purified by column chromatography (silica gel, 4:1 hexanes/ethyl acetate) to yield colorless oil (7.5 g, 79% yield). ^{1}H NMR (300 MHz, $CDCl_3$) δ 5.61 (2H,m); 4.80 (1H,m); 3.37 (2H, t, *J* =6.87); 2.36-1.40 (18H, m). ^{13}C NMR (75 MHz, $CDCl_3$) δ 172.8; 129.9; 129.7; 75.7; 34.8; 34.1; 34.0; 33.8; 32.7; 27.9; 25.9; 25.2; 24.5; 22.7.

Synthesis of 6-carbazol-9-yl-hexanoic acid cyclooct-4-enyl ester (5). Carbazole (3.7 g, 0.022 mol) was dissolved in anhydrous THF and added dropwise to an ice-cold mixture of NaH (0.5 g, 0.021 mol) in THF and stirred for one hour. Then, **4** (4.8 g, 0.016 mol), dissolved in 50 mL of anhydrous THF, was added dropwise to the reaction mixture. After the addition was complete, the mixture was refluxed overnight. After filtration, the solution was diluted with ether, washed with an aqueous solution of $NaHCO_3$, brine, and dried over Na_2SO_4. The solvent was removed and the crude product was purified by column chromatography (silica gel, 9:1 hexanes/ethyl acetate) yielding a viscous, colorless oil (3.7 g, 60% yield). ^{1}H NMR (300 MHz, $CDCl_3$) δ 8.12 (2H, d, *J* = 7.69); 7.48 (2H, dd, *J* =6.89, 15.11); 7.40 (2H, d, *J* =7.97); 7.26 (2H, dd, *J* = 6.89, 14.83); 5.65 (2H, m); 4.81 (1H, m); 4.31 (2H, t, *J* =7.14); 2.32-1.44 (18H, m). ^{13}C NMR (75 MHz, $CDCl_3$) δ 172.9, 140.5, 129.9, 129.8, 125.8, 123.0, 120.6, 118.9, 108.8, 75.8, 75.7, 43.2, 34.8, 34.1, 33.9, 29.1, 27.2, 25.9, 25.2, 22.7. MS m/z Calcd. (M^+): 390.2. Found (ESI): 390.2 (M^+).

Copolymerization of 3 and 5 (ratios of 3/5 = 1:5, 1:10, 1:20). Monomer **3** was dissolved in 1 mL of chloroform. A chloroform solution of the ruthenium catalyst in 1 mL of chloroform was added to the monomer solution and stirred for 30 seconds, followed by the addition of monomer **5** (in 5 mL chloroform). After stirring for ten minutes, ethyl vinyl ether (1 mL) was added. After stirring for an additional ten minutes, the solution was concentrated down to 1 mL and added dropwise to 100 mL of cold methanol. The polymer, which precipitated out of solution, was collected and redissolved in 1 mL of chloroform and reprecipitated into cold methanol. This purification procedure was repeated three times. The final product was collected as a brown solid **(6 a-c)**. ^{1}H NMR (300 MHz, $CDCl_3$) δ 8.77 (1H, broad); 8.44 (1H, broad); 8.13 (40H, broad); 7.45 (82H, broad); 7.26 (40H, broad); 7.14 (1H, broad); 5.38 (42H, broad); 4.89 (22H, broad); 4.28 (40H, broad); 3.54 (1H,m); 2.2-1.4 (370H, m). ^{13}C NMR (75 MHz, $CDCl_3$) δ 173.3, 152.5, 147.8, 140.5, 138.8, 133.9, 130.6, 130.4, 130.0, 129.8,

129.6, 128.9, 128.7, 127.7, 126.2, 125.9, 125.3, 123.0, 121.9, 120.6, 119.0, 108.9, 73.8, 68.8, 60.3, 43.1, 34.7, 34.4, 34.1, 33.5, 33.2, 33.0, 32.8, 29.1, 28.9, 27.4, 27.2, 25.7, 25.2, 23.7.

Formation of Ybq_3-copolymers 7a-c. Excess Ybq_3 was dissolved in a minimum amount of methanol and added to a chloroform solution of **6** (0.1 g/10 mL). After stirring overnight, the solution was concentrated down to 1 mL and added drop wise to 100 mL of cold methanol. The polymer, which precipitated out of solution, was collected and redissolved in 1 mL of chloroform and precipitated into cold methanol. This purification procedure was repeated three times. The final product was collected as a brown solid **7 a-c**. ^{1}H NMR (300 MHz, $CDCl_3$) δ 8.79 (broad); 8.13 (broad); 7.37 (broad); 5.40 (broad); 4.85 (broad); 4.30 (broad); 3.64 (broad); 2.4-1.2 (broad). ^{13}C NMR (75 MHz, $CDCl_3$) δ 173.3, 151.8, 147.6, 140.5, 138.1, 133.6,130.7,130.6, 130.5, 130.4,130.1,130.0, 129.9, 129.7, 126.2, 125.8, 122.9, 120.6, 118.9, 108.8, 73.8, 66.4, 43.1, 37.3, 34.7, 34.3, 34.1, 32.8, 29.0, 28.8, 27.2, 25.6, 25.2.

Syntheses of Alq_3-copolymers 9a-c. A solution of 8-hydroxyquinoline (50 mg, 0.34 mmol) and **8a-c** (33 mg, 67 mg, and 136 mg, respectively) in dry THF was added to triethylaluminum (0.11 mL, 0.11 mmol) via a syringe and stirred at room temperature under an argon atmosphere. During this period, the precipitation of Alq_3 was observed. After 24 hours, the mixture was filtered to remove any insoluble Alq_3. The filtrate was concentrated and precipitated into a large volume of methanol. The resulting precipitate was collected and dissolved in a small amount of $CHCl_3$ and reprecipitated into methanol. This purification procedure was repeated several times. The final polymers were collected as brown solids **9a-c**. ^{1}H NMR ($CDCl_3$): δ = 8.80 (broad, m, H-Ar), 8.13 (broad, m), 7.38 (broad, m), 5.40 (broad), 4.85 (broad), 4.30 (broad, m), 3.64 (broad, m), 2.4-1.2 (broad, m). ^{13}C NMR ($CDCl_3$): δ = 173.5, 158.9, 144.8, 142.6, 140.5, 139.9, 139.6, 131.5, 131.2, 129.9, 129.5, 125.8, 122.9, 121.9, 121.3, 120.6, 119.0, 112.7, 112.1, 108.8, 68.8, 67.6, 42.9, 34.5, 34.3, 33.5, 32.7, 28.9, 28.7, 27.0, 25.5, 25.0, 23.6.

3.6 References

(1) The contents of this chapter have been published. See: Meyers, A.; Kimyonok, A.; Weck, M. Infrared-Emitting Poly(norbornene)s and Poly(cyclooctene)s *Macromolecules* **2005**, *38*, 8671; and Kimyonok, A.; Weck, M. Poly(cyclooctene)s with Pendant Fluorescent and Phosphorescent Metal Complexes *Macromol. Rapid Commun.* **2007**, 28, 152.

(2) Hillmyer, M. A.; Laredo, W. R.; Grubbs, R. H. Ring-Opening Metathesis Polymerization of Functionalized Cyclooctenes by a Ruthenium-Based Metathesis Catalyst *Macromolecules* **1995**, *28*, 6311.

(3) Wang, X. Y.; Prabhu, R. N.; Schmehl, R. H.; Weck, M. Polymer-Based Tris(2-phenylpyridine)iridium Complexes *Macromolecules* **2006**, *39*, 3140.

(4) Chen, X. W.; Liao, J. L.; Liang, Y. M.; Ahmed, M. O.; Tseng, H. E.; Chen, S. A. High-Efficiency Red-Light Emission from Polyfluorenes Grafted with Cyclometalated Iridium Complexes and Charge Transport Moiety *J. Am. Chem. Soc.* **2003**, *125*, 636.

(5) Jiang, J. X.; Jiang, C. Y.; Yang, W.; Zhen, H. G.; Huang, F.; Cao, Y. High-Efficiency Electrophosphorescent Fluorene-alt-Carbazole Copolymers N-Grafted with Cyclometalated Ir Complexes *Macromolecules* **2005**, *38*, 4072.

(6) You, Y.; Kim, S. H.; Jung, H. K.; Park, S. Y. Blue Electrophosphorescence from Iridium Complex Covalently Bonded to the Poly (9-dodecyl-3-vinylcarbazole): Suppressed Phase Segregation and Enhanced Energy Transfer *Macromolecules* **2006**, *39*, 349.

(7) Sandee, A. J.; Williams, C. K.; Evans, N. R.; Davies, J. E.; Boothby, C. E.; Kohler, A.; Friend, R. H.; Holmes, A. B. Solution-Processible Conjugated Electrophosphorescent Polymers *J. Am. Chem. Soc.* **2004**, *126*, 7041.

(8) Weinfurtner, K. H.; Fujikawa, H.; Tokito, S.; Taga, Y. Highly Efficient Pure Blue Electroluminescence from Polyfluorene: Influence of the Molecular Weight Distribution on the Aggregation Tendency *Appl. Phys. Lett.* **2000**, *76*, 2502.

(9) Fürstner, A. Olefin Metathesis and Beyond *Angew. Chem. Int. Ed.* **2000**, *39*, 3013.

(10) Trnka, T. M.; Grubbs, R. H. The Development of L_2X_2Ru = CHR Olefin Metathesis Catalysts: An Organometallic Success Story *Acc. Chem. Res.* **2001**, *34*, 18.

(11) Frenzel, U.; Nuyken, O. Ruthenium-Based Metathesis Initiators: Development and Use in Ring-Opening Metathesis Polymerization *J. Polym. Sci., Part A: Polym. Chem.* **2002**, *40*, 2895.

(12) Bielawski, C. W.; Grubbs, R. H. Living Ring-Opening Metathesis Polymerization *Prog. Polym. Sci.* **2007**, *32*, 1.

(13) Carlise, J. R.; Wang, X. Y.; Weck, M. Phosphorescent Side-Chain Functionalized Poly(norbornene)s Containing Iridium Complexes *Macromolecules* **2005**, *38*, 9000.

(14) Meyers, A.; Weck, M. Design and Synthesis of Alq_3-Functionalized Polymers *Macromolecules* **2003**, *36*, 1766.

(15) Meyers, A.; Weck, M. Solution and Solid-State Characterization of Alq_3-Functionalized Polymers *Chem. Mater.* **2004**, *16*, 1183.

(16) Meyers, A.; South, C.; Weck, M. Design, Synthesis, Characterization and Fluorescent Studies of the First Zinc-Quinolate Polymer *Chem. Commun.* **2004**, 1176.

(17) Pollino, J. M.; Weck, M. Non-Covalent Side-Chain Polymers: Design Principles, Functionalization Strategies, and Perspectives *Chem. Soc. Rev.* **2005**, *34*, 193.

(18) Pollino, J. M.; Stubbs, L. P.; Weck, M. Living ROMP of Exo-Norbornene Esters Possessing Pd^{II} SCS Pincer Complexes or Diaminopyridines *Macromolecules* **2003**, *36*, 2230.

(19) Burckhalter, J.; Leib, R. I. Amino- and Chloromethylation of 8-Quinolinol - Mechanism of Preponderant Ortho Substitution in Phenols under Mannich Conditions *J. Org. Chem.* **1961**, *26*, 4078.

(20) Van Deun, R.; Fias, P.; Nockemann, P.; Schepers, A.; Parac-Vogt, T. N.; Van Hecke, K.; Van Meervelt, L.; Binnemans, K. Rare-Earth Quinolinates: Infrared-

Emitting Molecular Materials with a Rich Structural Chemistry *Inorg. Chem.* **2004**, *43*, 8461.

(21) Hasegawa, Y.; Kimura, Y.; Murakoshi, K.; Wada, Y.; Kim, J. H.; Nakashima, N.; Yamanaka, T.; Yanagida, S. Enhanced Emission of Deuterated Tris(hexafluoroacetylacetonato)neodymium(III) Complex in Solution by Suppression of Radiationless Transition *via* Vibrational Excitation *J. Phys. Chem.* **1996**, *100*, 10201.

(22) Kawa, M.; Takahagi, T. Improved Antenna Effect of Terbium(III)-Cored Dendrimer Complex and Green-Luminescent Hydrogel by Radical Copolymerization *Chem. Mater.* **2004**, *16*, 2282.

(23) Hasegawa, Y.; Yamamuro, M.; Wada, Y.; Kanehisa, N.; Kai, Y.; Yanagida, S. Luminescent Polymer Containing the Eu(III) Complex Having Fast Radiation Rate and High Emission Quantum Efficiency *J. Phys. Chem. A* **2003**, *107*, 1697.

(24) Curry, R. J.; Gillin, W. P. Electroluminescence of Organolanthanide Based Organic Light Emitting Diodes *Curr. Opin. Solid State Mater. Sci.* **2001**, *5*, 481.

(25) Hercules, D. M. *Fluorescence and Phosphorescence Analysis: Principles and Applications*; Interscience Publishers: New York, 1966.

(26) Hillmyer, M. A.; Laredo, W. R.; Grubbs, R. H. Ring-Opening Metathesis Polymerization of Functionalized Cyclooctenes by a Ruthenium-Based Metathesis Catalyst *Macromolecules* **1995**, *28*, 6311.

CHAPTER 4

POLY(NORBORNENE)S WITH PHOSPHORESCENT PLATINUM COMPLEXES

4.1 Abstract

This chapter describes the copolymerizations of a 2,7-di(carbazol-9-yl)fluorene-based host monomer with monomers containing terminal platinum complexes.[1] The homopolymerizations of the host monomer was found to be controlled, whereas the platinum complexes interfered with the polymerization, possibly due to an interaction between the ligands and the ruthenium of the initiator.

4.2 Introduction

In Section 2.4, advantages of 3rd row transition metal complexes in terms of OLED applications are discussed. Even though iridium complexes are by far the most widely employed metal complexes in OLED applications, other transition metal complexes are also studied.[2] Among these metal complexes, platinum complexes exhibit some unique properties.[3] Unlike iridium complexes, platinum complexes are square planar, which allows for intermolecular stacking.[4,5] Therefore, in addition to single molecule emission, excimer emission is also observed, which results in broad emission that can produce white light.[6,7] Obtaining white light from a single compound is quite appealing, as devices with multiple emitters are expected to lose their color purity over time due to differential aging of the different emitters.[7]

The ligands that are used for iridium complexes are also employed in platinum complexes (see Section 2.4 for structures). Of these, Pt(acac)(ppf) is the most promising

complex in terms of device properties.[7,8] Near white emission has been obtained for devices based on this complex.[7,8] Fréchet and coworkers attached this complex to a poly(styrene) backbone along with electron- and hole-transport compounds, and they fabricated devices that exhibit external quantum efficiencies as high as 4.6% with turn on voltages around 8V.[9] Unfortunately, emission was not pure white; they obtained emission with CIE coordinates of x = 0.33, y = 0.50 (pure white: x = 0.33, y = 0.33).[9]

In this chapter, the ring-opening metathesis polymerization of norbornenes with platinum complexes and a 2,7-di(carbazol-9-yl)fluorene-based host monomer are described. The host material has similar emission spectra and quantum yields as 4,4′-di(carbazol-9-yl)biphenyl (CBP).[10] CBP is one of the most widely used host materials in OLEDs due to its high triplet energy which enables it to transfer both singlet and triplet excitation to a wide range of iridium complexes.[11-15] DFT calculations suggest that use of the fluorene-diyl bridge, which can be readily functionalized with polymerizable groups such as norbornene, in place of the biphenyl bridge of CBP does not significantly affect the energy of lowest triplet state.[16] Therefore, the host material is expected to be as efficient as CBP in terms of device performance.

4.3 Results and Discussion

Polymerizations. Monomers **1**-**4** were synthesized by Jian-Yang Cho in Marder Group at Georgia Institute of Technology (see ref. 1 for the experimental procedures). The monomers were polymerized with the use of Grubbs' second- or third-generation ruthenium initiator (2 mol%) in dry CH_2Cl_2. Table 4.1 summarizes molecular weights estimated by GPC for the homopolymer of **1** (poly**1**) and random copolymers of **1** with 10 wt% of phosphor monomers: **5**-**7**. The synthesis of homopolymer of **2** was also attempted using the second-generation catalyst but the resulting material was too poorly soluble for characterization by GPC. The copolymers display much broader molecular

weight distributions than the homopolymer of the host. Indeed, three different carbene ^{1}H NMR spectroscopy signals are seen during the formation of the copolymers, whereas only one is seen during the homopolymerization of **1** (Figure 4.1).

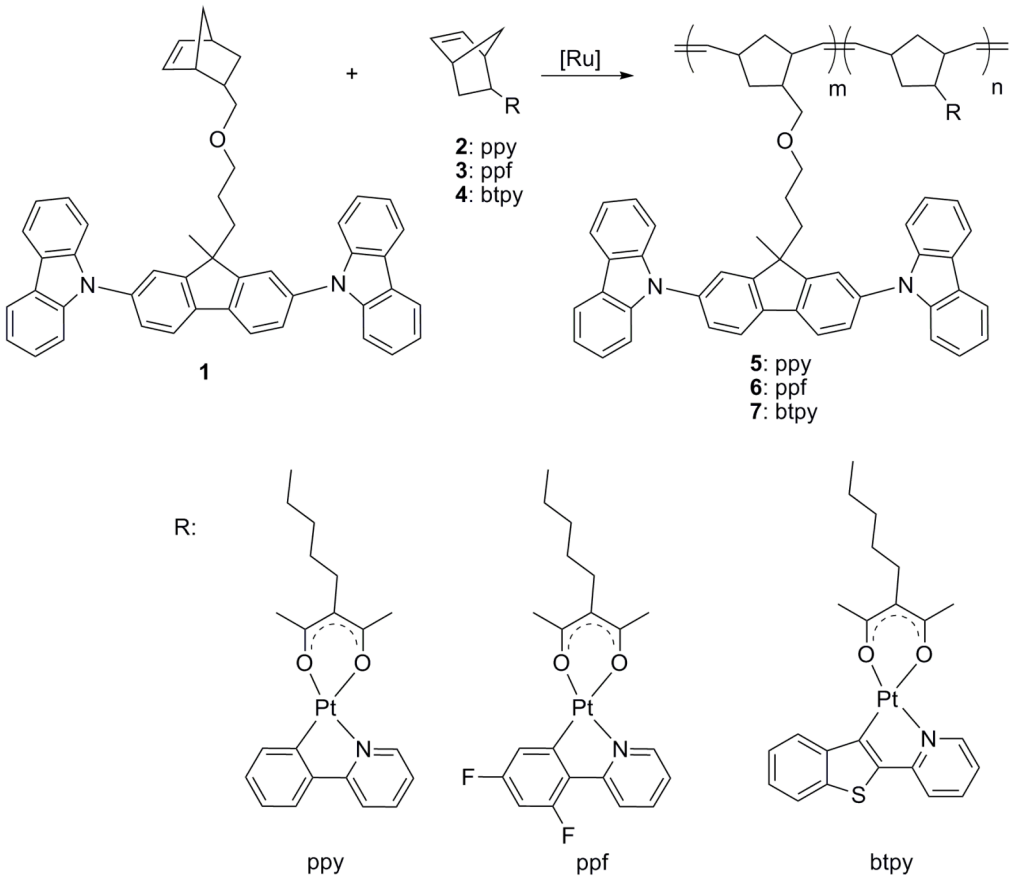

Scheme 4.1 Synthesis of the platinum containing polymers **5-7**.

Table 4.1 Polymer characterization data

Polymer	M_n **(kDa)**	M_w **(kDa)**	**PDI**	**Grubbs initi.**
Poly1	30.0	67.0	2.27	2nd
5	9.0	26.0	2.96	3rd
6	14.0	46.0	3.47	2nd
7	12.0	44.0	3.59	2nd

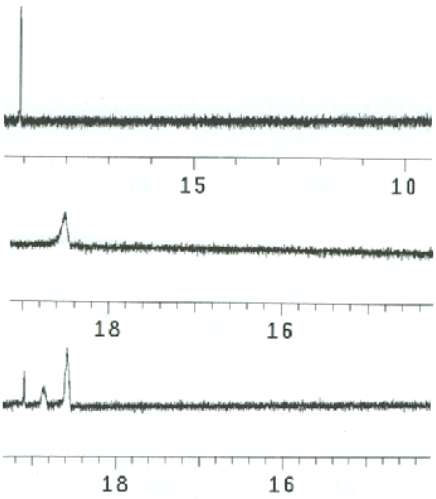

Figure 4.1. Carbene ^{1}H-NMR signals for the third generation Grubbs' catalyst (top), and during polymerizations of **1** (middle), and **5** (bottom)

In order to verify the living character of the polymerizations of **1**, four different polymerizations were carried out with monomer to catalyst ratios of 25:1, 50:1, 75:1, and 100:1 using Grubbs' third generation initiator. Figure 4.2 shows the plot of the molecular weights of these homopolymers versus the monomer to catalyst ratios. The linear relationship indicates that the polymerization is controlled. Furthermore, ^{1}H-NMR spectroscopy experiments showed the complete disappearance of the carbene signal of the initiator around 19.1 ppm, and the formation of a new, broad carbene signal around 18.5 ppm, indicating complete initiation (Figure 4.1). Both experiments strongly suggest that the polymerization of **1** proceeds in a living fashion. These findings suggest that while the polymerization of the host compound is controllable, the ruthenium species are not fully functional group tolerant towards the platinum complexes, perhaps due to transfer of the acetylacetonate ligand from platinum to ruthenium. Hence, the polymers may contain some different features from those indicated by their idealized structure.

More generally, ROMP appears to be unsuitable for the controlled polymerization of platinum acetylacetonate species.

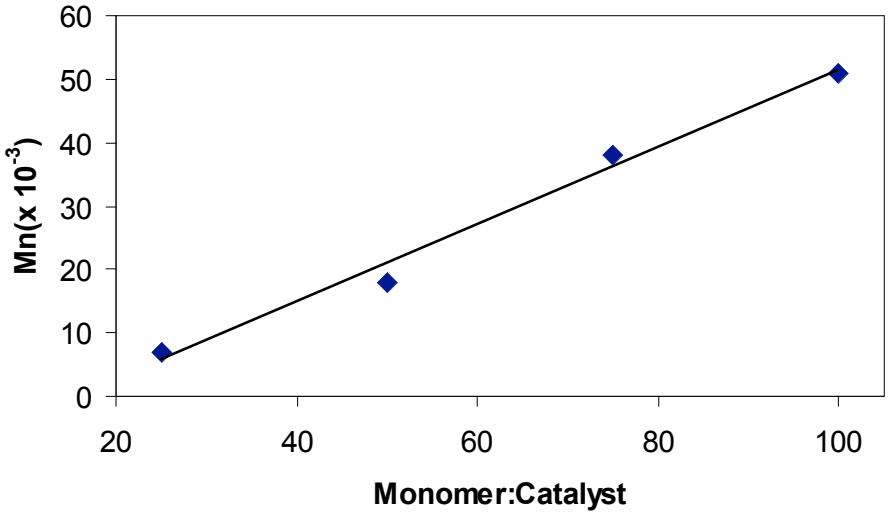

Figure 4.2 Plot of M_n vs. monomer-to-catalyst ratio for the homopolymerization of **1**.

4.4 Conclusion

Polymerization studies of a 2,7-di(carbazol-9-yl)fluorene-based host monomer and monomers with platinum complexes revealed that the homopolymerizations of the host monomer is controlled as indicated by the ^{1}H-NMR spectrum during the polymerization, which showed the complete disappearance of the carbene signal of the catalyst and the formation of a new carbene signal due to the polymerization, and by the molecular weight vs. monomer-to-catalyst plot, which showed that the molecular weight increases linearly with the increasing monomer-to-catalyst ratio. On the other hand, the platinum complexes interfered with the polymerization. ^{1}H-NMR spectra suggest that the acetyl acetonato groups of the complexes interact with the ruthenium center of the initiator. In the following chapters describing the iridium complexes, the acetyl acetonato

ligand will be replaced by ligands that will bind strongly to iridium will be employed in order to ensure that the iridium complexes will not interfere with the polymerizations.

4.5 Experimental

All Reagents were purchased either from Acros Organics or Aldrich and used without further purification. ^{1}H-NMR spectra (300 MHz) were taken using a Varian Mercury Vx 300 spectrometer. All spectra are referenced to residual proton solvent. Gel-permeation chromatography (GPC) analyses were carried out using a Waters 1525 binary pump coupled to a Waters 2414 refractive index detector with methylene chloride as an eluant on American Polymer Standards 10 μm particle size, linear mixed bed packing columns. The flow rate used for all the measurements was 1 mL/min. All GPC measurements were calibrated using poly(styrene) standards and carried out at room temperature.

General Polymerization Procedure. Monomers were polymerized with the use of Grubbs' second or third-generation catalysts (2 mol%) in dry CH_2Cl_2. After the polymerization was complete, the reaction mixture was quenched with few drops of ethyl vinyl ether. The reaction mixture was concentrated and precipitated into methanol. The resulting solid was collected by filtration, redissolved in CH_2Cl_2 and reprecipitated into methanol.

4.6 References

(1) The contents of this chapter have been published. See: Cho, J. Y.; Domercq, B.; Barlow, S.; Suponitsky, K. Y.; Li, J.; Timofeeva, T. V.; Jones, S. C.; Hayden, L. E.; Kimyonok, A.; South, C. R.; Weck, M.; Kippelen, B.; Marder, S. R. Synthesis and Characterization of Polymerizable Phosphorescent Platinum(II) Complexes for Solution-Processible Organic Light-Emitting Diodes *Organometallics* **2007**, *26*, 4816; and Kimyonok, A.; Domercq, B.; Haldi, A.; Cho, J. Y.; Carlise, J. R.; Wang, X. Y.; Hayden, L. E.; Jones, S. C.; Barlow, S.; Marder, S. R.; Kippelen, B.; Weck, M. Norbornene-Based Copolymers with Iridium Complexes and Bis(Carbazolyl)Fluorene Groups in Their Side-Chains and Their Use in Light-Emitting Diodes *Chem. Mater.* **2007**, *19*, 5602.

(2) Evans, R. C.; Douglas, P.; Winscom, C. J. Coordination Complexes Exhibiting Room-Temperature Phosphorescence: Evaluation of Their Suitability as Triplet Emitters in Organic Light Emitting Diodes *Coord. Chem. Rev.* **2006**, *250*, 2093.

(3) Ma, B. W.; Djurovich, P. I.; Thompson, M. E. Excimer and Electron Transfer Quenching Studies of a Cyclometalated Platinum Complex *Coord. Chem. Rev.* **2005**, *249*, 1501.

(4) D'Andrade, B.; Forrest, S. R. Formation of Triplet Excimers and Dimers in Amorphous Organic Thin Films and Light Emitting Devices *Chem. Phys.* **2003**, *286*, 321.

(5) Ionkin, A. S.; Marshall, W. J.; Wang, Y. Syntheses, Structural Characterization, and First Electroluminescent Properties of Mono-Cyclometalated Platinum(II) Complexes with Greater than Classical π-π Stacking and Pt-Pt Distances *Organometallics* **2005**, *24*, 619.

(6) Thompson, M. E.; Burrows, P. E.; Forrest, S. R. Electrophosphorescence in Organic Light Emitting Diodes *Curr. Opin. Solid State Mater. Sci.* **1999**, *4*, 369.

(7) D'Andrade, B. W.; Brooks, J.; Adamovich, V.; Thompson, M. E.; Forrest, S. R. White Light Emission Using Triplet Excimers in Electrophosphorescent Organic Light-Emitting Devices *Adv. Mater.* **2002**, *14*, 1032.

(8) Adamovich, V.; Brooks, J.; Tamayo, A.; Alexander, A. M.; Djurovich, P. I.; D'Andrade, B. W.; Adachi, C.; Forrest, S. R.; Thompson, M. E. High Efficiency

Single Dopant White Electrophosphorescent Light Emitting Diodes *New J. Chem.* **2002**, *26*, 1171.

(9) Furuta, P. T.; Deng, L.; Garon, S.; Thompson, M. E.; Fréchet, J. M. J. Platinum-Functionalized Random Copolymers for Use in Solution-Processible, Efficient, near-White Organic Light-Emitting Diodes *J. Am. Chem. Soc.* **2004**, *126*, 15388.

(10) Hreha, R. D.; George, C. P.; Haldi, A.; Domercq, B.; Malagoli, M.; Barlow, S.; Brédas, J. L.; Kippelen, B.; Marder, S. R. 2,7-Bis(diarylamino)-9,9-dimethylfluorenes as Hole-Transport Materials for Organic Light-Emitting Diodes *Adv. Funct. Mater.* **2003**, *13*, 967.

(11) Lamansky, S.; Djurovich, P.; Murphy, D.; Abdel-Razzaq, F.; Lee, H. E.; Adachi, C.; Burrows, P. E.; Forrest, S. R.; Thompson, M. E. Highly Phosphorescent Bis-Cyclometalated Iridium Complexes: Synthesis, Photophysical Characterization, and Use in Organic Light Emitting Diodes *J. Am. Chem. Soc.* **2001**, *123*, 4304.

(12) Tsuboyama, A.; Iwawaki, H.; Furugori, M.; Mukaide, T.; Kamatani, J.; Igawa, S.; Moriyama, T.; Miura, S.; Takiguchi, T.; Okada, S.; Hoshino, M.; Ueno, K. Homoleptic Cyclometalated Iridium Complexes with Highly Efficient Red Phosphorescence and Application to Organic Light-Emitting Diode *J. Am. Chem. Soc.* **2003**, *125*, 12971.

(13) Nazeeruddin, M. K.; Humphry-Baker, R.; Berner, D.; Rivier, S.; Zuppiroli, L.; Graetzel, M. Highly Phosphorescence Iridium Complexes and Their Application in Organic Light-Emitting Devices *J. Am. Chem. Soc.* **2003**, *125*, 8790.

(14) Chang, S. Y.; Kavitha, J.; Li, S. W.; Hsu, C. S.; Chi, Y.; Yeh, Y. S.; Chou, P. T.; Lee, G. H.; Carty, A. J.; Tao, Y. T.; Chien, C. H. Platinum(II) Complexes with Pyridyl Azolate-Based Chelates: Synthesis, Structural Characterization, and Tuning of Photo- and Electrophosphorescence *Inorg. Chem.* **2006**, *45*, 137.

(15) Kondakov, D. Y.; Lenhart, W. C.; Nichols, W. F. Operational Degradation of Organic Light-Emitting Diodes: Mechanism and Identification of Chemical Products *J. Appl. Phys.* **2007**, *101*.

(16) Marsal, P.; Avilov, I.; da Silva, D. A.; Brédas, J. L.; Beljonne, D. Molecular Hosts for Triplet Emission in Light Emitting Diodes: A Quantum-Chemical Study *Chem. Phys. Lett.* **2004**, *392*, 521.

CHAPTER 5

$Ir(ppy)_3$ FUNCTIONALIZED POLY(CYCLOOCTENE)S

5.1 Abstract

This chapter describes the synthesis and characterization of poly(cyclooctene)s with pendant carbazole groups and facial iridium tris-2-phenylpyridine (fac-$Ir(ppy)_3$).[1] Carbazole-based comonomers were used to increase the solubility of the polymers and to obtain energy transfer from carbazole units into the metal complexes. Excitation spectra of all polymers proved the presence of the energy transfer. All copolymers retained the optical properties associated to their corresponding metal complex analogues. Furthermore, it is established that the polymer backbone does not interfere with the optical properties of the metal complexes, making these polymers promising materials for OLEDs.

5.2 Introduction

The most promising iridium complexes in terms of device performances are 2-phenylpyridine based complexes such as $Ir(ppy)_3$ and $Ir(ppy)_2(acac)$.[2-6] External quantum efficiencies around 20% with near 100% internal quantum efficiencies have been obtained for devices utilizing these complexes doped into a wide energy gap host.[3] As discussed in Chapter 2, these complexes are attached to a variety of polymer backbones in the hopes of obtaining the outstanding device performances of the small molecule analogues.[7-9] Unfortunately, performances of the devices with these polymeric materials are not comparable to those of small molecule analogues. The potential advantages of

poly(cyclooctene)s over the polymer backbones discussed in Chapter 2 are described in Chapter 3. By using the same rationale, it can be concluded that $Ir(ppy)_3$ functionalized poly(cyclooctene)s might have properties that are appealing in terms of device performance. In this chapter, attachment of $Ir(ppy)_3$ to poly(cyclooctene) backbones, and a basic photoluminescence characterization of the polymers are reported.

5.3 Results and Discussion

Synthesis. The synthesis of the $Ir(ppy)_3$ containing monomer **3** is shown in Scheme 5.1. Coupling of **1**[10] with **2**[11] yielded target monomer **3**. The polymerizations using **3** were carried out using Grubbs' third generation catalyst. During the homopolymerization of **3**, the resulting polymers precipitated out of solution. Considering the fact that a large dipole moment of 6.5 D has been calculated for *fac*-$Ir(ppy)_3$,[12] we have recently proposed that aggregation may occur in homopolymers, where the *fac*-$Ir(ppy)_3$ complexes are forced to be in close proximity to each other.[11] Furthermore, it is also well-known that high concentration of metal complexes can give rise to self quenching due to triplet-triplet annihilation.[13] Therefore, in order to minimize self-quenching and to maximize solubility, compound **4** (see Section 3.3.1 for the synthesis of compound **4**) is employed as a comonomer. The copolymerization of **3** and **4** is also shown in Scheme 5.1. Again, the third generation Grubbs initiator[14] was used for the polymerization. The percentages of the metal complex containing monomer **3** in copolymers **5a**, **5b**, and **5c** were 20%, 10%, and 5%, respectively. The molecular weights of the copolymers are given in Table 1 and range from 13,000-22,000. While no glass transition temperature was observed for copolymers **5a-c**, they all underwent 5% weight loss at around 290 ^{o}C as determined by TGA.

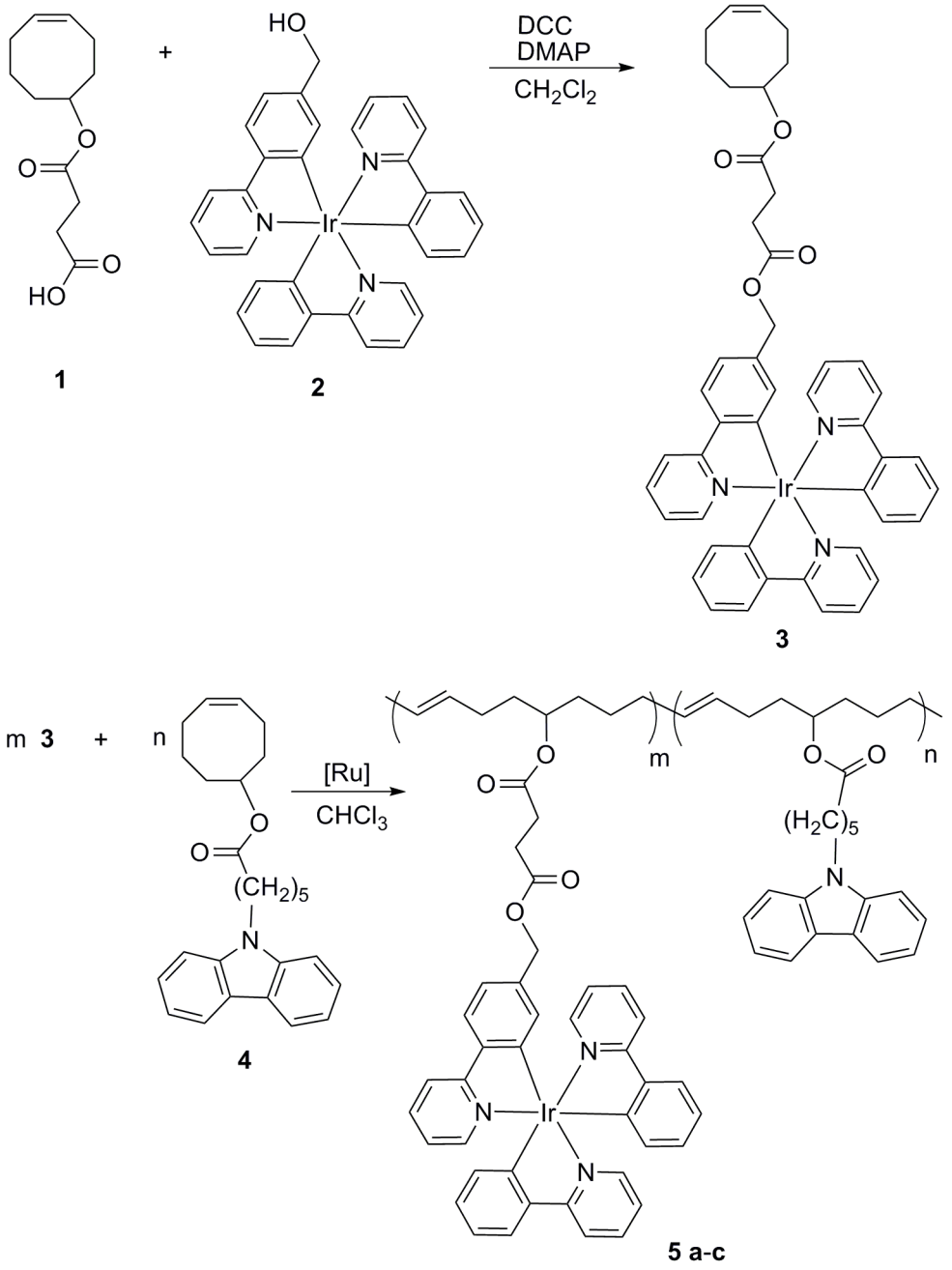

Scheme 5.1 Syntheses of $Ir(ppy)_3$ copolymers.

Table 5.1 Polymer characterization data.

Compound	M_n (kDa)	M_w (kDa)	PDI
5a	3.5	13.3	3.82
5b	4.2	21.8	5.20
5c	3.5	15.6	4.42

Photophysical Properties. After establishing the basic polymer properties, photophysical characterizations of the copolymers were carried out. The optical properties of all copolymers are listed in Table 5.2 and shown in Figure 5.1. For compound **3**, the absorption spectrum showed the typical metal to ligand charge-transfer (MLCT) transitions of *fac*-Ir(ppy)$_3$ around 380 nm. Copolymers **5a-c** retain the characteristic absorption bands of their corresponding monomers 3 and 4.

Table 5.2 Photophysical properties of the copolymers

Compound	λ_{abs}[a] (nm)	λ_{em}[a,b] (nm)	λ_{em}[b,c] (nm)	Φ[d,e]	τ[f] (ns)	τ[g] (ns)
5a	332, 344, 378	514	515	0.95	52	1419
5b	330, 344, 376	512	514	0.93	64	1400
5c	330, 344, 376	513	514	0.87	55	1263

[a] in chloroform solutions. [b] all polymers were excited at 380 nm. [c] in the solid state. [d] in degassed THF solutions. [e] relative to Ir(ppy)$_3$. [f] luminescence lifetime in THF solution. [g] luminescence lifetime in degassed THF solution.

The photoluminescence spectra of copolymers **5a-c** are shown in Figure 5.1(a) and are almost identical to the reference compound fac-Ir(ppy)$_3$. The solution and the solid-state emission maxima of all copolymers are almost identical (Table 2). These results in combination with the above described absorption spectra suggest that the poly(cyclooctene) backbone does not interfere with the photophysical properties of the pendant metal complexes.

To investigate whether energy transfer occurs between the carbazole units and the metal complexes, we measured the excitation spectra of polymers **5a-c**. Figure 5.1(b) shows the excitation spectra of **5a-c**, and the absorption spectra of **3**, **4**, and **5b**. As discussed in Section 3.3.2, the two local maxima at 330 and 345 nm in the absorption spectra of **5a-c** originate from the carbazole units, while the broad absorption maximum at 380 nm is attributable to the metal complex. Relative intensities of the carbazole bands and the MLCT band around 380 nm indicate the extent of the energy transfer. The high intensities of the carbazole bands compared to MLCT bands in the excitation spectra of **5a-c** indicate that there is significant energy transfer from the carbazole units into the metal moieties. These results prove that carbazole groups in copolymers **5a-c** act as efficient photoactive units that lead to enhanced optical properties. These results in combination with the known hole-transporting ability of carbazole make these copolymers promising candidates as materials for OLED applications.

Finally, we measured the emission quantum yields and lifetimes, which are listed in Table 5.2. The quantum yields and lifetimes of **5a-c** are close to those of the reference compound *fac*-Ir(ppy)$_3$. The emission lifetimes of **5a-c** are strongly affected by the presence of oxygen. This can be explained by the quenching of the relatively long-lived ^{3}MLCT state of Ir(ppy)$_3$ by oxygen (see Section 1.3 for the emission pathway).

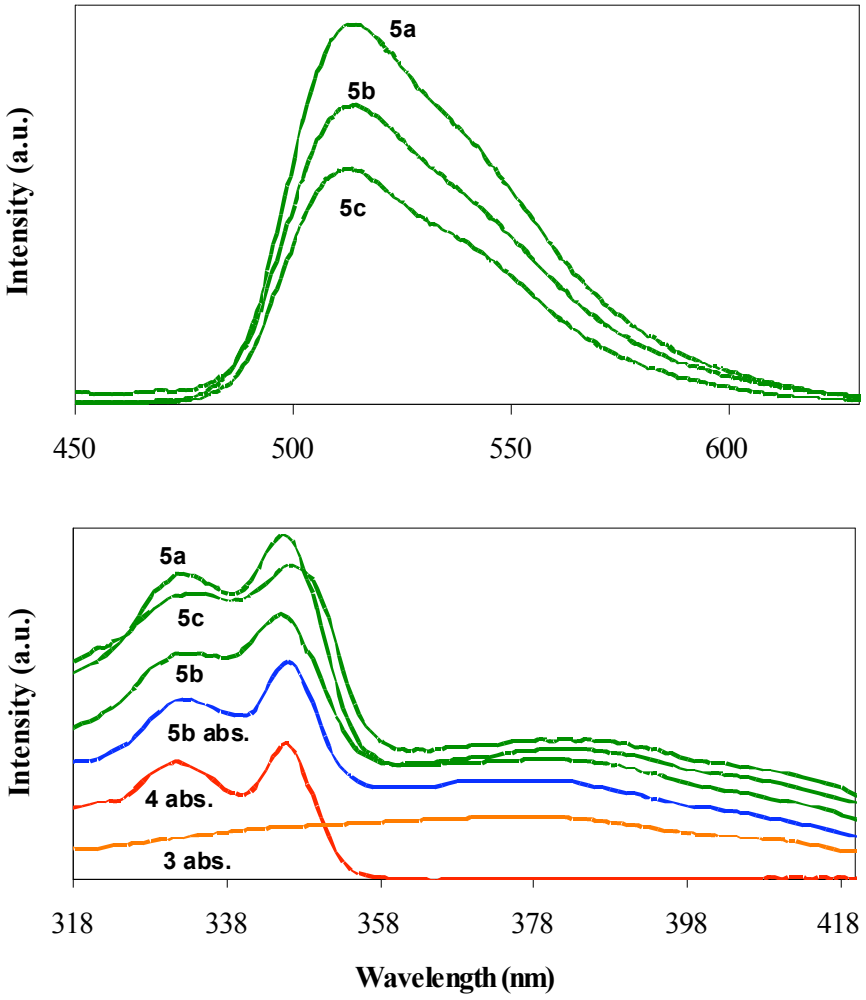

Figure 5.1 Solid state emission spectra of the copolymers (top); solid state excitation spectra of **5a-c** (monitored emission wavelength = 530 nm), and absorption spectra (in chloroform) of **5b**, **4,** and **3** (bottom).

5.4 Conclusion

We have synthesized via ring-opening metathesis polymerization poly(cyclooctene)s containing carbazole and *fac*-Ir(ppy)$_3$ moieties in the side-chains. By characterizing the optical properties of these materials, we were able to prove significant energy transfer from the carbazole units into the metal complex for each copolymer. Furthermore, we were able to show that the copolymers retained the optical properties of their corresponding metal complex analogues. These results in combination with the

random coil configuration of the poly(cyclooctene) backbone, which can provide a morphology that can be highly beneficial during device fabrication, make our copolymers promising candidates as materials for OLEDs.

5.5 Experimental

All Reagents were purchased either from Acros Organics or Aldrich and used without further purification. ^{1}H-NMR and ^{13}C-NMR spectra (300 MHz ^{1}H NMR, 75 MHz ^{13}C NMR) were taken using a Varian Mercury Vx 300 spectrometer. All spectra are referenced to residual proton solvent. Abbreviations used include singlet (s), doublet (d), triplet (t), and unresolved multiplet (m). Mass spectral analyses were provided by the Georgia Tech Mass Spectrometry Facility. Gel-permeation chromatography (GPC) analyses were carried out using a Waters 1525 binary pump coupled to a Waters 2414 refractive index detector with methylene chloride as an eluant on American Polymer Standards 10 μm particle size, linear mixed bed packing columns. The flow rate used for all the measurements was 1 mL/min. All GPC measurements were calibrated using poly(styrene) standards and carried out at room temperature. The glass-transition temperature of the polymers (Tg) was measured by differential-scanning calorimetry (DSC). The DSC analyses were performed under an atmosphere of nitrogen using a Mettler Toledo DSC 822e that was calibrated using indium standards. The temperature program provided two heating and cooling cycles between -50 and 100 ^{o}C at 10 ^{o}C/min, with the sample size ranging from 5 to 9 mg. The onset of thermal degradation for the polymers (T_d) was measured by thermal gravimetric analysis (TGA). The TGA analyses were performed under an atmosphere of nitrogen using a Shimadzu TGA-50 and all samples were heated from 25 to 450 ^{o}C at a rate of 10 ^{o}C /min. UV/vis absorption measurements were taken on a Shimadzu UV-2401 PC recording spectrophotometer. Emission measurements were acquired using a Shimadzu RF-5301 PC

spectrofluorophotometer. Lifetime measurements were taken using a PTI model C-72 fluorescence laser spectrophotometer with a PTI GL-3300 nitrogen laser.

Synthesis of *fac*-bis(2-phenyl-pyridine)iridium (III) cyclooct-4-enyl 4-(pyridin-2-yl)benzyl succinate, 3. Compounds **1** (320 mg, 0.48 mmol), **2** (130 mg, 0.57 mmol), and dimethylaminopyridine (DMAP) (6.4 mg, 0.05 mmol) were combined in 20 mL of dichloromethane. A solution of dicyclohexylcarbodiimide (DCC) (110 mg, 0.53 mmol) in 5 mL of dichloromethane was added and the reaction was stirred under argon at ambient temperatures for 24 h. The solvent was evaporated, and the residue was purified via column chromatography (silica, eluent: dichloromethane) to give compound **3** as a bright yellow powder in 30% yield. ^{1}H NMR ($CDCl_3$): δ = 7.82 (d, 3H, *J* = 8.1 Hz), 7.63 (m, 3H), 7.50 (m, 6H), 6.85 (m, 11H), 5.66 (m, 2H), 4.93 (s, 2H), 4.85 (m, 1H), 2.55 (t, 4H, *J* = 3.9 Hz), 2.32-213 (m, 4H), 1.85-1.60 (m, 6H). ^{13}C NMR ($CDCl_3$): δ = 172.5, 171.9, 166.8, 166.4, 161.8, 161.2, 160.9, 147.2, 143.9, 137.3, 136.8, 136.2, 130.0, 129.9, 124.1, 122.3, 120.1, 119.0, 76.3, 67.2, 33.9, 33.8, 29.9, 29.6, 25.8, 25.1, 22.6. MS Calcd (M): 893.3. Found (MALDI): 893.3 (M). EA Calcd: C, 61.87; H, 4.74; N, 4.71. Found: C, 61.36; H, 4.56; N, 5.08

Synthesis of Ir(ppy)$_3$-copolymers 5a-c. Monomers **3** and **4** were dissolved in chloroform (ratios of **3**:**4** = 1:4, 1:9, or 1:19). Then, a chloroform solution of Grubbs' third generation ruthenium initiator was added to the monomer solution (monomer: initiator ratio = 25:1) and the reaction mixture was stirred for 20 minutes. After the polymerization was complete, ethyl vinyl ether was added to terminate the polymerization. After stirring for an additional 10 minutes, the solution was concentrated and the residue was precipitated into methanol. The resulting precipitate was collected and dissolved in a small amount of $CHCl_3$ and reprecipitated into methanol. This purification procedure was repeated several times. The final polymers were collected as brown solids **5a-c**. ^{1}H NMR ($CDCl_3$, 300 MHz): δ = 8.08 (broad, m), 7.83 (broad), 7.62 (broad), 7.41 (broad, m), 7.22 (broad, m), 6.84 (broad), 5.34 (broad), 4.87 (broad), 4.27

(broad), 2.56 (broad), 2.23 (broad), 2.07-1.79 (broad), 1.73-1.23 (broad, m). ^{13}C NMR (75 MHz, $CDCl_3$): δ = 173.5, 172.5, 172.3, 166.9, 166.5, 161.9, 161.3, 161.2, 147.3, 143.9, 140.7, 137.4, 136.9, 136.3, 130.7, 130.6, 130.1, 129.9, 129.6, 129.4, 128.8, 126.3, 125.9, 124.3, 123.1, 122.2, 120.7, 120.2, 119.4, 119.1, 108.9, 74.3, 73.8, 67.2, 43.1, 34.7, 34.4, 34.0, 33.6, 32.8, 29.8, 29.7, 29.0, 28.8, 27.3, 27.1, 25.6, 25.3, 25.1, 23.6.

5.6 References

(1) The contents of this chapter have been published. See: Kimyonok, A.; Weck, M. Poly(cyclooctene)s with Pendant Fluorescent and Phosphorescent Metal Complexes *Macromol. Rapid Commun.* **2007**, *28*, 152.

(2) Adachi, C.; Baldo, M. A.; Forrest, S. R.; Thompson, M. E. High-Efficiency Organic Electrophosphorescent Devices with Tris(2-phenylpyridine)iridium Doped into Electron-Transporting Materials *Appl. Phys. Lett.* **2000**, *77*, 904.

(3) Adachi, C.; Baldo, M. A.; Thompson, M. E.; Forrest, S. R. Nearly 100% Internal Phosphorescence Efficiency in an Organic Light-Emitting Device *J. Appl. Phys.* **2001**, *90*, 5048.

(4) Baldo, M. A.; Lamansky, S.; Burrows, P. E.; Thompson, M. E.; Forrest, S. R. Very High-Efficiency Green Organic Light-Emitting Devices Based on Electrophosphorescence *Appl. Phys. Lett.* **1999**, *75*, 4.

(5) Lamansky, S.; Djurovich, P.; Murphy, D.; Abdel-Razzaq, F.; Lee, H. E.; Adachi, C.; Burrows, P. E.; Forrest, S. R.; Thompson, M. E. Highly Phosphorescent Bis-Cyclometalated Iridium Complexes: Synthesis, Photophysical Characterization, and Use in Organic Light Emitting Diodes *J. Am. Chem. Soc.* **2001**, *123*, 4304.

(6) Kawamura, Y.; Brooks, J.; Brown, J. J.; Sasabe, H.; Adachi, C. Intermolecular Interaction and a Concentration-Quenching Mechanism of Phosphorescent Ir(III) Complexes in a Solid Film *Phys. Rev. Lett.* **2006**, *96*.

(7) Chen, X. W.; Liao, J. L.; Liang, Y. M.; Ahmed, M. O.; Tseng, H. E.; Chen, S. A. High-Efficiency Red-Light Emission from Polyfluorenes Grafted with Cyclometalated Iridium Complexes and Charge Transport Moiety *J. Am. Chem. Soc.* **2003**, *125*, 636.

(8) Jiang, J. X.; Jiang, C. Y.; Yang, W.; Zhen, H. G.; Huang, F.; Cao, Y. High-Efficiency Electrophosphorescent Fluorene-alt-Carbazole Copolymers N-Grafted with Cyclometalated Ir Complexes *Macromolecules* **2005**, *38*, 4072.

(9) You, Y.; Kim, S. H.; Jung, H. K.; Park, S. Y. Blue Electrophosphorescence from Iridium Complex Covalently Bonded to the Poly (9-dodecyl-3-vinylcarbazole):

Suppressed Phase Segregation and Enhanced Energy Transfer *Macromolecules* **2006**, *39*, 349.

(10) Breitenkamp, K.; Simeone, J.; Jin, E.; Emrick, T. Novel Amphiphilic Graft Copolymers Prepared by Ring-Opening Metathesis Polymerization of Poly(ethylene glycol)-Substituted Cyclooctene Macromonomers *Macromolecules* **2002**, *35*, 9249.

(11) Carlise, J. R.; Wang, X. Y.; Weck, M. Phosphorescent Side-Chain Functionalized Poly(norbornene)s Containing Iridium Complexes *Macromolecules* **2005**, *38*, 9000.

(12) Breu, J.; Stössel, P.; Schrader, S.; Starukhin, A.; Finkenzeller, W. J.; Yersin, H. Crystal Structure of *fac*-Ir(ppy)$_3$ and Emission Properties under Ambient Conditions and at High Pressure *Chem. Mater.* **2005**, *17*, 1745.

(13) Hercules, D. M. *Fluorescence and Phosphorescence Analysis: Principles and Applications*; Interscience Publishers: New York, 1966.

(14) Love, J. A.; Morgan, J. P.; Trnka, T. M.; Grubbs, R. H. A Practical and Highly Active Ruthenium-Based Catalyst that Effects the Cross Metathesis of Acrylonitrile *Angew. Chem. Int. Ed.* **2002**, *41*, 4035.

CHAPTER 6

FUNCTIONALIZATION OF POLYMERS WITH PHOSPHORESCENT IRIDIUM COMPLEXES *VIA* 1,3 DIPOLAR CYCLOADDITIONS

6.1 Abstract

In this Chapter, a simple yet highly efficient route to prepare polymers with a variety of pendant iridium complexes as potential materials in organic light-emitting diodes by employing click chemistry is reported.[1] A quantitative conversion is observed for the post-polymerization functionalization of the azide containing polymers with the alkyne functionalized iridium complexes. Photophysical characterization of the polymers revealed that the polymers retain the photoluminescence properties of the small molecule analogues. In contrast, electroluminescence studies indicate that the triazole ring on the spacer adversely affects the device performance.

6.2 Introduction

In Chapter 2, polymers with emissive metal complexes are reviewed. In these reports, the functionalized polymers were synthesized either by the polymerization of monomers containing the desired metal complex as a side-chain or by the modification of polymers with the metal complex in a post polymerization reaction. While the former strategy can have a highly controlled and quantitative metal complex functionalization, the latter approach is modular, with the potential to attach a library of metal complexes onto the polymer backbone. However, a high yielding orthogonal covalent functionalization is crucial for the success of the modular post polymerization approach.

In this chapter such a strategy is presented by taking advantage of the 1,3-dipolar cycloaddition reactions, often referred to as "click chemistry".[2-5] This transformation is widely used due to its high tolerance to functional groups, high reaction yields, and mild reaction conditions.[6,7]

The polymers described in this chapter are based on two different comonomers, styrene and *N*-vinyl carbazole. Styrene was functionalized with azide units for easy, high yielding click reactions with alkyne-containing iridium complexes. As discussed in the previous chapters, the role of the second comonomer, *N*-vinyl carbazole is manifold. Firstly, poly (*N*-vinyl carbazole) has been employed extensively as a host material in OLEDs due to its hole-transport properties and its high-energy singlet excited state.[8-10] Moreover, it prevents self quenching and aggregation of metal centers by decreasing the concentration of the iridium complexes along the polymer backbone. Three different iridium complexes with different emission colors are employed to demonstrate the versatility of the approach.

6.3 Results and Discussion

Synthesis. The synthetic route toward the fully functionalized copolymers is outlined in Scheme 6.1. All compounds described in this chapter were synthesized by Dr. Xian-Yong Wang, a postdoctoral fellow in the Weck group (see ref. 1 for the experimental procedures). For ease of characterization, relatively low molecular weight polymers were prepared. *N*-vinylcarbazole or styrene were copolymerized with *p*-(chloromethyl)styrene (in ratios of 9:1) using AIBN as the initiator. The chloromethylated copolymers were then converted to the corresponding azides **1** and **2** in 90-95% yields. NMR spectroscopy showed that all chlorine units were transformed into the azide groups. Copolymers **1** and **2** were then reacted with complexes **3-5** *via* click chemistry to yield the desired fully functionalized copolymers **6-11** in 71-93% yields. NMR spectra of copolymers **6-11**

showed complete conversion of the azide groups to the 1,4-disubstituted 1,2,3-triazoles. Copolymers **6-11** are soluble in common organic solvents such as chloroform and THF.

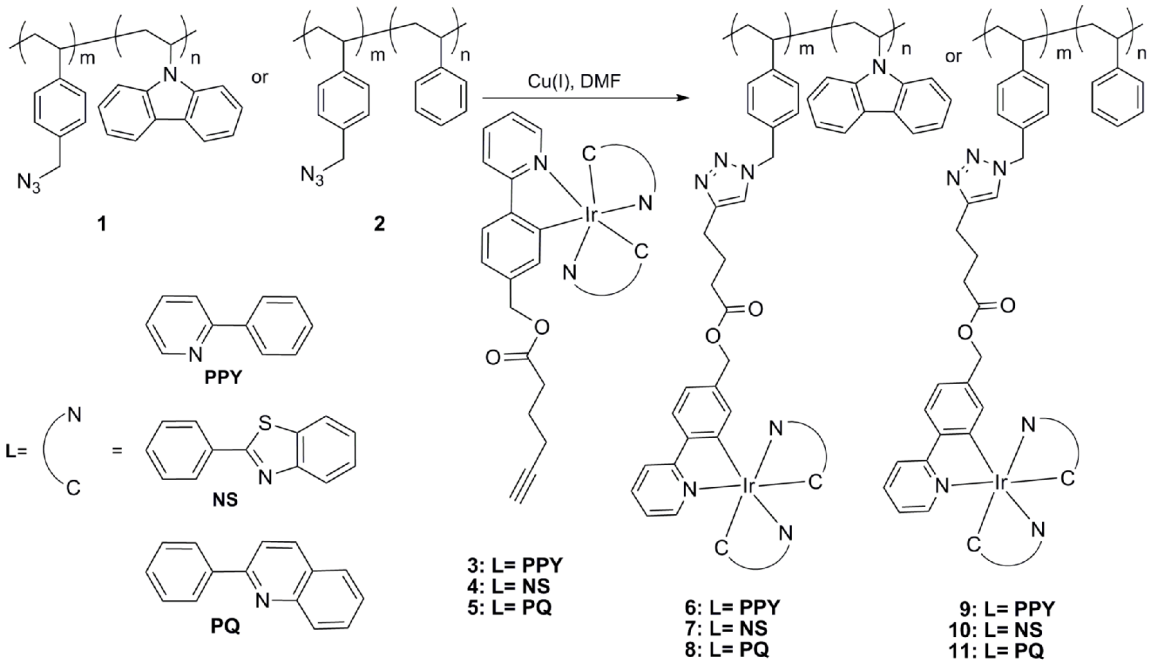

Scheme 6.1 Functionalization of the polymers via click chemistry

Photophysical Properties. Table 6.1 lists the photophysical properties of all copolymers and the corresponding small molecule iridium complex precursors. Figure 6.1(a) and 6.1(b) shows the photoluminescence spectra of the alkyne-functionalized complexes **3-5** and copolymers **6-11** in chloroform solutions and solid state, respectively. UV-vis absorption spectra of **6-11** reveals the characteristic π-π* transitions originating from the ligands of the iridium complexes and the carbazole moiety in the high energy region, whereas in the lower energy region, starting around 380 nm and extending to around 500 nm, weak and broad metal-to-ligand charge-transfer (MLCT) transitions of the iridium complexes are observed. Emission maxima of the copolymers are similar to those of the corresponding small molecule iridium complexes. Compared to the solution emission, the solid state emissions are slightly red shifted for all copolymers (Figure 6.1). These

results indicate that the polymer backbones do not affect the absorption or emission maxima of the tethered metal complexes. On the other hand, slightly different emission quantum yields are obtained for different polymers in comparision to their small molecule analogues (Table 6.1). The emission lifetimes of all compounds are strongly affected by the presence of oxygen, which is due to the quenching of the relatively long-lived ^{3}MLCT state by oxygen, causing a decrease in the emission lifetimes. On the other hand, copolymers with and without carbazole groups have similar lifetimes, indicating that there is no emission quenching related to carbazole units.

Table 6.1. Photophysical data for the complexes **3-5** and copolymers **6-11**

Compound	λ_{max}[a] **(nm)**	λ_{max}[a,b] **(nm)**	λ_{max}[b,c] **(nm)**	Φ[d]	τ[e] **(ns)**	τ[f] **(ns)**
3	282, 383	515	517	0.40	34	1484
9	282, 384	515	522	0.29	45	1000
6	282, 295, 344, 384	515	517	0.40	51	1297
4	290, 310, 324, 395	554	557	0.36	109	1612
10	290, 310, 325, 395	555	556	0.22	95	1393
7	296, 330, 344, 395	554	555	0.19	87	1485
5	273, 293, 329, 410	597	606	0.11	98	1735
11	273, 293, 329, 411	606	612	0.07	88	862
8	282, 295, 332, 345, 407	606	609	0.05	81	740

[a] in THF solution. [b] all the compounds were excited at 400 nm. [c] in the solid-state. [d] photoluminescence quantum yield in THF. [e] emission lifetime in THF. [f] emission lifetime in degassed THF.

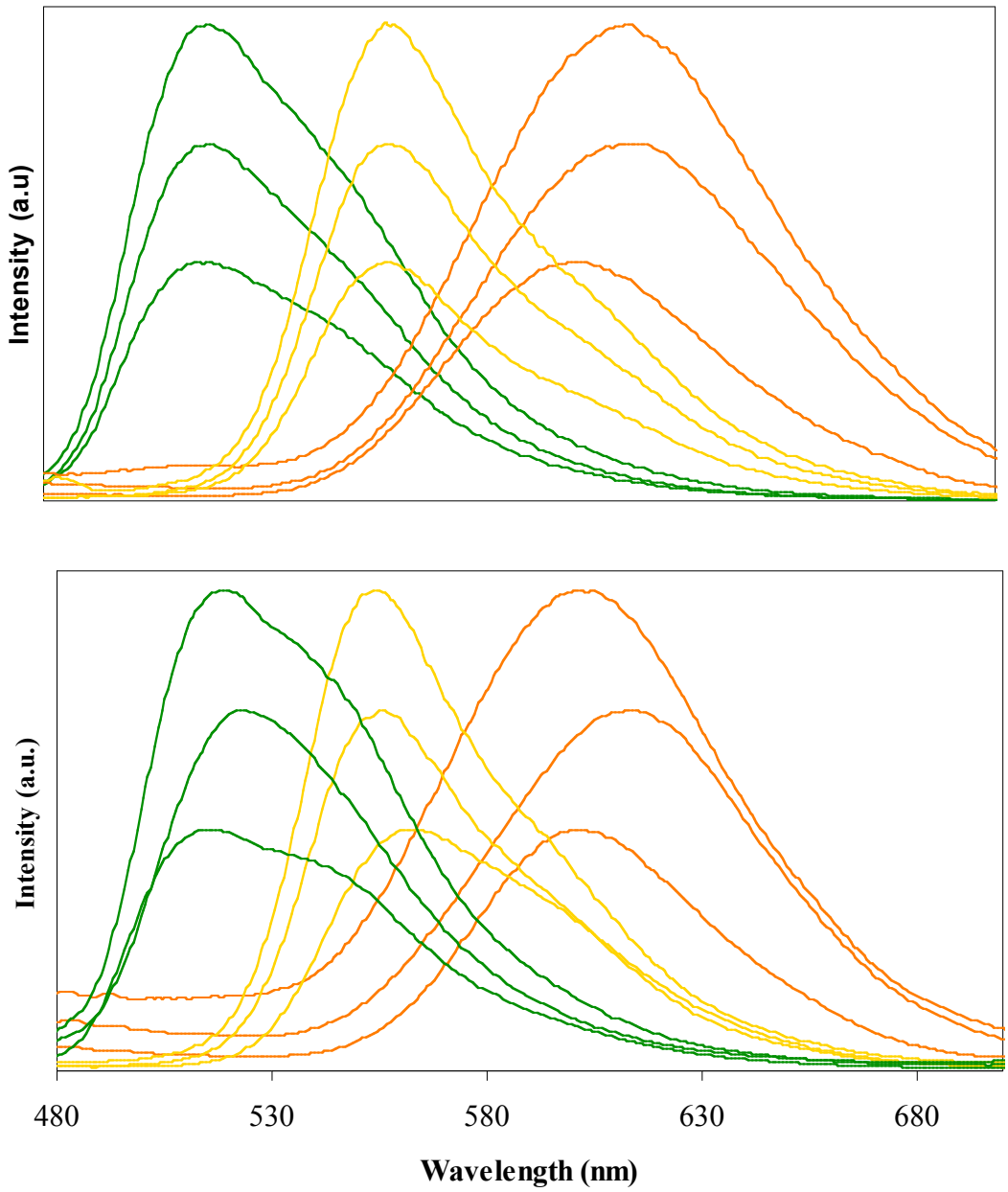

Figure 6.1. Solution emission (top) and solid state emission (bottom) spectra of **3-5** and **6-11.** From top to bottom: green curves: **6**, **9**, **3**; yellow curves: **7**, **10**, **4**; orange curves: **8**, **11**, **5.**

Electroluminescence. Electroluminescence studies were conducted by Andreas Haldi in the Kippelen group at Georgia Institute of Technology. In order to determine the effect of the triazole ring on the device performance, two OLEDs based on either polymer **6** or

an analogue of polymer **6** without the triazole ring, polymer **12**[11], were fabricated. Figure 6.2 shows the structures of polymer **12** and the hole-transport polymer **13** (provided by the Marder Group), which contains crosslinking cinnamate groups that undergo [2+2] cycloaddition upon exposure to UV light.[12,13] Device with polymer **6** as the emissive layer gives an external quantum efficiency of 0.2 % at 100 cd/m^2. When PBD is mixed with the polymer as the electron-transport compound, a slight increase in the efficiency is observed. On the other hand, device with polymer **12** gives EQE of 1.0 % at 100 cd/m^2. The efficieny of the device increases significantly upon blending with PBD (Figure 6.3). These results indicate that although click chemistry is a powerful synthetic tool, the resulting triazole ring adversely affects the device performance, however, the reason for this behavior is not clear, and needs to be further investigated.

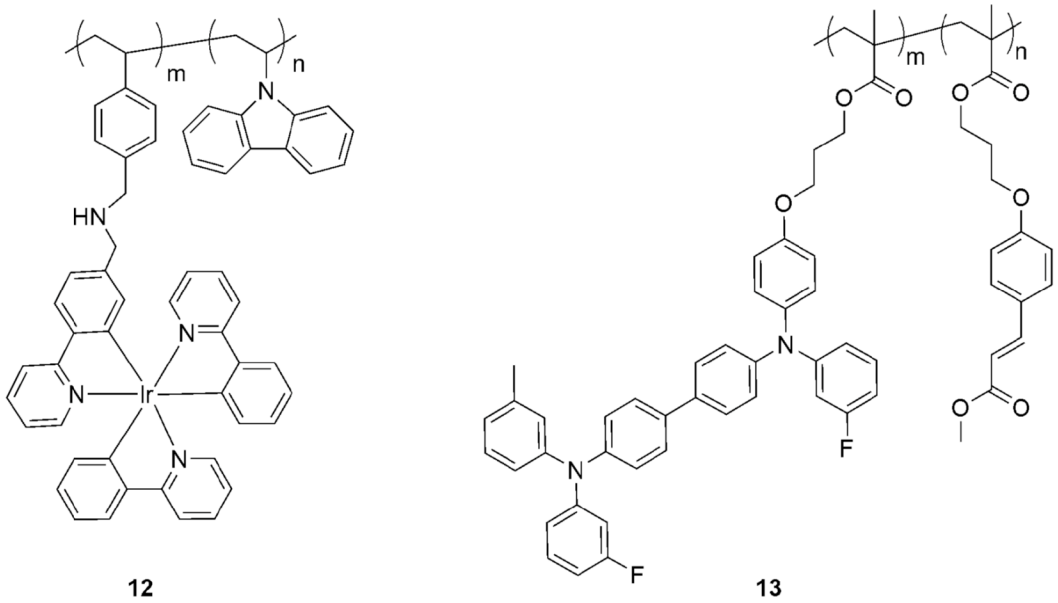

Figure 6.2 Structures of polymer **12** and **13** (for **12**, m:n = 9:1, for **13** m:n = 7:3).

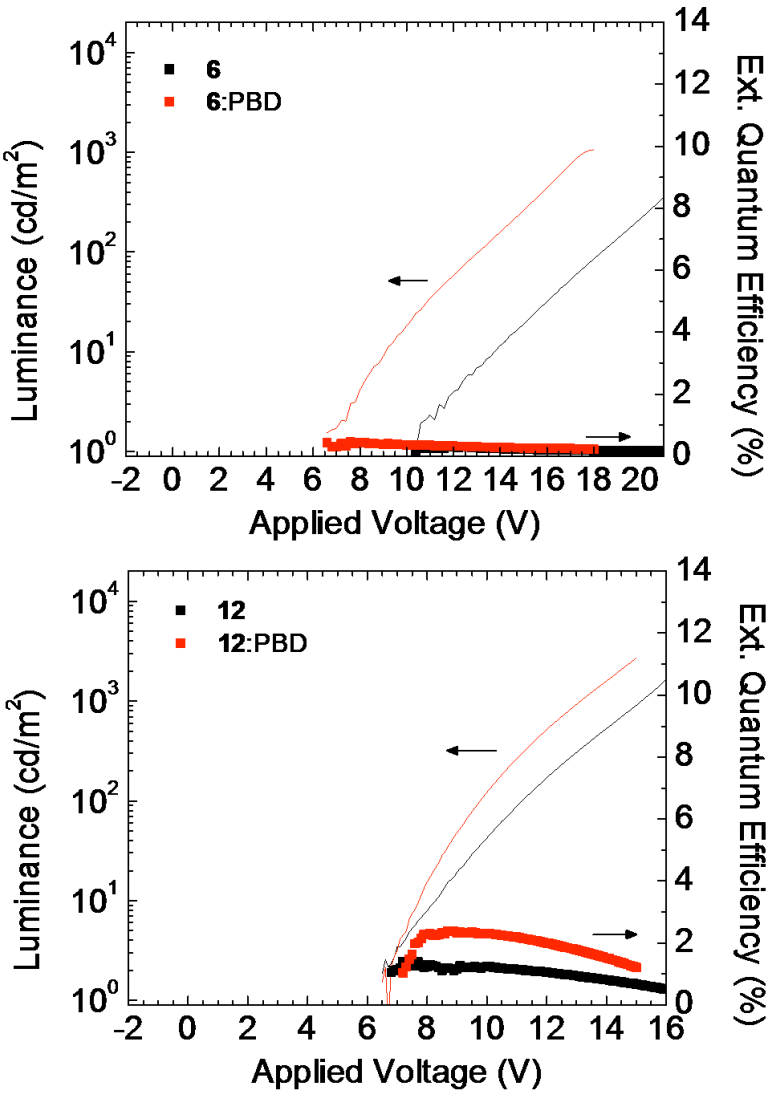

Figure 6.3 Current density, luminance and external quantum efficiency as a function of applied voltage for device with structure ITO/**13** (35 nm)/**(6** or **12)** (35 nm)/BCP (40 nm)/LiF/Al.

6.4 Conclusion

Using high yielding and fully orthogonal 1, 3 dipolar cycloadditions, we have synthesized copolymers with pendant iridium complexes. This functionalization strategy is modular, *i. e.* any alkyne containing the iridium complex can be used. The copolymers

retained the photoluminescence properties associated with their small molecule analogues both in solution and the solid state. The method described herein offers a straightforward synthesis of functionalized polymeric materials with potential applications in OLEDs. On the other hand, effect of the triazole ring on the electroluminescence behavior needs to be further investigated.

6.5 Experimental

All Reagents were purchased either from Acros Organics or Aldrich and used without further purification. UV/vis absorption measurements were taken on a Shimadzu UV-2401 PC recording spectrophotometer. Emission measurements were acquired using a Shimadzu RF-5301 PC spectrofluorophotometer. Lifetime measurements were taken using a PTI model C-72 fluorescence laser spectrophotometer with a PTI GL-3300 nitrogen laser.

6.6 References

(1) The contents of this chapter have been published. See: Wang, X. Y.; Kimyonok, A.; Weck, M. Functionalization of Polymers with Phosphorescent Iridium Complexes *via* Click Chemistry *Chem. Commun.* **2006**, 3933.

(2) Appukkuttan, P.; Van der Eyeken, E. Recent Developments in Microwave-Assisted, Transition-Metal-Catalysed C-C and C-N Bond-Forming Reactions *Eur. J. Org. Chem.* **2008**, 1133.

(3) Nandivada, H.; Jiang, X. W.; Lahann, J. Click Chemistry: Versatility and Control in the Hands of Materials Scientists *Adv. Mater.* **2007**, *19*, 2197.

(4) Moses, J. E.; Moorhouse, A. D. The Growing Applications of Click Chemistry *Chem. Soc. Rev.* **2007**, *36*, 1249.

(5) Binder, W. H.; Sachsenhofer, R. 'Click' Chemistry in Polymer and Materials Science *Macromol. Rapid Commun.* **2007**, *28*, 15.

(6) Kolb, H. C.; Finn, M. G.; Sharpless, K. B. Click Chemistry: Diverse Chemical Function from a Few Good Reactions *Angew. Chem. Int. Ed.* **2001**, *40*, 2004.

(7) Bock, V. D.; Hiemstra, H.; van Maarseveen, J. H. Cu^{I}-Catalyzed Alkyne-Azide "Click" Cycloadditions from a Mechanistic and Synthetic Perspective *Eur. J. Org. Chem.* **2006**, 51.

(8) Kido, J.; Hongawa, K.; Okuyama, K.; Nagai, K. Bright Blue Electroluminescence from Poly(N-vinylcarbazole) *Appl. Phys. Lett.* **1993**, *63*, 2627.

(9) Zhu, W. G.; Liu, C. Z.; Su, L. J.; Yang, W.; Yuan, M.; Cao, Y. Synthesis of New Iridium Complexes and Their Electrophosphorescent Properties in Polymer Light-Emitting Diodes *J. Mater. Chem.* **2003**, *13*, 50.

(10) Gong, X.; Ostrowski, J. C.; Bazan, G. C.; Moses, D.; Heeger, A. J. Red Electrophosphorescence from Polymer Doped with Iridium Complex *Appl. Phys. Lett.* **2002**, *81*, 3711.

(11) Wang, X. Y.; Prabhu, R. N.; Schmehl, R. H.; Weck, M. Polymer-Based Tris(2-phenylpyridine)iridium Complexes *Macromolecules* **2006**, *39*, 3140.

(12) Domercq, B.; Hreha, R. D.; Zhang, Y. D.; Larribeau, N.; Haddock, J. N.; Schultz, C.; Marder, S. R.; Kippelen, B. Photo-Patternable Hole-Transport Polymers for Organic Light-Emitting Diodes *Chem. Mater.* **2003**, *15*, 1491.

(13) Domercq, B.; Hreha, R. D.; Zhang, Y. D.; Haldi, A.; Barlow, S.; Marder, S. R.; Kippelen, B. Organic Light-Emitting Diodes with Multiple Photocrosslinkable Hole-Transport Layers *J. Polym. Sci., Part B:Polym. Phys.* **2003**, *41*, 2726.

CHAPTER 7

POLY(NORBORNENE)S WITH PHOSPHORESCENT IRIDIUM COMPLEXES

7.1 Abstract

Solution-processable copolymers with pendant phosphorescent iridium complexes and 2,7-di(carbazol-9-yl)fluorene type host moieties were synthesized using ruthenium-catalyzed ring-opening metathesis polymerization.[1] Low polydispersity indices, ranging between 1.2–1.3, and molecular weights around 20,000 Daltons were obtained for all copolymers. As a result of the living character of the polymerization of the monomer containing the host moiety, a high degree of control over the molecular weights of all copolymers can be obtained. The photo and electroluminescence properties of all copolymers were investigated. All copolymers retained the photo- and electrophysical properties of the corresponding non-polymeric iridium complexes. Furthermore, as a proof of principle for the potential use of these materials, organic light-emitting devices were fabricated using the orange-emitting copolymer. A maximum external quantum efficiency of 1.9% at 100 cd/m^2 and a turn on voltage of 3.7 V were obtained with photoluminescence quantum yield of 0.10 demonstrating the potential of these copolymers as emissive materials for display and lighting applications.

7.2 Introduction

In Chapters 5 and 6, poly(cyclooctene)s and poly(styrene)s with iridium complexes are described. In this chapter, another type of polymer backbone, poly(norbornene), is investigated. Unlike poly(cyclooctene)s of Chapter 5,

poly(norbornene)s can be synthesized in a living fashion via ROMP.[2] High control over polymerization is desirable in order to have reproducible polymer properties. Furthermore, low PDIs obtained for poly(norbornene)s minimize potentially adverse effects of chain length differences on device performance. Moreover, by simply changing the monomer to catalyst ratio, it is possible to change molecular weights of the polymers, which allows for determination of the molecular weight effect on the device performance. Finally, poly(norbornene)-based backbones are expected to have little or no adverse effects on the charge-carrier mobilities in devices. Indeed, higher hole mobilities have been measured for bis(diarylamino)fluorene-functionalized poly(norbornene)s in comparison to analogous materials based on the more polar poly(acrylate) backbone.[3]

In this Chapter, the synthesis of random copolymers containing 2,7-di(carbazol-9-yl)fluorene-type host moieties and various iridium complexes in the side-chains that emit in various regions of the visible spectrum and their solution and solid-state photoluminescence properties and their solid-state electroluminescence properties are described.

7.3 Results and Discussion

Synthesis. The coupling of 2-phenyl-pyridine (ppy) to *exo*-norbornene carboxylic acid is the key step for the synthesis of the iridium complex-based monomers **10** – **12** (Scheme 1). The emission color of the iridium complexes, and, therefore, the monomers and polymers, can be tuned through variation of the ligand. In our case, we utilized either 2-phenyl-pyridine, 2-phenylquinoline (pq), or 2-benzo[b]thiophen-2-yl-pyridine (btpy) as ligands. This synthetic strategy could not be applied to the synthesis of a blue/green-emitting monomer based on the 2-(2,4-difluoro-phenyl)pyridinato (ppf) ligand since we anticipated that the emission would be red-shifted by the presence of the functionalized

ppy ligand relative to that expected for a $Ir(ppf)_3$-type complex.[4] Therefore, monomer **3** consisting of three ppf-type ligands was synthesized according to the route shown in Scheme 1.

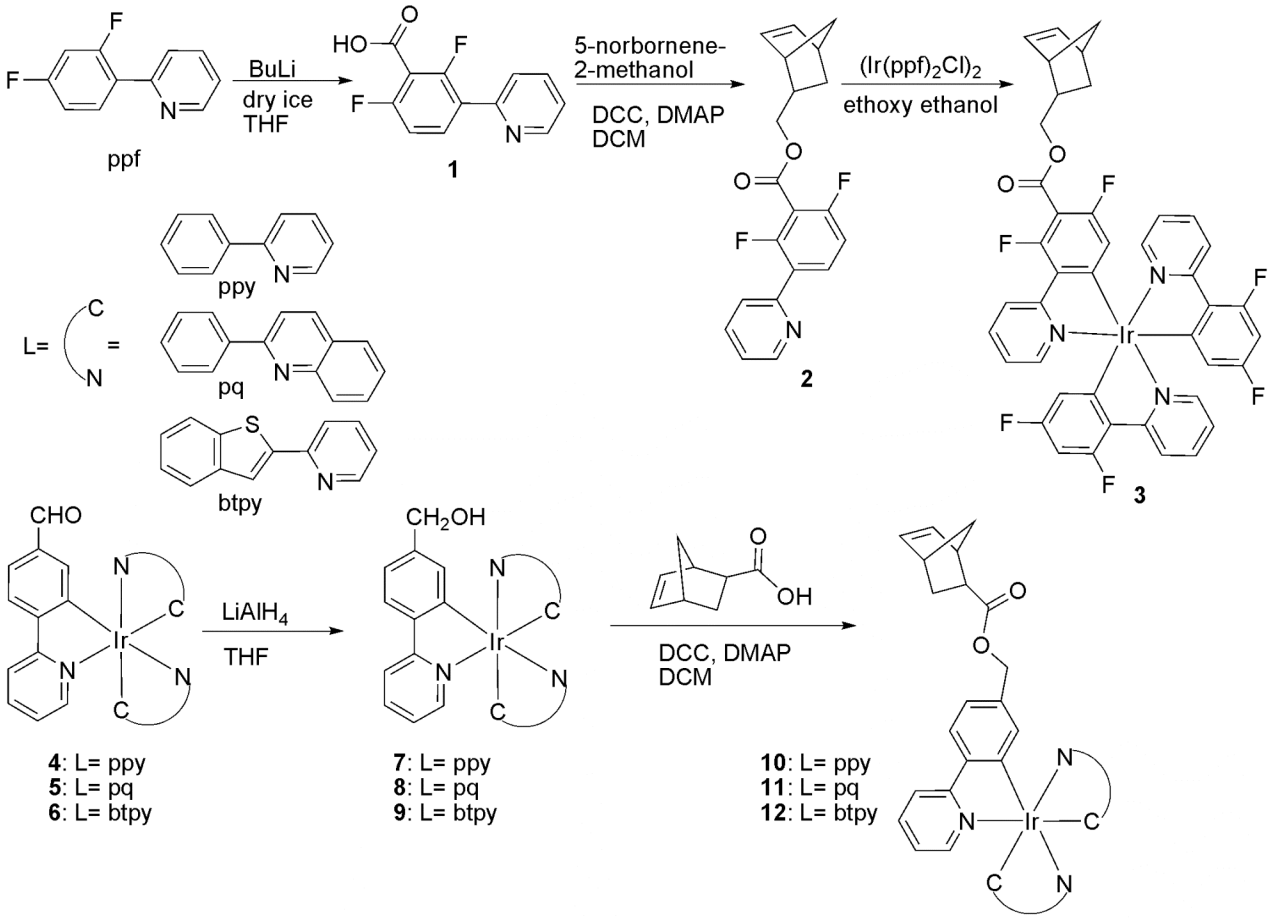

Scheme 7.1 Syntheses of iridium-complex containing monomers **3** and **10** – **12**.

Compounds **4**,[4] **7**,[5] and **10**,[5] were prepared according to literature procedures. Compounds **5** and **8** were prepared by Dr. Xian-Yong Wang and monomer **13** was synthesized by scientists from the Marder Group (see Chapter 4). Compound **1** was obtained by taking advantage of the most acidic hydrogen in the benzene ring of ppf through the reaction of ppf with BuLi, followed by treatment with CO_2 (Scheme 1).[6-8] Coupling of **1** to 5-norbornene-2-methanol yielded **2**, which was metalated to yield the

$Ir(ppf)_3$-based monomer **3**. Complex **6** was synthesized by the reaction of the iridium dimer $(Ir(btpy)_2Cl)_2$ with 4-(2-pyridine)benzaldehyde. The aldehyde group in **6** was reduced to an alcohol using $LiAlH_4$ to give **9**, which was esterified with *exo*-5-norbornene-2-carboxylic acid to yield monomer **12**. Monomer **11** was prepared in the same manner starting with compound **8**.

A living polymerization is key to the successful reproducibility of all desired copolymers. As discussed in Chapter 4, the polymerization of **13** proceeds in a living fashion. Attempts to investigate the living character of the homopolymerization of **3**, and **10**-**12** were not possible because the addition of the ruthenium initiator to the monomer solutions resulted in precipitation of insoluble materials (see Chapter 5 for a detailed discussion on this phenomenon). Therefore, in our materials, comonomer **13** also serves as a spacer and solubilizing unit between the metal complexes in addition to its role in accepting electrons and holes.

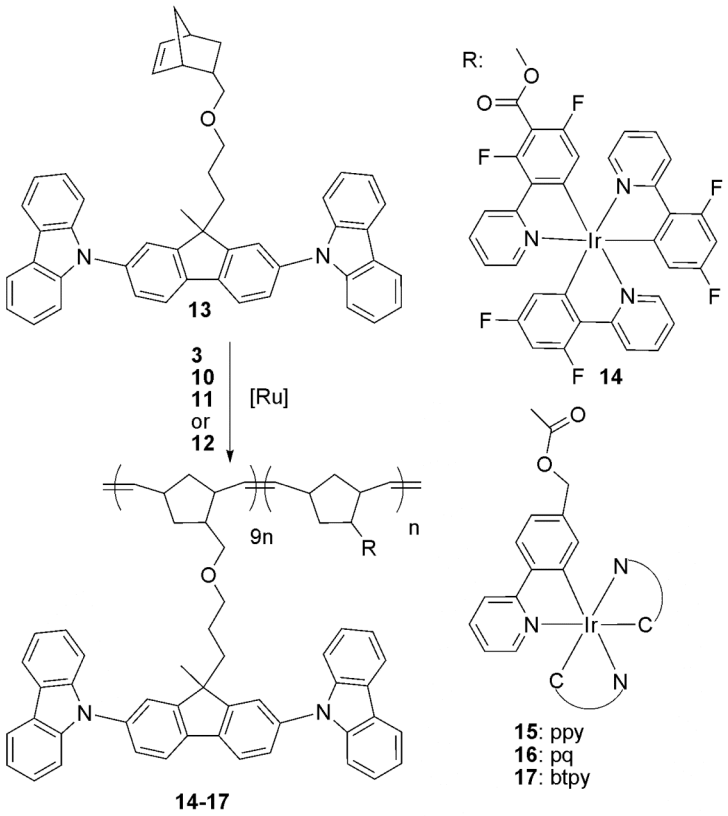

Scheme 7.2 Synthesis of copolymers **14** – **17**.

Copolymerizations of **3**, **10**, **11**, or **12** with **13** were carried out in chloroform at room temperature using Grubbs' third generation initiator (Scheme 7.2). All copolymerizations were complete within 10 minutes. In all copolymers, a 9:1 ratio of **13** to the iridium complex containing monomer was employed and the target degree of polymerization was 50, i.e. monomer to catalyst ratios of 50:1 were employed. As mentioned, attempts to homopolymerize **3**, and **10** – **12** resulted in precipitation of insoluble materials. The high solubilities of copolymers **14** – **17** in common organic solvents suggest a random distribution of the two monomers along the backbone. Table 7.1 lists the polymer properties of copolymers **14** – **17**. All copolymers have molecular weights around 20 kD and polydispersities between 1.22 and 1.31. The low PDIs of the copolymers indicate some degree of control of the polymerizations and ensure that the approximate lengths of the polymer chains are reproducible, minimizing potentially adverse effects of chain length differences on device performance. We observed no glass-transition temperatures for any of the copolymers. All copolymers underwent 5% weight loss at temperatures slightly higher than 300 ^{0}C as measured by thermal gravimetric analysis.

Table 7.1 Polymer characterization data.

Compound	**M_w (kDa)**	**M_n (kDa)**	**PDI**	**T_d[a] (^{o}C)**
14	23.5	18.5	1.24	318
15	25.5	19.5	1.31	324
16	24.5	19.0	1.29	302
17	23.0	19.0	1.22	303

[a]Temperature at 5% weight loss.

Photophysical Properties. The photophysical and electroluminescence properties of the small molecule analogues of the iridium complexes used in this study have been well-characterized in the literature, and devices based on these complexes exhibit promising performances.[9-14] Therefore, we compared the basic photophysical properties of our copolymers to their small molecule analogues to evaluate their potential as materials for OLEDs. Table 7.2 lists the photophysical properties of copolymers **14** – **17**. In solution, the high-energy regions of the absorption spectra of the copolymers are dominated by monomer **13** since its concentration is nine times higher than those of the iridium complex-containing monomers. Thus, the ligand-centered (LC) π-π* transitions typically observed for iridium complexes in the region of 250-350 nm are obscured by transitions attributable to **13** at around 295 nm and 340 nm. In the lower energy region, starting around 380 nm, broad features assignable to metal-to-ligand charge transfer (MLCT) transitions of the iridium complexes are observed.

Table 7.2 Photophysical and electroluminescence properties of copolymers **14** – **17**.

Compound	λ_{abs}[a] **(nm)**	λ_{em}[a,f] **(nm)**	λ_{em}[b,f] **(nm)**	**Φ**[c]	**τ**[d] **(μs)**	**τ**[e] **(μs)**	λ_{el}[g] **(nm)**
14	296, 343, 379	468	474	0.41	0.0637	1.30	511
15	295, 343, 382	512	517	0.33	0.0848	1.43	521
16	295, 342, 408	591	595	0.10	0.1936	1.34	603
17	297, 339, 408	600	600	0.07	0.1664	3.71	602

[a]In chloroform solutions. [b]Peak emission in solid state. [c]In degassed solutions using *fac*-$Ir(ppy)_3$ (Φ = 0.40, in toluene). [d]Luminescence lifetimes in THF solution. [e]Luminescence lifetimes in degassed THF solution. [f]All polymers were excited at 400 nm. [g]Peak EL emission.

The solid-state emissions of the copolymers are slightly red shifted compared to the solution emissions with the exception of **17**. Figure 7.1 shows the solid-state emission spectra of the copolymers. The tunability of the emission of cyclometallated iridium species is well established; relative to $Ir(ppy)_3$, a blue-shifted emission can be obtained by employing electron-withdrawing groups such as fluorine, while the emission of the complexes with extended conjugation is red-shifted.[9-14] The shapes of the peaks and the emission maxima of our copolymers are identical to the corresponding small-molecule iridium complexes, indicating that polymer backbones do not interfere with the emission.

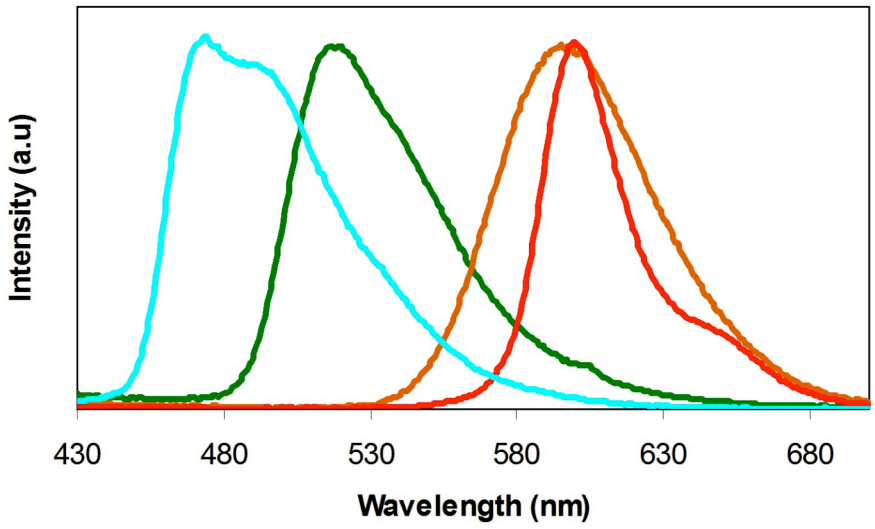

Figure 7.1 Solid-state photoluminescence spectra of copolymers **14** (blue), **15** (green), **16** (orange), and **17** (red).

The solution phosphorescence quantum efficiencies of **14** – **17** were measured using *fac*-$Ir(ppy)_3$ as reference (Φ = 0.40, in toluene) and range from 0.07 to 0.41. The emission lifetimes are strongly affected by the presence of oxygen due to the quenching of the ^{3}MLCT state by oxygen.[15] In degassed solutions, the lifetimes are in the

microsecond region. The measured values of the emission efficiencies and the lifetimes are comparable to those of the corresponding small-molecule complexes.

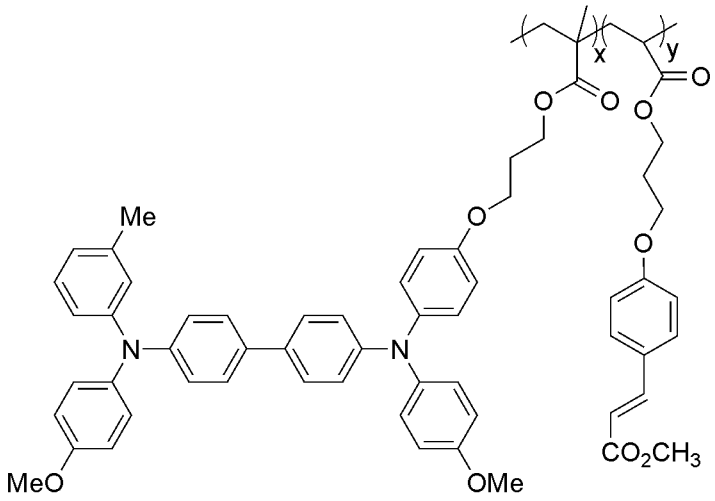

Figure 7.2 Structure of the crosslinkable hole-transport polymer (x:y = 4:1, synthesized by scientists in the Marder Group).

Electroluminescence. Electroluminescence studies were conducted by Andreas Haldi, and Benoit Domercq in the Kippelen group at Georgia Institute of Technology (see ref. 1 for the experimental details). Figure 7.3 shows the electroluminescence spectra of devices in which the copolymers **14** – **17** are used as emitting layers between the cross-linked TPD-based copolymer (Figure 7.2) as a hole-transport material and vacuum-deposited BCP and AlQ_3 as hole-blocking and electron-transport materials, respectively. The similar photoluminescence and electroluminescence spectra of the copolymers suggest that the emission stems from the iridium complex. However, the electroluminescence (EL) spectrum of the device fabricated using copolymer **14** is red-shifted compared to the photoluminescence spectrum. Figure 7.4 shows the electrical characteristics of devices fabricated using copolymer **16** and **17** as emitting layers. The turn-on voltage for the current density is low (ca. 2.4 V) for both devices, and the turn-on voltage for the light for both devices is 3.7 V. External quantum efficiencies at 100

cd/m^2 are 1.9 and 0.9 % for devices with **16** and **17**, respectively. Considering that copolymers **16** and **17** have low photoluminescence quantum efficiencies (10 and 7%, respectively), these results are encouraging. Devices fabricated from copolymers **14** and **15** yielded low light output, indicating inefficient triplet energy transfer from the host material in the copolymer to the metal complex even though previous studies on small molecule devices fabricated from the vapor phase on mixtures of 4,4′-di(carbazol-9-yl)biphenyl (CBP) and Ir(ppy)$_3$ have shown efficient energy transfer between CBP to the phosphor.[16,17] The origin of the lower performance in our red-emitting co-polymer materials compared to their small molecule counterparts is not well understood at this stage and will be further investigated.

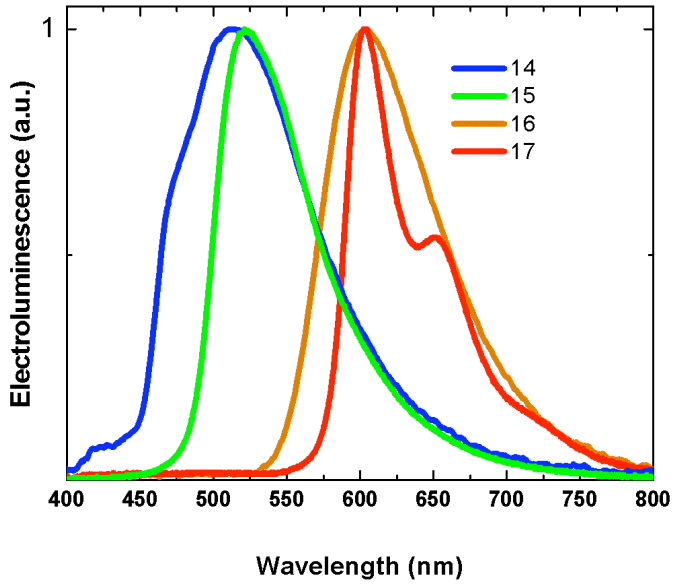

Figure 7.3 Electroluminescence spectra for devices with structure ITO/HT polymer (Fig. 7.2)/**(14 – 17)**/BCP/AlQ$_3$/LiF/Al (35 nm/25 nm/6 nm/20 nm/1 nm/150 nm).

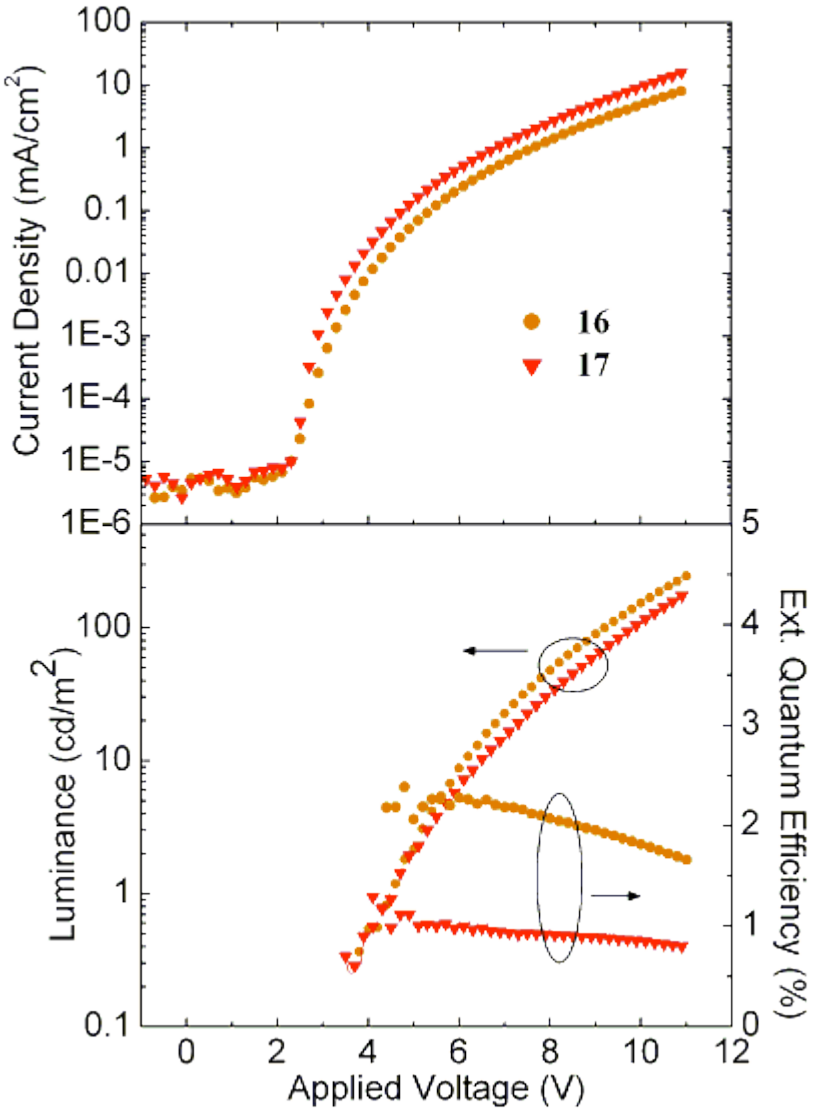

Figure 7.4 Current density, luminance and external quantum efficiency as a function of applied voltage for device with structure ITO/ HT polymer (Fig. 7.2)/**(16** or **17)**/BCP/AlQ_3/LiF/Al (35 nm/25 nm/6 nm/20 nm/1 nm/150 nm).

7.4 Conclusion

We have synthesized a series of norbornene-based copolymers via ROMP that combine emissive iridium complexes with a host material. This design allows for solution processibility and prevents phase separation. Controllable polymerizations and the low PDIs assured that molecular weight differences of the polymer chains are minimized to prevent any possible adverse effect of chain length difference on the device performance. By comparing the iridium containing copolymers to their small molecule analogues, we established that the polymer backbones do not interfere with the basic photophysical properties of the iridium complexes. Furthermore, we employed these copolymers as the emissive layer in OLED devices. Devices based on the orange-emitting copolymer gave encouraging results despite the low phosphorescence quantum yields of the copolymer. These results demonstrate that our methodology allows for the solution-based fabrication of OLED devices from functionalized poly(norbornene)s.

7.5 Experimental

All reagents were purchased either from Acros Organics or Aldrich and used without further purification. ^{1}H-NMR and ^{13}C-NMR spectra (300 MHz ^{1}H NMR, 75 MHz ^{13}C NMR) were obtained using a Varian Mercury Vx 300 spectrometer. All spectra are referenced to residual proton solvent. Abbreviations used include singlet (s), doublet (d), doublet of doublets (dd), triplet (t), triplet of doublets (td) and unresolved multiplet (m). Mass spectral analyses were provided by the Georgia Tech Mass Spectrometry Facility. Gel-permeation chromatography (GPC) analyses were carried out using a Waters 1525 binary pump coupled to a Waters 2414 refractive index detector with methylene chloride as the eluant on American Polymer Standards 10 μm particle size, linear mixed bed packing columns. The flow rate used for all the measurements was 1 mL/min. All GPC measurements were calibrated using poly(styrene) standards and

carried out at room temperature. The onset of thermal degradation for the polymers was measured by thermal gravimetric analysis (TGA) using a Shimadzu TGA-50. UV/vis absorption measurements were taken on a Shimadzu UV-2401 PC recording spectrophotometer. Emission measurements were acquired using a Shimadzu RF-5301 PC spectrofluorophotometer. Elemental analyses for C, H, and N were performed using Perkin Elmer Series II CHNS/O Analyzer 2400. Elemental analyses for iridium were provided by Galbraith Laboratories.

Synthesis of 2,6-difluoro-3-pyridin-2-yl-benzoic acid (1). Under an argon atmosphere, 10.5 mL of a ^{n}BuLi solution (1.6 M in hexanes, 16.8 mmol) was added dropwise at -78 ^{o}C to a THF (55 mL) solution of 2-(2,4-diflouro-phenyl)pyridine (3.2 g, 16.8 mmol). The mixture was stirred for 20 minutes, followed by the addition of freshly crushed dry ice. After stirring for an additional 5 minutes, 10 mL of an aq. HCl solution (1M) was added, followed by the addition of diethyl ether (30 mL). The organic layer was collected and the aqueous layer was washed three times with diethyl ether (30 mL). The combined organic layers were concentrated *in vacuo*, and the target compound was obtained by precipitation into hexanes (2.7 g, 68% yield). ^{1}H NMR (DMSO): δ = 8.72 (d, 1H, J = 3.3 Hz), 8.04 (d, 1H, J = 6.9 Hz), 7.91 (m, 1H), 7.76 (m, 1H), 7.41 (m, 1H), 7.33 (t, 1H, J = 8.7 Hz). ^{13}C NMR (DMSO): δ = 162.8, 161.5, 158.9, 158.0, 155.6, 151.8, 150.6, 137.8, 134.1, 124.9, 124.8, 123.9, 113.6, 113.4, 113.1. MS Calcd (M+1): 236.0. Found (ESI): 236.0 (M+1).

Synthesis of 2,6-difluoro-3-pyridin-2-yl-benzoic acid bicyclo[2.2.1]hept-5-en-2-ylmethyl ester (2). Compound **1** (2.7 g, 11.5 mmol), *exo*-5-norbornene-2-methanol (1.4 g, 11.5 mmol), and dimethylaminopyridine (0.3 g, 2.45 mmol) were combined in 100 mL of THF. A solution of dicyclohexylcarbodiimide (2.7g, 13.1 mmol) in 10 mL of THF was added, and the reaction was stirred under argon at ambient temperatures for 24 h. The solvent was evaporated and the residue was purified via column chromatography (silica, 4:1 hexanes:ethyl acetate) to give compound **2** as a clear oil (2.6 g, 66% yield).

^{1}H NMR ($CDCl_3$): δ = 8.71 (d, 1H, *J* = 4.8 Hz), 8.10 (m, 1H), 7.76 (t, 1H, *J* = 1.5 Hz), 7.74 (m, 1H) 7.26 (m, 1H), 7.07 (td, 1H, *J* = 8.7 Hz, 1.5 Hz), 6.09 (m, 2H), 4.45 (dd, 1H, *J* = 6.6 Hz, 10.8 Hz), 4.28 (dd, 1H, *J* = 9.3 Hz, 10.8 Hz), 2.85 (s, 1H), 2.80 (s, 1H), 1.86 (m, 1H), 1.37 (s, 2H), 1.30 (d, 1H, *J* = 8.4 Hz), 1.24 (m, 1H). ^{13}C NMR ($CDCl_3$): δ = 162.5, 162.4, 159.9, 159.1,158.9, 156.5, 151.9, 150.1,137.2, 136.8, 136.4, 134.2, 134.1, 134.0, 124.6, 124.5, 123.0, 112.8, 112.7, 112.5, 112.4, 70.4, 45.2, 43.9, 41.9, 38.1, 29.8. MS Calcd (M): 341.2. Found (EI): 341.2 (M).

Synthesis of *fac*-exo-bis(2-(4′,6′-difluorophenyl)-pyridinato, N, $C^{2'}$)(2-(5′-bicyclo[2.2.1]hept-5-ene-2-yl ethanoyl-4′,6′-difluorophenyl)pyridinato, N, $C^{2'}$) iridium(III) (3). Compound **2** (75 mg, 0.22 mmol), $(Ir(ppf)_2Cl)_2$ (90 mg, 0.074 mmol),[14] and $AgCF_3SO_3$ (38 mg, 0.148 mmol) were combined in 3 mL of ethoxyethanol. The mixture was purged with argon for 30 minutes followed by stirring at 150 ^{o}C for 24 h under an argon atmosphere. The mixture was cooled to room temperature and water (10 mL) was added to precipitate the product. After filtration, the collected solid was purified via column chromatography (silica, CH_2Cl_2) to yield compound **3** (36 mg, 27% yield). ^{1}H NMR ($CDCl_3$): δ = 8.33 (m, 3H), 7.72 (m, 3H), 7.45 (m, 3H), 6.96 (m, 3H), 6.41 (m, 3H), 6.25 (m, 2H), 6.09 (m, 2H), 4.39 (dd, 1H, *J* = 6.6 Hz, 10.8 Hz), 4.19 (dd, 1H, *J* = 9.3 Hz, 10.8 Hz), 2.84 (s, br, 2H), 1.85 (m, 1H), 1.37 (s, 2H), 1.28 (m, 2H). ^{13}C NMR ($CDCl_3$): δ = 163.7, 163.2, 160.1, 147.3, 147.1, 137.7, 132.6, 123.8, 123.5, 122.9, 122.5, 119.1, 118.2, 97.6, 68.9, 49.6, 44.2, 42.5, 37.9, 29.9, 29.2. MS Calcd (M): 912.9. Found (EI): 912.9 (M). Anal. Calcd. ($C_{42}H_{28}F_6IrN_3O_2$): C, 55.26; H, 3.09; N, 4.60. Found: C, 55.11; H, 3.22; N, 4.66.

Synthesis of *fac*-bis(2-(benzo[b]thiophen-2-yl)-pyridinato, N, $C^{3'}$)(2-(4′-formylphenyl)pyridinato, N, $C^{2'}$) iridium(III) (6). $(Ir(btpy)_2Cl)_2$[9] (1.0 g, 0.77 mmol), 4-(2-pyridyl)benzaldehyde (0.42 g, 2.3 mmol) and $AgCF_3SO_3$ (0.40 g, 1.5 mmol) were combined in 11 mL of ethoxyethanol. The reaction mixture was purged with argon for 30 minutes and then stirred at 150 ^{o}C for 24 h under an argon atmosphere. The solution

was cooled to room temperature and water (20 mL) was added to precipitate the product. After filtration, the collected solid was purified via column chromatography (silica, CH_2Cl_2) to yield compound **6** (0.18 g, 15% yield). ^{1}H NMR ($CDCl_3$): δ = 9.62 (s, 1H), 7.78 (m, 4H), 7.51(m, 7H), 7.39 (d, 1H, *J* = 5.7 Hz), 7.33 (d, 1H, *J* = 1.8 Hz), 7.24 (d, 1H, *J* = 5.4 Hz) 7.09 (m, 2H), 6.93 (td, 1H, *J* = 5.9 Hz, 1.5 Hz), 6.78 (t, 1H, *J* = 7.6 Hz), 6.68 (m, 5H). ^{13}C NMR ($CDCl_3$): δ = 194.7, 165.6, 163.2, 162.6, 160.8, 156.6, 155.9, 150.7, 148.9, 148.1, 147.6, 146.9, 143.7, 143.3, 142.6, 137.6, 137.1, 136.2, 134.6, 134.4, 128.7, 125.2, 124.3, 123.8, 123.7, 122.5, 122.3, 119.9, 119.7, 118.9, 118.8. MS Calcd (M+1): 796.1. Found (ESI): 796.1 (M+1).

Synthesis of *fac*-bis(2-(benzo[b]thiophen-2-yl)-pyridinato, N, $C^{3\prime}$)(2-(4′-hydroxymethylphenyl) pyridinato, N, $C^{2\prime}$) iridium(III) (9). Compound **6** (50 mg, 0.062 mmol) was dissolved in 5 mL of THF and 0.08 mL of lithium aluminum hydride (1M in diethyl ether) was added dropwise. The reaction mixture was stirred at ambient temperatures for 45 minutes and then quenched by the addition of excess water. The crude product, which showed no remaining aldehyde signals by ^{1}H NMR spectroscopy, was dissolved in dichloromethane, washed three times with water, dried with $MgSO_4$ and used without further purification.

Synthesis of *fac*-exo-bis(2-phenyl-quinolinato, N, $C^{2\prime}$)(2-(4′-methyl bicyclo[2.2.1]hept-5-ene-2-carboxyl phenyl)pyridinato, N, $C^{2\prime}$) iridium(III) (11). Compound **8** (1.220 g, 1.55 mmol), *exo*-5-norbornene-2-carboxylic acid (0.245 g, 1.77 mmol), and dimethylaminopyridine (0.100 g, 0.82 mmol) were combined in 60 mL of CH_2Cl_2. A solution of dicyclohexylcarbodiimide (0.370 g, 1.79 mmol) in 10 mL of CH_2Cl_2 was added and the reaction was stirred under argon at ambient temperatures for 24 h. The solvent was evaporated and the residue was purified via column chromatography (silica, CH_2Cl_2) to give compound **11** as an orange powder (1.07 g, 76% yield). ^{1}H NMR ($CDCl_3$): δ = 8.09 (m, 5H), 7.91 (d, 1H, *J* = 8.4 Hz), 7.86 (d, 1H, *J* = 6.9 Hz), 7.70 (m, 2H), 7.62 (d, 2H, *J* = 9.0 Hz), 7.57 (d, 1H, *J* = 9.0 Hz), 7.46 (td, 1H, *J* = 9.0

Hz, 3.0 Hz), 7.40 (d, 1H, *J* = 9.0 Hz), 7.22 (t, 1H, *J* = 7.8 Hz), 7.16 (t, 1H, *J* = 7.8 Hz), 6.95 (m, 3H), 6.71 (m, 7H), 6.50 (d, 1H, *J* = 1.2 Hz), 6.14 (m, 2H), 4.82 (m, 2H), 2.97 (s, br, 1H), 2.91(s, br, 1H), 2.20 (dd, 1H, *J* = 7.2, 4.2), 1.88 (m, 1H), 1.44 (m, 1H), 1.33 (m, 2H). ^{13}C NMR ($CDCl_3$): δ = 176.2, 167.5, 167.4, 165.8, 163.2, 160.6, 158.4, 149.2, 148.8, 148.2, 146.4, 144.9, 143.7, 138.3, 137.6, 137.2, 137.1, 136.3, 136.1, 135.9, 133.3, 133.2, 130.4, 129.8, 129.7, 129.2, 128.4, 127.9, 127.8, 127.7, 127.1, 126.4, 126.3, 125.9, 125.3, 123.6, 122.3, 120.6, 120.2, 119.8, 119.2, 118.4, 118.1, 66.9, 46.8, 43.5, 41.9, 30.6, 30.5. MS Calcd (M): 905.3. Found (EI): 905.3 (M). Anal. Calcd. ($C_{50}H_{38}IrN_3O_2$): C, 66.35; H, 4.23; N, 4.64. Found: C, 66.21; H, 4.38; N, 4.67.

Synthesis of *fac*-bis(2-benzo[b]thiophen-2-yl-pyridinato, N, $C^{3\prime}$)(2-(4′-methyl bicyclo[2.2.1]hept-5-ene-2-carboxyl phenyl)pyridinato, N, $C^{2\prime}$) iridium(III) (12). Compound **9** (143 mg, 0.18 mmol), *exo*-5-norbornene-2-carboxylic acid (29 mg, 0.21 mmol), and dimethylaminopyridine (10 mg, 0.08 mmol) were combined in 15 mL of CH_2Cl_2. A solution of dicyclohexylcarbodiimide (42 mg, 0.21 mmol) in 5 mL of CH_2Cl_2 was added, and the reaction was stirred under argon at ambient temperatures for 24 h. The solvent was evaporated and the residue was purified via column chromatography (silica, CH_2Cl_2) to give compound **12** (81 mg, 49% yield). ^{1}H NMR ($CDCl_3$): δ = 7.76 (d, 2H, *J* = 8.1 Hz), 7.69 (d, 1H, *J* = 8.1 Hz), 7.62 (d, 1H, *J* = 8.4 Hz), 7.47 (m, 6H), 7.36 (d, 1H, *J* = 6.0 Hz), 7.26 (d, 1H, *J* = 5.1 Hz), 7.12 (td, 1H, *J* = 7.2 Hz, 1.5 Hz), 7.05 (m, 1H), 6.93 (dd, 1H, *J* = 6.3 Hz, 1.5 Hz), 6.85 (m, 3H), 6.67 (m, 5H), 6.06 (m, 2H), 4.87 (s, 2H), 2.83 (m, 2H), 2.01 (m, 1H), 1.55 (m, 1H), 1.34 (m, 1H), 1.23 (m, 2H). ^{13}C NMR ($CDCl_3$): δ = 176.2, 166.7, 163.4, 162.7, 161.8, 157.4, 155.3, 149.3, 147.8, 147.7, 147.5, 147.1, 144.6, 143.2, 142.6, 138.5, 138.0, 137.2, 136.9, 136.7, 136.2, 129.2, 128.8, 125.1, 124.9, 124.1, 123.7, 122.4, 122.3, 122.2, 120.4, 119.8, 118.8, 118.7, 66.7, 46.6, 43.3, 41.8, 30.4. MS Calcd (M) 917.2. Found (EI): 917.2 (M). Anal. Calcd. ($C_{46}H_{34}IrN_3O_2S_2$): C, 60.24; H, 3.74; N, 4.58. Found: C, 58.53; H, 3.62; N, 4.59.

General polymerization procedure. A solution of Grubbs' third generation initiator in chloroform (0.05 M) was added to a chloroform solution (0.01M) containing a mixture of **13** and the desired iridium-containing monomer (**3**, **10** – **12**) in a ratio of 9:1, respectively. The reaction mixture was stirred for 20 minutes at ambient temperatures. After 20 minutes, the polymerization was quenched by the addition of ethyl vinyl ether. The reaction mixture was concentrated and precipitated into methanol. The resulting solid was collected by filtration, redissolved in CH_2Cl_2 and reprecipitated into methanol. This procedure was repeated until the methanol solution was clear to yield copolymers **14** – **17** for which ^{1}H-NMR spectra showed no remaining monomer or other impurity peaks. All copolymers were synthesized with a total monomer to catalyst ratio of 50:1.

Copolymer 14. ^{1}H NMR ($CDCl_3$): δ = 8.07 (br), 7.78 (br), 7.42 (br), 7.22 (br), 6.85 (br), 6.38 (br), 6.26 (br), 4.97 (br), 2.98 (br), 2.00 (br), 1.68 (br), 1.44 (br). ^{13}C NMR ($CDCl_3$): δ = 163.5, 163.0, 162.3, 154.0, 147.1, 141.1, 138.8, 137.6, 137.1, 134.1, 129.9, 126.3, 123.6, 121.8, 121.4, 120.6, 120.3, 118.2, 110.0, 97.4, 73.1, 71.0, 51.2, 42.7, 41.6, 37.1, 29.9, 26.8, 25.3. Anal. Calcd.: Ir, 2.75. Found: Ir, 2.16.

Copolymer 15. ^{1}H NMR ($CDCl_3$): δ = 8.05 (br), 7.76 (br), 7.38 (br), 7.20 (br), 6.76 (br), 4.98 (br), 2.98 (br), 2.16 (br) 1.92 (br), 1.67 (br), 1.43 (br). ^{13}C NMR ($CDCl_3$): δ = 166.8, 166.3, 161.7, 161.2, 160.9, 154.1, 147.1, 143.7, 141.1, 138.7, 137.3, 137.0, 136.0, 134.6, 134.1, 133.1, 130.7, 130.1, 129.9, 127.9, 126.2, 124.1, 123.6, 121.8, 121.4, 120.6, 120.2, 118.9, 110.0, 73.0, 71.0, 51.2, 44.1, 42.3, 41.7, 38.9, 37.1, 29.9, 26.7, 25.4. Anal. Calcd.: Ir, 2.79. Found: Ir, 3.06.

Copolymer 16. ^{1}H NMR ($CDCl_3$): δ = 8.07 (br), 7.81 (br), 7.42 (br), 7.21 (br), 6.82 (br), 6.63 (br), 4.98 (br), 3.05 (br), 1.98 (br), 1.68 (br), 1.42 (br). ^{13}C NMR ($CDCl_3$): δ = 167.4, 165.8, 160.4, 158.3, 154.0, 149.1, 148.4, 143.5, 141.1, 138.7, 137.0, 135.9, 133.3, 129.8, 128.3, 126.2, 125.2, 123.6, 121.8, 121.4, 120.6, 120.2, 119.3, 110.0, 72.9, 71.0, 51.2, 42.6, 41.5, 39.2, 37.1, 26.8, 25.4. Anal. Calcd.: Ir, 2.75. Found: Ir, 2.99.

Copolymer 17. ^{1}H NMR ($CDCl_3$): δ = 8.06 (br), 7.77 (br), 7.40 (br), 7.21 (br), 6.82 (br), 6.65 (br), 4.97 (br), 2.98 (br), 1.92 (br), 1.68 (br), 1.43 (br). ^{13}C NMR ($CDCl_3$): δ = 167.5, 161.8, 157.8, 155.2, 154.0, 149.2, 147.8, 143.2, 142.6, 141.1, 138.7, 137.0, 134.1, 129.9, 126.2, 125.1, 123.6, 121.8, 121.4, 120.6, 120.2, 118.6, 110.0, 73.0, 71.0, 51.2, 46.0, 42.7, 39.2, 37.1, 26.8, 25.3. Anal. Calcd.: Ir, 2.75. Found: Ir, 2.77.

7.6 References

(1) The contents of this chapter have been published. See: Kimyonok, A.; Domercq, B.; Haldi, A.; Cho, J. Y.; Carlise, J. R.; Wang, X. Y.; Hayden, L. E.; Jones, S. C.; Barlow, S.; Marder, S. R.; Kippelen, B.; Weck, M. Norbornene-Based Copolymers with Iridium Complexes and Bis(Carbazolyl)Fluorene Groups in Their Side-Chains and Their Use in Light-Emitting Diodes *Chem. Mater.* **2007**, *19*, 5602.

(2) Pollino, J. M.; Stubbs, L. P.; Weck, M. Living Romp of Exo-Norbornene Esters Possessing Pd^{II} SCS Pincer Complexes or Diaminopyridines *Macromolecules* **2003**, *36*, 2230.

(3) Hreha, R. D.; Haldi, A.; Domercq, B.; Barlow, S.; Kippelen, B.; Marder, S. R. Synthesis of Acrylate and Norbornene Polymers with Pendant 2,7-Bis(Diarylamino)Fluorene Hole-Transport Groups *Tetrahedron* **2004**, *60*, 7169.

(4) Beeby, A.; Bettington, S.; Samuel, I. D. W.; Wang, Z. J. Tuning the Emission of Cyclometalated Iridium Complexes by Simple Ligand Modification *J. Mater. Chem.* **2003**, *13*, 80.

(5) Carlise, J. R.; Wang, X. Y.; Weck, M. Phosphorescent Side-Chain Functionalized Poly(norbornene)s Containing Iridium Complexes *Macromolecules* **2005**, *38*, 9000.

(6) Schlosser, M.; Heiss, C. Exploring Structural Opportunities: The Regioflexible Substitution of 1,3-Difluorobenzene *Eur. J. Org. Chem.* **2003**, 4618.

(7) Coe, P. L.; Waring, A. J.; Yarwood, T. D. The Lithiation of Fluorinated Benzenes and Its Dependence on Solvent and Temperature *J. Chem. Soc. Perkin Trans. 1* **1995**, 2729.

(8) Bridges, A. J.; Patt, W. C.; Stickney, T. M. A Dramatic Solvent Effect During Aromatic Halogen Metal Exchanges - Different Products from Lithiation of Polyfluorobromobenzenes in Ether and THF *J. Org. Chem.* **1990**, *55*, 773.

(9) Lamansky, S.; Djurovich, P.; Murphy, D.; Abdel-Razzaq, F.; Lee, H. E.; Adachi, C.; Burrows, P. E.; Forrest, S. R.; Thompson, M. E. Highly Phosphorescent Bis-Cyclometalated Iridium Complexes: Synthesis, Photophysical Characterization, and Use in Organic Light Emitting Diodes *J. Am. Chem. Soc.* **2001**, *123*, 4304.

(10) Lamansky, S.; Djurovich, P.; Murphy, D.; Abdel-Razzaq, F.; Kwong, R.; Tsyba, I.; Bortz, M.; Mui, B.; Bau, R.; Thompson, M. E. Synthesis and Characterization of Phosphorescent Cyclometalated Iridium Complexes *Inorg. Chem.* **2001**, *40*, 1704.

(11) Adachi, C.; Baldo, M. A.; Forrest, S. R.; Lamansky, S.; Thompson, M. E.; Kwong, R. C. High-Efficiency Red Electrophosphorescence Devices *Appl. Phys. Lett.* **2001**, *78*, 1622.

(12) Tsuboyama, A.; Iwawaki, H.; Furugori, M.; Mukaide, T.; Kamatani, J.; Igawa, S.; Moriyama, T.; Miura, S.; Takiguchi, T.; Okada, S.; Hoshino, M.; Ueno, K. Homoleptic Cyclometalated Iridium Complexes with Highly Efficient Red Phosphorescence and Application to Organic Light-Emitting Diode *J. Am. Chem. Soc.* **2003**, *125*, 12971.

(13) Nazeeruddin, M. K.; Humphry-Baker, R.; Berner, D.; Rivier, S.; Zuppiroli, L.; Graetzel, M. Highly Phosphorescence Iridium Complexes and Their Application in Organic Light-Emitting Devices *J. Am. Chem. Soc.* **2003**, *125*, 8790.

(14) Tamayo, A. B.; Alleyne, B. D.; Djurovich, P. I.; Lamansky, S.; Tsyba, I.; Ho, N. N.; Bau, R.; Thompson, M. E. Synthesis and Characterization of Facial and Meridional Tris-Cyclometalated Iridium(III) Complexes *J. Am. Chem. Soc.* **2003**, *125*, 7377.

(15) Hercules, D. M. *Fluorescence and Phosphorescence Analysis: Principles and Applications*; Interscience Publishers: New York, 1966.

(16) Baldo, M. A.; Lamansky, S.; Burrows, P. E.; Thompson, M. E.; Forrest, S. R. Very High-Efficiency Green Organic Light-Emitting Devices Based on Electrophosphorescence *Appl. Phys. Lett.* **1999**, *75*, 4.

(17) Pfeiffer, M.; Forrest, S. R.; Leo, K.; Thompson, M. E. Electrophosphorescent p-i-n Organic Light-Emitting Devices for Very-High-Efficiency Flat-Panel Displays *Adv. Mater.* **2002**, *14*, 1633.

CHAPTER 8

OPTIMIZATION OF OLED PERFORMANCES BY OPTIMIZATION OF THE POLYMER STRUCTURE

8.1 Abstract

This chapter studies the polymer structure-device performance relationship in order to discover general principles that can be used to optimize polymer structures. As a model system, orange-emitting copolymers containing iridium complexes and bis(carbazolyl)fluorene groups in their side-chains were prepared, and the molecular weight, iridium loading, spacer type, and spacer length were systematically changed. The optimum polymer structure resulted in a device with an external quantum efficiency of 4.9±0.4%, and a luminance of 8.8±0.7cd A^{-1} at 100 cd m^{-2}. It was found that these principles can be applied to the polymers containing other types of iridium complexes. Finally, in order to optimize the device fabrication, an orange-emitting copolymer with cinnamate type crosslinking units in the side chains was prepared, and its use in fully solution-processed OLEDs was demonstrated.

8.2 Introduction

In Chapter 7, synthesis and characterization of copolymers containing iridium complexes and bis(carbazolyl)fluorene groups in their side-chains were described. The best device performance was obtained for the orange-emitting copolymers. In this chapter, while the structures of the orange-emitting iridium complex and the host compound remain the same as in Chapter 7, the device performance was attempted to be maximized by changing the molecular weights and iridium contents of the polymers, and

by changing the types and lengths of the linkers between the electroactive groups on the side chains and the polymer backbone.

The molecular weight of the polymer might have a significant impact on the device performance, since it will affect the processability and the morphology of the emissive layer. As in the previous chapter, ring-opening metathesis polymerization[1,2] was employed to obtain polymers with different molecular weights in order to study the effect of the chain length on the device performance. Another factor that can influence the device performance is the concentration of the iridium complex. High concentrations of the iridium complex can give rise to concentration quenching, whereas low concentrations might result in insufficient energy transfer from the host to the complex.[3,4] Therefore, it is clear that finding the optimum iridium loading on the polymer will lead to an enhancement in device performance. Finally, spacer groups might also affect the electroluminescence behavior of polymers. For example, replacing an ether group on the spacer with an ester group can have an impact on the hole mobility of the polymer due to a change in the polarity of the spacer.[5-7] Furthermore, increasing the spacer length might result in a better performance due to a better mixing of the iridium complex with the host compound.[8]

The electron-transport layers that are described in the previous chapters contain small molecules that are vacuum deposited on top of the emissive layer. Solution-processing of the electron-transport layer was not possible due to the fact that the emissive layer would dissolve during the deposition of the electron-transport layer. An ideal device would have each layer solution-processed on top of each other. In Section 8.4, in order to demonstrate the fabrication of a fully solution-processed device, an orange-emitting copolymer with cinnamate type crosslinking units[9-11] in the side chains was described, and the device performance was compared to that of the optimized orange-emitting copolymer.

8.3 Results and Discussion

8.3.1 Optimization of Orange-emitting Copolymers

Synthesis. The structures of monomers **1-4**, which are used to prepare the different polymers, are shown in Fig. 8.1. For the host monomers **1** and **2** (synthesized by Lauren E. Hayden, and Simon C. Jones in the Marder Group), we selected 2,7-di(carbazol-9-yl)fluorene as the building block, as discussed in Chapters 4 and 7. The promising performance of the combination of the bis(carbazolyl)fluorene host material and an orange-emitting iridium complex in the emissive layer of an OLED device in Chapter 7 indicates an efficient energy transfer from the host to the iridium complex.

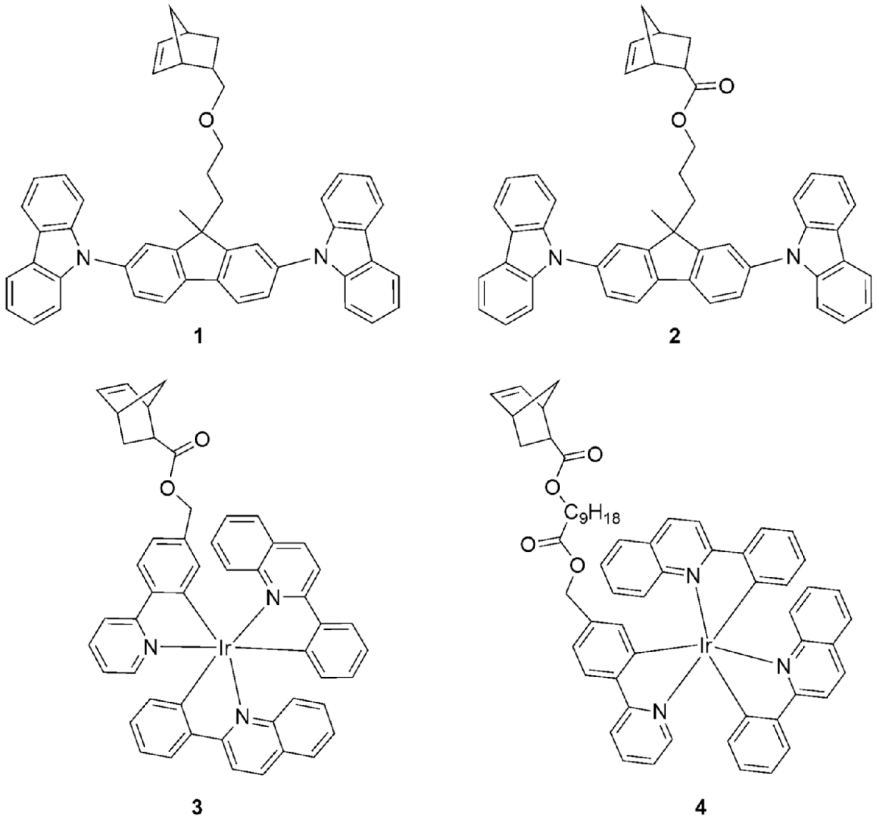

Figure 8.1. Structures of the monomers for the optimization of orange-emitting copolymers

The synthesis of monomer **3** (Fig. 8.1) was described in Chapter 7. Monomer **4** was synthesized by the reaction of compound **5**[12] with the alcohol functionalized iridium complex **6** (Scheme 8.1).

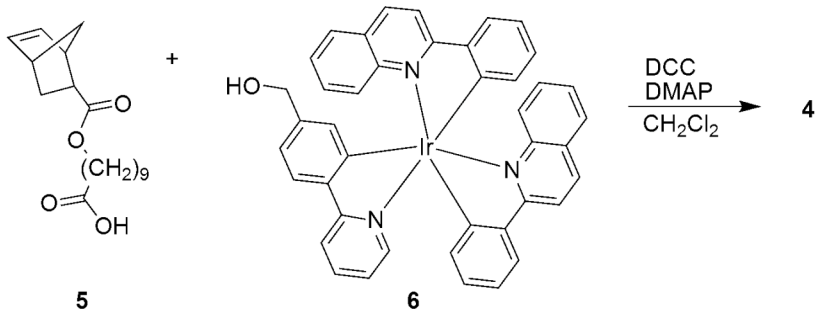

Scheme 8.1 Synthesis of iridium containing monomer **4**.

Copolymerizations of **1** or **2** with **3** or **4** were carried out in chloroform at room temperature using Grubbs' third generation initiator (Scheme 8.2). All copolymerizations were complete within 10 minutes. A range of monomer to catalyst ratios as well as host monomer to the iridium complex containing monomer ratios were employed in order to obtain polymers with tunable polymer properties such as molecular weight and iridium content. Table 8.1 lists the polymer properties of copolymers **7-19**. For **7-9**, we have varied the monomer to catalyst ratio, *i.e.* the molecular weights of the resulting polymers. Copolymers **7-9** have molecular weights between 19 kD and 238 kD, and polydispersities between 1.29 and 1.47. For copolymers **10-16**, we kept the monomer to catalyst ratio constant (50:1 molar ratio) leading to molecular weight in a range comparable to that of polymer **7** but varied the relative percentages of the iridium containing monomer in the copolymers from a 98:2 to a 60:40 molar ratio. The final incorporation of iridium in the copolymers has been calculated from elemental analysis and ranges from 2 to 29 mol% (Table 8.1). The iridium monomer feed ratios and the measured iridium content in the copolymers are in good agreement for copolymers with less than or equal to 20 mol%

iridium. For higher iridium loading levels (30 mol% and 40 mol%), the measured iridium loadings are lower than the theoretical ones (the molar feed ratio for **16** was m:n = 60:40 with an incorporation of m:n = 71:29 while for **15** the molar feed ratio of m:n = 70:30 resulted in m:n = 75:25). This can be explained potentially from a loss of oligomeric iridium containing materials that aggregate during purification. It has already been proposed previously that aggregation might occur during the polymerization due to the close proximity of the iridium complexes.[13] For lower iridium level, the host material acts as a spacer between the metal complexes preventing, at least partially, potential aggregation.

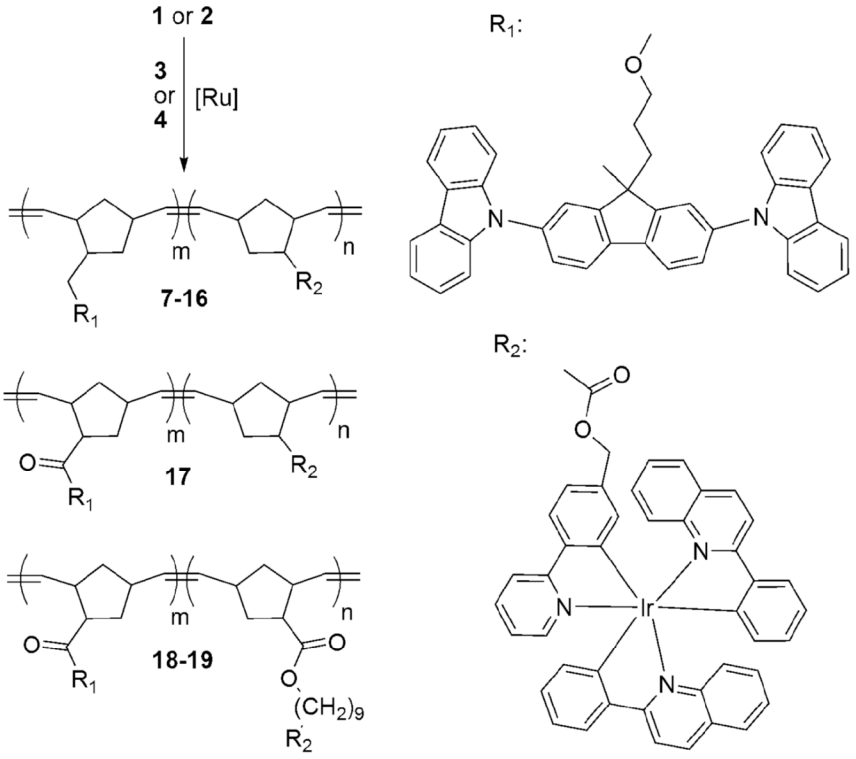

Scheme 8.2 Synthesis of copolymers **7-19**.

Photophysical Properties. The absorption and photoluminescence spectra of **7** have been reported in Chapter 7. Comparable spectra have been measured of copolymers **7-9**, **17**, and **18**, indicating that the polymer chain length (**7-9** and spacer length or type (**17** and **18**) do not affect the emission properties (Table 8.1). Increasing the iridium

concentration, on the other hand, resulted in a red shift in the solid-state emission. The photoluminescence spectrum of the polymer with the lowest iridium loading (2 mol%) peaks at 595 nm, whereas the polymer with highest iridium loading (29 mol%) has its maximum at 613 nm. The photoluminescence quantum yield of the iridium-based orange organometallic complex in toluene is 10% which is low compared to that of the well-known green complex *fac* tris(2-phenylpyridine)iridium ($Ir(ppy)_3$, Φ=0.41).

Table 8.1 Characterization of copolymers with peak maxima of solid-state photoluminescence and electroluminescence spectra, plus external quantum efficiency and luminous efficiency at 100 cd/m^2 for devices based on phosphorescent copolymers with different molecular weight, different iridium concentration, and different linkages between the side groups and the polymer backbone. The device structure was ITO/**20** (35 nm)/**7-19** (20-25 nm)/BCP (40 nm)/LiF (1 nm)/Al.

Polymer	m:n (mol%)	M_n (kDa)	PDI	$\lambda_{max,PL}$ (nm)	$\lambda_{max,EL}$ (nm)	EQE (%)	Luminous efficiency (cd/A)
7	89:11	19.0	1.29	594	600	2.9±0.3	3.9±0.4
8	92:8	70.0	1.33	590	602	3.2±0.3	4.9±0.4
9	90:10	238.0	1.47	591	607	1.5±0.1	2.0±0.1
10	98:2	16.0	1.34	595	596	1.9±0.3	2.6±0.4
11	95:5	23.0	1.26	595	598	3.4±0.4	4.6±0.5
12	93:7	16.0	1.43	597	602	3.0±0.4	4.1±0.5
13	81:19	21.0	1.48	605	607	2.4±0.2	3.2±0.3
14	79:21	19.5	1.44	604	607	2.0±0.1	2.7±0.2
15	75:25	19.5	1.32	612	611	1.9±0.1	2.6±0.1
16	71:29	27.0	1.25	613	612	1.7±0.1	2.3±0.1
17	90:10	16.0	1.31	592	605	3.9±0.3	5.3±0.4
18	90:10	20.0	1.21	594	603	4.5±0.5	8.0±0.9
19	95:5	16.5	1.21	595	597	4.9±0.4	8.8±0.7

Electroluminescence. Electroluminescence studies were conducted by Andreas Haldi and Benoit Domercq in the Kippelen group at Georgia Institute of Technology. Table 8.1 lists the external quantum efficiencies and luminous efficiencies at 100 cd/m^2 for devices based on the orange-emitting copolymers. The device with the highest molecular weight (238,000 g/mol) copolymer **9** exhibited poor performance compared to the polymers with lower molecular weights. However, similar device performances were obtained for the polymers with molecular weights of 19,000 g/mol and 70,000 g/mol.

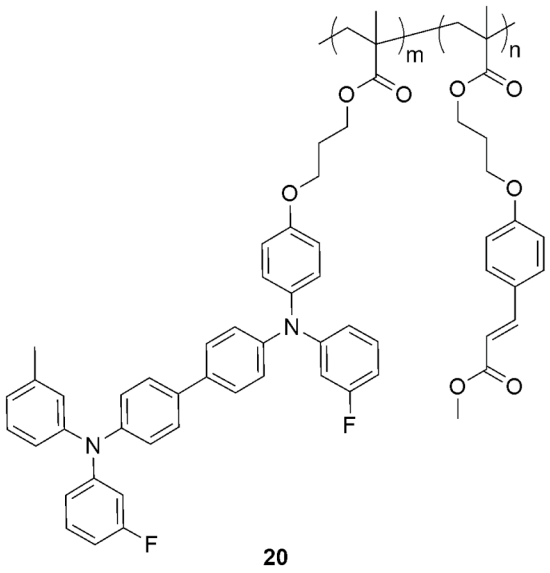

20

Figure 8.2 Structure of the hole-transport polymer **20**.

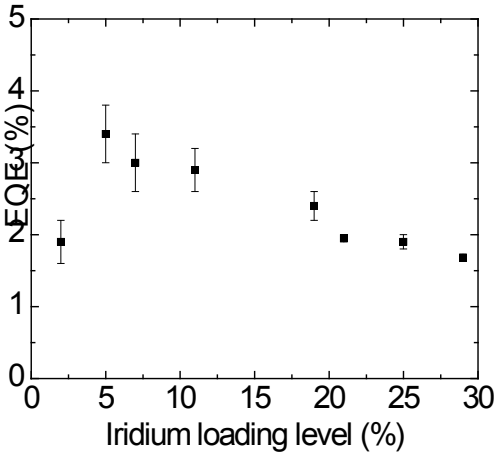

Figure 8.3 External quantum efficiency as a function of the loading level of the iridium complex in the copolymer for OLEDs with device configuration ITO/ **20** (35 nm)/ **7, 10-16** (20-25 nm)/BCP (40 nm)/LiF (1 nm)/Al.

For the polymers with different iridium loadings, the highest performance was obtained for **11**, which contains 5% iridium containing monomer (Figure 8.3). Similar results have been reported for the studies on evaporated or molecularly doped OLEDs.[4,14-18] For high loading levels, concentration quenching is expected,[19] whereas for low concentrations, light emission from the host and the guest can be observed simultaneously,[18] indicating incomplete energy transfer from the host to the guest. As in the case of photoluminescence, increasing the iridium concentration resulted in a red shift in the electroluminescence spectrum (Figure 8.4). For example, the maximum electroluminescence wavelength is 596 nm for the copolymer with an iridium complex concentration of 5 mol%, whereas it is 612 nm for the copolymer with 29 mol% iridium concentration. With a 5 mol% iridium concentration, the CIE coordinates of the emission were x=0.58, y=0.42.

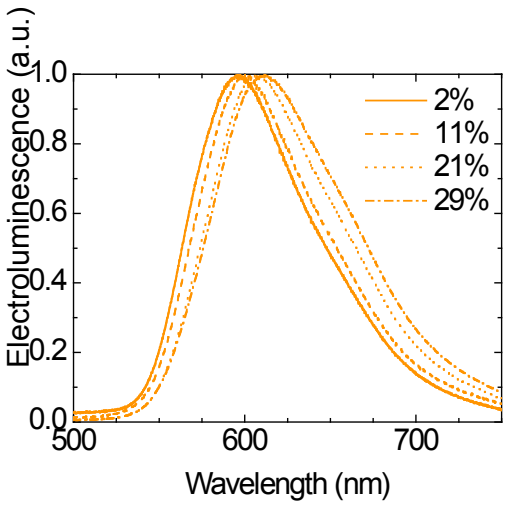

Figure 8.4 Electroluminescence spectra for OLED devices using **7, 10, 14, 16** with increasing iridium complex content as emitting layer.

Finally, the influences of the spacer type and length on the device performance were studied. Higher efficiencies were obtained for the copolymers with ester linkage on the host material compared to the ether linkage. Furthermore, increasing the spacer length on the iridium containing monomer led to more efficient devices, probably due to a better mixing of the metal complex with the host. The best result was obtained for **19** with 5% iridium complex loading, a long spacer on the iridium complex, and an ester linkage on the host monomer (Figure 8.5).

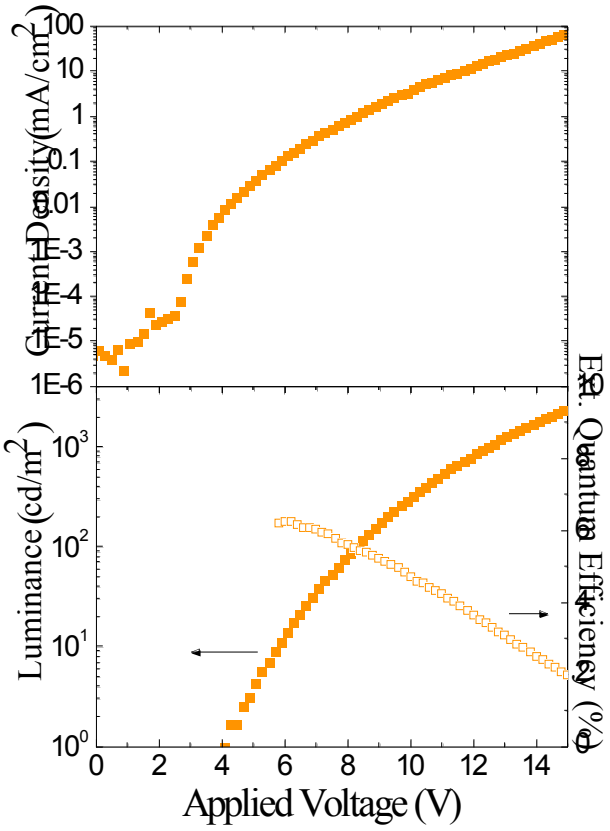

Figure 8.5 Current density (solid symbols, top), luminance (solid symbols, bottom), and external quantum efficiency (empty symbols, bottom) as a function of applied voltage for a device with structure ITO/**20** (35 nm)/**19** (25 nm)/BCP (40 nm)/LiF (1 nm)/Al.

8.3.2 Crosslinkable Orange-Emitting Copolymer

Synthesis. The synthesis of the crosslinkable orange copolymer is depicted in Scheme 8.3. The host material **2** and the crosslinking unit **21** were synthesized by scientists in the Marder Group. Copolymerization of **2**, **21**, and **4** was carried out in chloroform at room temperature using Grubbs' third generation initiator with a monomer to catalyst ratio of 50. The calculated feed ratio of the monomers was 70:5:25 for m:n:o. Elemental analysis revealed the actual ratio to be 66:6:28. The polymer has a molecular weight (M_w) of 12.0 kDa with a PDI of 1.73.

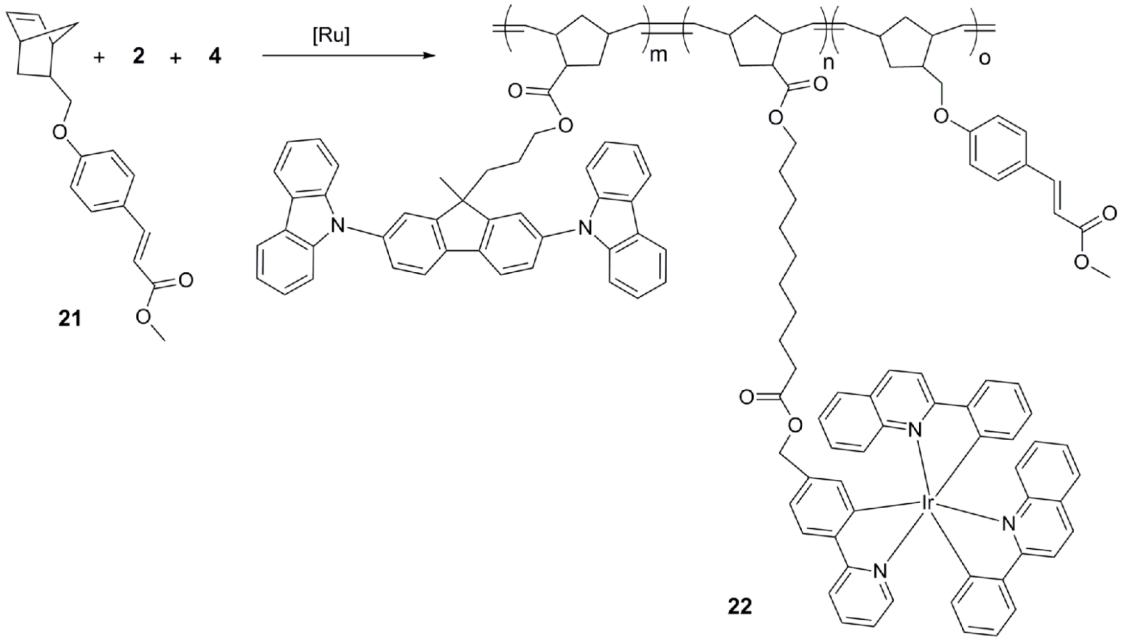

Scheme 8.3 Synthesis of the crosslinkable orange-emitting copolymer **22**.

Electroluminescence. Electroluminescence studies were conducted by Andreas Haldi in the Kippelen group at Georgia Institute of Technology. OLEDs with polymer **22** as the emissive layer were fabricated in order to determine the potential of our crosslinking approach. Figure 8.6 shows the electroluminescence data of devices with copolymer **22**. The photocrosslinkable hole-transport polymer **20** (Figure 8.2) was spin-coated onto ITO and crosslinked by UV radiation. Then, copolymer **22** was spin-coated onto the hole-transport layer, crosslinked by UV radiation, followed by the depositions of the electron-transport layer, and the cathode. Three different electron-transport compounds were used. The device with vacuum deposited BCP gave an EQE of 0.5%. On the other hand, the device with solution-processed polymer **24** (synthesized by scientists in the Marder Group) had an EQE of 1.3%. Finally, when polymer **22** was mixed with the electron-transport compound **23** (synthesized by scientists in the Marder Group), the external quantum efficiency increased to 2.7%. As mentioned in Section 8.3, the optimized

device with the orange-emitting copolymer without a crosslinking group gave EQE of 4.9%. Although lower performances obtained for the devices with copolymer **22** compared to the device with copolymer **19**, the results are still highly promising, considering that fully solution-processable devices can be fabricated by employing copolymer **22**.

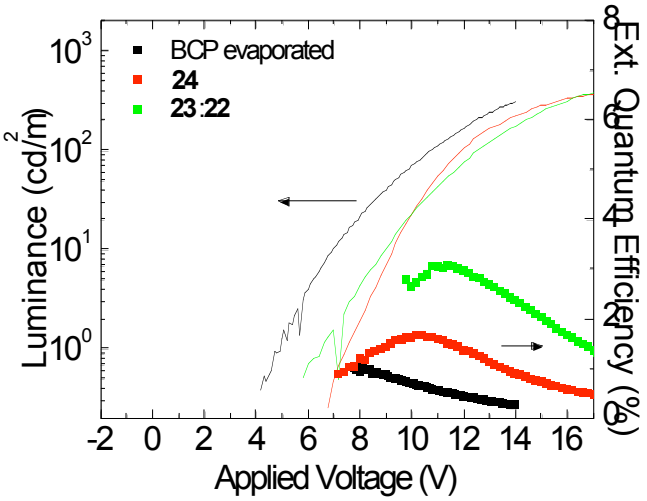

Figure 8.6 Luminance and external quantum efficiency as a function of applied voltage for device with structure ITO/**20** (35 nm)/**22** (25 nm)/ETL (40 nm)/LiF (1 nm)/Al.

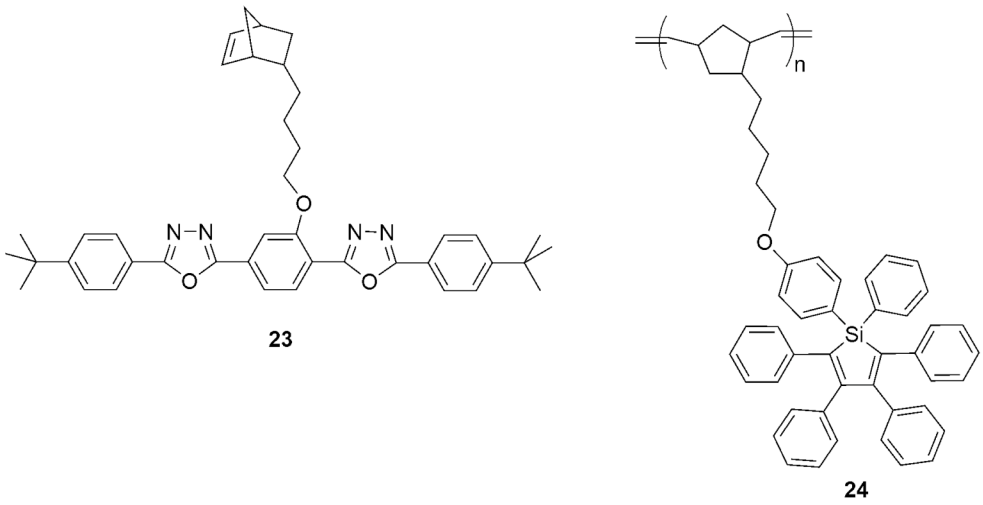

23 **24**

Figure 8.7 Structures of the electron-transport compounds **23** and **24**.

8.3.3 Optimization of Green-Emitting Copolymers

Synthesis. In Section 8.3.1, it was shown that a long spacer on the orange-emitting iridium-containing monomer resulted in a significant increase in the device performance. Assuming that this principle will also be valid for other iridium containing monomers, we prepared compound **26**, a green-emitting monomer with a long spacer. Figure 8.8 shows the structures of compound **26**, and the host materials (synthesized by Marder Group) that are copolymerized with **26**. Monomer **26** was synthesized by the reaction of compound **5**[12] with the alcohol functionalized iridium complex **6** (Scheme 8.3).

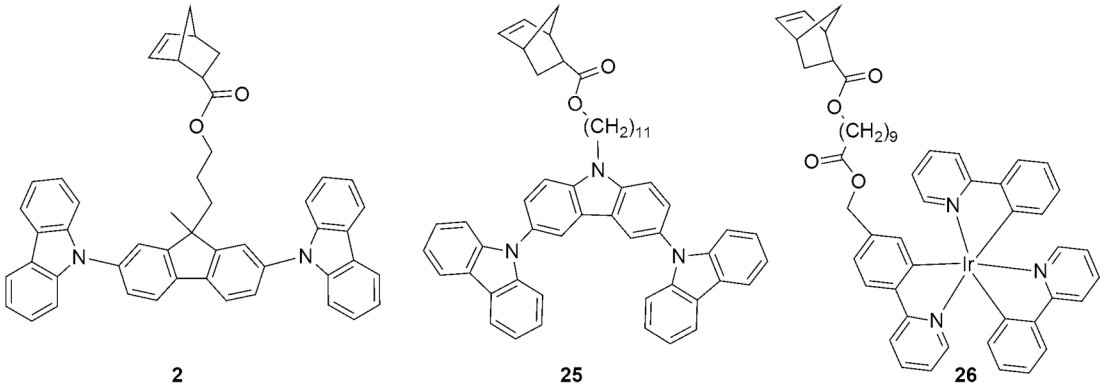

Figure 8.8 Structures of the monomers for the optimization of the green-emitting copolymers.

As mentioned above, two different host materials are copolymerized with **26** (Scheme 8.4). Monomer **2** contains 2,7-di(carbazol-9-yl)fluorene group that was described previously in this chapter and Chapters 4 and 7. The second host compound contains a carbazole trimer. As described in Chapters 3, 5, and 6, carbazole based compounds have been widely used as the host materials for luminescent metal complexes due to their hole transporting properties.[20-23] The carbazole trimer in compound **25** has been studied extensively for applications in electronics[24-28] and employed successfully as a host material for a green-emitting iridium complex.[29]

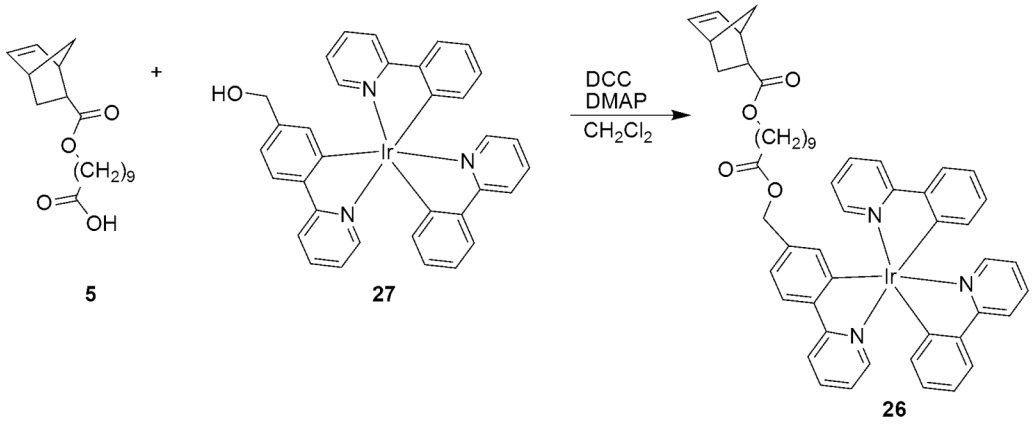

5 27 26

Scheme 8.4 Synthesis of green-emitting monomer **26**.

Copolymerizations of **26** with **2** or **25** were carried out in chloroform at room temperature using Grubbs' third generation initiator with monomer to catalyst ratio of 50:1(Scheme 8.4). Each polymer has 5 mol% iridium containing monomer, as this is the optimum loading for the orange-emitting copolymer. Both copolymerizations were complete within 10 minutes. Polymer **28** has a molecular weight (Mw) of 10 kDa with a PDI of 1.51, whereas polymer **29** has a molecular weight of 13.5 kDa and a PDI of 1.48.

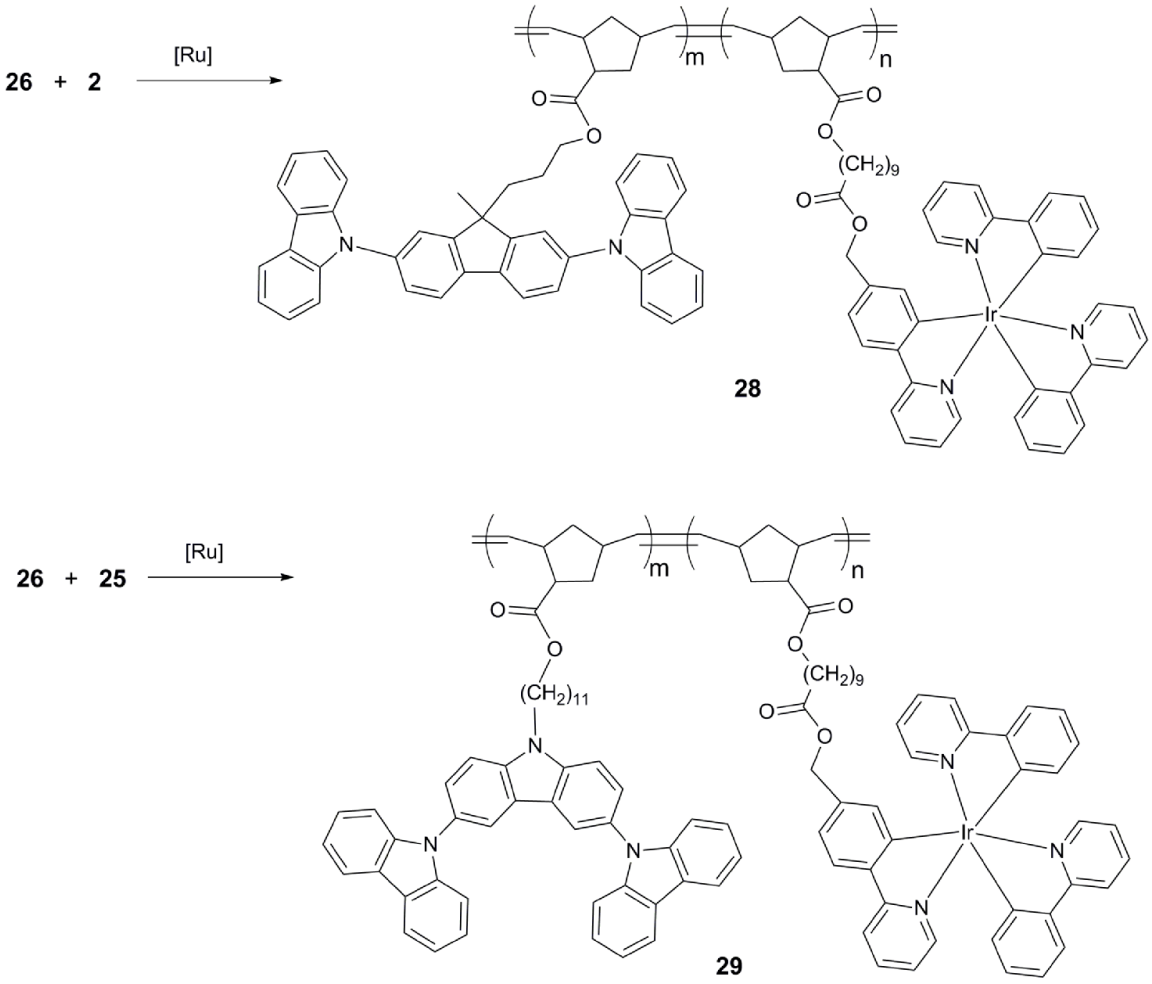

Scheme 8.5 Synthesis of green-emitting copolymers **28** and **29**.

Photoluminescence. The photoluminescence spectra of copolymers **28** and **29** are shown in Figure 8.9 and are almost identical to the reference compound *fac*-Ir(ppy)$_3$. The solution and the solid-state emission maxima of the copolymers are almost identical. These results suggest that the polymer backbone and the host groups do not interfere with the photoluminescence properties of the pendant metal complexes.

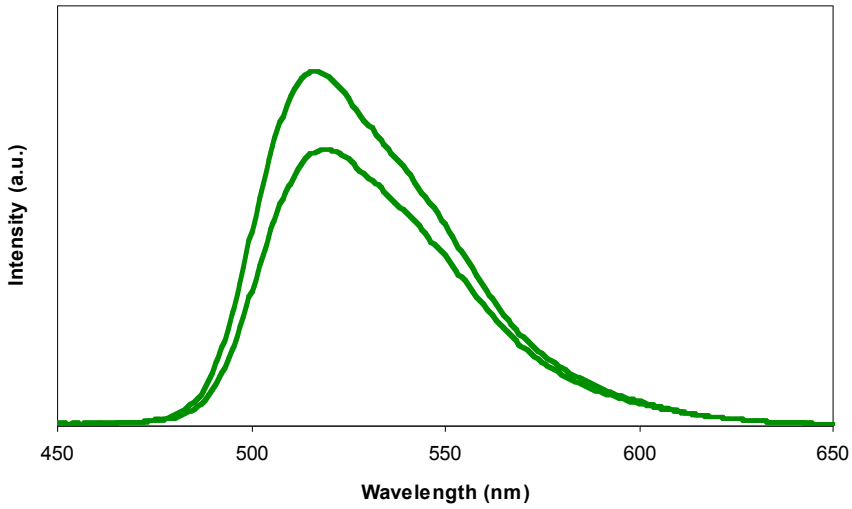

Figure 8.9 Solid-state photoluminescence data for polymers **28** (bottom curve) and **29** (top curve)

Electroluminescence. Electroluminescence studies were conducted by Andreas Haldi in the Kippelen group at Georgia Institute of Technology. OLEDs with polymer **28** as the emissive layer were fabricated in order to determine the effect of the spacer length on the device performance. Figure 8.10 shows the electroluminescence data of devices with copolymer **28**. The photocrosslinkable hole-transport polymer **20** (Figure 8.2) was spin-coated onto ITO and crosslinked by UV radiation. Then, Copolymer **28** was spin-coated onto the hole-transport layer, followed by the depositions of the electron-transport compound BCP, and the cathode. The device exhibited an external quantum efficiency of 2.7% and a luminance of 9 cd/A at 100 cd/m^2. In Chapter 7, the green-emitting polymer with 10 mol% iridium containin monomer and a slightly different linker on the host material resulted in a device with EQE of 1.1% and a luminance of 4.1 cd/A at 100 cd/m^2. Therefore it is clear that a long spacer on the iridium containing monomer and a decrease in iridium loading lead to an increase in device performance. These results are in accord with Section 8.4, where the same phenomena were observed for the orange-emitting copolymers. On the other hand, the device with polymer **29** gave a poor

performance. At this point, the reason for the poor performance is not clear, and needs to be further investigated.

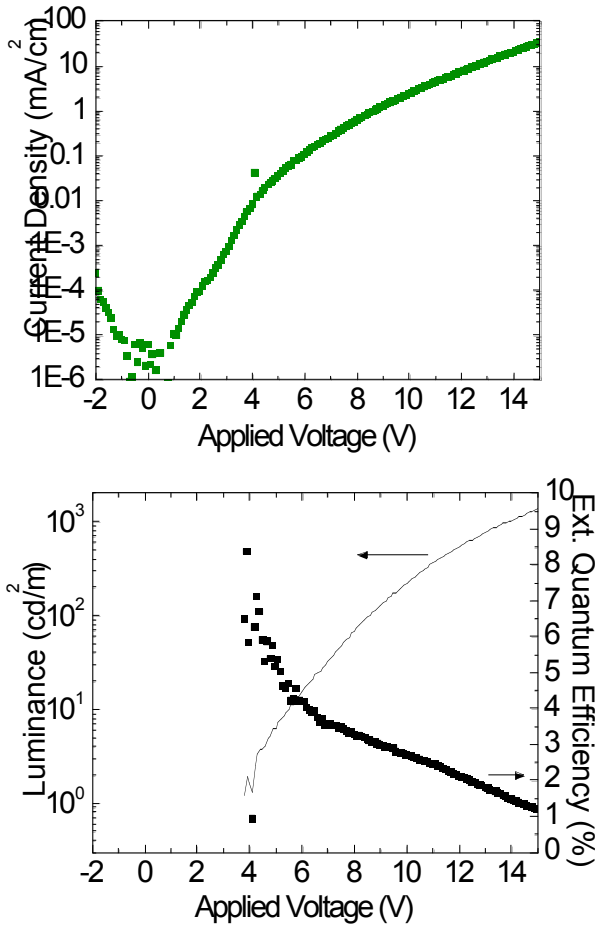

Figure 8.10 Current density, luminance, and external quantum efficiency as a function of applied voltage for a device with structure ITO/**20** (35 nm)/**28** (20 nm)/BCP (40 nm)/LiF (1 nm)/Al.

8.4 Conclusion

Copolymers with an orange- or green-emitting iridium complex and host groups in their side-chains were synthesized and incorporated into phosphorescent organic light-emitting diodes. For the orange-emitting copolymers, the effects of molecular weight,

iridium content, spacer type and length on the device performance were investigated in detail. Unless it is too high (i.e. more than 200 kDa), the molecular weight of the copolymer did not significantly influence the device performance. On the other hand, the optimum iridium complex loading was found to be 5 mol%. Changing the linker type on the host material from an ether group to an ester group resulted in a slight increase on the device performance. Finally, replacing a short spacer on the iridium containing monomer with a long one led to further improvement.

Incorporation of a crosslinking unit as a side-chain of the orange-emitting copolymer made it possible to fabricate fully solution-processed OLEDs. However, the crosslinked polymer resulted in a decrease in the efficiency of the device. External quantum efficiencies as high as 4.9±0.4% at 100 cd/m^2 were measured for the orange-emitting copolymers. In order to determine the applicability of these findings to the other type of iridium complexes, a green-emitting copolymer with 5 mol% iridium containing monomer and a long spacer on the iridium containing monomer was prepared. An improvement on the device performance was observed by employing this copolymer, suggesting that the principles that are used to optimize the orange-emitting copolymer can also be applied to other types of iridium containing polymers.

8.5 Experimental

All reagents were purchased either from Acros Organics or Aldrich and used without further purification. ^{1}H-NMR and ^{13}C-NMR spectra (300 MHz ^{1}H NMR, 75 MHz ^{13}C NMR) were obtained using a Varian Mercury Vx 300 spectrometer. All spectra are referenced to residual proton solvent. Abbreviations used include singlet (s), doublet (d), doublet of doublets (dd), triplet (t), triplet of doublets (td) and unresolved multiplet (m). Mass spectral analyses were provided by the Georgia Tech Mass Spectrometry Facility. Gel-permeation chromatography (GPC) analyses were carried out using a

Waters 1525 binary pump coupled to a Waters 2414 refractive index detector with methylene chloride as the eluant on American Polymer Standards 10 μm particle size, linear mixed bed packing columns. The flow rate used for all the measurements was 1 mL/min. All GPC measurements were calibrated using poly(styrene) standards and carried out at room temperature. UV/vis absorption measurements were taken on a Shimadzu UV-2401 PC recording spectrophotometer. Emission measurements were acquired using a Shimadzu RF-5301 PC spectrofluorophotometer. Elemental analyses for iridium were provided by Galbraith Laboratories.

***fac-exo*-bis(2-phenyl-quinolinato, N, C2′)(2-(4′-(10-methoxy-10-oxodecyl bicyclo[2.2.1]hept-5-ene-2-carboxyl) phenyl)pyridinato, N, C2′) iridium(III) (4)**. Compounds **5**[12] (98 mg, 0.31 mmol) and **6** (200 mg, 0.25 mmol) and dimethylaminopyridine (17 mg, 0.14 mmol) were combined in 10 mL of CH_2Cl_2. A solution of dicyclohexylcarbodiimide (60 mg, 0.30 mmol) in 2 mL of CH_2Cl_2 was added and the reaction was stirred under argon at ambient temperatures for 24 h. The solvent was evaporated and the residue was purified via column chromatography (silica, CH_2Cl_2) to give compound **4** as an orange powder (210 mg, 77% yield). ^{1}H NMR ($CDCl_3$): δ = 8.19 (d, 1H, *J* = 9 Hz), 8.09 (m, 3H), 7.99 (d, 1H, *J* = 9 Hz), 7.88 (m, 2H), 7.67 (m, 2H), 7.62 (m, 2H), 7.56 (d, 1H, *J* =8.7 Hz), 7.47 (m, 1H), 7.38 (d, 1H, *J* = 8.1 Hz), 7.19 (m, 3H), 6.92 (m, 3H), 6.73 (m, 4H), 6.63 (m, 2H), 6.45 (d, 1H, *J* =1.8 Hz), 6.13 (m, 2H), 4.72 (s, 2H), 4.09 (t, 2H, *J* = 6.9 Hz), 3.05 (s, 1H), 2.92 (s, 1H), 2.24 (t, 2H, J= 7.5), 1.95 (m, 1H), 1.58 (m, 6H), 1.34 (m, 12H). ^{13}C NMR ($CDCl_3$): δ =176.6, 173.9, 167.4, 165.8, 163.2, 160.6, 158.4, 149.2, 148.7, 148.2, 146.5, 144.9, 143.6, 138.3, 137.6, 137.1, 137.0, 136.3, 136.1, 135.9, 133.1, 130.4, 129.8, 129.6, 129.2, 128.4, 127.9, 127.8, 127.7, 127.1, 126.4, 126.3, 125.8, 125.3, 123.5, 122.3, 120.6, 120.2, 119.6, 119.1, 118.4, 118.2, 66.6, 64.9, 46.9, 46.6, 43.5, 41.9, 34.6, 30.6, 29.6, 29.5, 29.4, 29.3, 28.9, 26.2, 25.1. MS (ESI): *m/z* 1008.3 ([M-C_5H_7]) Anal. Calcd. ($C_{60}H_{56}IrN_3O_4$): C, 67.02; H, 5.25; N, 3.91. Found: C, 67.07; H, 5.43; N, 4.12.

***fac-exo*-bis(2-phenyl-pyridine, N, C2′)(2-(4′-(10-methoxy-10-oxodecyl bicyclo[2.2.1]hept-5-ene-2-carboxyl) phenyl)pyridinato, N, C2′) iridium(III) (26).** Compounds 5[12] (125 mg, 0.41 mmol), 27 (250 mg, 0.37 mmol) and dimethylaminopyridine (22 mg, 0.18 mmol) were combined in 8 mL of CH_2Cl_2. A solution of dicyclohexylcarbodiimide (92 mg, 0.46 mmol) in 2 mL of CH_2Cl_2 was added and the reaction was stirred under argon at ambient temperatures for 24 h. The solvent was evaporated and the residue was purified via column chromatography (silica, CH_2Cl_2) to give compound 28 as a yellow powder (295 mg, 83% yield). ^{1}H NMR ($CDCl_3$): δ = 7.85 (d, 3H, *J* = 7.8 Hz), 7.63 (m, 3H), 7.50 (m, 6H), 6.85 (m, 11H), 6.12 (m, 2H), 4.91 (s, 2H), 4.07 (t, 2H, *J* = 6.9), 3.04 (s, 1H), 2.91 (s, 1H), 2.24 (m, 3H), 1.92 (m, 2H), 1.59 (m, 5H), 1.25-1.41 (m, 11H). ^{13}C NMR ($CDCl_3$): δ = 176.6, 174.0, 166.9, 166.8, 166.4, 161.8, 161.2, 160.9, 147.3, 147.2, 143.9, 138.3, 137.4, 137.3, 137.1, 136.2, 136.0, 130.1, 130.0, 124.1, 122.3, 122.2, 120.1, 119.3, 119.0, 118.9, 66.7, 64.8, 46.8, 46.6, 43.4, 41.8, 34.6, 30.6, 29.6, 29.5, 29.4, 29.3, 28.9, 26.2, 25.1. MS Calcd (M): 975.3. Found (ESI): 976.3 (M+1). Anal. Calcd. ($C_{52}H_{52}IrN_3O_4$): C, 64.04; H, 5.37; N, 4.31. Found: C, 62.73; H, 5.17; N, 4.23.

General polymerization procedure. A solution of Grubbs' third generation initiator[30] in chloroform (0.05 M) was added to a chloroform solution (0.01M) containing a mixture of monomers **3** or **4** and **5** or **6** in the desired ratios (Table 1). The reaction mixture was stirred for 15 minutes at ambient temperatures. After 15 minutes, the polymerization was quenched by the addition of ethyl vinyl ether. The reaction mixture was concentrated and precipitated into methanol. The resulting solid was collected by filtration, redissolved in CH_2Cl_2 and reprecipitated into methanol. This procedure was repeated until the methanol solution was clear to yield copolymers for which ^{1}H-NMR spectra showed no remaining monomer or other impurity signals.

Copolymer 17. ^{1}H NMR ($CDCl_3$): δ = 8.07 (br), 7.81 (br), 7.40 (br), 7.23 (br), 6.79 (br), 6.63(br), 5.02 (br), 4.71 (br), 3.78 (br), 2.56 (br), 1.90 (br), 1.49 (br), 1.12 (br). ^{13}C NMR ($CDCl_3$): δ = 167.0, 165.2, 160.3, 158.1, 153.3, 148.7, 145.9,144.5, 143.0, 140.6, 138.1, 137.2, 136.7, 130.0, 129.3, 128.1, 127.5, 125.9, 125.3, 123.2, 121.5, 121.2, 120.4, 119.8, 117.7, 109.8, 66.4, 63.8, 50.9, 41.7, 36.7, 26.6, 24.4.

Copolymer 18. ^{1}H NMR ($CDCl_3$): δ = 8.06 (br), 7.84 (br), 7.48 (br), 7.21 (br), 6.89 (br), 6.68 (br), 4.99 (br), 4.74 (br), 3.72 (br), 2.64 (br), 1.95 (br), 1.50 (br), 1.09 (br). ^{13}C NMR ($CDCl_3$): δ = 167.5, 165.6, 163.1, 160.5, 158.5, 153.7, 149.2, 148.8, 148.2, 146.5, 144.9, 143.6, 141.1, 138.8, 137.6, 137.2, 136.3, 133.1, 132.4, 130.5, 129.8, 128.4, 127.9, 126.5, 123.7, 121.9, 121.6, 120.7, 120.4, 119.7, 119.1, 118.2, 110.0, 66.8, 64.3, 60.7, 51.2, 49.7, 46.2, 45.8, 43.6, 42.5, 37.0, 34.9, 32.1, 29.7, 26.9, 25.5, 24.4, 22.9.

Copolymer 22. ^{1}H NMR ($CDCl_3$): δ = 8.17 (br), 7.92 (br), 7.48 (br), 7.29 (br), 6.95 (br), 6.78 (br, m), 6.30 (br), 5.10 (br), 3.81 (br), 2.64 (br), 2.03 (br), 1.59 (br), 1.19 (br). Anal. Calcd.: C, 82.70; H, 5.94; N, 3.58; O, 6.19; Ir, 1.58. Found: C, 81.96; H, 6.03; N, 3.62; O, 6.40; Ir,1.92.

Copolymer 28. ^{1}H NMR ($CDCl_3$): δ = 8.07 (br), 7.84 (br), 7.39 (br), 7.21 (br), 6.88 (br), 6.69 (br, m), 5.00 (br), 4.75 (br), 3.73 (br), 3.11 (br), 2.50 (br), 1.92 (br), 1.48 (br), 1.08 (br).

Copolymer 29. ^{1}H NMR ($CDCl_3$): δ = 8.16 (br), 7.59 (br), 7.35 (br), 7.26 (br), 6.86 (br), 5.30(br, m), 4.90 (br), 4.37 (br), 3.99 (br), 3.11 (br), 2.85 (br), 2.48 (br), 2.22 (br), 1.96 (br), 1.75 (br, m), 1.55 (br), 1.29 (br).

8.6 References

(1) Fürstner, A. Olefin Metathesis and Beyond *Angew. Chem. Int. Ed.* **2000**, *39*, 3013.

(2) Trnka, T. M.; Grubbs, R. H. The Development of L_2X_2Ru = CHR Olefin Metathesis Catalysts: An Organometallic Success Story *Acc. Chem. Res.* **2001**, *34*, 18.

(3) Baldo, M. A.; Adachi, C.; Forrest, S. R. Transient Analysis of Organic Electrophosphorescence. II. Transient Analysis of Triplet-Triplet Annihilation *Phys. Rev. B* **2000**, *62*, 10967.

(4) Gong, X.; Robinson, M. R.; Ostrowski, J. C.; Moses, D.; Bazan, G. C.; Heeger, A. J. High-Efficiency Polymer-Based Electrophosphorescent Devices *Adv. Mater.* **2002**, *14*, 581.

(5) Bellmann, E.; Shaheen, S. E.; Thayumanavan, S.; Barlow, S.; Grubbs, R. H.; Marder, S. R.; Kippelen, B.; Peyghambarian, N. New Triarylamine-Containing Polymers as Hole Transport Materials in Organic Light-Emitting Diodes: Effect of Polymer Structure and Cross-Linking on Device Characteristics *Chem. Mater.* **1998**, *10*, 1668.

(6) Borsenberger, P. M.; Pautmeier, L.; Richert, R.; Bassler, H. Hole Transport in 1,1-Bis(di-4-tolylaminophenyl)cyclohexane *J. Chem. Phys.* **1991**, *94*, 8276.

(7) Markham, J. P. J.; Samuel, I. D. W.; Lo, S. C.; Burn, P. L.; Weiter, M.; Bassler, H. Charge Transport in Highly Efficient Iridium Cored Electrophosphorescent Dendrimers *J. Appl. Phys.* **2004**, *95*, 438.

(8) Evans, N. R.; Devi, L. S.; Mak, C. S. K.; Watkins, S. E.; Pascu, S. I.; Kohler, A.; Friend, R. H.; Williams, C. K.; Holmes, A. B. Triplet Energy Back Transfer in Conjugated Polymers with Pendant Phosphorescent Iridium Complexes *J. Am. Chem. Soc.* **2006**, *128*, 6647.

(9) Hreha, R. D.; Zhang, Y. D.; Domercq, B.; Larribeau, N.; Haddock, J. N.; Kippelen, B.; Marder, S. R. Synthesis of Photo-Crosslinkable Hole-Transport Polymers with Tunable Oxidation Potentials and Their Use in Organic Light-Emitting Diodes *Synthesis* **2002**, 1201.

(10) Hreha, R. D.; Haldi, A.; Domercq, B.; Barlow, S.; Kippelen, B.; Marder, S. R. Synthesis of Acrylate and Norbornene Polymers with Pendant 2,7-Bis(Diarylamino)Fluorene Hole-Transport Groups *Tetrahedron* **2004**, *60*, 7169.

(11) Domercq, B.; Hreha, R. D.; Zhang, Y. D.; Larribeau, N.; Haddock, J. N.; Schultz, C.; Marder, S. R.; Kippelen, B. Photo-Patternable Hole-Transport Polymers for Organic Light-Emitting Diodes *Chem. Mater.* **2003**, *15*, 1491.

(12) South, C. R.; Higley, M. N.; Leung, K. C. F.; Lanari, D.; Nelson, A.; Grubbs, R. H.; Stoddart, J. F.; Weck, M. Self-Assembly with Block Copolymers through Metal Coordination of SCS-Pd^{II} Pincer Complexes and Pseudorotaxane Formation *Chem. Eur. J.* **2006**, *12*, 3789.

(13) Carlise, J. R.; Wang, X. Y.; Weck, M. Phosphorescent Side-Chain Functionalized Poly(norbornene)s Containing Iridium Complexes *Macromolecules* **2005**, *38*, 9000.

(14) Adachi, C.; Baldo, M. A.; Thompson, M. E.; Forrest, S. R. Nearly 100% Internal Phosphorescence Efficiency in an Organic Light-Emitting Device *J. Appl. Phys.* **2001**, *90*, 5048.

(15) Baldo, M. A.; Lamansky, S.; Burrows, P. E.; Thompson, M. E.; Forrest, S. R. Very High-Efficiency Green Organic Light-Emitting Devices Based on Electrophosphorescence *Appl. Phys. Lett.* **1999**, *75*, 4.

(16) Wu, F. I.; Su, H. J.; Shu, C. F.; Luo, L. Y.; Diau, W. G.; Cheng, C. H.; Duan, J. P.; Lee, G. H. Tuning the Emission and Morphology of Cyclometalated Iridium Complexes and Their Applications to Organic Light-Emitting Diodes *J. Mater. Chem.* **2005**, *15*, 1035.

(17) Zhen, H. Y.; Luo, C.; Yang, W.; Song, W. Y.; Du, B.; Jiang, J. X.; Jiang, C. Y.; Zhang, Y.; Cao, Y. Electrophosphorescent Chelating Copolymers Based on Linkage Isomers of Naphthylpyridine-Iridium Complexes with Fluorene *Macromolecules* **2006**, *39*, 1693.

(18) Yang, X. H.; Neher, D. Polymer Electrophosphorescence Devices with High Power Conversion Efficiencies *Appl. Phys. Lett.* **2004**, *84*, 2476.

(19) Ramos-Ortiz, G.; Oki, Y.; Domercq, B.; Kippelen, B. Förster Energy Transfer from a Fluorescent Dye to a Phosphorescent Dopant: A Concentration and Intensity Study *Phys. Chem. Chem. Phys.* **2002**, *4*, 4109.

(20) Wang, X. Y.; Prabhu, R. N.; Schmehl, R. H.; Weck, M. Polymer-Based tris(2-phenylpyridine)iridium Complexes *Macromolecules* **2006**, *39*, 3140.

(21) Chen, X. W.; Liao, J. L.; Liang, Y. M.; Ahmed, M. O.; Tseng, H. E.; Chen, S. A. High-Efficiency Red-Light Emission from Polyfluorenes Grafted with Cyclometalated Iridium Complexes and Charge Transport Moiety *J. Am. Chem. Soc.* **2003**, *125*, 636.

(22) Jiang, J. X.; Jiang, C. Y.; Yang, W.; Zhen, H. G.; Huang, F.; Cao, Y. High-Efficiency Electrophosphorescent Fluorene-alt-Carbazole Copolymers N-Grafted with Cyclometalated Ir Complexes *Macromolecules* **2005**, *38*, 4072.

(23) You, Y.; Kim, S. H.; Jung, H. K.; Park, S. Y. Blue Electrophosphorescence from Iridium Complex Covalently Bonded to the Poly (9-dodecyl-3-vinylcarbazole): Suppressed Phase Segregation and Enhanced Energy Transfer *Macromolecules* **2006**, *39*, 349.

(24) Konno, T.; El-Khouly, M. E.; Nakamura, Y.; Kinoshita, K.; Araki, Y.; Ito, O.; Yoshihara, T.; Tobita, S.; Nishimura, J. Photoinduced Intramolecular Electron Transfer of Carbazole Trimer-[60]Fullerene Studied by Laser Flash Photolysis Techniques *J. Phys. Chem. C* **2008**, *112*, 1244.

(25) McClenaghan, N. D.; Passalacqua, R.; Loiseau, F.; Campagna, S.; Verheyde, B.; Hameurlaine, A.; Dehaen, W. Ruthenium(II) Dendrimers Containing Carbazole-Based Chromophores as Branches *J. Am. Chem. Soc.* **2003**, *125*, 5356.

(26) Zhang, Q.; Hu, Y. F.; Cheng, Y. X.; Su, G. P.; Ma, D. G.; Wang, L. X.; Jing, X. B.; Wang, F. S. Carbazole-Based Hole-Transporting Materials for Electroluminescent Devices *Synth. Met.* **2003**, *137*, 1111.

(27) Promarak, V.; Ichikawa, M.; Sudyoadsuk, T.; Saengsuwan, S.; Jungsuttiwong, S.; Keawin, T. Synthesis of Electrochemically and Thermally Stable Amorphous Hole-Transporting Carbazole Dendronized Fluorene *Synth. Met.* **2007**, *157*, 17.

(28) Xu, T. H.; Lu, R.; Liu, X. L.; Zheng, X. Q.; Qiu, X. P.; Zhao, Y. Y. Phosphorus(V) Porphyrins with Axial Carbazole-Based Dendritic Substituents *Org. Lett.* **2007**, *9*, 797.

(29) Ding, J. Q.; Gao, J.; Cheng, Y. X.; Xie, Z. Y.; Wang, L. X.; Ma, D. G.; Jing, X. B.; Wang, F. S. Highly Efficient Green-Emitting Phosphorescent Iridium Dendrimers Based on Carbazole Dendrons *Adv. Funct. Mater.* **2006**, *16*, 575.

(30) Love, J. A.; Morgan, J. P.; Trnka, T. M.; Grubbs, R. H. A Practical and Highly Active Ruthenium-Based Catalyst That Effects the Cross Metathesis of Acrylonitrile *Angew. Chem. Int. Ed.* **2002**, *41*, 4035.

CHAPTER 9

CONCLUSION AND OUTLOOK

9.1 Abstract

This chapter provides a broad overview of the projects that are described in this thesis, and summarizes the basic findings. Furthermore, suggestions for future studies are presented.

9.2 Summary of the Results

In this thesis, syntheses and characterizations of polymers with metal complexes along their side-chains for OLED applications are described. The physical and photophysical properties of the polymers were tuned by changing the backbone and the metal complex. Poly(norbornene)s, poly(cyclooctene)s, and poly(styrene)s were studied. The differences in the glass transition temperatures and PDIs of the polymers indicated that device performances might be affected by the polymer type due to the differences in the processability of the polymers. However, no direct comparison was made in order to determine the most promising polymer type for OLED applications. In addition to the backbone, it was found that the molecular weights of the polymers had an impact on the device performance. It was shown that devices based on high molecular weight poly(norbornene)s (200 kDa) had lower efficiencies than those with low molecular weight (15-50 kDa). In each case, it was found that the polymer backbone does not interfere with the basic photopysical properties of the metal complexes.

The two main classes of metal complexes studied in this thesis are metalloquinolates and iridium complexes. It was shown that the emission properties of

poly(cyclooctene)s containing 8-hydroxyquinolines in their side-chains could be altered by simply changing the metal. Green- and near IR-emitting polymers were synthesized by employing aluminum and ytterbium, respectively. On the other hand, for the iridium complexes, changes in color were achieved by varying the ligands. Iridium containing polymers with emission spectra that span the entire visible spectrum were synthesized by employing the appropriate ligands. All homopolymers based on these complexes (metalloquinolates and iridium complexes) had solubility problems that could be attributed to different reasons. For polymers with metalloquinolates, ligand exchange reactions between the complexes can result in a crosslinked network due to the binding of the metal to ligands on different polymer chains[1-3], whereas, for the iridium containing polymers, the insolubility is believed to be due to the aggregation between the complexes.[4] Regardless of the reason, it is clear that comonomers had to be used in order to increase the solubility. Comonomers that could also function as a host material for the metal complex were chosen to increase charge transfer and to facilitate exciton formation. The comonomers that are described in this thesis are based on carbazole or a 2,7-di(carbazol-9-yl)fluorene-type material. These compounds have been employed extensively as host materials in OLEDs.[5-9] In Chapter 3, it was shown that there is significant energy transfer from carbazole to aluminum tris(8-hydroxyquinoline) for the poly(cyclooctene) based systems, proving the efficiency of our approach. Similarly, the electroluminescence spectra of poly(norbornene)s with iridium complexes and a 2,7-di(carbazol-9-yl)fluorene type host material did not show emission from the host, indicating an efficient energy transfer from the host to the complex.

The main focus in terms of device studies was on the poly(norbornene)s with iridium complexes (Chapters 7 and 8). The best results were obtained for the orange-emitting polymer, which was used as the model system to study polymer structure-device performance relationships in order to develop general principles that can be used to optimize iridium-containing polymers for OLED applications. It was found that the

device performance is dependent on various parameters such as molecular weight, iridium loading, spacer type, and spacer length. As mentioned above, high molecular weight (*i.e*. more than 200 kDa) had an adverse effect on the device performance. On the other hand, the optimum iridium complex loading was found to be 5 mol%. Changing the linker type on the host material from an ether group to an ester group resulted in a slight increase on the device performance. Finally, replacing a short spacer on the iridium containing monomer with a long one led to a further improvement. External quantum efficiencies as high as 4.9 ± 0.4% at 100 cd/m^2 were measured for the orange-emitting copolymers. It was found that these principles can be applied to other types (*i.e*. green-emitting) of iridium containing polymers.

Finally, in order to fabricate fully solution-processable OLEDs, an orange-emitting random copolymer with a crosslinking unit in the side-chain was prepared. The polymer was crosslinked by exposure to UV light after spin-coating it on top of ITO. Although a lower efficiency (2.7% EQE) was obtained for the device with the crosslinked copolymer than that of the optimized orange-emitting copolymer without the crosslinking unit, the results are still highly promising, considering that fully solution-processable devices can be fabricated.

These results show that every unit of the polymer structure has an impact on the device performance. Therefore, polymers for OLED applications should be carefully designed. For example, the host material should be specifically chosen for the metal complex in order to maximize energy transfer and charge transport. The polymerization method of choice should be tolerant to functional groups on monomers to minimize interference during the polymerization process. Each project described in the thesis has enhanced our knowledge in terms of structure-property relationship, which in turn led to the fabrication of OLEDs with systematically improved performances. The efficiencies of our OLEDs are now among the best examples of side-chain functionalized polymers for OLED applications. The general principles described in this thesis for the

optimization of the polymer structure can provide guide lines for the future studies. The next section describes future ideas to further optimize the polymer structure.

9.3 Future Ideas

9.3.1 Postpolymerization Functionalization

In Chapter 6, it was shown that click chemistry is a highly effective tool for the functionalization of polymers with various iridium complexes. However, preliminary studies indicated that the triazole ring has an impact on the device performance. Indeed, it was reported that the triazole ring formed by a click reaction can participate in electron transfer between redox species,[10] suggesting that the ring might affect the exciton formation in the device. On the other hand, it needs to be determined whether this effect is positive or negative. A decisive conclusion can be drawn by changing the device structure systematically, and by employing a different iridium complex with a different emission color than $Ir(ppy)_3$. If the performance of the device based on a polymer with the triazole ring is lower in each case, it can be concluded that another postpolymerization functionalization strategy is needed. One of the possibilities is the hydrazone formation between the polymer and the metal complex as shown in Scheme 9.1. Quantitative conversions are obtained for this type of postpolymerization reactions between a ketone and a hydrazine.[11]

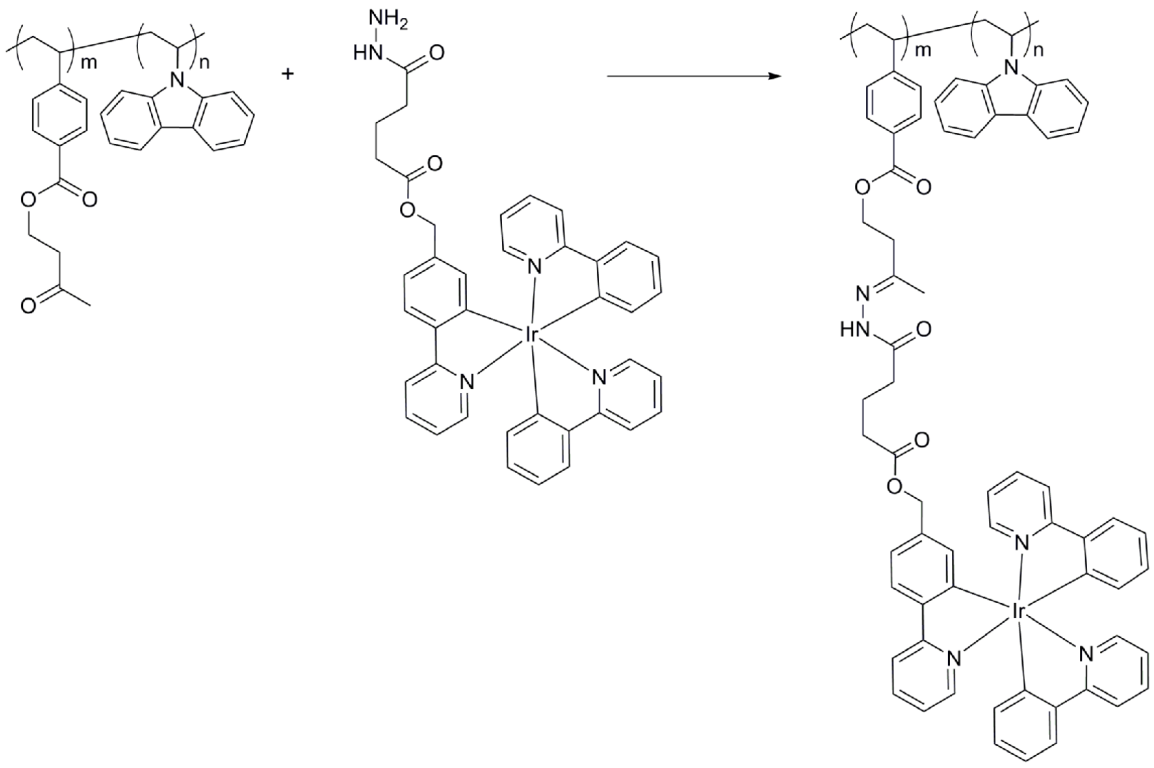

Scheme 9.1 Proposed quantitative postpolymerization functionalization.

9.3.2 Optimization of the Iridium-Containing Polymers

In Chapters 5-8, the iridium containing polymers are also functionalized with the materials that are mainly hole-transporters in order to facilitate the charge mobility and exciton formation. This strategy can be taken one step further by the attachment of an electron-transport compound to the polymer backbone (Figure 9.1). Co-existence of an electron-transport compound such as an oxadiazole derivative and a hole-transport material can improve the charge balance in the emissive layer, leading to an increased device performance.[12-15] Ultimately, a crosslinking agent can be included in the polymer structure to produce a polymer with four functional groups (hole- and electron-transporters, an emissive metal complex, and a crosslinking unit) for fully solution-processible OLEDs.

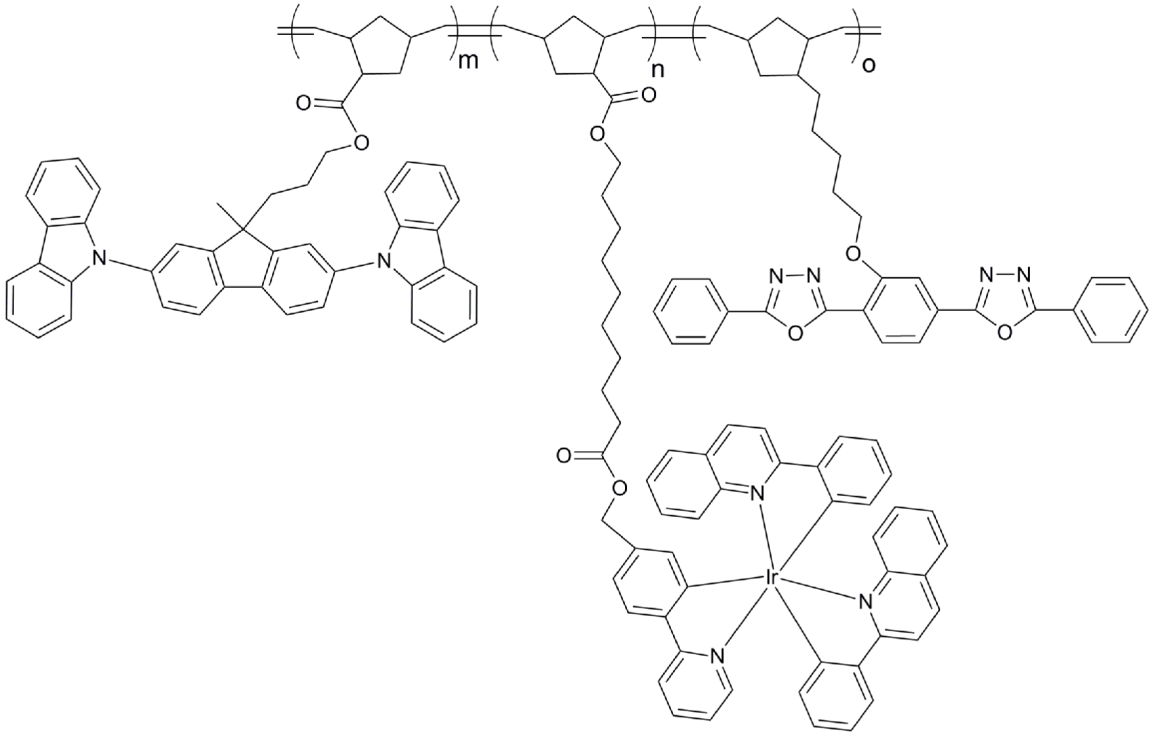

Figure 9.1 Example of a multi-functionalized polymer with a metal complex and hole- and electron-transporters.

Another issue that should be addressed in order to optimize device performance is the effect of the double bonds of the polymer backbone on the device performance. The double bonds on poly(norbornene) can be hydrogenated as shown in Scheme 9.2. Comparison of the performances of the devices with or without these double bonds should determine the importance of the presence of the double bonds. However, it should be noted that the complete removal of the hydrogenation catalyst is crucial in order to have a fair comparison.

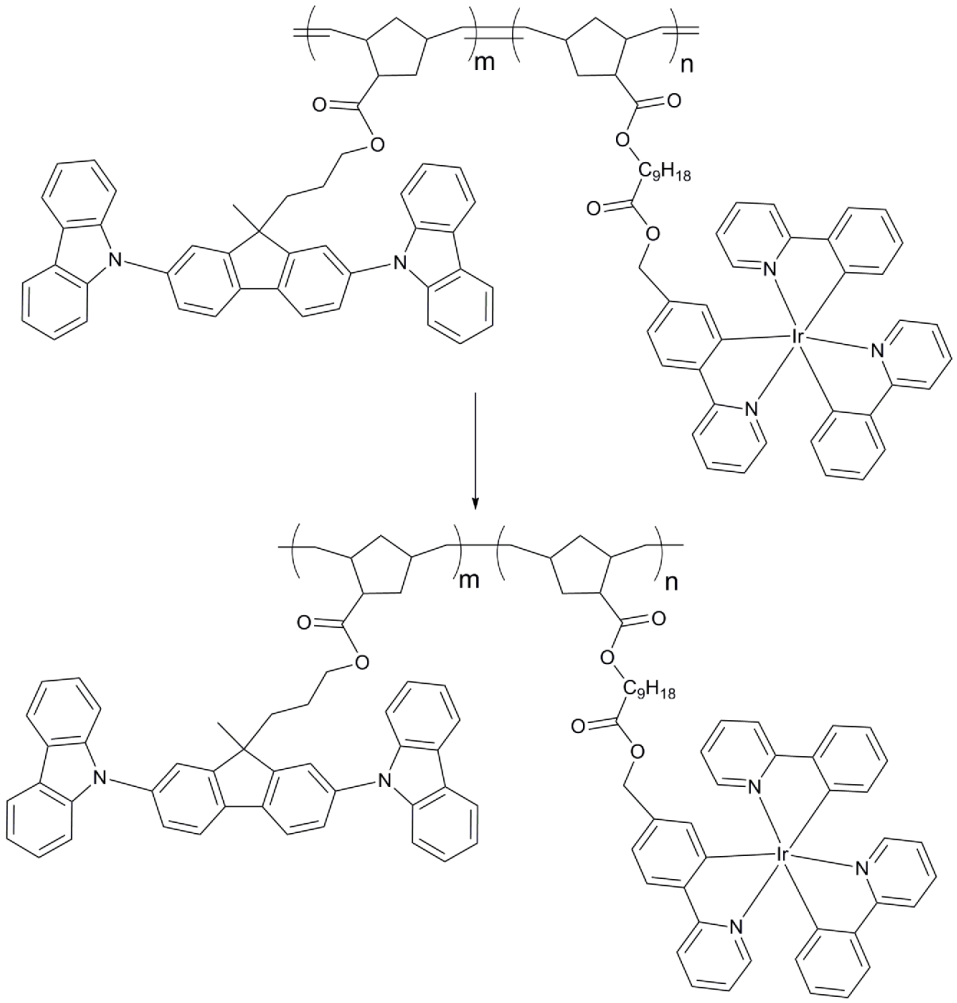

Scheme 9.2 Hydrogenation of the poly(norbornene) backbone.

The PL quantum efficiency of the orange-emitting iridium complex that is mentioned in Chapter 7 is 10%. Comparison of the devices based on the orange-emitting polymer and a polymer with a similar emission spectrum but with a higher PL efficiency (Figure 9.2) can clarify the importance of the PL quantum efficiency. The iridium complex that is shown in Figure 9.2 has a PL quantum efficiency of 32% (three times higher than the orange-emitting complex) with an emission maximum of 598 nm,[16] which is the same as our orange emitting polymer. If the devices give similar performances, it can be concluded that the limiting factor is not the PL efficiency.

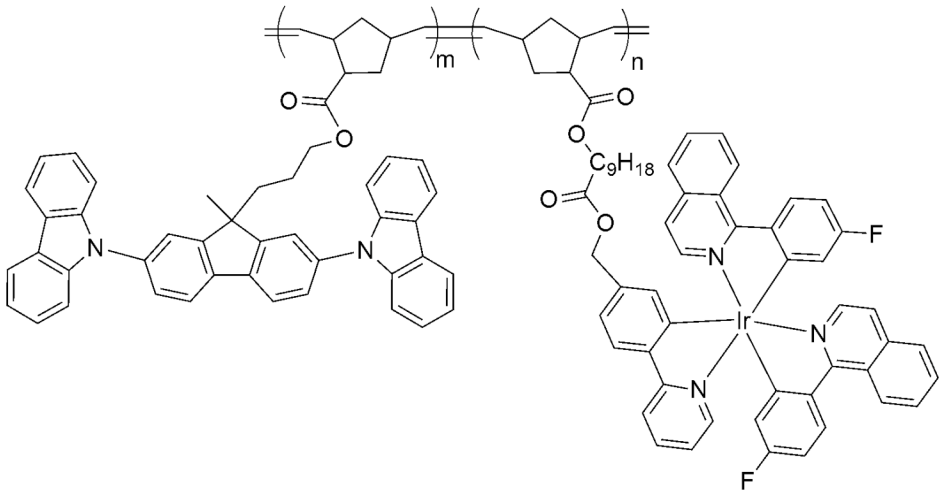

Figure 9.2 Structure of the proposed orange-emitting polymer with high PL efficiency.

9.4 References

(1) Meyers, A.; Weck, M. Design and Synthesis of Alq_3-Functionalized Polymers *Macromolecules* **2003**, *36*, 1766.

(2) Meyers, A.; Weck, M. Solution and Solid-State Characterization of Alq_3-Functionalized Polymers *Chem. Mater.* **2004**, *16*, 1183.

(3) Wang, X. Y.; Weck, M. Poly(styrene)-Supported Alq_3 and BPh_2q *Macromolecules* **2005**, *38*, 7219.

(4) Carlise, J. R.; Wang, X. Y.; Weck, M. Phosphorescent Side-Chain Functionalized Poly(norbornene)s Containing Iridium Complexes *Macromolecules* **2005**, *38*, 9000.

(5) Jiang, J. X.; Jiang, C. Y.; Yang, W.; Zhen, H. G.; Huang, F.; Cao, Y. High-Efficiency Electrophosphorescent Fluorene-alt-Carbazole Copolymers N-Grafted with Cyclometalated Ir Complexes *Macromolecules* **2005**, *38*, 4072.

(6) You, Y.; Kim, S. H.; Jung, H. K.; Park, S. Y. Blue Electrophosphorescence from Iridium Complex Covalently Bonded to the Poly (9-dodecyl-3-vinylcarbazole): Suppressed Phase Segregation and Enhanced Energy Transfer *Macromolecules* **2006**, *39*, 349.

(7) Chen, X. W.; Liao, J. L.; Liang, Y. M.; Ahmed, M. O.; Tseng, H. E.; Chen, S. A. High-Efficiency Red-Light Emission from Polyfluorenes Grafted with Cyclometalated Iridium Complexes and Charge Transport Moiety *J. Am. Chem. Soc.* **2003**, *125*, 636.

(8) Hreha, R. D.; George, C. P.; Haldi, A.; Domercq, B.; Malagoli, M.; Barlow, S.; Bredas, J. L.; Kippelen, B.; Marder, S. R. 2,7-Bis(diarylamino)-9,9-dimethylfluorenes as Hole-Transport Materials for Organic Light-Emitting Diodes *Adv. Funct. Mater.* **2003**, *13*, 967.

(9) Marsal, P.; Avilov, I.; da Silva, D. A.; Brédas, J. L.; Beljonne, D. Molecular Hosts for Triplet Emission in Light Emitting Diodes: A Quantum-Chemical Study *Chem. Phys. Lett.* **2004**, *392*, 521.

(10) Devaraj, N. K.; Decreau, R. A.; Ebina, W.; Collman, J. P.; Chidsey, C. E. D. Rate of Interfacial Electron Transfer through the 1,2,3-Triazole Linkage *J. Phys. Chem. B* **2006**, *110*, 15955.

(11) Yang, S. K.; Weck, M. Modular Covalent Multifunctionalization of Copolymers *Macromolecules* **2008**, *41*, 346.

(12) Xiang, N. J.; Lee, T. H.; Gong, M. L. A.; Tong, K. L.; So, S. K.; Leung, L. M. Synthesis of 2-Phenylquinoline-Based Ambipolar Molecules Containing Multiple 1,3,4-Oxadiazole Spacer Groups *Synth. Met.* **2006**, *156*, 270.

(13) Bugatti, V.; Concilio, S.; Iannelli, P.; Piotto, S. P.; Bellone, S.; Ferrara, M.; Neitzert, H. C.; Rubino, A.; Della Sala, D.; Vacca, P. Synthesis and Characterization of New Electroluminescent Molecules Containing Carbazole and Oxadiazole Units *Synth. Met.* **2006**, *156*, 13.

(14) Gong, X.; Robinson, M. R.; Ostrowski, J. C.; Moses, D.; Bazan, G. C.; Heeger, A. J. High-Efficiency Polymer-Based Electrophosphorescent Devices *Adv. Mater.* **2002**, *14*, 581.

(15) Lee, J. H.; Tsai, H. H.; Leung, M. K.; Yang, C. C.; Chao, C. C. Phosphorescent Organic Light-Emitting Device with an Ambipolar Oxadiazole Host *Appl. Phys. Lett.* **2007**, *90*, 243501.

(16) Okada, S.; Okinaka, K.; Iwawaki, H.; Furugori, M.; Hashimoto, M.; Mukaide, T.; Kamatani, J.; Igawa, S.; Tsuboyama, A.; Takiguchi, T.; Ueno, K. Substituent Effects of Iridium Complexes for Highly Efficient Red OLEDs *Dalton Trans.* **2005**, 1583.

APPENDIX A

N-HETEROCYCLIC CARBENE BASED BLUE-EMITTING IRIDIUM COMPLEXES

A.1 Abstract

This section describes a procedure for the synthesis of a blue emitting N-heterocyclic carbene-based iridium complex in high yields. Furthermore, a method for the separation of the meridional isomer from the facial isomer is depicted. Finally, emission spectra in solution and the solid state are compared to those reported in the literature.

A.2 Introduction

The synthesis and characterization of numerous iridium complexes with emission spectra that span the visible spectrum have been reported in the literature, as described in the previous chapters. However, blue-emitting iridium complexes are still scarce. Most iridium complexes that emit in the blue have broad emission spectra that expand into the green region, resulting in low color purity.[1-3] Exceptions to this behavior are the N-heterocyclic carbene-based iridium complexes, which emit in the blue or near-UV regions.[3,4] In general, these complexes have low photoluminescence quantum yields in solution (i.e. <10%). However, the emission quantum yields increase significantly when the complexes are doped in polymer films.[5] Furthermore, promising performances were obtained for devices from N-heterocyclic carbene based iridium complexes,[6,7] making

them outstanding candidates for the attachment to polymer backbones for solution-processable OLEDs.

In this section, the synthesis of an N-heterocyclic carbene based blue-emitting iridium complex is described. Although the complex has been reported in the literature,[5] the methodology described in this section provides a more efficient synthesis of the complex in terms of chemical yield. Furthermore, the solution and solid state emission spectra of the complex are reported to demonstrate the color purity of the complex.

A.3 Results and Discussion

Synthesis. Ligand **1** was synthesized according to the literature procedures.[5] The reported procedure for the synthesis of complex **3**, involving a base, KHMDS (Potassium hexamethyldisilazane), and 10 times excess of ligand **1** with respect to the iridium dimer **2**, results in 24% yield.[5] Recently, Mashima and coworkers described a strategy for the synthesis of N-heterocyclic carbene-base iridium complexes that employs excess amounts of Ag_2O.[4] By employing a similar procedure that involves stoichiometric amounts of the ligand and Ag_2O, iridium complex **3** was obtained in 61% yield (Scheme A.1), a significant increase from the reported 24%. The proportion of the meridional and the facial isomers was found to be 11:1 according to ^{1}H-NMR spectroscopy. However, recrystallization from dichloromethane/methanol solution afforded pure *mer*-**3** (Figure A.1)

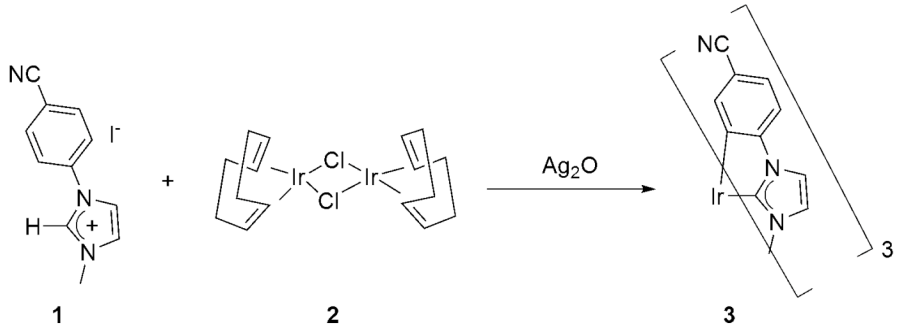

Scheme A.1 Synthesis of the blue-emitting complex **3**.

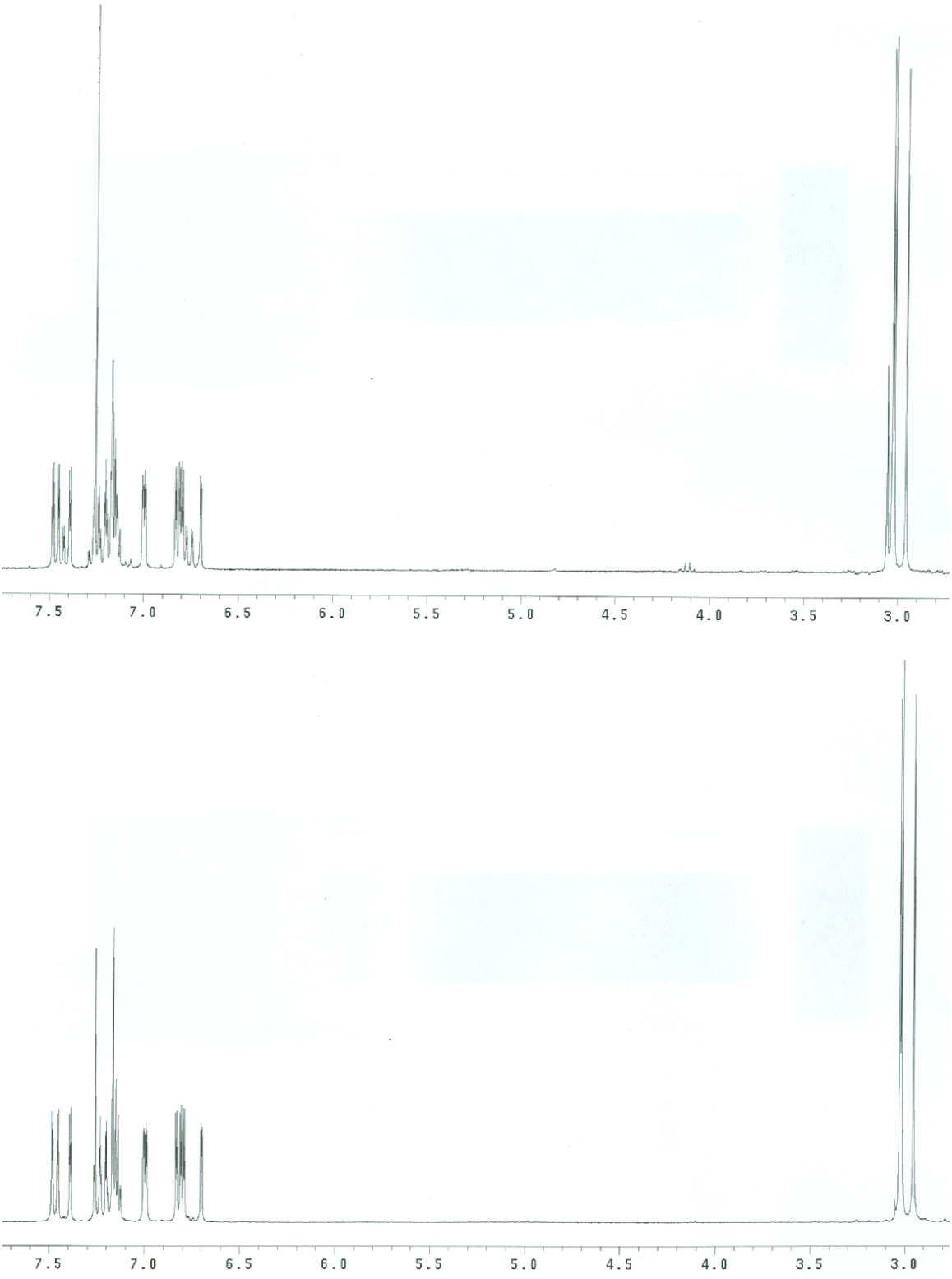

Figure A.1 ^{1}H-NMR spectra of **3** (top: mixture of facial and meridional isomers, bottom: meridional).

In order to determine the applicability of the strategy to the syntheses of iridium complexes with 2 different ligands, a second methyl-ether functionalized N-heterocyclic carbene ligand was synthesized as shown in Scheme A.2. Pd_2dba_3 and BINAP were employed to catalyze the coupling of compound **4** and bromobenzene to give compound **5**, which was then reacted with ethyl orthoformate and ammonium tetrafluoroborate to yield the target ligand **6**.

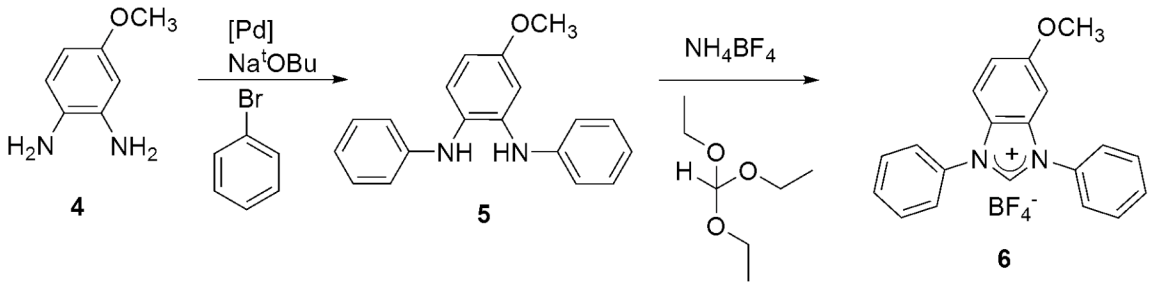

Scheme A.2 Synthesis of ligand **6**.

In order to synthesize target complex **8**, based on ligands **1** and **3**, compound **7** (synthesized in a single step from complex **2** in 30% yield)[7] was reacted with **6** in the presence of Ag_2O (Scheme A.3). Unfortunately, this reaction did not produce the desired compound. In a control reaction, ligand **1** was reacted with compound **7** as shown in Scheme A.3, and complex **3** was obtained in 20% yield. As described above, complex **3** was synthesized in 61% yield in one step from iridium dimer **2**. Overall yield for the two-step synthesis for the same compound is 6%, indicating the inefficiency of the procedure described in Scheme A.3.

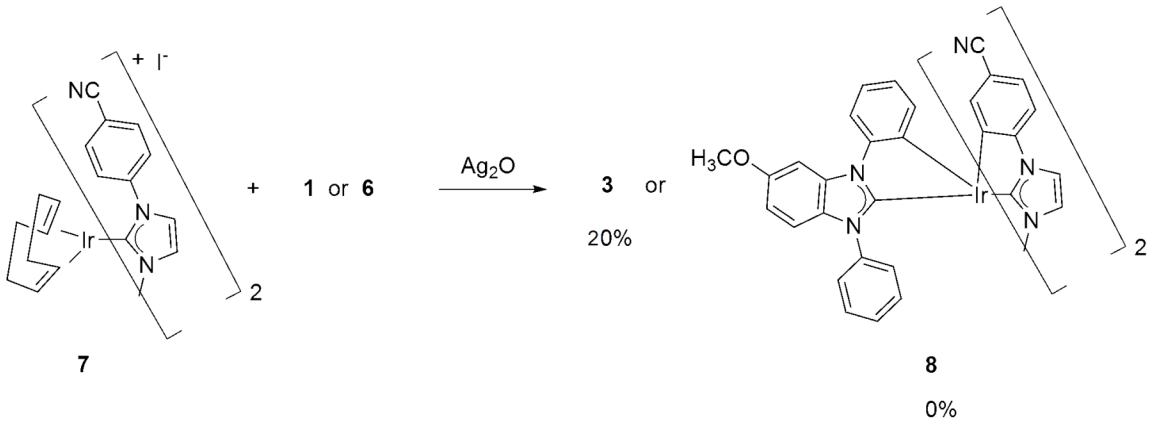

Scheme A.3 Attempted synthesis of a complex with two different ligands.

Photoluminescence. Unlike the iridium complexes discussed in the previous chapters, both isomers of N-heterocyclic based iridium complexes have high PL quantum efficiencies.[5] For example, as reported in the literature, *mer*-**3** has 57% PL efficiency in PMMA films.[5] Figure A.2 shows the emission spectra of *mer*-**3** both in chloroform solution and the solid state. The emission maximum in solution is 457 nm, which is in agreement with the literature value.[5] However, the solid state emission spectrum is shifted towards to the green region with an emission maximum of 503 nm. This large red-shift might be due to excimer formation, as suggested by the broad and featureless spectrum.[8] The solution emission maximum and the solid state emission maximum in PMMA films are similar,[5] indicating that the excimer formation can be prevented by doping the complex in a suitable host.

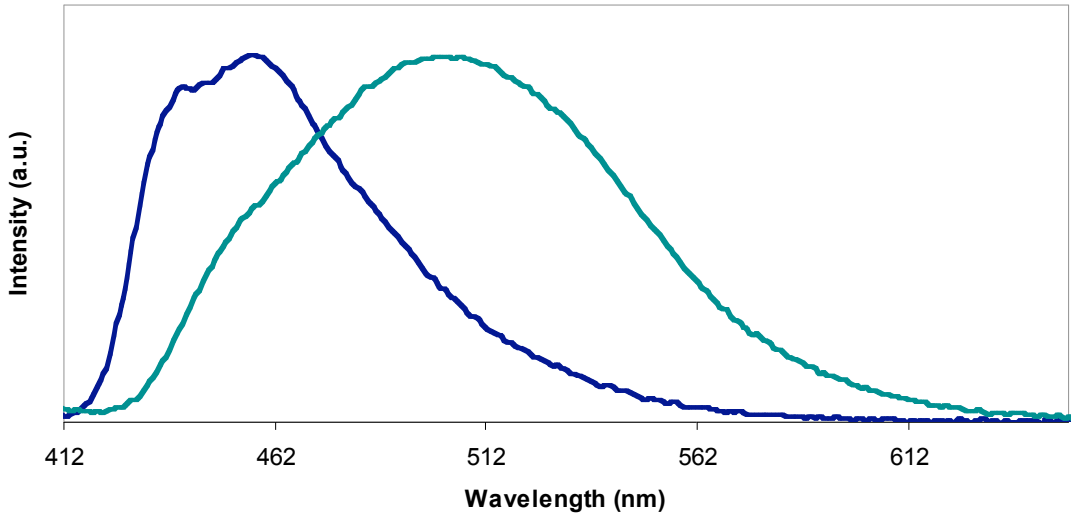

Figure A.2 Solution (blue) and solid state (green) emission spectra of mer-**3**.

A.4 Conclusion

A blue emitting N-heterocyclic carbene based iridium complex was synthesized. Recrystallization from dichloromethane/methanol solution gave pure meridianal isomer, which displayed blue emission in solution. However, the complex emits in the green region in solid state most likely due to aggregation. Therefore, employment of a host material is crucial in order to prevent the aggregation.

A.5 Experimental

All Reagents were purchased either from Acros Organics or Aldrich and used without further purification. ^{1}H-NMR and ^{13}C-NMR spectra (300 MHz ^{1}H NMR, 75 MHz ^{13}C NMR) were taken using a Varian Mercury Vx 300 spectrometer. All spectra are referenced to residual proton solvent. Mass spectral analyses were provided by the

Georgia Tech Mass Spectrometry Facility. Emission measurements were acquired using a Shimadzu RF-5301 PC spectrofluorophotometer.

Synthesis of tris-[1-(4′-cyanophenyl)-3-methylimidazol-2-yliden-C^2,$C^{2'}$]-iridium(III), 3. A mixture of compounds **1** (1.41 g, 4.53 mmol), **2** (0.50 g, 0.74 mmol), and Ag_2O (1.04 g, 4.48 mmol) in 2-ethoxy ethanol (60 mL) was stirred for 24 hours at 135 ^oC under argon. After the solvent was removed *in vacuo*, the resulting solid was purified by column chromatography (silica, CH_2Cl_2) to give compound **3** as a light yellow powder (0.67 g, 61% yield). The spectral data for **3** were consistent with that reported in the literature.[5]

4-Methoxybenzene-1,2-diamine, 5. A Mixture of compound **4** (1.75 g, 12.6 mmol)), bromobenzene (4.25 g, 27.1 mmol), NaO^tBu (3.08 g, 32.0 mmol), Pd_2dba_3 (0.225 g, 0.25 mmol), and BINAP (0.325 g, 0.52 mmol) in 50 mL toluene was stirred at 80 ^oC under argon for 2 days. Diethyl ether was added and the mixture was filtered. The solution was concentrated *in vacuo*, followed by column chromatography (silica, 10:1 hexane/ethyl acetate) to give compound **5** in 52%. ^1H NMR (300 MHz, $CDCl_3$) δ 7.30-7.07 (7H, m); 6.96 (1H, t, J = 7.5); 6.91 (1H, d, J = 3.0); 6.81 (1H, t, J = 7.5); 6.73 (2H, d, J = 8.1); 6.44 (1H, dd, J = 8.4, 3.0); 6.14 (1H, s); 5.09 (1H, s); 3.77 (3H, s). ^{13}C NMR (75 MHz, $CDCl_3$) δ 158.2, 146.7, 142.6, 141.1, 129.6, 127.3, 123.9, 121.9, 119.5, 119.4, 115.0, 105.7, 101.9, 55.7. MS m/z Calcd. (M^+): 291.1. Found (ESI): 291.1 (M^+).

6-Methoxy-1,3-diphenylbenzoimidazolium tetrafluoroborate, 6. Triethyl orthoformate (90 mg, 0.60 mmol)) was added dropwise to the mixture of compound **2** (145 mg, 0.50 mmol) and ammonium tetrafluoroborate (55 mg, 0.52 mmol) under argon. The mixture was stirred at 120 ^oC for 2 hours. After cooling to room temperature, hexane was added, the mixture was filtered, and the solid was washed with hexane and ethyl acetate to give compound **3** as a white powder (160 mg, 83%). ^1H NMR (300 MHz, $CDCl_3$) δ 9.51 (1H, s); 7.85 (4H, m); 7.67 (7H, m); 7.26 (1H, m); 7.04 (1H, m); 3.88 (3H,

s). ^{13}C NMR (75 MHz, $CDCl_3$) δ 160.6, 139.6, 132.8, 131.4, 131.0, 130.9, 129.6, 125.6, 125.4, 118.8, 114.9, 95.8, 56.5. MS m/z Calcd. (M): 388.1. Found (ESI): 301.1 (M-BF_4).

A.6 References

(1) Tamayo, A. B.; Alleyne, B. D.; Djurovich, P. I.; Lamansky, S.; Tsyba, I.; Ho, N. N.; Bau, R.; Thompson, M. E. Synthesis and Characterization of Facial and Meridional Tris-Cyclometalated Iridium(III) Complexes *J. Am. Chem. Soc.* **2003**, *125*, 7377.

(2) Li, J.; Djurovich, P. I.; Alleyne, B. D.; Yousufuddin, M.; Ho, N. N.; Thomas, J. C.; Peters, J. C.; Bau, R.; Thompson, M. E. Synthetic Control of Excited-State Properties in Cyclometalated Ir(III) Complexes Using Ancillary Ligands *Inorg. Chem.* **2005**, *44*, 1713.

(3) Sajoto, T.; Djurovich, P. I.; Tamayo, A.; Yousufuddin, M.; Bau, R.; Thompson, M. E.; Holmes, R. J.; Forrest, S. R. Blue and near-Uv Phosphorescence from Iridium Complexes with Cyclometalated Pyrazolyl or N-Heterocyclic Carbene Ligands *Inorg. Chem.* **2005**, *44*, 7992.

(4) Chien, C. H.; Fujita, S.; Yamoto, S.; Hara, T.; Yamagata, T.; Watanabe, M.; Mashima, K. Stepwise and One-Pot Syntheses of Ir(III) Complexes with Imidazolium-Based Carbene Ligands *Dalton Trans.* **2008**, 916.

(5) Egen, M.; Kahle, K.; Bold, M.; Gessner, T.; Lennartz, C.; Nord, S.; Schmidt, H. W.; Thelakkat, M.; Baete, M.; Neuber, C.; Kowalsky, W.; Schieldknecht, C.; Johannes, H.-H. Preparation of Transition Metal N-Heterocyclic Carbene Complexes for Use in Organic Light Emitting Diodes (OLEDs) *Patent: WO2006056418*.

(6) Schieldknecht, C.; Ginev, G.; Kammoun, A.; Riedl, T.; Kowalsky, W.; Johannes, H.-H.; Lennartz, C.; Kahle, K.; Egen, M.; Gebner, T.; Bold, M.; Nord, S.; Erk, P. Novel Deep-Blue Emitting Phosphorescent Emitter *Proc. SPIE* **2005**, *5937*, 59370E.

(7) Fuchs, E.; Egen, M.; Kahle, K.; Lennartz, C.; Molt, O.; Nord, S.; Kowalsky, W.; Schieldknecht, C.; Johannes, H.-H. Heteroleptic Cyclometalated Transition Metal-Carbene Complexes Containing at Least Two Differently Substituted N-Heterocyclic Carbene Ligands and Their Use in Organic Light Emitting Diodes (OLEDs) *Patent: WO2007115970.*

(8) Hercules, D. M. *Fluorescence and Phosphorescence Analysis: Principles and Applications*; Interscience Publishers: New York, 1966.

APPENDIX B

CROSSLINKABLE HOLE-TRANSPORT POLYMERS FOR SOLUTION-PROCESSABLE OLEDS

B.1 Abstract

A carbazole based copolymer with crosslinking cinnamate groups was synthesized and employed as a hole-transport layer in OLEDs. An External quantum efficiency of 8.4 %, and a luminous efficiency of 28 cd/A were obtained for a device with the crosslinked copolymer. On the other hand, it was found that UV exposure during the crosslinking process gives rise to partial decomposition of the carbazole groups, resulting in declined device performance.

B.2 Introduction

The hole-transport compounds that are described in Chapters 6-8 are TPD based copolymers that contain crosslinking cinnamate groups.[1-4] These polymers were spin-coated onto ITO and crosslinked by UV radiation, which allowed for the spin-coating of the emissive polymers onto the hole-transport layer. This strategy can be applied to other types of hole-transport compounds as well. As mentioned in the previous chapters, carbazole is extensively used in OLEDs due to its hole-transport properties and its high-energy singlet excited state.[5-7] Therefore, it is highly desirable to synthesize carbazole based crosslinkable polymers to improve the processability of carbazole. In this section, synthesis of such a polymer is described and the application of the polymer in OLEDs is illustrated.

B.3 Results and Discussion

Synthesis. Scheme B.1 depicts the synthesis of the cinnamate functionalized carbazole based polymer **3**. The synthesis of polymer **1** was described in Chapter 6.[8] Polymer **3** was obtained by the reaction of compound **2** and polymer **1** in the presence of potassium carbonate. The ^{1}H-NMR spectrum of polymer **3** showed complete disappearance of the –CH_2Cl band of polymer **1** at around 4.20 ppm, and the formation of a broad singlet at around 3.80 ppm due to the –OCH_3 group of the cinnamate units of polymer **3** (Figure B.1). Polymer **3** (m:n = 75:25) has a molecular weight (M_w) of 15.4 kDa, and a PDI of 2.49.

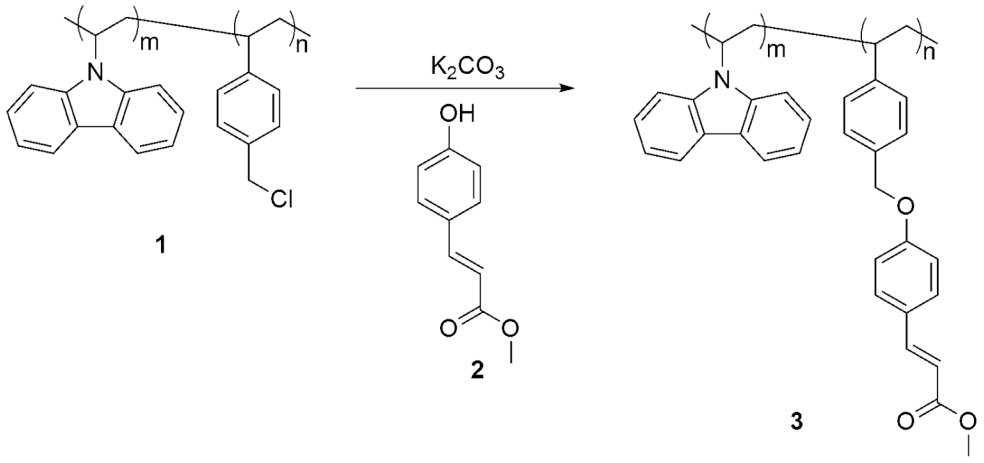

Scheme B.1 Synthesis of the crosslinkable hole-transport polymer.

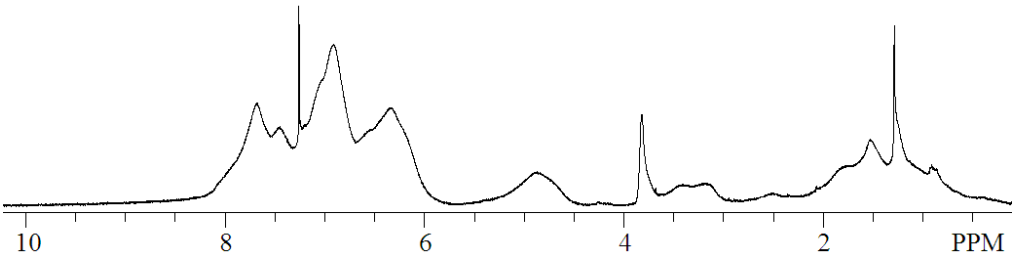

Figure B.1 ^{1}H-NMR spectrum of polymer **3**.

Electroluminescence. Electroluminescence studies were conducted by Andreas Haldi in the Kippelen group at Georgia Institute of Technology. Figure B.2 shows the electroluminescence spectra of devices in which copolymer **3** was used as the hole-transport layer. Polymer **3** was spin-coated onto ITO, and crosslinked upon exposure to UV radiation for 30 minutes. Subsequently, $Ir(ppy)_3$ doped in CBP was spin-coated on top of the hole-transport layer, followed by the depositions of BCP and the cathode. Figure B.2 indicates that the device performance is affected by the energy dose of UV exposure to crosslink copolymer **3**. UV exposure of 450 mJ resulted in a device with an EQE of 8.4%, and a luminous efficiency of 28 cd/A, and decreasing or increasing the energy of the UV light did not significantly affect the device performance (Table B.1). For example, when the error range is taken into consideration (Table B.1), it can be stated that there is almost no difference between 250 mJ and 450 mJ of UV exposure.

In order to determine the effect of the crosslinking on the device performance, a similar device with poly(N-vinyl carbazole) but without a crosslinking unit was fabricated. It was found that the efficiency of the device without a crosslinking group is twice as high as that of the device based on polymer **3**. Therefore, it can be concluded that, long term UV radiation (i.e. 30 min) partially decomposes the carbazole ring.

Indeed, higher performances were observed for the devices, where polymer **3** was not exposed to UV light compared to the devices listed in Table 1. Nevertheless, 8% external quantum efficiency is promising, considering that fully solution-processable devices can be fabricated by employing copolymer **3**.

Table B.1 Device performance as a function of UV exposure.

UV Dose (mJ)	**External Quantum Efficiency**	**Luminous Efficiency (cd/A)**
250	7.8 ± 0.4 %	26 ± 2
350	7.0 ± 0.4 %	24 ± 2
450	8.4 ± 0.1 %	28 ± 1
600	6.6 ± 0.6 %	22 ± 2

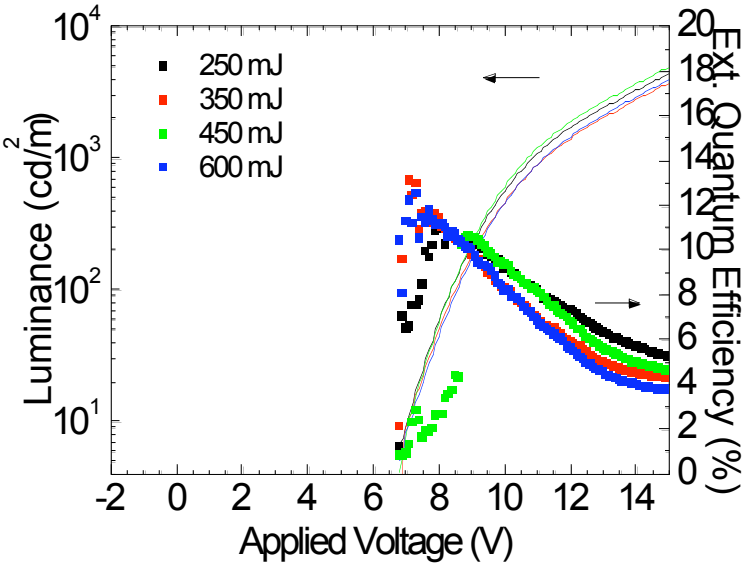

Figure B.2 Luminance and external quantum efficiency as a function of applied voltage for device with structure ITO/**3** (17 nm)/CBP:Ir(ppy)$_3$ (20 nm)/BCP (40 nm)/LiF/Al.

B.4 Conclusion

A polymer with hole-transporting carbazole groups and crosslinking cinnamate units was synthesized. It was found that the crosslinking process, where the polymer is exposed to UV light for 30 minutes, adversely affects the device performance, possibly due to a partial decomposition of the carbazole groups on the polymer. On the other hand external quantum efficiencies as high as 8.4% were obtained by employing the polymer as the hole-transport layer in OLEDs.

B.5 Experimental

All reagents were purchased either from Acros Organics or Aldrich and used without further purification unless otherwise noted. ^{1}H-NMR and ^{13}C-NMR spectra (300 MHz ^{1}H NMR, 75 MHz ^{13}C NMR) were taken using a Varian Mercury Vx 300 spectrometer. All spectra are referenced to residual proton solvent. Gel-permeation chromatography (GPC) analyses were carried out using a Waters 1525 binary pump coupled to a Waters 2414 refractive index detector with methylene chloride as an eluant on American Polymer Standards 10 μm particle size, linear mixed bed packing columns. The flow rate used for all the measurements was 1 mL/min. All GPC measurements were calibrated using poly(styrene) standards and carried out at room temperature.

Synthesis of polymer 3. A mixture of polymer **1** (500 mg), compound **2** (375 mg, 2.1 mmol), and potassium carbonate (375 mg, 2.7 mmol) in 10 ml of DMF was stirred at 85 ^{o}C for 24 hours. The mixture was poured into water, followed by the addition of methylene chloride. The organic layer was collected, washed with brine, and concentrated in vacuo, followed by the precipitation in methanol. Polymer **3** was obtained as a white solid, for which ^{1}H-NMR spectrum showed the complete disappearence of the chlorine groups . ^{1}H NMR (300 MHz, $CDCl_3$) (ppm): δ = 0.85-1.75 (m, br), 2.47 (br), 3.25 (m, br), 3.82 (s, br), 4.90 (br), 6.37 (br), 7.05 (br), 7.48 (br), 7.65

(br). ^{13}C NMR (75 MHz, $CDCl_3$) (ppm): δ = 167.5, 160.3, 144.2, 139.8, 139.7, 139.5, 137.2, 137.1, 129.6, 127.1, 127.0, 124.9, 124.8, 123.6, 121.7, 120.1, 118.7, 118.6, 115.3, 114.9, 110.3, 107.8, 107.3, 69.5, 50.0, 49.9, 38.9, 35.7.

B.6 References

(1) Hreha, R. D.; Zhang, Y. D.; Domercq, B.; Larribeau, N.; Haddock, J. N.; Kippelen, B.; Marder, S. R. Synthesis of Photo-Crosslinkable Hole-Transport Polymers with Tunable Oxidation Potentials and Their Use in Organic Light-Emitting Diodes *Synthesis* **2002**, 1201.

(2) Hreha, R. D.; Haldi, A.; Domercq, B.; Barlow, S.; Kippelen, B.; Marder, S. R. Synthesis of Acrylate and Norbornene Polymers with Pendant 2,7-Bis(diarylamino)fluorene Hole-Transport Groups *Tetrahedron* **2004**, *60*, 7169.

(3) Domercq, B.; Hreha, R. D.; Zhang, Y. D.; Larribeau, N.; Haddock, J. N.; Schultz, C.; Marder, S. R.; Kippelen, B. Photo-Patternable Hole-Transport Polymers for Organic Light-Emitting Diodes *Chem. Mater.* **2003**, *15*, 1491.

(4) Domercq, B.; Hreha, R. D.; Zhang, Y. D.; Haldi, A.; Barlow, S.; Marder, S. R.; Kippelen, B. Organic Light-Emitting Diodes with Multiple Photocrosslinkable Hole-Transport Layers *J. Polym. Sci., Part B:Polym. Phys.* **2003**, *41*, 2726.

(5) Kido, J.; Hongawa, K.; Okuyama, K.; Nagai, K. Bright Blue Electroluminescence from Poly(N-vinylcarbazole) *Appl. Phys. Lett.* **1993**, *63*, 2627.

(6) Zhu, W. G.; Liu, C. Z.; Su, L. J.; Yang, W.; Yuan, M.; Cao, Y. Synthesis of New Iridium Complexes and Their Electrophosphorescent Properties in Polymer Light-Emitting Diodes *J. Mater. Chem.* **2003**, *13*, 50.

(7) Gong, X.; Ostrowski, J. C.; Bazan, G. C.; Moses, D.; Heeger, A. J. Red Electrophosphorescence from Polymer Doped with Iridium Complex *Appl. Phys. Lett.* **2002**, *81*, 3711.

(8) Wang, X. Y.; Prabhu, R. N.; Schmehl, R. H.; Weck, M. Polymer-Based Tris(2-phenylpyridine)Iridium Complexes *Macromolecules* **2006**, *39*, 3140.

APPENDIX C

ORGANOCATALYTIC ONE POT TANDEM REACTIONS

C.1 Abstract

Organocatalysts are studied for homogenous one-pot tandem reactions with a focus on oxidations of alcohols, enantioselective aldol reactions, acetylation of secondary alcohols, and Michael additions. It was found that it is possible to perform three reactions, which are catalyzed by three different catalysts, in a tandem fashion in one pot.

C.2 Introduction

Sequential catalytic reactions that take place in one pot by the employment of different catalysts are highly desirable, as the isolation and purification of intermediates are avoided, making these reactions more economical and environmentally friendly.[1-5] Organocatalysis is attractive for such applications since it avoids the use of expensive and toxic metal based catalysts.[6] However, it suffers from the disadvantage of high catalyst loading compared to the metal-catalyzed reactions.[7] Therefore, it is beneficial to attach organocatalysts to polymer backbones, which might result in recyclable catalysts that eliminate the drawback of high catalyst loading.[8-10] This section is focused on the identification of two or three different organocatalysts that can be attached to the same polymer backbone in order to produce recyclable catalysts for homogeneous one pot tandem reactions.

Four different types of reactions are studied in this section: Proline-catalyzed enantioselective aldol reactions, quinine catalyzed Michael additions, DMAP- or tetramisole-catalyzed acetylation of the secondary alcohols, and TEMPO-catalyzed

oxidation of the primary alcohols to aldehydes (Figure C.1). Proline and its derivatives are extensively used for a wide variety of reactions including aldol reactions.[11,12] In general, high catalyst loadings (~30 mol%) are necessary for the reactions to proceed, which makes proline an ideal candidate for polymer support.[13-15] Therefore, in our studies, we kept the proline-catalyzed aldol reaction as one of the reactions of the one pot reactions, and varied the second reaction. As a first step, in Section C.3, the effects of the reaction conditions on proline-catalyzed aldol reactions are studied. In Section C.4, as a first attempt to accomplish tandem reactions, quinine is employed as a catalyst for Michael additions[16-20] along with proline. Combination of Michael addition and intramolecular aldol reaction can be envisioned to produce cyclic structures that are intermediates in natural product synthesis.[21-23]

Another reaction that can be complimentary to the aldol reaction is the acetylation of the secondary alcohols by DMAP.[24-26] In Section C.4, it will be shown that the alcohol produced by the aldol reaction can be acetylated effectively by DMAP, making proline and DMAP promising candidates for one pot reactions.

The kinetic resolution of the secondary alcohol produced by the aldol reaction can be achieved by employing a chiral acetylation catalyst instead of achiral DMAP. In Section C.5, DMAP is replaced with tetramisole, which is an enantioselective acetylation catalyst,[27] and as a third reaction, TEMPO-catalyzed oxidation of the primary alcohols to aldehydes is introduced.[28-31] Thus, it will be possible to synthesize an enantiomerically pure β-hydroxyketone starting from a primary alcohol after three reactions in one pot. Finally, in Section C.6, preliminary results for poly(styrene) supported proline are presented.

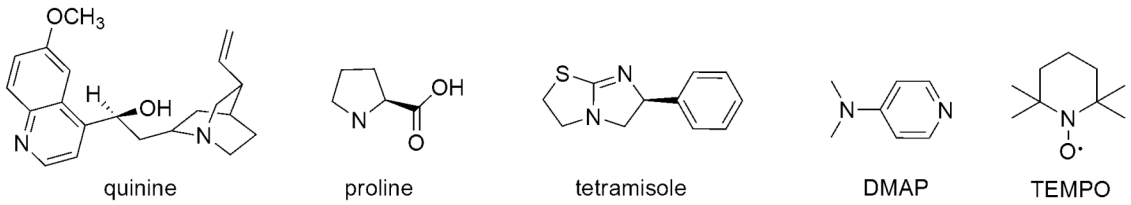

Figure C.1. Organocatalysts studied for one pot tandem reactios

C.3 Proline-Catalyzed Aldol Reactions

Proline and its derivatives have been widely employed as catalysts for aldol reactions of aldehydes and ketones.[11] For these reactions, a large excess of the ketone, and 30 mol% catalyst with respect to the aldehyde are employed.[32] In order to determine the effects of the catalyst loading, ketone concentration, and the reaction time on the chemical yield, 4-nitro benzaldehyde and acetone in DMF were reacted as shown in Scheme C.1. This reaction has been used as a model system to determine the activity of the catalysts.[14,15,32,33] The reported procedure for this reaction with 30 mol% (with respect to 4-nitro benzaldehyde) proline and 70 times excess (with respect to 4-nitro benzaldehyde) of acetone affords the product in 68%.[32] Table C.1 lists the yields of the reaction as a function of catalyst loading, acetone concentration, and reaction time. Decreasing the catalyst loading to 20 mol% did not significantly affect the reaction, whereas no product was obtained when the loading was 10%. The concentration of acetone is also found to play a significant role. When the concentration was decreased to one fifth of the reported concentration, the yield decreased to around 45% from 67%. On the other hand, increasing the reaction time has no effect on the yield, indicating that there is no side-product formation after the reaction is complete. Enantioselectivities of the reactions were not determined for this preliminary study.

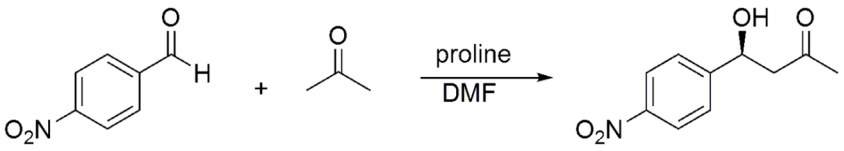

Scheme C.1 Aldol reaction between 4-nitro benzaldehyde and acetone

Table C.1 Yields of the reactions between 4-nitro benzaldehyde and acetone as a function of catalyst loading (with respect to 4-nitro benzaldehyde), acetone concentration, and reaction time.

Reaction	Proline (mol%)	Acetone (x excess)	Time (hour)	Yield (%)
Literature	30	70	4	68
1	30	70	5	67
2	30	70	12	68
3	30	14	5	47
4	30	14	16	42
5	20	70	12	65

C.4 DMAP-Catalyzed Acetylation of Alcohols

DMAP can be used as the second catalyst for the acetylation of the secondary alcohol produced by the aldol reaction (Scheme C.2). Table C.2 lists the reaction yield as a function of catalyst concentration, catalyst type, and the reaction time. The reaction is complete in 1 hour with a catalyst concentration of 0.1M. The reaction goes to completion even upon decreasing the catalyst concentration by half but the reaction time increases by a factor of two. The reaction yield decreases with increasing reaction time

(Table C.2, entries **1-3**). Upon completion of the reaction, the product starts decomposing, producing acetic acid and an α,β unsaturated ketone. Therefore, unlike the aldol reaction described in the previous section, it is crucial to stop the reaction as soon as the reaction is complete. The control experiment with proline as the only catalyst showed that proline cannot catalyze this reaction (Table C.2, entry **4**). Furthermore, the presence of proline along with DMAP did not affect the reaction yield, suggesting that proline and DMAP are compatible with each other, making them suitable catalysts for attachment to a polymer backbone for one pot tandem reactions.

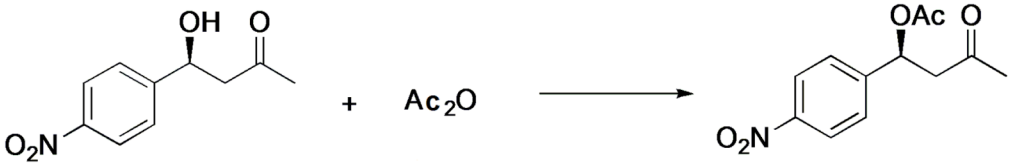

Scheme C.2 Acetylation of the product of the Aldol reaction of Figure 1.

Table C.2 Dependence of the reaction yield on catalyst concentration, catalyst type, and the reaction time.

Reaction	M[a]	Catalyst[b]	Time (h)	Yield (%)
1	0.1	DMAP	20	26%
2	0.1	DMAP	1.5	73%
3	0.1	DMAP	1	quantitative[c]
4	0.1	Proline	30	0
5	0.1	Proline+DMAP	1	quantitative[c]
6	0.05	Proline+DMAP	2.5	quantitative[c]

[a] catalyst concentration in DMF. [b] catalyst loading with respect to the alcohol: **1-3**, 10%; **4**, 30%; **5-6**, 30% proline, 10% DMAP. [c] NMR yields

C.5 One Pot Tandem Michael Addition and Aldol Reaction

Another possibility for one-pot two-reaction system is the combination of Michael addition and Aldol reaction. The reactions shown in Figure C.3 (Michael addition to obtain compound **3**, and then aldol reaction to obtain **4**) have been reported to be catalyzed by proline.[21] However, the reaction is carried out at 35 ^{o}C and the reaction time is almost 4 days (Table C.3). Employment of two different catalysts, one for the Michael addition, and one for the aldol reaction might result in a shorter reaction time. Table C.3 lists the chemical yields of compounds **3** or **4** as a function of the catalyst type and concentration. Quinine is employed as the catalyst for the Michael addition and as indicated in Table C.3, it cannot catalyze the aldol reaction but it is effective for the Micheal addition (entry **3**). When proline is the only catalyst and the catalyst concentration is increased to 0.5M, the reaction time becomes shorter (about 2 days). Furthermore, when proline and quinine are used together, compound **4** was obtained in 1 day (entry **5**), indicating that the two-catalyst approach is more efficient than the one catalyst approach. On the other hand a slight decrease in enantioselectivity is observed for the two-catalyst system. Unfortunately, similar reactions between cyclic diketones and methyl vinyl ketone failed to give the desired products. Therefore, these reactions are not ideal to be studied for polymeric systems.

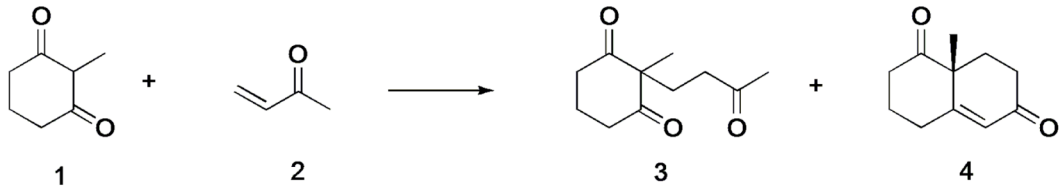

Scheme C.3 One Pot Tandem Michael addition and Aldol Rection.

Table C.3 One Pot Tandem Michael addition and Aldol reaction.

Reaction	M	Reactant	Catalyst	Product	Yield (%)	ee (%)	T (^{o}C)	Time (hour)
Literature	0.16	1+2	proline	4	49	76	35	89
1	0.5	1+2	proline	4	52	70	25	54
2	0.5	3	proline	4	57	75	25	-
3	1	1+2	quinine	3	64	-	25	-
4	0.1	1+2	quinine	-	0	-	25	24
5	0.5	1+2	2 catalysts	4	49	63	25	24

C.6 One-Pot Tandem Alcohol Oxidation, Aldol Reaction, and Acetylation

According to the findings of Sections C.3, C.4, and C.5, the two catalysts that can be attached to the same polymer backbone might be proline and a catalyst for acetylation reactions. A third catalyst that can be added to the reaction sequence is TEMPO for the oxidation of the primary alcohols. Thus, it might be possible to carry out three reactions in one pot as shown in Scheme C.4. The first reaction is the oxidation of a primary alcohol to the corresponding aldehyde, which then can react with acetone for the aldol reaction as the second reaction. Finally, the third reaction is the kinetic resolution of the product of the aldol reaction by a chiral acetylation catalyst such as tetramisole. In order to determine the feasibility of the approach, reactions shown in Scheme C.4 were carried out with small molecule catalysts. Bromobenzyl alcohol was oxidized to 4-bromobenzaldehyde in the presences of TEMPO as the catalyst and [bis(acetoxy)iodo]benzene as the stoichiometric oxidant.[34] After the reaction is complete (1 hour), the other two catalysts, proline and tetramisole were added along with acetone and DMF. After 16 hours, acetic anhydride was added as the final reactant. Yields of the compounds **5** and **7** are 40% and 10%, respectively. A side product, compound **8**, was

formed during the acetylation of compound **6** in 13% yield. This side reaction might be avoided by carefully adjusting the reaction conditions, as demonstrated in Section B.4. Although the ee's of the products are not determined, the low yield of the acetylation reaction indicates that tetramisole reacts preferentially with compound **6** ((S)-enantiomer of the aldol product) rather than **5** ((R)-enantiomer of the aldol product), which is in accord with the literature report.[27] These results show that it is possible to carry out three reactions in one pot in a tandem fashion. On the other hand it should be noted that proline and tetramisole should be added to the reaction medium after the alcohol oxidation is complete. When all three catalysts mixed at the same time, the aldol reaction failed, and the yield of the oxidation reaction decreased, suggesting that [bis(acetoxy)iodo]benzene reacts with proline. In a test reaction, proline-catalyzed aldol reaction in the presence of TEMPO preceded without any difficulty, indicating the adverse effect of [bis(acetoxy)iodo]benzene on proline. Nevertheless, it is possible to attach proline and tetramisole to a polymer backbone to accomplish two reactions in one pot, and TEMPO can be used as a small molecule catalyst along with the polymer for the third reaction.

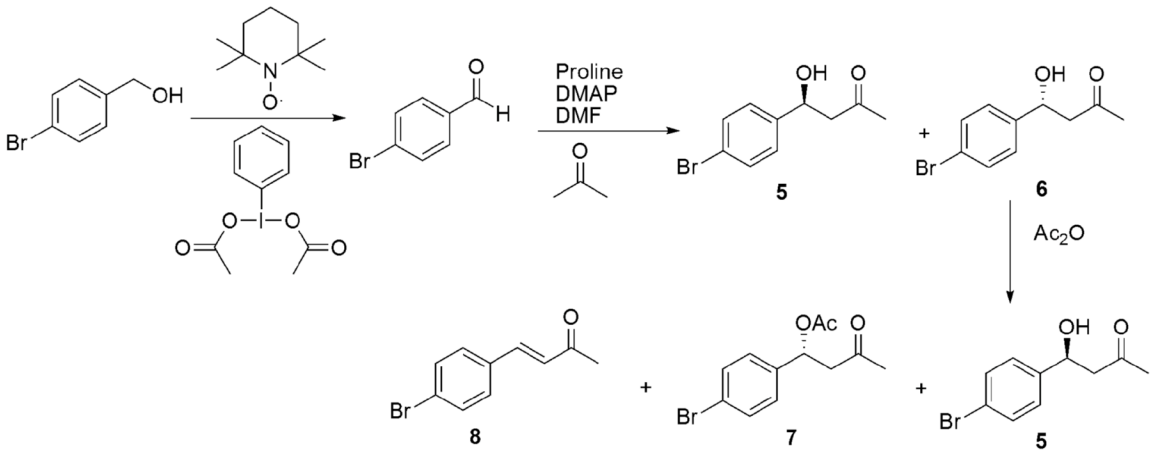

Scheme C.4 One-Pot Tandem Alcohol Oxidation, Aldol Reaction, and Acetylation.

C.7 Poly(styrene) with Side-Chain Proline

Proline plays a crucial role in our polymeric catalyst design. Therefore, it is important to determine the catalytic activity of a polymer with side-chain proline as the only catalyst. If the catalytic activities of the small molecule proline and polymeric proline are similar, a second catalyst can be attached to the polymer along with proline to construct a more complex system. In this section, covalent attachment of proline to polystyrene backbone is described (Scheme C.5). Compounds **9** and **10** were synthesized according to the literature procedures.[15,35] Monomer **11** was obtained by the coupling of **9** and **10** in the presences of DCC and DMAP. Polymerization of **11** using AIBN as the initiator yielded polymer **12** (M_w = 9.7 kDa, PDI = 2.51). Removing the protecting groups on the amine and carboxylic acid groups of proline is the final step to obtain the polymeric catalyst. Unfortunately, deprotection using HCl or TFA resulted in insoluble materials, which could not be characterized. After deprotection, the amine and carboxylic acid groups on proline might provide sites for hydrogen bonding that can lead to a crosslinked polymer network, which can explain the insolubility of the polymer. However, the polymer is still insoluble in solvents such as DMSO, which is expected to disrupt the hydrogen bonding. Furthermore, heating the polymer in various solvents did not cause any changes in solubility. At this stage, the origin of the insolubility is not clear, and needs to be further investigated.

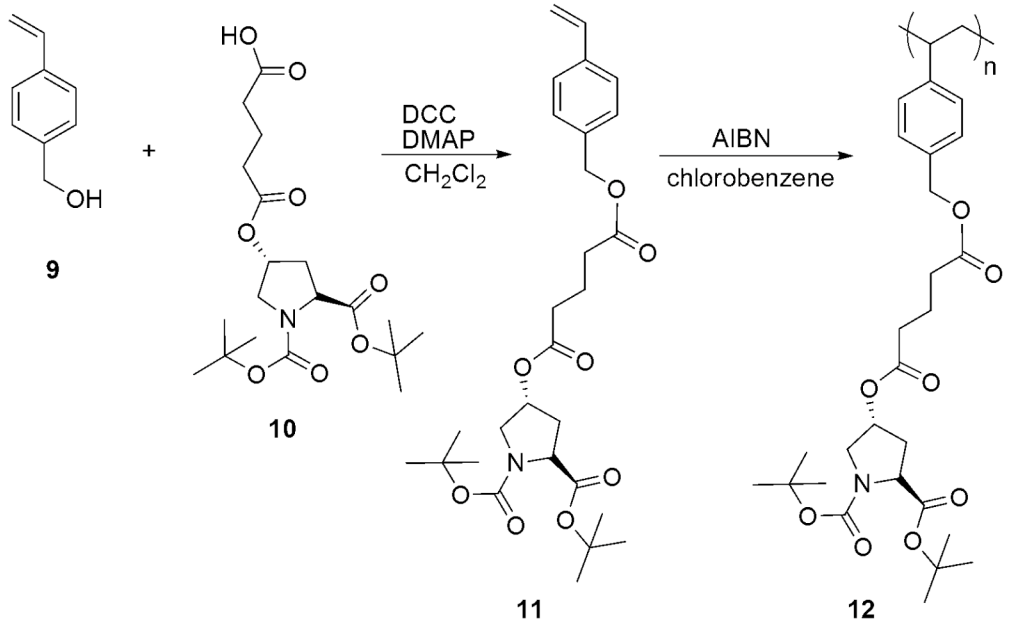

Scheme C.5 Synthesis of poly(styrene) with side-chain protected proline.

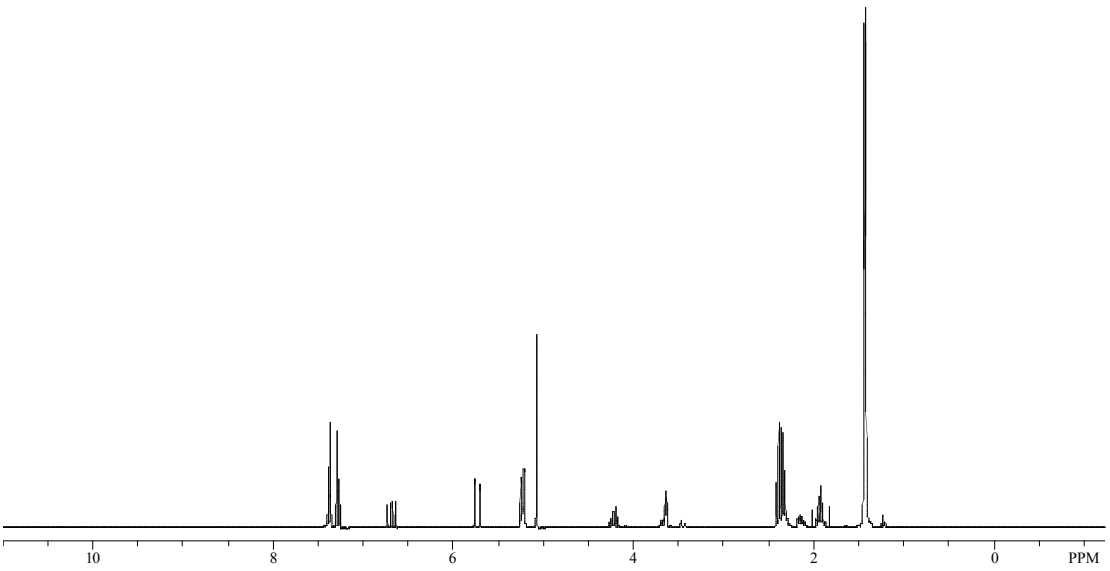

Figure C.2 ^{1}H-NMR spectrum of monomer **11**.

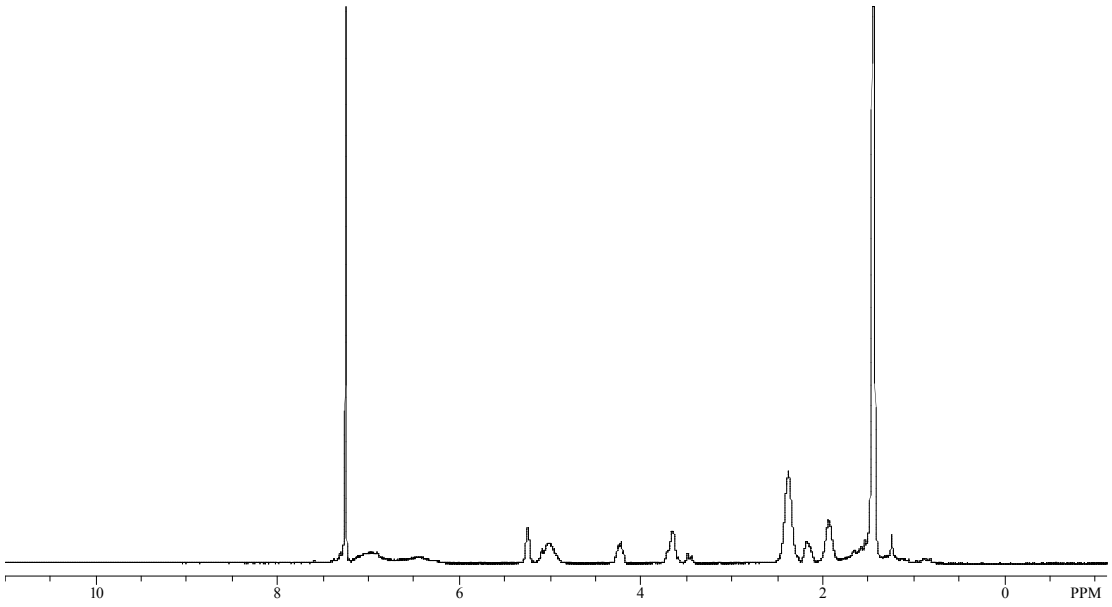

Figure C.3 ^{1}H-NMR spectrum of polymer **12**.

C.8 Conclusion

Organocatalysis for one pot tandem reactions are studied. It was found that proline is compatible with acetylation catalysts such as DMAP or tetramisole, indicating that aldol reactions and acetylation reactions can be carried out sequentially in one pot. On the other hand, the reaction conditions should be carefully adjusted in order to optimize the reaction yield. For example, there is no side product formation for the aldol reaction upon increasing the reaction time, whereas, the yield of the acetylation reaction decreases rapidly with increasing reaction time due to the side reactions. Furthermore, it was found that TEMPO-catalyzed oxidation reactions can be added to the reaction sequence in order to perform three reactions in one pot. Finally, a protected proline-functionalized poly(styrene) was synthesized to create a recyclable catalyst for aldol reactions. Unfortunately, the deprotection step resulted in insoluble materials.

C.9 Experimental

All Reagents were purchased either from Acros Organics or Aldrich and used without further purification. ^{1}H-NMR and ^{13}C-NMR spectra (300 MHz ^{1}H NMR, 75 MHz ^{13}C NMR) were taken using a Varian Mercury Vx 300 spectrometer. All spectra are referenced to residual proton solvent. Abbreviations used include singlet (s), doublet (d), triplet (t), and unresolved multiplet (m). Mass spectral analyses were provided by the Georgia Tech Mass Spectrometry Facility. Gel-permeation chromatography (GPC) analyses were carried out using a Waters 1525 binary pump coupled to a Waters 2414 refractive index detector with methylene chloride as an eluant on American Polymer Standards 10 μm particle size, linear mixed bed packing columns. The flow rate used for all the measurements was 1 mL/min. All GPC measurements were calibrated using poly(styrene) standards and carried out at room temperature.

Synthesis of (2R,4R)-di-tert-butyl 4-(5-oxo-5-(4-vinylbenzyloxy)pentanoyloxy)pyrrolidine-1,2-dicarboxylate, 11. A mixture of compounds 9 (0.39 g, 2.9 mmol), 10(1.16 g, 2.9 mmol), DCC (0.66 g, 3.2 mmol), and DMAP (0.12 g, 1.0 mmol) in 30 mL CH_2Cl_2 was stirred for 24 hours at ambient temperatures. The solvent was evaporated and the residue was purified via column chromatography (silica, 1:1 hexanes/ethyl acetate) to give compound **11** (1.30 g, 87% yield). ^{1}H NMR (300 MHz, $CDCl_3$) δ 7.39 (2H, d, *J* =8.7); 7.29 (2H, d, *J* =8.7); 6.69 (1H, dd, *J* =18.0, 10.8); 5.74 (1H, dd, *J* =18.0, 1.0); 5.24 (2H, m); 5.07 (2H, s); 4.22 (1H, m); 3.72-3.42 (2H, m); 2.37 (5H, m); 2.15 (1H, m); 1.93 (2H, pentate, *J* = 6.9); 1.44 (18H, m). ^{13}C NMR (75 MHz, $CDCl_3$) δ 172.8; 172.6; 172.5; 171.8; 171.6; 154.0; 137.8; 136.5; 135.6; 128.8; 126.6; 114.6; 81.6; 80.5; 80.3; 72.9; 72.1; 66.3; 58.6; 52.4; 52.2; 36.8; 35.7; 33.4; 28.6; 28.5; 28.2; 28.1; 20.2. MS Calcd (M): 517.3. Found (ESI): 518.3 (M+1).

Synthesis of polymer 12. A solution of monomer **11** (350 mg, 0.67 mmol) and AIBN (4.0 mg, 0.024 mmol) in 1.7 mL chlorbenzene was stirred at 80 ^{o}C under argon for 3

days. The reaction mixture was cooled to room temperature and poured into hexane to precipitate the product. The powder was collected by filtration, dissolved in CH_2Cl_2, and precipitated into hexane to give polymer 12 as a white powder. ^{1}H NMR (300 MHz, $CDCl_3$) (ppm): δ = 6.99 (br), 6.46 (br), 5.26 (s, br), 5.02 (br), 4.23 (br), 3.66(br), 3.48 (br), 2.39 (br), 2.17 (br), 1.94(br), 1.45 (s, br).

C.10 References

(1) Helms, B.; Guillaudeu, S. J.; Xie, Y.; McMurdo, M.; Hawker, C. J.; Fréchet, J. M. J. One-Pot Reaction Cascades Using Star Polymers with Core-Confined Catalysts *Angew. Chem. Int. Ed.* **2005**, *44*, 6384.

(2) Voit, B. Sequential One-Pot Reactions Using the Concept Of "Site Isolation" *Angew. Chem. Int. Ed.* **2006**, *45*, 4238.

(3) Poe, S. L.; Kobaslija, M.; McQuade, D. T. Microcapsule Enabled Multicatalyst System *J. Am. Chem. Soc.* **2006**, *128*, 15586.

(4) Bruggink, A.; Schoevaart, R.; Kieboom, T. Concepts of Nature in Organic Synthesis: Cascade Catalysis and Multistep Conversions in Concert *Org. Process Res. Dev.* **2003**, *7*, 622.

(5) Phan, N. T. S.; Gill, C. S.; Nguyen, J. V.; Zhang, Z. J.; Jones, C. W. Expanding the Utility of One-Pot Multistep Reaction Networks through Compartmentation and Recovery of the Catalyst *Angew. Chem. Int. Ed.* **2006**, *45*, 2209.

(6) Marques, M. M. B. Catalytic Enantioselective Cross-Mannich Reaction of Aldehydes *Angew. Chem. Int. Ed.* **2006**, *45*, 348.

(7) Cozzi, F. Immobilization of Organic Catalysts: When, Why, and How *Adv. Synth. Catal.* **2006**, *348*, 1367.

(8) Benaglia, M.; Puglisi, A.; Cozzi, F. Polymer-Supported Organic Catalysts *Chem. Rev.* **2003**, *103*, 3401.

(9) Benaglia, M. Recoverable and Recyclable Chiral Organic Catalysts *New J. Chem.* **2006**, *30*, 1525.

(10) Dickerson, T. J.; Reed, N. N.; Janda, K. D. Soluble Polymers as Scaffolds for Recoverable Catalysts and Reagents *Chem. Rev.* **2002**, *102*, 3325.

(11) Notz, W.; Tanaka, F.; Barbas, C. F. Enamine-Based Organocatalysis with Proline and Diamines: The Development of Direct Catalytic Asymmetric Aldol, Mannich, Michael, and Diels-Alder Reactions *Acc. Chem. Res.* **2004**, *37*, 580.

(12) Allemann, C.; Gordillo, R.; Clemente, F. R.; Cheong, P. H. Y.; Houk, K. N. Theory of Asymmetric Organocatalysis of Aldol and Related Reactions: Rationalizations and Predictions *Acc. Chem. Res.* **2004**, *37*, 558.

(13) Benaglia, M.; Celentano, G.; Cozzi, F. Enantioselective Aldol Condensations Catalyzed by Poly(ethylene glycol)-Supported Proline *Adv. Synth. Catal.* **2001**, *343*, 171.

(14) Kucherenko, A. S.; Struchkova, M. I.; Zlotin, S. G. The (S)-Proline/Polyelectrolyte System: An Efficient, Heterogeneous, Reusable Catalyst for Direct Asymmetric Aldol Reactions *Eur. J. Org. Chem.* **2006**, 2000.

(15) Bellis, E.; Kokotos, G. Proline-Modified Poly(propyleneimine) Dendrimers as Catalysts for Asymmetric Aldol Reactions *J. Mol. Cat. A-Chem.* **2005**, *241*, 166.

(16) Kumar, A.; Salunkhe, R. V.; Rane, R. A.; Dike, S. Y. Novel Catalytic Enantioselective Protonation (Proton-Transfer) in Michael Addition of Benzenethiol to Alpha-Acrylacrylates - Synthesis of (S)-Naproxen and Alpha-Arylpropionic Acids or Esters *Chem. Commun.* **1991**, 485.

(17) Bartoli, G.; Bosco, M.; Carlone, A.; Cavalli, A.; Locatelli, M.; Mazzanti, A.; Ricci, P.; Sambri, L.; Melchiorre, P. Organocatalytic Asymmetric Conjugate Addition of 1,3-Dicarbonyl Compounds to Maleimides *Angew. Chem. Int. Ed.* **2006**, *45*, 4966.

(18) Szollosi, G.; Bartok, M. Enantioselective Michael Addition Catalyzed by Cinchona Alkaloids *Chirality* **2001**, *13*, 614.

(19) Sekino, E.; Kumamoto, T.; Tanaka, T.; Ikeda, T.; Ishikawa, T. Concise Synthesis of Anti-Hiv-1 Active (+)-Inophyllum B and (+)-Calanolide A by Application of (-)-Quinine-Catalyzed Intramolecular Oxo-Michael Addition *J. Org. Chem.* **2004**, *69*, 2760.

(20) Hodge, P.; Khoshdel, E.; Waterhouse, J.; Fréchet, J. M. J. Michael Additions Catalyzed by Cinchona Alkaloids Bound via Their Vinyl Groups to Preformed Crosslinked Polymers *J. Chem. Soc. Perkin Trans. 1* **1985**, 2327.

(21) Bui, T.; Barbas, C. F. A Proline-Catalyzed Asymmetric Robinson Annulation Reaction *Tetrahedron Lett.* **2000**, *41*, 6951.

(22) Shigehisa, H.; Mizutani, T.; Tosaki, S. Y.; Ohshima, T.; Shibasaki, M. Formal Total Synthesis of (+)-Wortmannin Using Catalytic Asymmetric Intramolecular Aldol Condensation Reaction *Tetrahedron* **2005**, *61*, 5057.

(23) Davies, S. G.; Sheppard, R. L.; Smith, A. D.; Thomson, J. E. Highly Enantioselective Organocatalysis of the Hajos-Parrish-Eder-Sauer-Wiechert Reaction by the Beta-Amino Acid Cispentacin *Chem. Commun.* **2005**, 3802.

(24) Deratani, A.; Darling, G. D.; Horak, D.; Fréchet, J. M. J. Heterocyclic Polymers as Catalysts in Organic-Synthesis - Effect of Macromolecular Design and Microenvironment on the Catalytic Activity of Polymer-Supported (Dialkylamino)pyridine Catalysts *Macromolecules* **1987**, *20*, 767.

(25) Delaney, E. J.; Wood, L. E.; Klotz, I. M. Poly(ethylenimines) with Alternative (Alkylamino)pyridines as Nucleophilic Catalysts *J. Am. Chem. Soc.* **1982**, *104*, 799.

(26) Xu, S. J.; Held, I.; Kempf, B.; Mayr, H.; Steglich, W.; Zipse, H. The Dmap-Catalyzed Acetylation of Alcohols - a Mechanistic Study (DMAP=4-(Dimethylamino)pyridine) *Chem. Eur. J.* **2005**, *11*, 4751.

(27) Birman, V. B.; Li, X. M. Benzotetramisole: A Remarkably Enantioselective Acyl Transfer Catalyst *Org. Lett.* **2006**, *8*, 1351.

(28) Sheldon, R. A.; Arends, I. W. C. E.; Ten Brink, G. J.; Dijksman, A. Green, Catalytic Oxidations of Alcohols *Acc. Chem. Res.* **2002**, *35*, 774.

(29) Ferreira, P.; Phillips, E.; Rippon, D.; Tsang, S. C.; Hayes, W. Poly(ethylene glycol)-Supported Nitroxyls: Branched Catalysts for the Selective Oxidation of Alcohols *J. Org. Chem.* **2004**, *69*, 6851.

(30) Fey, T.; Fischer, H.; Bachmann, S.; Albert, K.; Bolm, C. Silica-Supported TEMPO Catalysts: Synthesis and Application in the Anelli Oxidation of Alcohols *J. Org. Chem.* **2001**, *66*, 8154.

(31) Pozzi, G.; Cavazzini, M.; Quici, S.; Benaglia, M.; Dell'Anna, G. Poly(ethylene glycol)-Supported TEMPO: An Efficient, Recoverable Metal-Free Catalyst for the Selective Oxidation of Alcohols *Org. Lett.* **2004**, *6*, 441.

(32) Sakthivel, K.; Notz, W.; Bui, T.; Barbas, C. F. Amino Acid Catalyzed Direct Asymmetric Aldol Reactions: A Bioorganic Approach to Catalytic Asymmetric Carbon-Carbon Bond-Forming Reactions *J. Am. Chem. Soc.* **2001**, *123*, 5260.

(33) Tang, Z.; Jiang, F.; Yu, L. T.; Cui, X.; Gong, L. Z.; Mi, A. Q.; Jiang, Y. Z.; Wu, Y. D. Novel Small Organic Molecules for a Highly Enantioselective Direct Aldol Reaction *J. Am. Chem. Soc.* **2003**, *125*, 5262.

(34) DeMico, A.; Margarita, R.; Parlanti, L.; Vescovi, A.; Piancatelli, G. A Versatile and Highly Selective Hypervalent Iodine (III)/2,2,6,6-Tetramethyl-1-Piperidinyloxyl-Mediated Oxidation of Alcohols to Carbonyl Compounds *J. Org. Chem.* **1997**, *62*, 6974.

(35) Shimomura, O.; Lee, B. S.; Meth, S.; Suzuki, H.; Mahajan, S.; Nomura, R.; Janda, K. D. Synthesis and Application of Polytetrahydrofuran-Grafted Polystyrene (PS-PTHF) Resin Supports for Organic Synthesis *Tetrahedron* **2005**, *61*, 12160.

APPENDIX D

^{1}H-NMR SPECTRA OF THE MONOMERS AND POLYMERS

Chapter 3

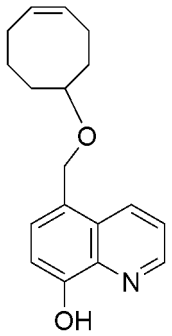

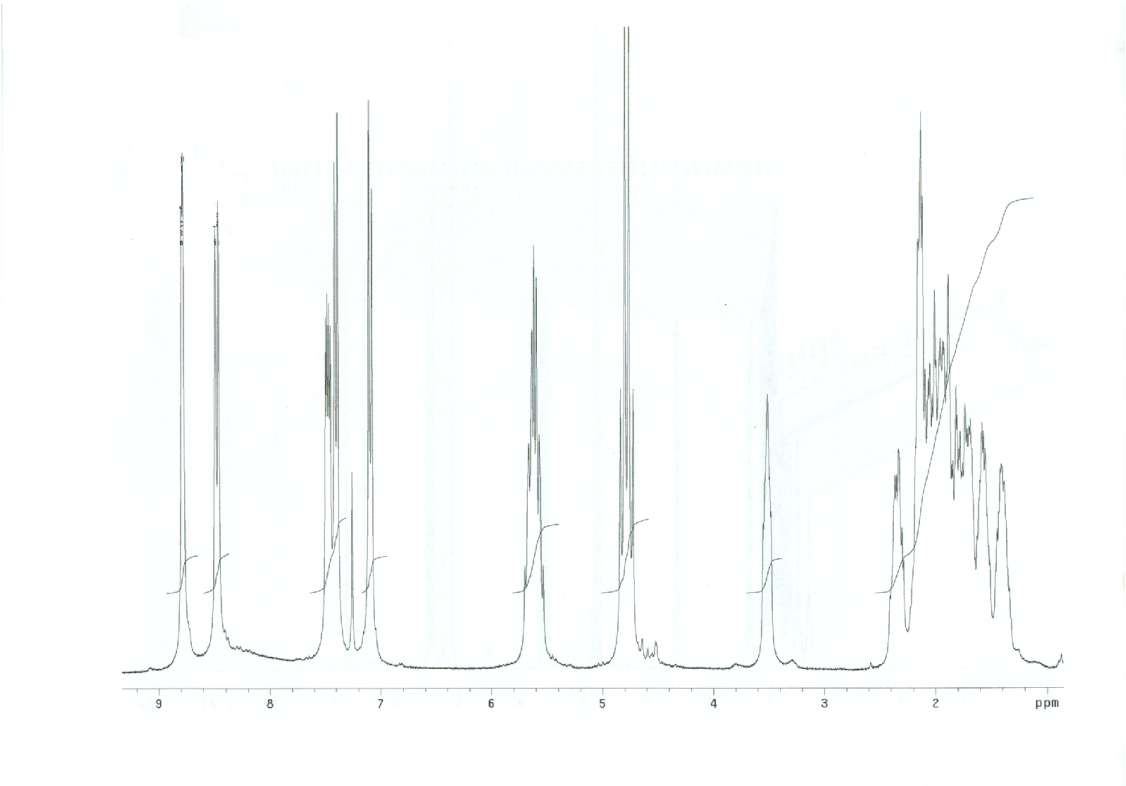

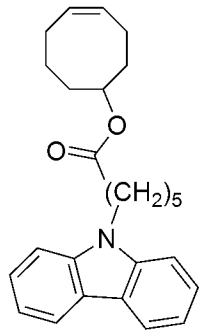
O
O
(CH2)5
N


9
8
7
6
5
4
3
2
1

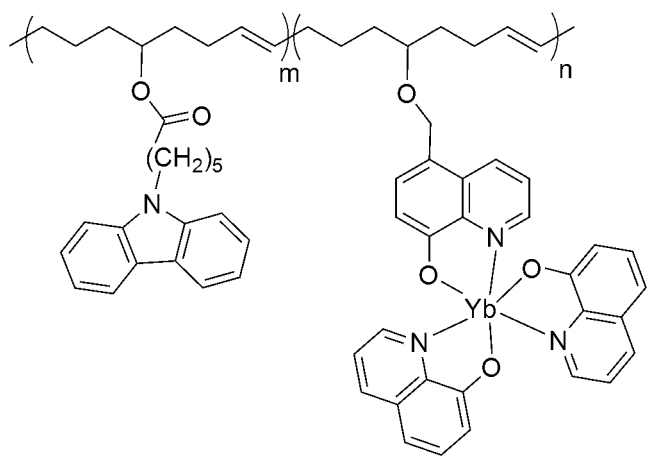
m
n
O
O
(CH2)5
N
O
N
O
Yb
O
N
N
O

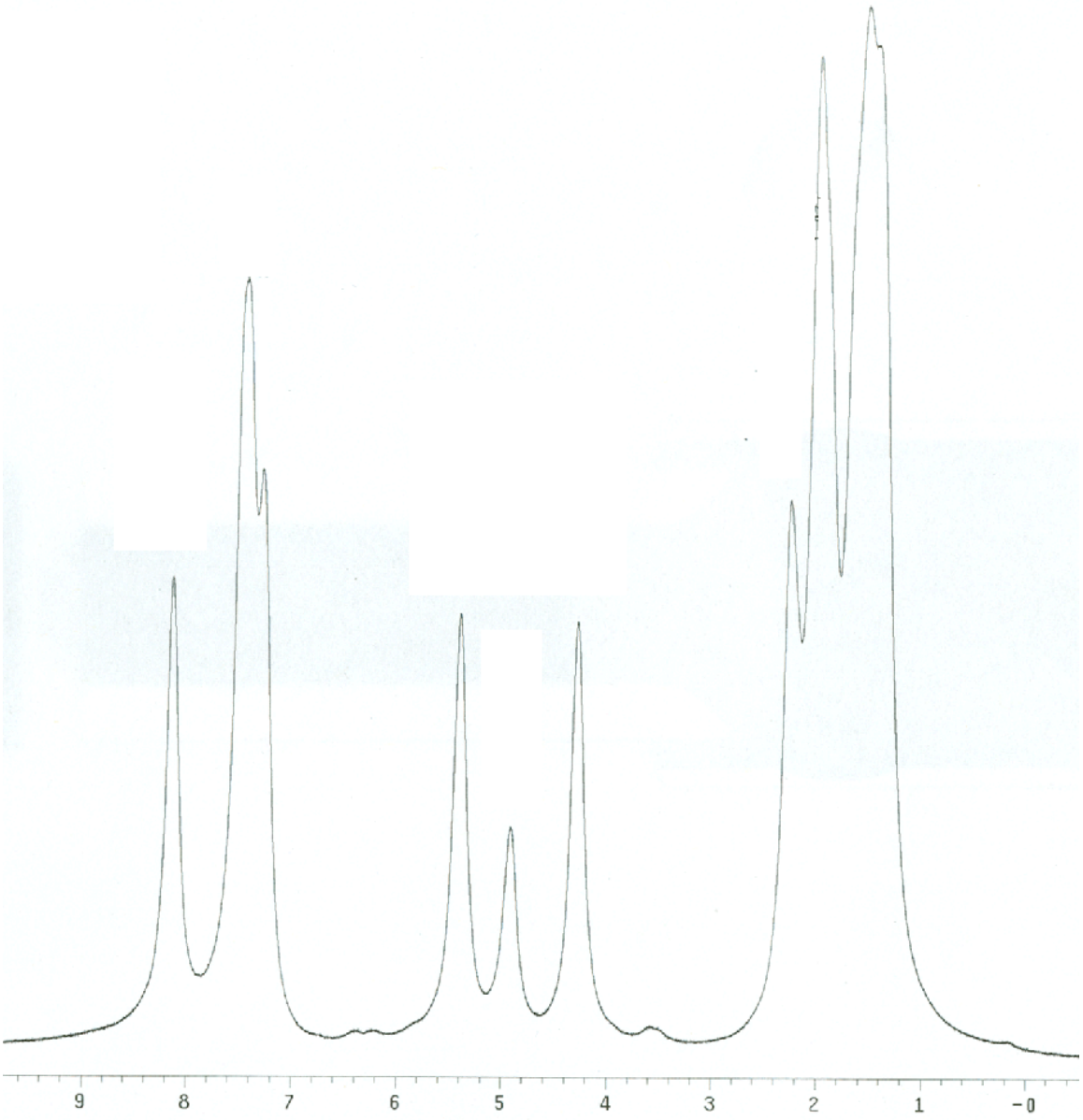
9
8
7
6
5
4
3
2
1
-0

Chapter 5

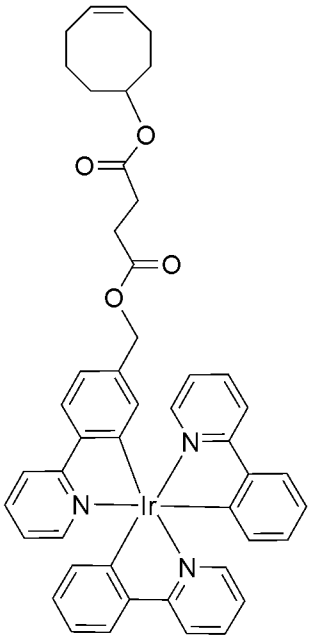

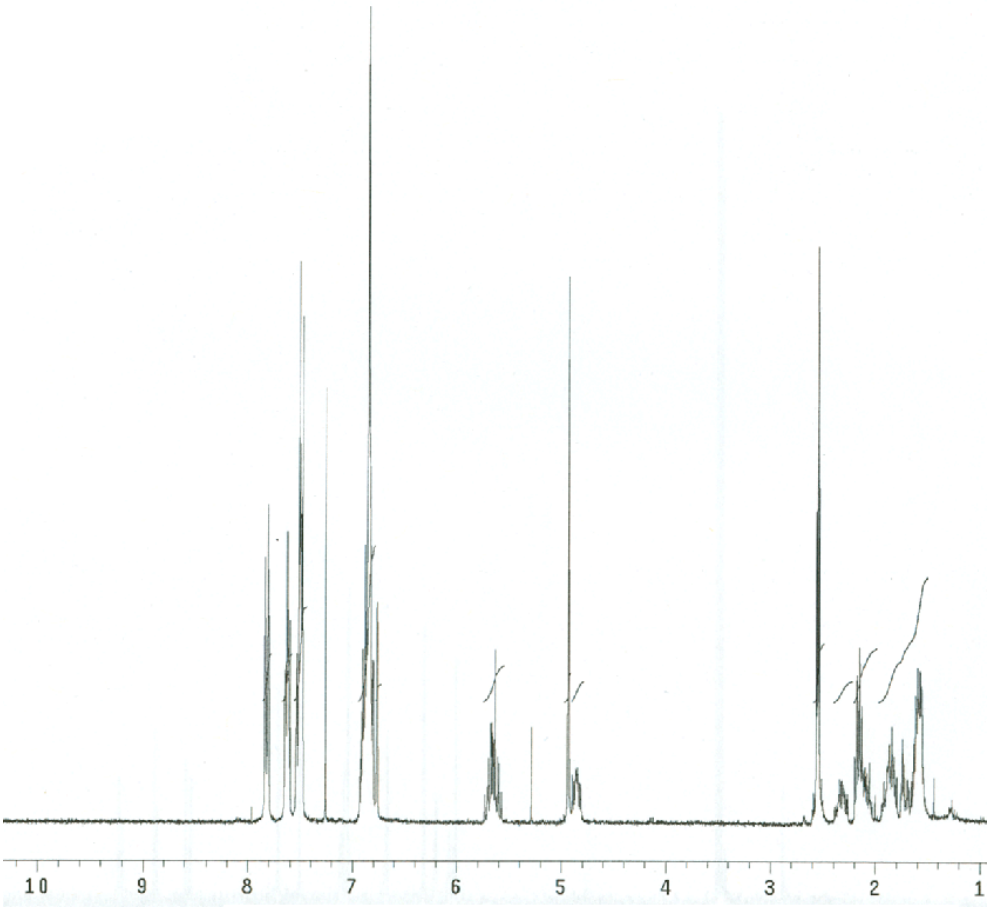

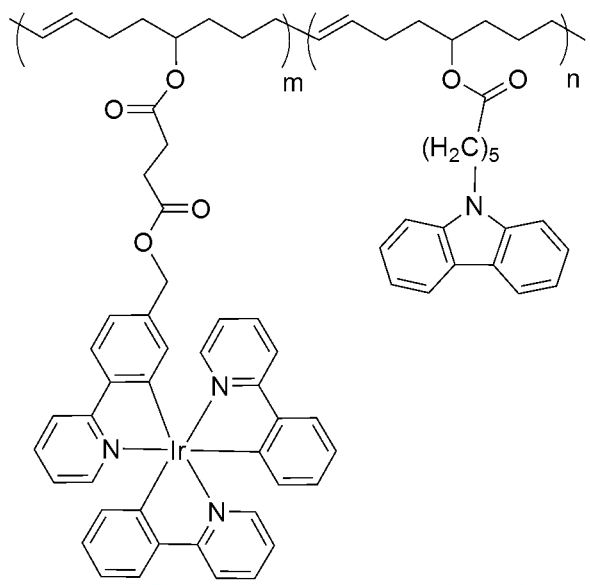
m
n
O
O
O
O
O
O
$(H_2C)_5$
N
N
N
Ir
N

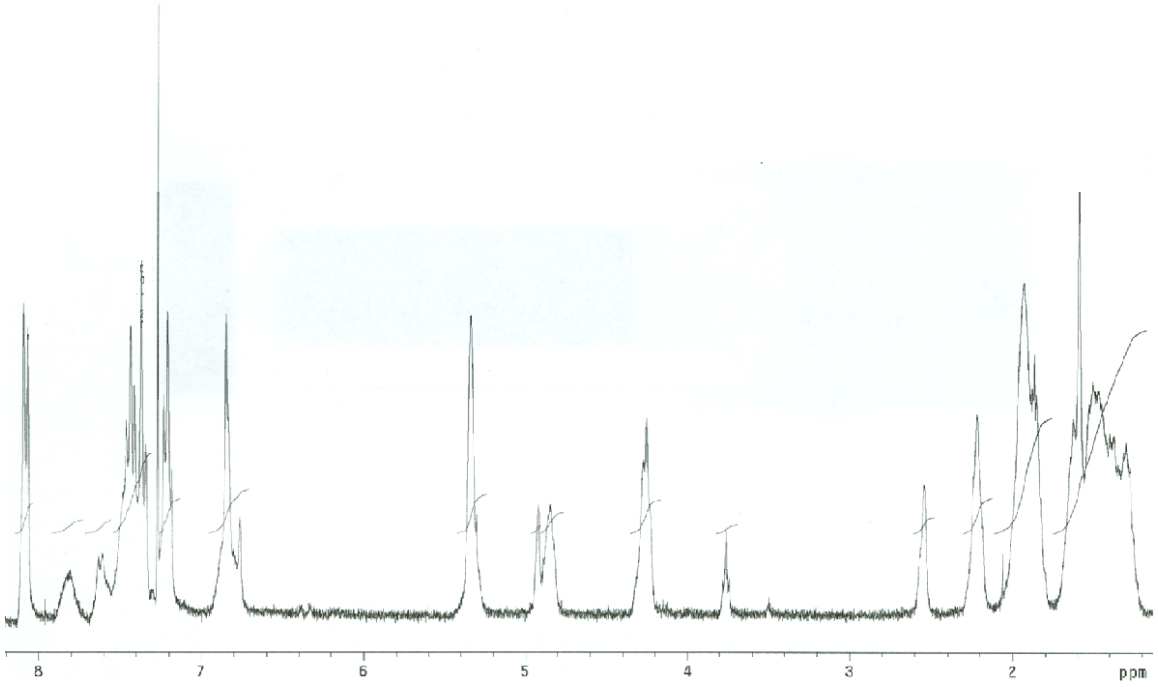
8
7
6
5
4
3
2
ppm

Chapter 7

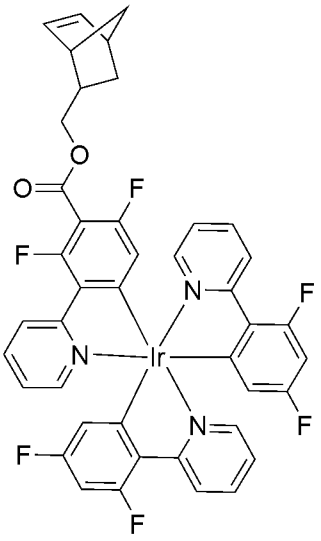

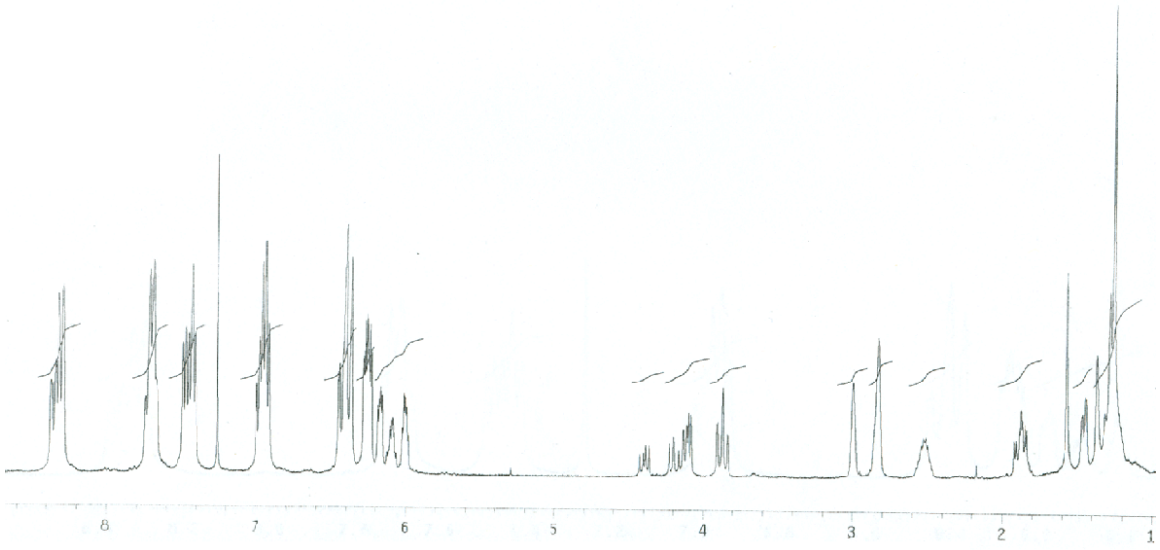

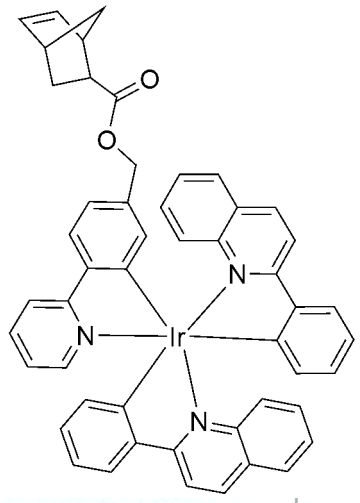
O
O
N
Ir
N
N

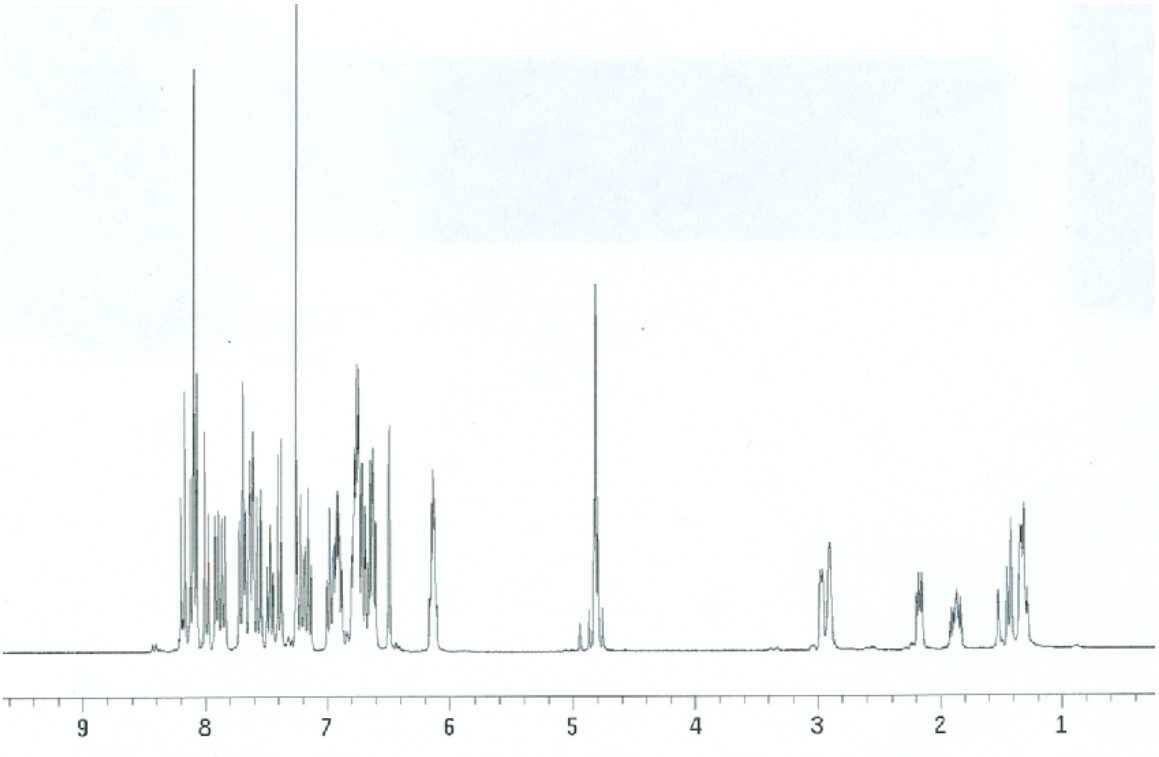
9
8
7
6
5
4
3
2
1

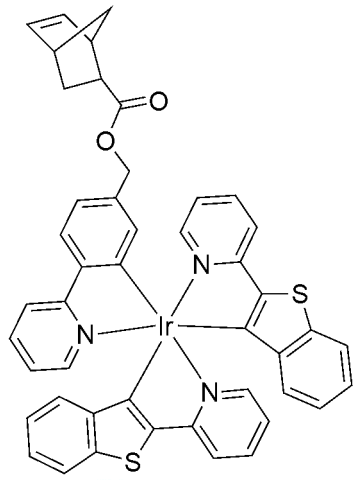
O
O
N
S
N
Ir
N
S

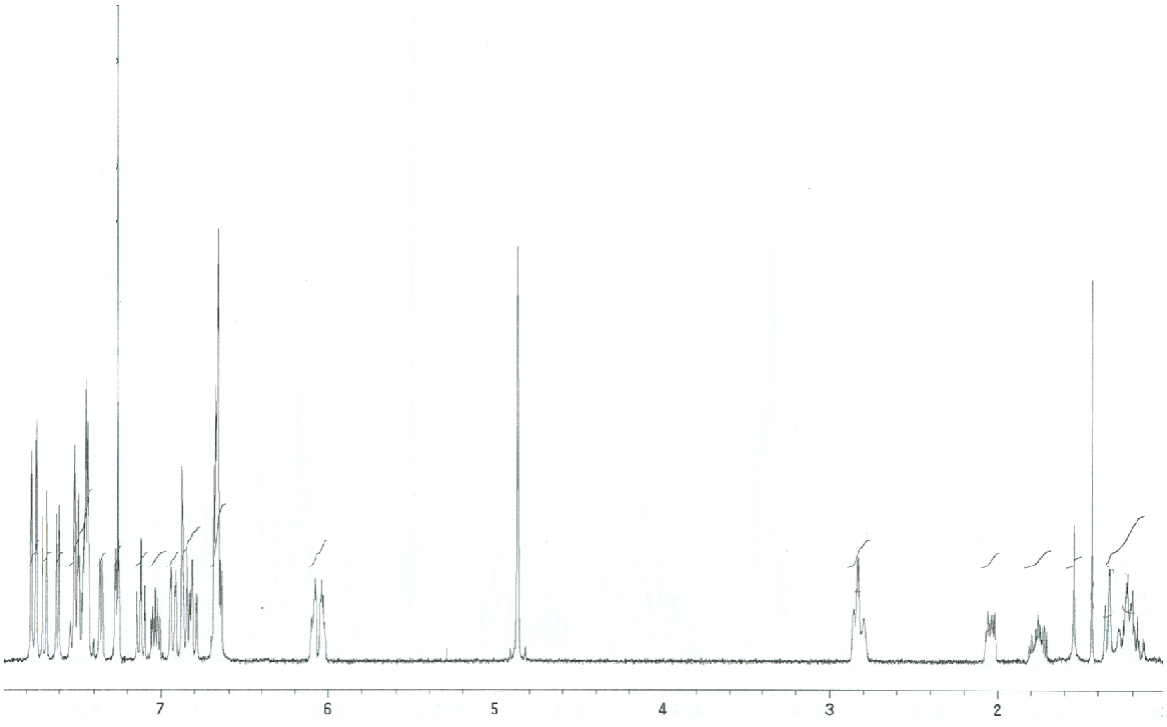
7
6
5
4
3
2

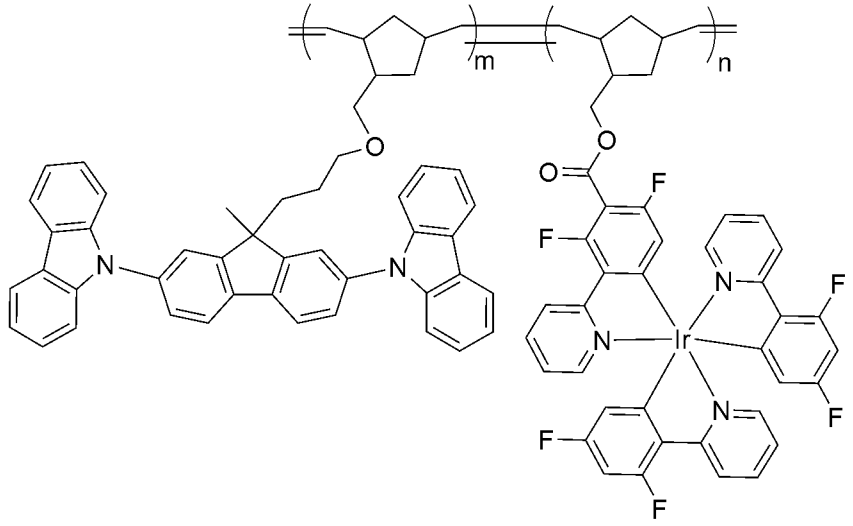
m
n
O
O
O
F
F
N
N
N
Ir
F
F
N
F
F

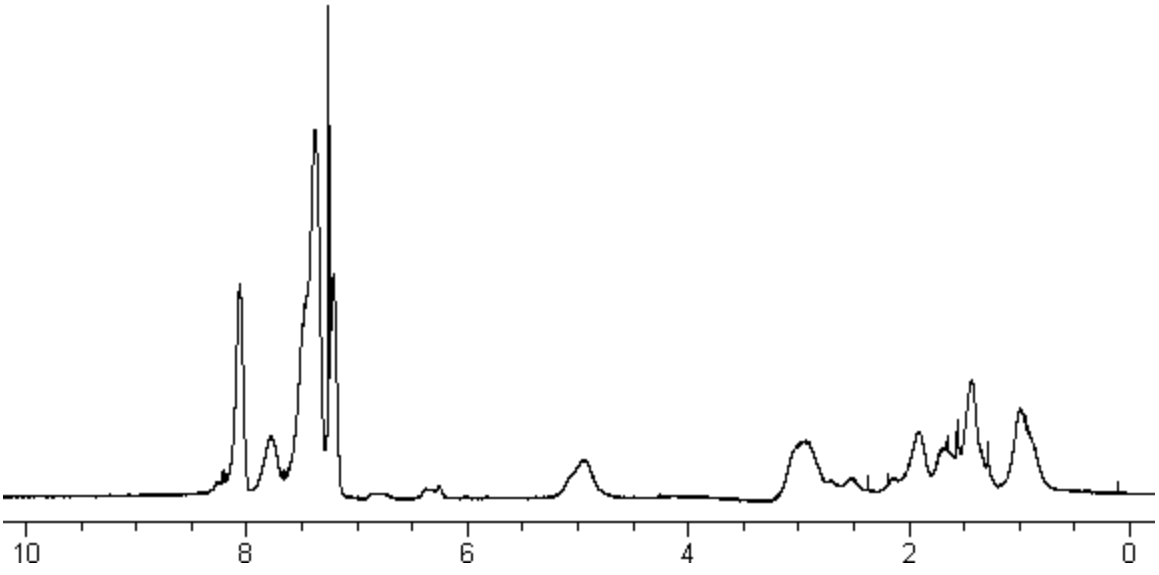
10
8
6
4
2
0

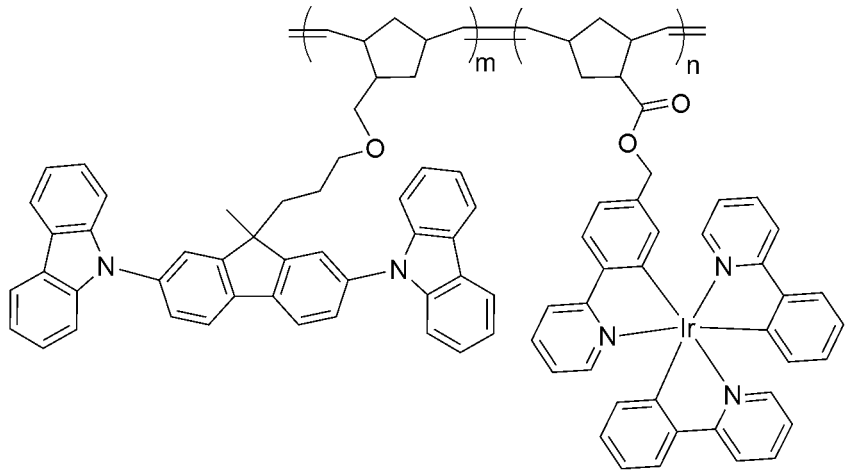
m
n
O
O
O
N
N
N
N
Ir
N

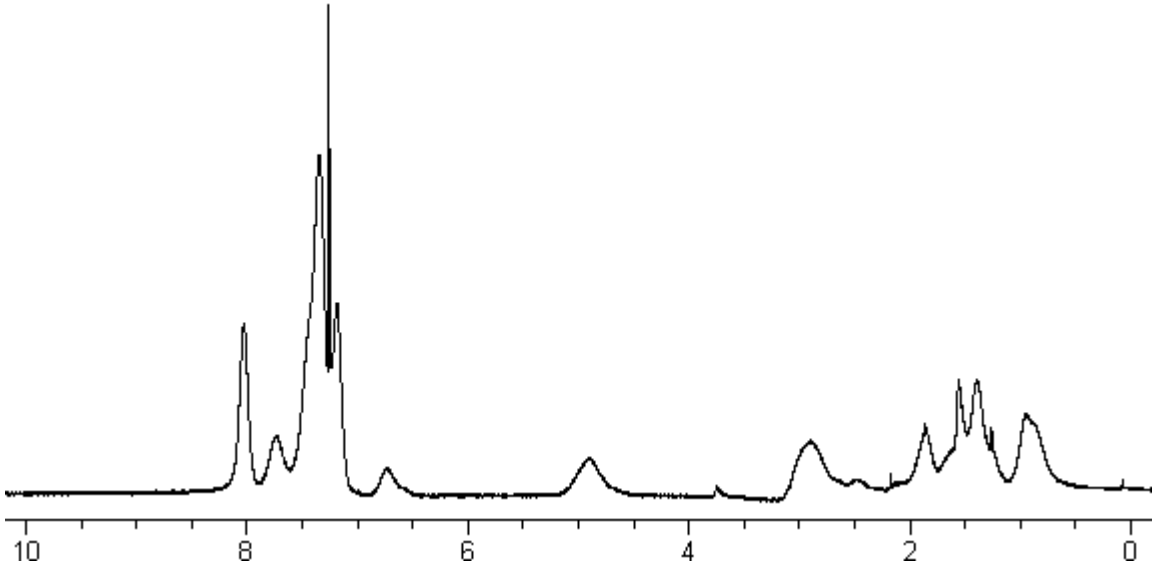
10
8
6
4
2
0

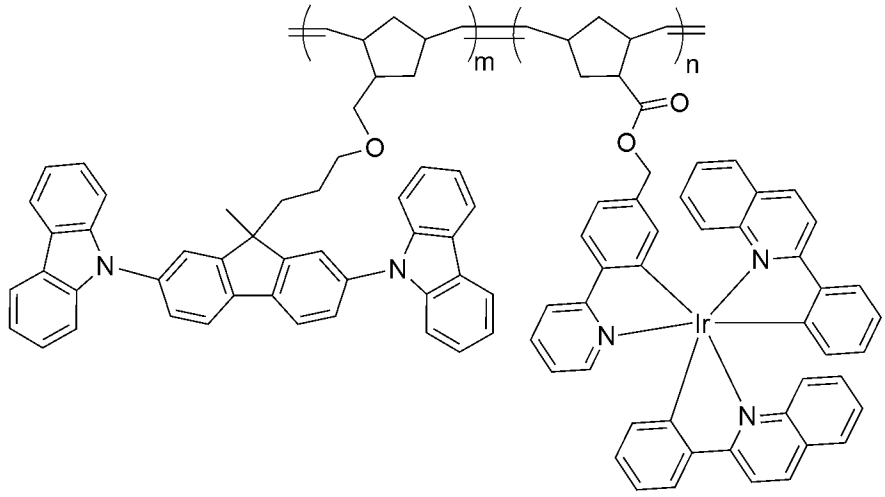
m
n
O
O
O
N
N
N
N
Ir

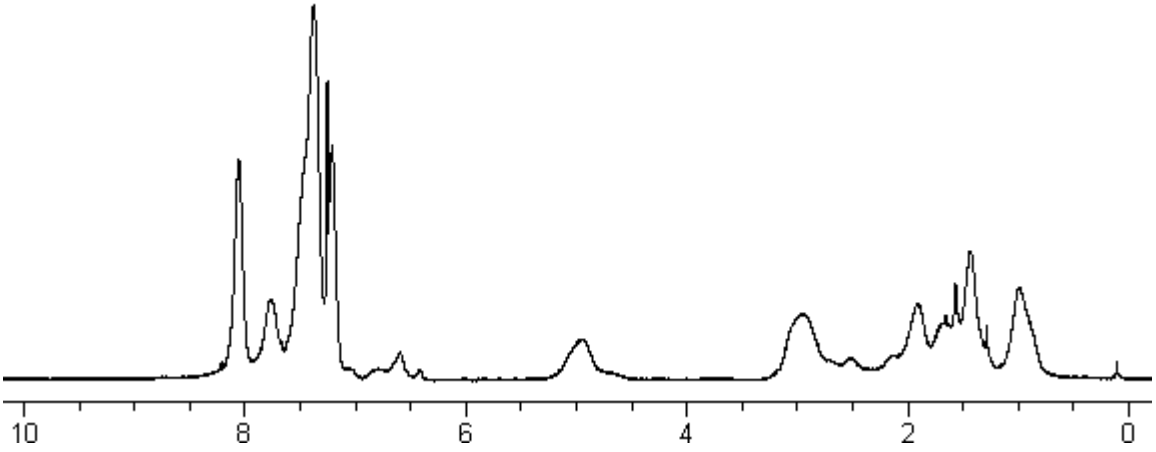
10
8
6
4
2
0

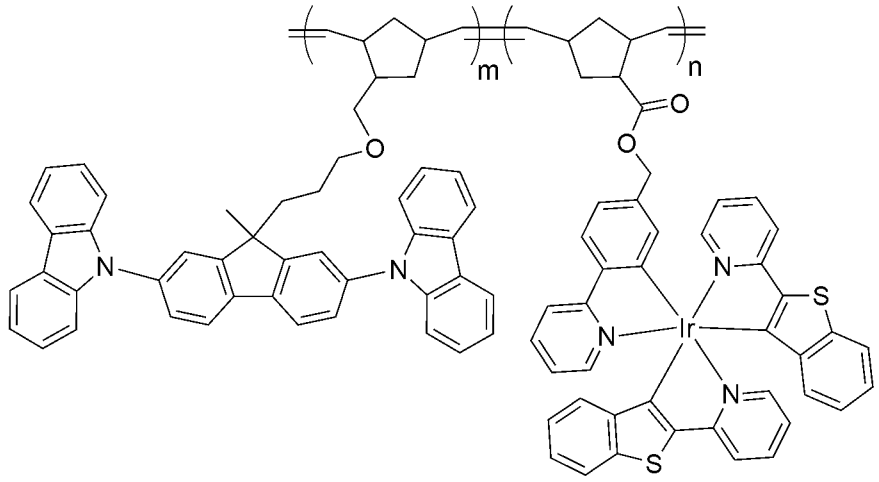
m
n
O
O
O
N
N
N
N
Ir
S
S

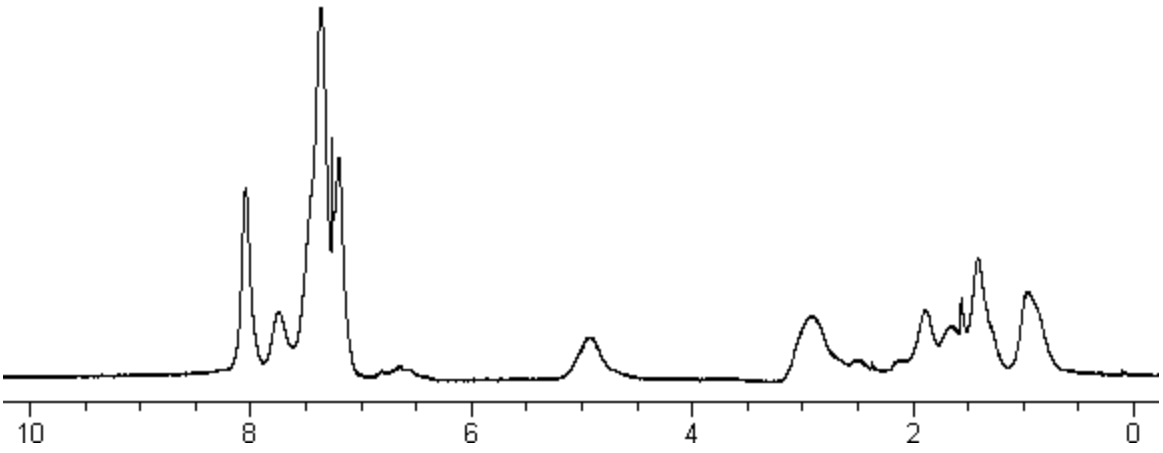
10
8
6
4
2
0

Chapter 8

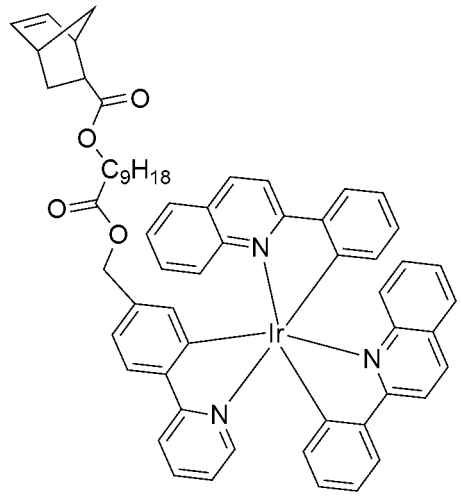

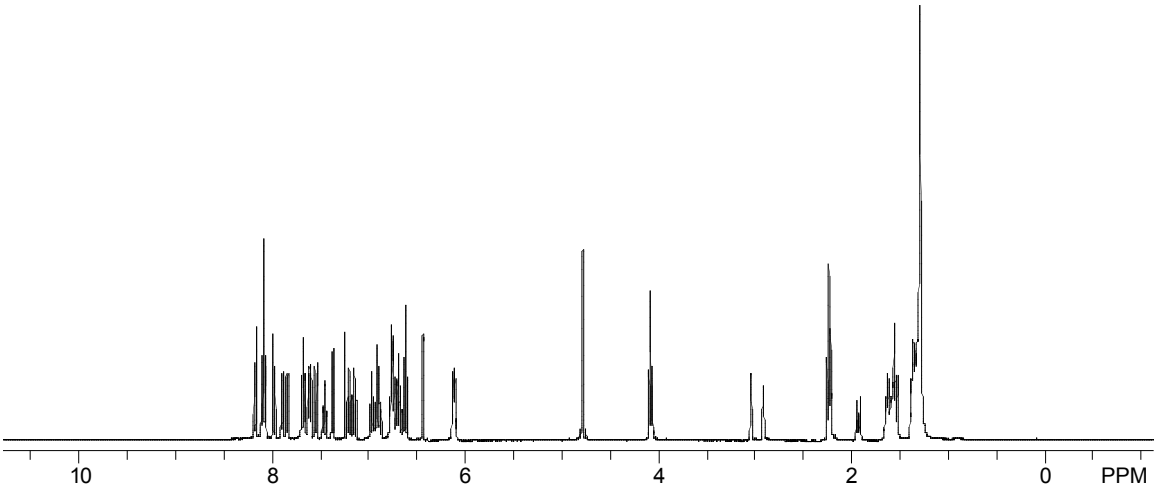

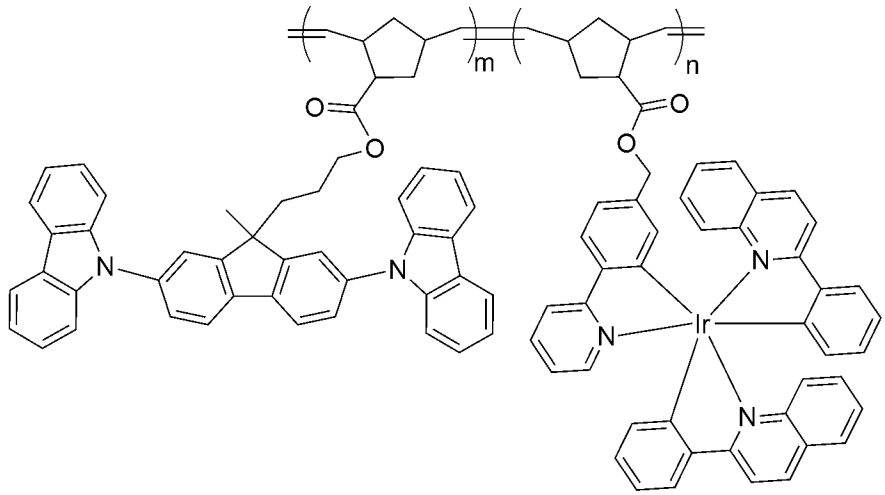
m
n
O
O
O
O
N
N
N
Ir
N
N

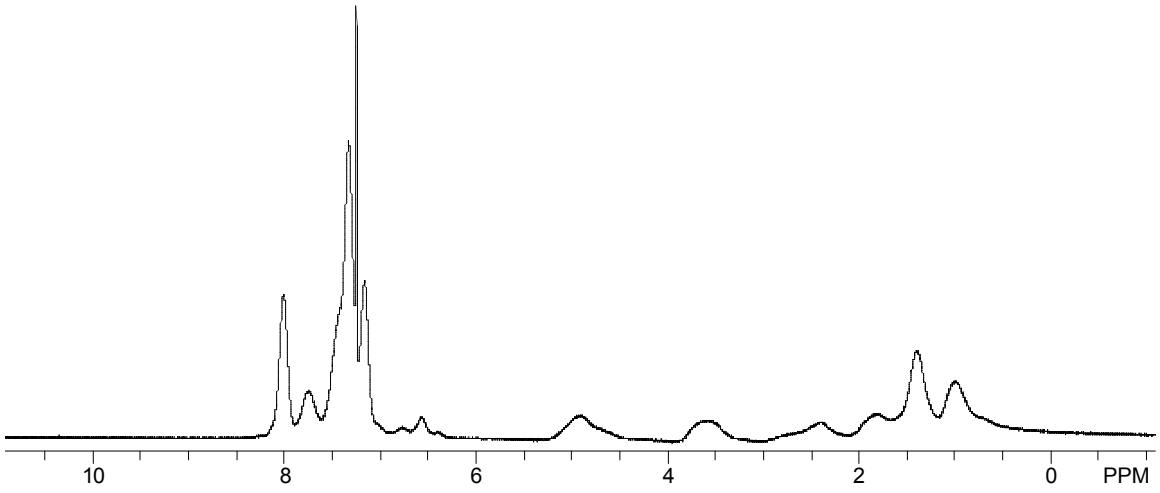
10
8
6
4
2
0
PPM

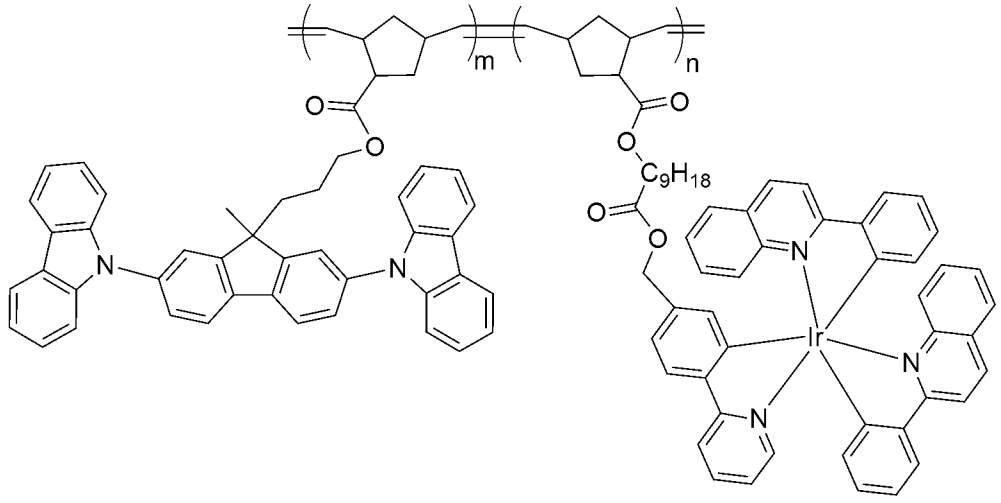
m
n
O
O
O
O
O
C_9H_{18}
O
N
N
N
Ir
N
N

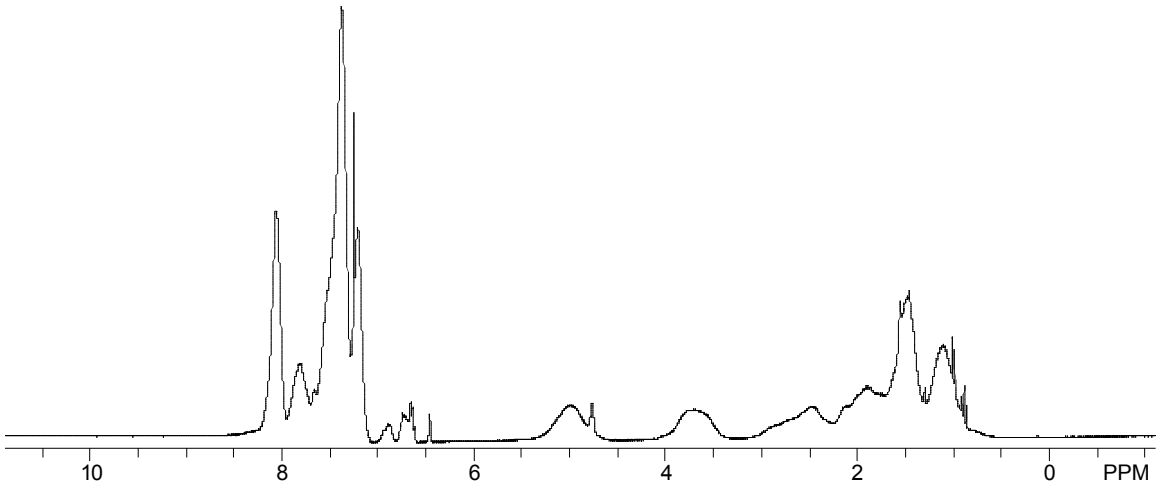
10
8
6
4
2
0
PPM

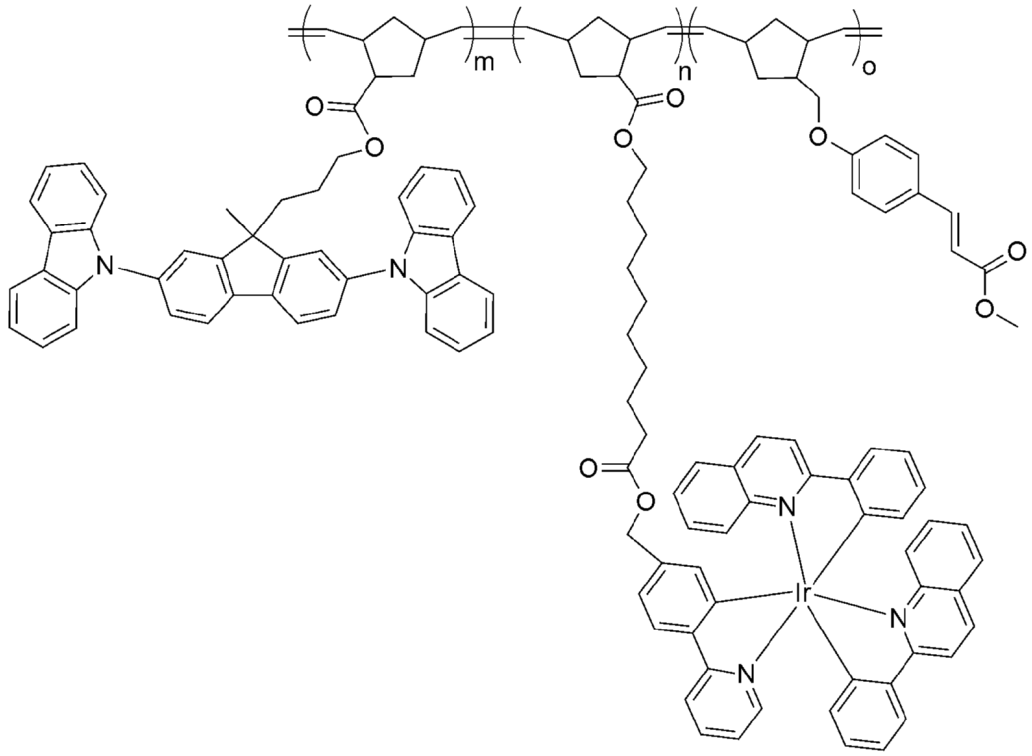
m
n
o
O
O
O
O
O
O
O
O
N
N
N
Ir
N
N

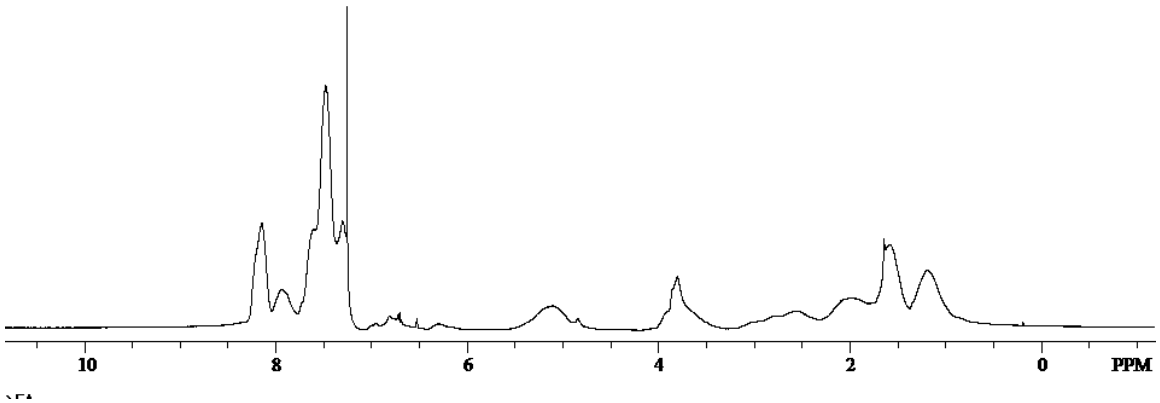
10
8
6
4
2
0
PPM

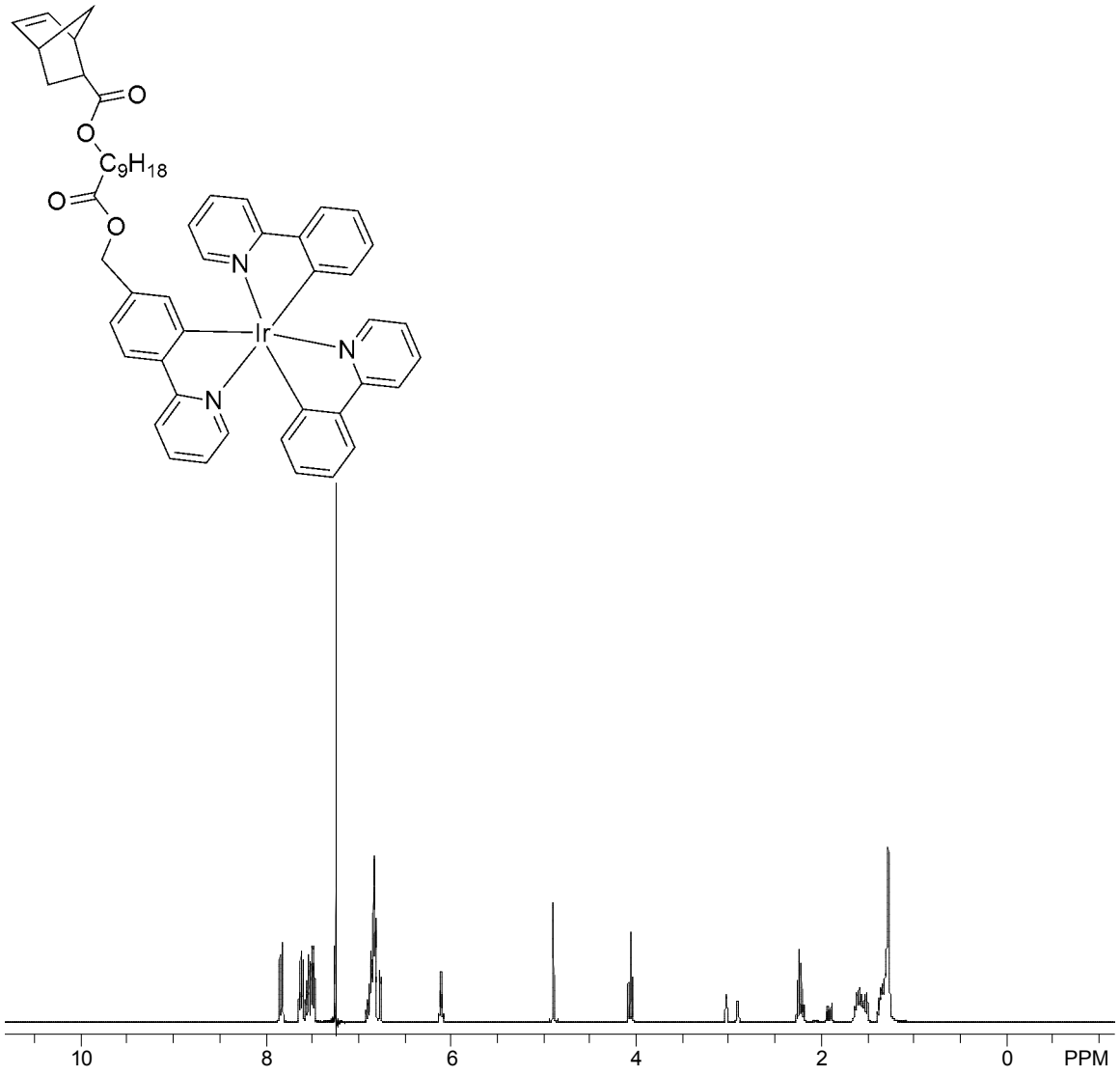
O
O
C9H18
O
O
N
Ir
N
N
10
8
6
4
2
0
PPM

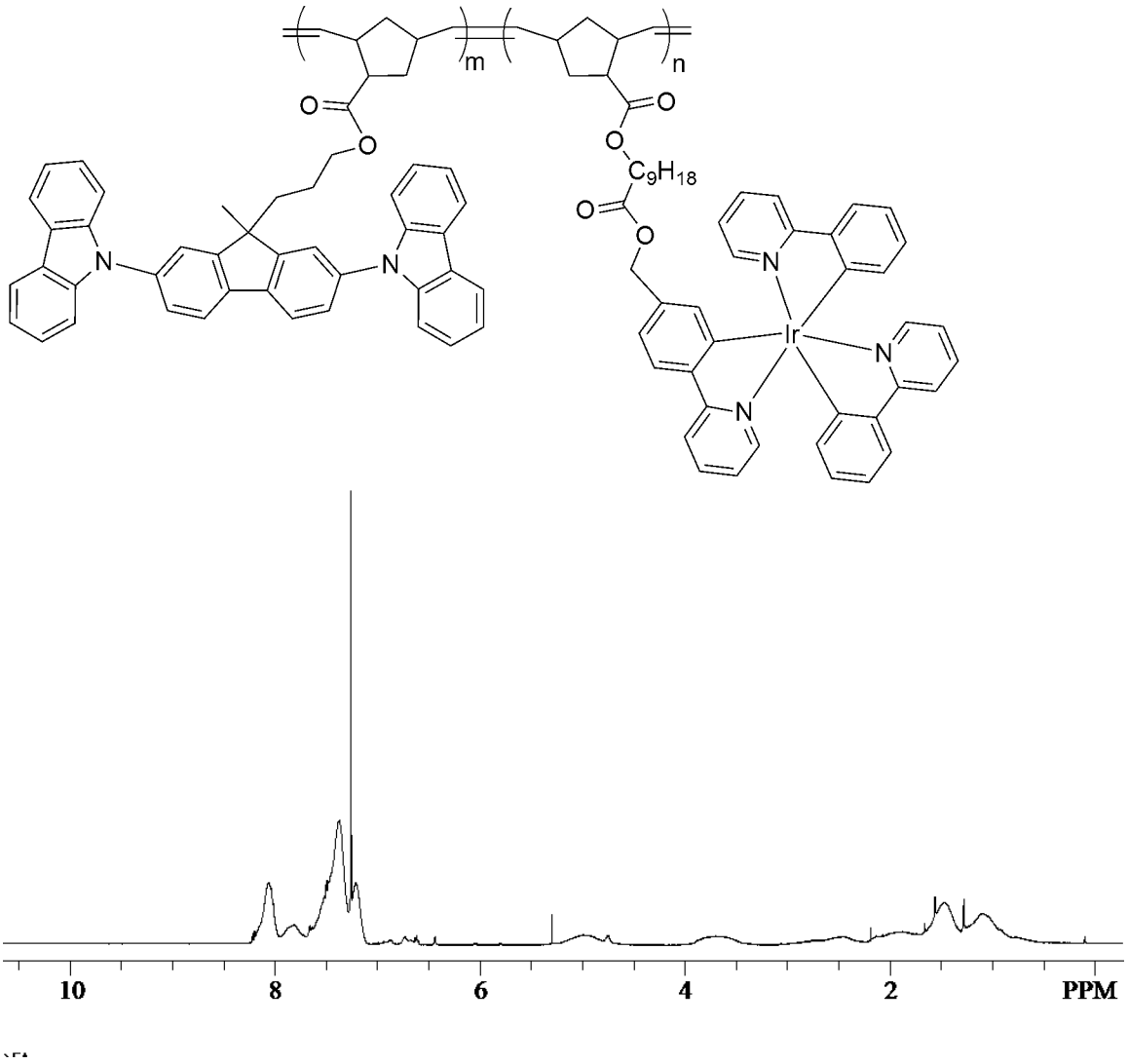
m
n
O
O
O
O
O
O
C_9H_{18}
N
N
N
N
Ir
N
10
8
6
4
2
PPM

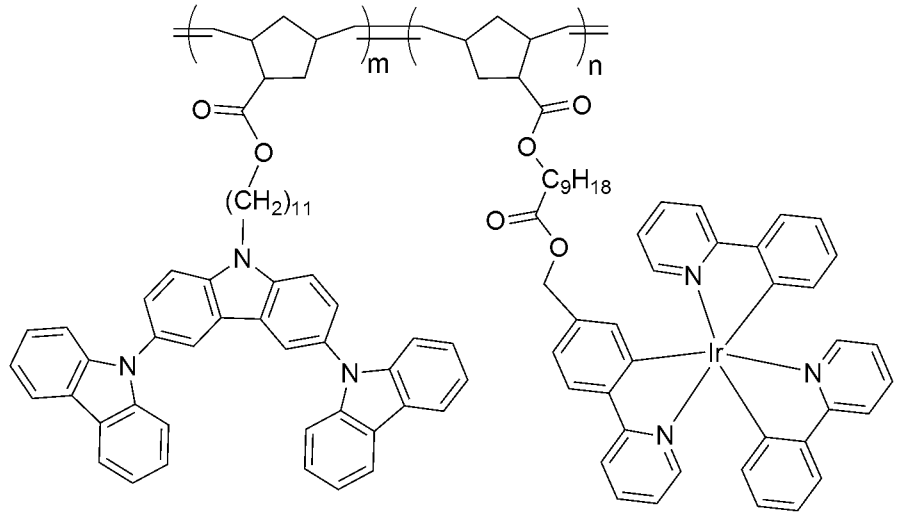
m
n
O
O
O
O
O
$(CH_2)_{11}$
C_9H_{18}
O
N
N
N
N
Ir
N
N

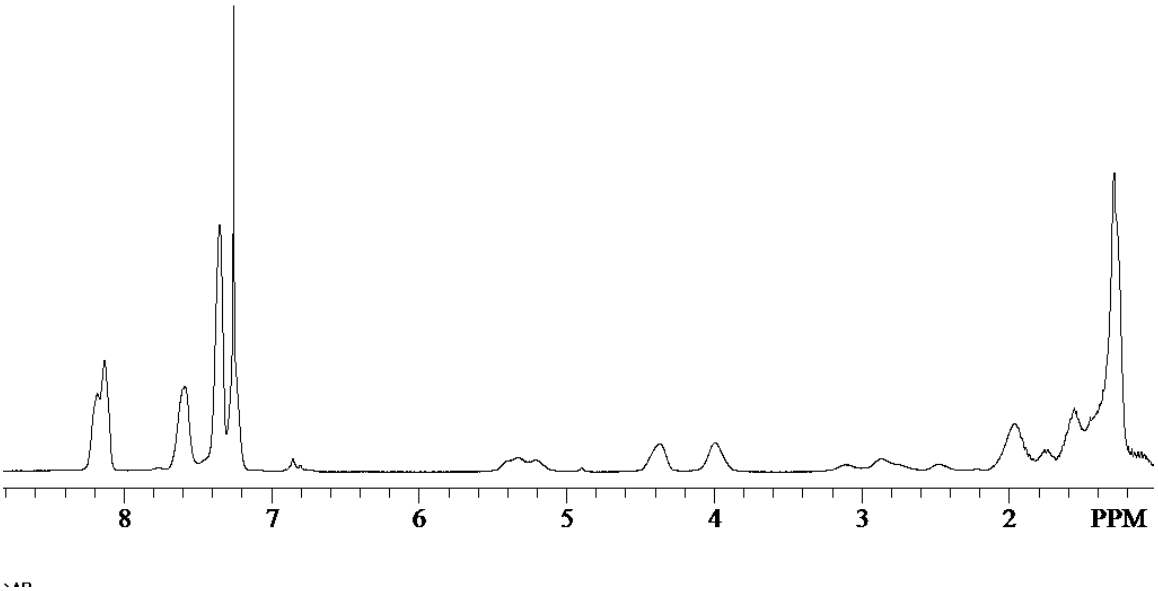
8
7
6
5
4
3
2
PPM